UNIVERSITÀ
DEGLI STUDI
FIRENZE

DOTTORATO DI RICERCA IN SCIENZE CLINICHE

Indirizzo in Fisiopatologia Clinica e dell'invecchiamento

e Scienze Infermieristiche

CICLO XXX

COORDINATORE Prof. Matucci Cerinic Marco

Ruolo dei canali Transient Receptor Potential (TRP) nella neuropatia periferica indotta da chemioterapici

Settore Scientifico Disciplinare BIO/14

Dottorando
Dr.ssa Marone Ilaria Maddalena

Tutore
Prof. Geppetti Pierangelo

Coordinatore
Prof. Matucci Cerinic Marco

Anni 2014/2017

Index

Chapter I – Introduction

1.1 Definition of Pain

A widely accepted definition of pain was developed by the International Association for the Study of Pain (IASP): pain is "*an unpleasant sensory and emotional experience associated with actual or potential tissue damage, or described in terms of such damage*". It represents a multidimensional sensory experience that is intrinsically unpleasant and associated with hurting and soreness. There is no single standard taxonomy of pain, but distinctions are frequently made between chronic and acute pain and between cancer and non cancer pain. Chronic pain is generally differentiated from acute pain by its duration, with chronic pain lasting longer than some specified time, often 3 or 6 months [1]. Conditions that cause intermittent recurring pain, for example, migraine headaches or sickle-cell anemia, have characteristics of both chronic and acute pain.

It may vary in intensity (mild, moderate, or severe), quality (sharp, burning, or dull), duration (transient, intermittent, or persistent), and referral (superficial or deep, localized or diffuse). Although it is essentially a sensation, pain has strong cognitive and emotional components; it is mainly linked to, or described in terms of, suffering. It is also associated with avoidance motor reflexes and alterations in autonomic output. All of these features are inextricably linked to the experience of pain. Pain can also be divided into two broad categories: adaptive and maladaptive. Adaptive pain contributes to survival by protecting the organism from injury or promoting healing when injury has occurred. Maladaptive pain, in contrast, is an expression of the pathologic operation of the nervous system; it is pain as disease.

The sensory experience of acute pain caused by a noxious stimulus is mediated by the nociceptive system. To prevent damage to tissue, we have learnt to associate certain categories of stimuli with danger that must be avoided. This association is formed by linking noxious stimuli with a sensation that is intense and unpleasant. The sensation of pain must be strong enough it demands immediate attention. This nociceptive pain system is a key early warning device, an alarm system that announces the presence of a potentially damaging stimulus. Nociceptive pain must be controlled only under specific clinical situations, such as during surgery or medical procedures that damage tissue and, after a trauma. It is important that this system not be chronically disabled, because loss of

its protective function inevitably leads to tissue damage, including self-induced mutilation of the tongue and lips, destruction of joints, loss of the tips of fingers, and pressure ulcers. Nociceptive pain is therefore a vital physiologic sensation. Lack of it in patients with congenital insensitivity to pain due to a mutation of the Nerve growth factor (NGF) tyrosine kinase A receptor, which results in a loss of high-threshold sensory neurons, reduces life expectancy [2]. If tissue damage occurs despite the nociceptive defensive system (e.g. through trauma, surgery, or inflammatory diseases), the body shifts from protecting against noxious, potentially damaging stimuli to promoting healing of the injured tissue. The term inflammatory pain is used to accomplish this goal. In this state, sensitivity to stimuli that usually do not cause pain is increased.

Chronic pain is a disabling condition that affects about 20% of the general population [3]. Although strong efforts have been made in pain research during the past decade, translation of preclinical results into clinical practice has been minor. Currently, very few novel therapeutic opportunities have been offered to patients, and older drugs have considerable side effects and incomplete efficacy. Thus, patients are frequently undertreated, and new potent analgesic drugs with a better safety profile are clearly needed. Response to tissue injury may evolve in a chronic status of allodynia and hyperalgesia, typically represented by hypersensitivity to both mechanical and thermal stimuli. In addition to central mechanisms, such hypersensitivity is primarily driven by over-activity of the peripheral nociceptors via sensitization of their nerve terminals [4]. Different etiologic agents, including physical trauma, neurotoxins, cancer and chemotherapeutic treatment, infections, immune and metabolic diseases, and migraine, produce pain symptoms, in which different molecular mechanisms eventually contribute to the sensitization of small diameter unmyelinated C-fibres and medium-diameter thinly myelinated Aδ-fibres [4]. Unlike inflammatory pain, neuropathic pain is not associated with an overt tissue inflammatory condition, but rather is dependent from a damage or dysfunction of the nervous system and is most frequently due to peripheral nerve injury.

Peripheral sensitization is produced when nociceptor terminals are exposed to by-products of tissue damage and inflammation, referred to collectively as the "inflammatory soup" [4]. Some of the main components of the "inflammatory soup" include peptides (bradykinin), lipids (prostaglandins), neurotransmitters (serotonin and ATP) and neurotrophins (NGF). The acidic nature of the "inflammatory soup" is also a crucial factor. Each of these factors sensitize or excite the terminals of the nociceptor by interacting with cell-surface receptors expressed by nociceptor neurons [4]. As a result, we prevent contact with or movement of the injured part until repair is complete, minimizing

further damage. Inflammatory pain typically decreases as the damage and inflammatory response resolve.

Maladaptive pain is uncoupled from a noxious stimulus or healing tissue. Such pain may occur in response to damage to the nervous system (neuropathic pain) or result from abnormal operation of the nervous system (functional pain). Maladaptive pain is the expression of abnormal sensory processing and usually is persistent or recurrent. This is an area of enormous unmet clinical need because treatment options are limited and our understanding incomplete. In the maladaptive pain, the fire alarm system is constantly switched on even though there is no emergency, or repeated false alarms occur. Neuropathic pain may result from lesions to the peripheral nervous system, as in patients with diabetic or AIDS polyneuropathy, post-herpetic neuralgia, or lumbar radiculopathy, or to the central nervous system, such as in patients with spinal cord injury, multiple sclerosis, or stroke [5].

In functional form of pain sensitivity, no neurologic deficit or peripheral abnormality can be detected. The pain is due to an abnormal responsiveness or function of the nervous system, in which heightened gain or sensitivity of the sensory apparatus amplifies symptoms. Several common conditions have features that may place them this category: fibromyalgia, irritable bowel syndrome, some forms of non-cardiac chest pain, and tension-type headache [6-8]. It is unknown why the central nervous system of patients with functional pain displays abnormal sensitivity or hyperresponsiveness. Although inflammatory, neuropathic, and functional pain each have different causes, they share some characteristics. The pain in these syndromes may arise spontaneously in the apparent absence of any peripheral stimulus, or it may be evoked by stimuli. Evoked pain may arise from a low-intensity, normally innocuous stimulus, such as a light touch to the skin in a patient with post-herpetic neuralgia or vibration during an acute attack of gout, or it may be an exaggerated and prolonged response to a noxious stimulus. The former condition is called allodynia and the latter hyperalgesia. Spontaneous pain and changes in sensitivity to stimuli are fundamental features of clinical pain, distinguishing it from nociceptive pain, in which pain occurs only in the presence of an intense or noxious stimulus.

Classic migraine represents a kind of pain inserted in a different category of pain syndromes. Migraine is characterized by attacks of often throbbing and frequently unilateral severe headache, which are usually associated with nausea, vomiting, and/or sensitivity to light (photophobia), sound (phonophobia), or odours (osmophobia), and aggravated by movement. If untreated, attacks typically last 4–72 h. In about 30% of patients, migraine attacks are preceded or accompanied by transient focal neurologic

symptoms, which are usually visual, but that could also consist in paresthesias or language disturbances, commonly known as 'aura'. The last update of the World Health Organization, Global Burden of Disease, states that migraine alone is responsible for almost 3% of disability attributable to a specific disease worldwide. It is an episodic neurologic condition that has been related to abnormal cortical activity that alters sensory input from dural and cerebrovascular sensory fibers and is associated with an abnormal sensory processing in the brainstem. It possesses features of inflammatory and functional pain, as well as of objective neurologic dysfunction [9].

Pain caused by cancer varies greatly in character and source; it depends on the tumor, its location, and its proximity to other tissues. In some cases, tumor cells produce chemical signals that contribute directly to the pain, as in osteosarcomas. In other tumors, the pain may be due to mechanical compression or invasion of a nerve, distention of an organ, ischemia, or an inflammatory reaction to tissue necrosis. It may also represent a neurotoxic side effect of chemotherapy [10].

1.2 The primary afferent nociceptors

The sensory experience of pain begins in the periphery, where the peripheral terminals of primary afferent fibers respond to many stimuli and translate this information into the dorsal horn of the spinal cord, where the central ends of these fibers terminate. Nearly a century ago, Sherrington proposed the existence of the nociceptor, a primary sensory neuron that is activated by stimuli capable of causing tissue damage [11]. According to this model, nociceptors have characteristic thresholds or sensitivities that distinguish them from other sensory nerve fibers. Electrophysiological studies have shown the existence of primary sensory neurons that can be excited by noxious heat, intense pressure or irritant chemicals, but not by innocuous stimuli such as warming or light touch [4]. Primary afferent fibers have a unique morphology, called pseudo-unipolar, wherein both central and peripheral terminals emanate from a common axonal stalk. Primary sensory neurons have the cell somata in sensory ganglia, dorsal root and trigeminal ganglia (DRG and TG, respectively). The peripheral axons of these neurons innervate tissue, such as skin and whose terminals react to sensory stimuli, and the central axons enter the spinal cord, where it forms synapse with second order neurons to transfer information to the central nervous system (CNS). Many neurons innervating the viscera are located in the nodose ganglia and, their peripheral fibers travel with the vagus nerve whereas their central axons project to the area postrema. All sensory systems form an anatomic

connection between the potentially harmful external and internal milieu and the CNS and convert all the stimuli into electro-chemical signals. The heterogeneous population of sensory fibers originated from the ganglia can be distinguished into three main groups based on anatomical and functional criteria (Figure 1). Cell bodies with the largest diameters give rise to myelinated, rapidly conducting Aβ primary sensory fibers. Most, but not all, Aβ fibers detect innocuous stimuli applied to skin, muscle and joints and thus do not contribute to pain. By contrast, small- and medium-diameter cell bodies give rise to most of the nociceptors, including unmyelinated, slowly conducting C fibers and thinly myelinated, more rapidly conducting Aδ fibers (Figure 1a). It has long been assumed that Aδ and C nociceptors mediate "first" and "second" pain, respectively, namely the rapid, acute, sharp pain and the delayed, more diffuse, dull pain evoked by noxious stimuli (Figure 1b). There are two main classes of Aδ nociceptor and both respond to intense mechanical stimuli, but can be distinguished by their differential responsiveness to intense heat or how they are affected. The Aδ and C nociceptive fibers either respond to one type of physical stimulus (unimodal nociceptors), or more commonly integrate and generate a response to potentially damaging thermal, mechanical and/or chemical stimuli (polymodal nociceptors) [4].

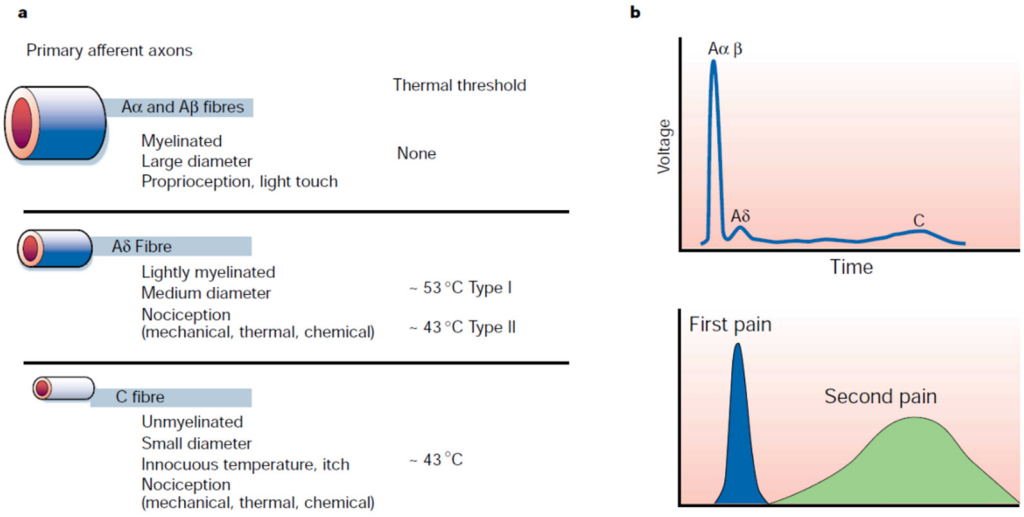

Figure 1. Different nociceptors detect different types of pain. a Peripheral nerves include small-diameter (Aδ) and medium- to large-diameter (Aα,β) myelinated afferent fibres, as well as small-diameter unmyelinated afferent fibres (C). **b** Conductive velocity is related to fiber diameter. Aδ and C nociceptors mediate "first" and "second" pain. (Julius, 2001).

Primary sensory neurons are the interface of the nervous system with the external and internal environment of our body. A major function of the sensory apparatus is to detect potentially damaging stimuli and warn of the risk of injury. All primary sensory nociceptors make synaptic connections with neurons in the grey matter (dorsal horn) of the spinal cord. Subsets of dorsal horn neurons, in turn, project axons and transmit pain messages to higher brain centers, including the reticular formation, thalamus and

ultimately the cerebral cortex (Figure 2). Primary afferent nerve fibers project to the dorsal horn of the spinal cord, which is organized into anatomically and electrophysiological distinct laminae. For example, the spinal cord neurons within lamina I and II are generally responsive to noxious stimulation (*via* Aδ and C fibers), neurons in laminae III and IV are primarily responsive to innocuous stimulation (*via* Aβ), and neurons in lamina V receive a convergent non-noxious and noxious input *via* direct (monosynaptic) Aδ and Aβ inputs and indirect (polysynaptic) C fiber inputs [12]. In animal models, the expression of c-Fos protein is a useful marker for monitoring neural activities in the central pathways of the sensory system, mainly in the pain pathway including thermal, mechanical and chemical stimuli [13]. Spinal neurons expressing c-Fos after noxious stimulation are located in laminae I and II, and laminae V and VI of the dorsal horn.

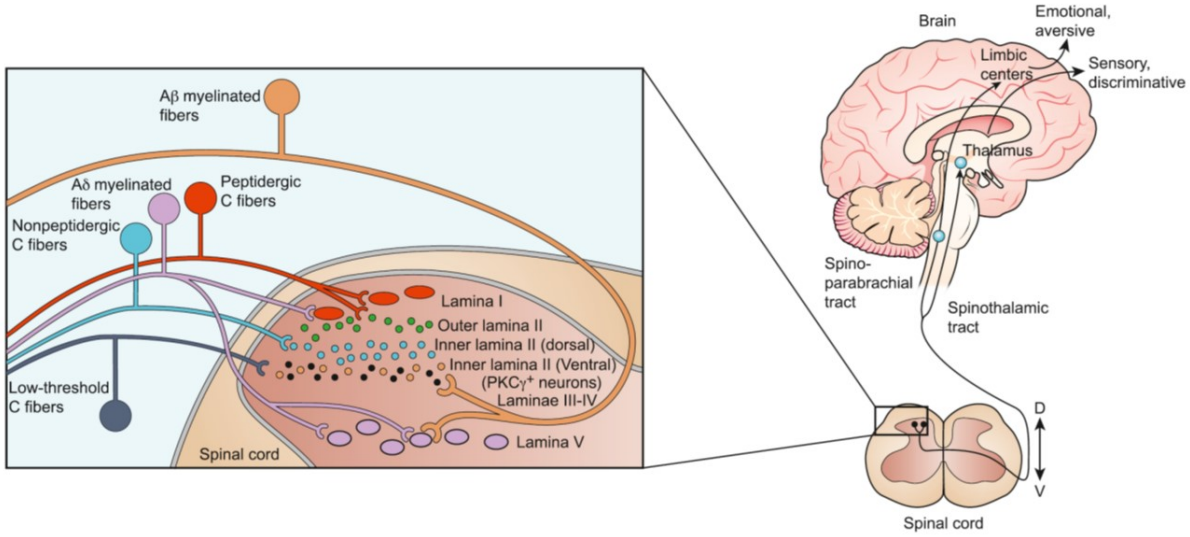

Figure 2. Spinal Cord Neuroanatomy: inputs and projections. Different populations of primary afferent fibers target different regions of the dorsal horn of the spinal cord, with the input from C nociceptors concentrated in the superficial dorsal horn (laminae I and II). The small myelinated Aδ nociceptors target both laminae I and V. The low-threshold C mechanoreceptors, in contrast, target neurons in the ventral part of inner lamina II, which contains many PKCγ-expressing populations of interneurons. The right side of the figure illustrates the major ascending pathways that derive from the spinal cord dorsal horn. (Braz, 2014).

Most C-fibers nociceptors respond to noxious chemical stimuli such as capsaicin, the pungent ingredient in hot chili peppers, and for this reason they are defined as capsaicin-sensitive sensory neurons. Histochemical studies of adult DRG reveal two broad classes of unmyelinated C-fibers: the so-called peptidergic population, containing the peptide neurotransmitter substance P (SP) and express TrkA, the high-affinity tyrosine kinase receptor for NGF [14]. The second population does not express SP or TrkA, but can be labelled selectively with the α-D-galactosyl-binding lectin, IB4, and expresses P2X3 receptors, a specific subtype of ATP-gated ion channel. This categorization is a first approximation at best, as additional molecular markers become available, new subsets

are likely to be recognized. The ability of sensing and transmitting noxious stimuli and nociceptive information is intrinsically associated to the release of neuropeptides from their peripheral terminals. The ionic event, gating by noxious stimuli, results in an excitatory effect with the subsequent depolarization of the nerve fibers and the initiation of an action potential propagation. Calcium (Ca^{2+}) influx into the peptidergic nerve endings causes the local release of proinflammatory neuropeptides, such as the calcitonin gene-related peptide (CGRP) and tachykinins, SP and neurokinin A (NKA). Activation of CGRP and tachykinin receptors (NK1, NK2 and NK3) on effector cells, particularly at the vascular levels, causes a series of inflammatory responses, collectively referred to as neurogenic inflammation [15].

Sir Thomas Lewis in his pioneering studies [16] precisely defined the dual "nocifensor" role of these neurons as characterized by the capacity of one portion of the widely branching sensory fiber to respond to the injury, and to generate action potentials, which are carried, antidromically, to other branches of the fiber, where they release a chemical substance that causes the flare and increases the sensitivity of other sensory axons responsible for pain. There is now a bulk of information suggesting that this phenomenon, firstly described at the somatic (skin) level, occurs in a variety of visceral organs. In addition, sensory neuropeptide release may occur not only from collateral fibers invaded antidromically by action potentials, through a tetrodotoxin-sensitive axon reflex, but also, as in the case of capsaicin, by the stimulated terminal itself *via* a tetrodotoxin-insensitive mechanism [17].

1.3 Neurogenic inflammation

The term neurogenic inflammation refers to a series of responses that occur at peripheral level following the activation of capsaicin-sensitive sensory neurons, mainly present at the vascular level. These events also occur in other tissues and organs with a large variability according to the mammal species under investigation. At the vascular level, the release of CGRP, SP and NKA induces vasodilatation, mediated by CGRP, plasma protein extravasation and leukocyte adhesion to the vascular endothelium of postcapillary venules, mediated by SP/NKA and the NK1 receptor [15]. In non-vascular tissues, neurogenic inflammatory responses include cardiac positive chronotropic effects (CGRP-mediated), contraction of the smooth muscle of the iris sphincter (SP/NKA, NK2 receptor), ureter, bladder neck and urethra (SP/NKA, NK2/NK1 receptors), relaxation of bladder dome (CGRP), exocrine gland secretion (SP/NKA, NK1 receptor). Species-

related variations in neurogenic inflammatory responses are clearly illustrated by the motor effect produced by sensory nerve activation and tachykinins in the airways. The release of SP/NKA from capsaicin-sensitive nerve terminals causes direct bronchoconstriction in the guinea-pig, indirect and nitric oxide/prostanoid-mediated bronchodilatation in the rat and mouse. In humans, as in guinea-pigs, activation of both NK2 and, in part, NK1 receptors mediates a robust bronchoconstriction in human isolated bronchi [18]. Noteworthy is the ability of tachykinins (NK1) to stimulate seromucous secretion [19] from bronchial glands, and to excite (NK3) postganglionic cholinergic nerve terminals in the human bronchus [20]. Neurogenic inflammation markedly contributes to inflammatory responses both at the somatic and visceral levels in different mammal species. In the human skin there is compelling evidence that capsaicin or histamine causes a flare response that being blocked by local anesthetics or by repeated application of topical capsaicin (capsaicin desensitization), is mediated by stimulation of terminals of capsaicin-sensitive neurons and the subsequent release of neuropeptides. However, whether in man, neurogenic inflammation plays a pathophysiological role at the visceral level it not well understood. There is evidence that CGRP is released by capsaicin from human tissues *in vitro* [21] and during migraine attacks [22]. A major role of CGRP released from trigeminal perivascular nerve fibers derived from the observation that BIBN 4096BS, a peptide with high affinity for the CGRP receptor [23] that does not cross the blood brain barrier, reduces the pain and other symptoms associated with migraine attacks [24]. This finding supports the hypothesis that sensory CGRP is released from terminals of primary sensory neurons and exerts a pathophysiological role in human disease.

1.4 Transient Receptor Potential (TRP) channels

The TRP ion channels are a large class of channel subunits united by a common primary structure and permeability to monovalent cations and Ca^{2+} ions. The first gene encoding a TRP channel was discovered in the fruit-fly *Drosophila melanogaster* where mutants for that gene exhibited impaired vision due to the lack of a specific Ca^{2+} influx pathway into photoreceptors [25]. Phototransduction in the fruit-fly involves activation of membrane cation channels leading to a depolarizing current. *Drosophila* photoreceptors contain the light-sensitive G protein-coupled receptor rhodopsin, whose activation results in stimulation of phospholipase C-β (PLC-β). Resolving components of the light-induced current (LIC) led to the identification of a *Drosophila* mutant displaying a transient LIC in response to light, in contrast to the sustained LIC in wild-type flies. This mutant strain

was termed *trp*, for transient receptor potential. Mutations in this gene led to a disruption of a Ca^{2+} entry channel in the photoreceptors, indicating that TRP, the protein encoded by the *trp* gene, forms all, or part, of a Ca^{2+} influx channel [26].

More than 50 members of the TRP family have been characterized in many tissues and cell types in both vertebrates and invertebrates making them one of the largest groups of ion channels [27]. A unifying theme in this group is that TRP proteins play critical roles in sensory physiology, which include contributions to vision, taste, olfaction, hearing, touch, and thermo- and osmo-sensation. TRP cation channels are unique cellular sensors characterized by a promiscuous activation mechanism [28]. For example, yeasts use a TRP channel to perceive and respond to hypertonicity [29], nematodes use TRP channels at the tips of neuronal dendrites in their "noses" to detect and avoid noxious chemicals [30], male mice use a pheromone-sensing TRP channel to tell males from females [31]. Humans use TRP channels to appreciate sweet, bitter and umami (amino acid) [32] and to discriminate warmth, heat and cold. In each of these cases, TRPs mediate sensory transduction, not only in a classical sense, for the entire multicellular organism, but also at the level of single cells.

1.4.1 Classification and structural features

TRPs are classified essentially according to their primary amino acid sequence rather than selectivity or ligand affinity, because their properties are heterogenous and their regulation is complex. The 28 mammalian TRPs channel superfamily can be divided into six families [33,34] (Figure 3). The TRPC (Canonical) and TRPM (Melastatin) subfamilies consist of seven and eight different channels, respectively (i.e. TRPC1-TRPC7 and TRPM1-TRPM8). The TRPV (Vanilloid) subfamily presently comprises six members (TRPV1-TRPV6). The most recently identified subfamily, TRPA (Ankyrin), has only one mammalian member (TRPA1). The TRPP (Polycystin) and TRPML (mucolipin) families, each containing three mammalian members, are not sufficiently characterized, but gain increasing interest because of their involvement in several human diseases.

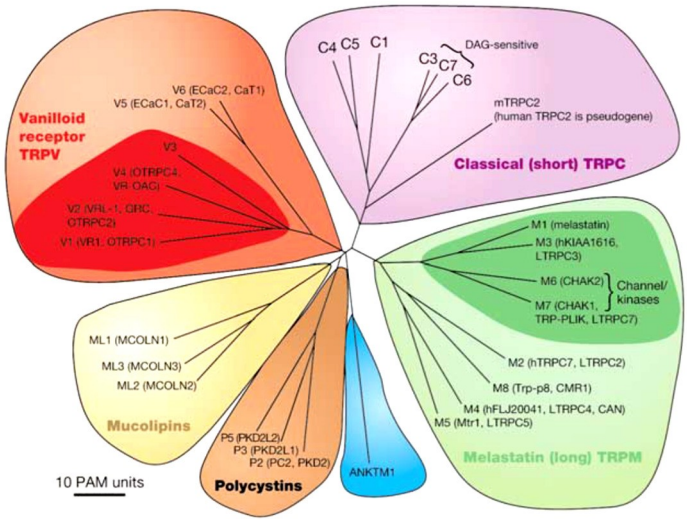

Figure 3. Mammalian TRP family tree. The evolutionary distance is shown by the total branch lengths in point accepted mutations (PAM) units, which is the mean number of substitutions per 100 residues. Adapted from Clapham (2003).

All TRP channels comprise six transmembrane domains (S1-S6) and a pore region formed by a short, hydrophobic stretch between S5 and S6 to form cation-permeable pores. Both the N- and C-termini are located intracellularly (Figure 4). Despite the topographic similarities between the TRPs and the voltage-gated potassium channels, the TRPs are actually only distantly related to these channels. Voltage-gating refers to channel opening results from movement of the charged S4 segment in K_V/Na_V/Ca_V channels upon a change in transmembrane voltage. In TRPs channels, S4 lacks the complete set of positively charged residues necessary for the voltage sensor in many voltage-gated ion channels [35]. In general, TRP channel gating is not dominated by voltage but rather is affected by the energy differences accompanying changes in temperature, binding, and voltage. Functional TRP channels consist of either homo- or hetero-multimers of four TRP subunits (Figure 4). Whereas the C-terminus is a highly conserved residue, most TRP channels contain N-terminus ankyrin repeats, which are 33-residue motifs with a conserved backbone and variable residues that mediate specific protein-protein interactions [36]. It is notable that ankyrin repeats are prominent in the assembly of macromolecular complexes between the plasma membrane and the cytoskeleton. It is also possible that the ankyrin repeats play a functional role in transmitting mechanical forces to the gate of the channels.

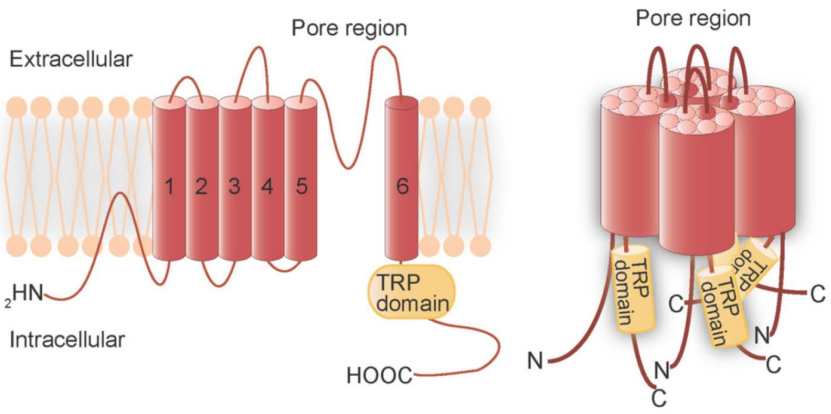

Figure 4. Transmembrane topology of TRP channels. Transmembrane topology (left) and the quartenary structure of TRP channels (right). The TRP protein has six putative transmembrane domains, a pore region between the fifth and sixth transmembrane domains and a TRP domain in the C-terminal region. The TRP protein assembles into homotetramers or heterotetramers to form channels (Takahashi, 2012).

Although a single defining characteristic of TRP channels function has not yet emerged, TRPs may be generally described as calcium-permeable cation channels with polymodal activation properties. By integrating multiple concomitant stimuli and coupling their activity to downstream cellular signal amplification *via* Ca^{2+} permeation and membrane depolarization, TRP channels appear well adapted to function in cellular sensation. Indeed, their localization in the plasma membranes of neurons or other cells and a large body of evidence collected using a plethora of stimuli, indicates that they are sensors of chemical, mechanical and thermal stimuli. All functionally characterized TRP channels mediate the transmembrane flux of cations down their electrochemical gradients, thereby raising intracellular Ca^{2+} and Na^{+} concentrations and depolarizing the cell. As they are widely expressed in mammalian tissues, TRPs are well positioned to regulate intracellular Ca^{2+} and Na^{+}, and transmembrane voltage in both excitable and non-excitable cells. Most Ca^{2+}-permeable TRP channels are only poorly selective for Ca^{2+}, with permeability ratio relative to Na^{+} (P_{Ca}/P_{Na}) in the range between 0.3 and 10. Exceptions are TRPV5 and TRPV6, two highly Ca^{2+}-selective TRP channels with P_{Ca}/P_{Na} >100. TRP channels are gated by different stimuli that include the binding of intracellular and extracellular messengers, changes in temperature, and chemical and/or mechanical (osmotic) stress. Sensitivity to polymodal activation suggests that the physiologically relevant stimulus for any given TRP will be governed by the specifics of cellular context (i.e., phosphorylation status, lipid environment, interacting proteins, and concentrations of relevant ligands). Ligands that activate TRP channels may be classified as (a) exogenous small organic molecules, including synthetic compounds and natural products; (b) endogenous lipids or products of lipid metabolism; (c) purine nucleotides and their metabolites; (d) inorganic ions, with Ca^{2+} and Mg^{2+} being the most likely to have physiological relevance [37].

In addition, from their first identification, several members of other TRP subfamilies have been described as store operated channels (SOCs). Store-operated Ca^{2+} entry channels are considered channels that are activated whenever intracellular Ca^{2+} stores become depleted. In many cases, the classification of TRP channels as SOCs is mainly based on the results of Ca^{2+} imaging protocols, in which store-dependent Ca^{2+} influx is estimated from the rise in intracellular Ca^{2+} concentration that occurs in cells to which extracellular Ca^{2+} is readded after artificial store depletion. However, most TRP channels are not gated by the usual mechanism defined as activating store-operated Ca^{2+} entry. Thus it is not accurate to refer to TRP channels as store-operated channels, although it may turn out that one or more of these channels participate to this process [38].

1.4.2 The TRPC subfamily

The mammalian TRP channels most closely related to Drosophila TRP are classified in the TRPC subfamily. TRPC channels are nonselective, Ca^{2+}-permeable cation channels, but the permeability ratio (PCa/PNa) varies significantly between different members of the family. In general, TRPC members can be considered as channels activated after stimulation of receptors that activate different isoforms of phospholipase C (PLC). A recent study reported that TRPC1 is directly activated by membrane stretch, independent of PLC activity [39].

1.4.3 The TRPV subfamily

The TRPV family includes six mammalian members divided into two group: TRPV1-TRPV4 and TRPV5-TRPV6. The vanilloid receptor TRPV1 is the best characterized ion channel in this class. Members of the TRPV family contain three to five ankyrin repeats in their cytosolic NH_2-termini. TRPV1-TRPV4 are all heat-activated channels that are non-selective for cations and modestly permeable to Ca^{2+}. In addition, they also function as chemosensors for a broad array of endogenous and synthetic ligands. Recently, it has been described that TRPV4 is also activated upon cell swelling [40]. Interestingly, these different chemical and physical activator stimuli mostly have an additive, or even supra-additive, effect on the gating of TRPV channels, which endows these channels with the ability to act as signal integrators. This form of signal integration is of great importance to several pathological states. The properties of the two other members of this subfamily, TRPV5 and TRPV6, are quite different from those of TRPV1-TRPV4. They are the only highly Ca^{2+}-selective channels in the TRP family, and both are

tightly regulated by intracellular Ca^{2+} [41]. These properties allow TRPV5 and TRPV6 to play a crucial role as gatekeepers in epithelial Ca^{2+} transport, and as selective Ca^{2+} influx pathways in non-excitable cells [42]. In addition, in contrast to the other TRPVs, the temperature sensitivity of TRPV5 and TRPV6 is relatively low. TRPV1 is commonly referred as the capsaicin receptor, and was first described as a polymodal receptor activated by vanilloid compounds (capsaicin, resiniferatoxin), moderate heat (≥43 °C) and low pH (<5.9) [43,44]. Since then, TRPV1 has been reported to be also activated by camphor [45], allicin [46,47] nitric oxide [48], spider toxins [49] potentiated by ethanol [50] and modulated by extracellular cations [51]. TRPV1 was initially described in a subpopulation of small- to medium-diameter neurons in DRG, TG and nodose ganglia [43,44]. While TRPV1 has since been described in many neuronal and non-neuronal cells [52], its highest expression level is in sensory neurons. Several studies have demonstrated that inflammatory mediators, such as bradykinin, prostaglandin E_2, extracellular ATP, glutamate and NGF indirectly sensitize TRPV1 [53]; following exposure of sensory neurons to inflammatory mediators, responses to capsaicin or heat are dramatically enhanced to the extent that body temperature can be sufficient to activate nociceptors [44]. Inflammatory mediators sensitize TRPV1 function by various mechanisms: they may increase TRPV1 expression levels in the membrane [54,55] induce TRPV1 phosphorylation by protein kinases [56] or release the inhibition of TRPV1 by phosphatidylinositol 4,5-bisphosphate, which render the channel more responsive to agonist stimulation [57]. In addition, these inflammatory mediators act on receptors that are coupled to G proteins or tyrosine kinase pathways thus activating PLC and/or PLA2 which, in turn, induce the release of arachidonic acid metabolites. Several amide derivatives of arachidonic acid (anandamide) and lipoxygenase products of arachidonic acid, such as 12-(S)-HPETE, are agonists of TRPV1 and therefore are candidates for endogenous capsaicin like substances [58]. In addition to inflammatory mediators, proteases released during inflammation or nerve injury, such as trypsin and mast cell tryptase, can also sensitize TRPV1. These proteases cleave the protease activated receptor 2 (PAR2) to sensitize TRPV1 to induce thermal hyperalgesia through PKA and PKCε second messenger pathways [59,60]. These findings demonstrate that TRPV1 not only participates in pain evoked by chemical and moderate heat but that TRPV1 contributes to peripheral sensitization, acting as the final substrate for multiple inflammatory mediators that operate *via* distinct intracellular signaling pathways.

TRPV4 channel is a polymodal receptor with a wide expression pattern and a corresponding variety of physiological roles [61]. TRPV4 is widely expressed on nervous and non-nervous organs, tissues and cells, including urinary bladder, kidney, vascular

endothelium, keratinocytes, cochlear hair cells, and Merkel cells [62-64]. TRPV4 activation on sensory neurons, TG and DRG neurons [65] causes SP and CGRP release, thus evoking neurogenic inflammation in peripheral tissues [66]. TRPV4 was firstly identified as an osmo-transducer activated by decrease in osmolarity, suggesting a role in the regulation of cell swelling [61,67]. Later studies demonstrated that TRPV4 is activated by shear stress [68], innocuous warmth (27-35 °C) [65,69], low pH, citrate [64], endocannabinoids and arachidonic acid (AA) metabolites [27,70], NO[48] and synthetic selective agonists, such as the phorbol ester 4α-phorbol 12,13-didecanoate (4α-PDD) [69]. The mechanosensitive nature of TRPV4 and its implication in sensing shear stress suggest a role in flow-sensitive cells, such as vascular endothelial and renal tubular epithelial cells. The mechanism through which TRPV4 is activated by mechanical stress is still under debate. Two transduction pathways have been proposed to regulate TRPV4 activation: the PLC/diacylglycerol (DAG) pathway and the PLA2/ AA pathway [71,72]. Some evidence suggests that activation of TRPV4 by hypotonicity involves its phosphorylation by Src family of tyrosine kinase [73]. Although the molecular mechanism of hypotonicity-induced TRPV4 activation should be further investigated, studies addressing the gating mechanism of the channel by cell swelling exclude that it is directly gated by mechanotransduction since it does not respond to membrane stretch [67]. It was shown that hypotonicity becomes painful to the animals when nociceptive fibers are sensitized by the PGE2, whose levels increase during inflammation or in response to mechanical, chemical and thermal injury. TRPV4 also plays a crucial role in mechanical hyperalgesia elicited by exposure to inflammatory mediators. Indeed, PGE2 and serotonin, can act synergistically through cAMP/PKA and PKCε to engage TRPV4 in hyperalgesia to mechanical and osmotic stimuli [74]. In addition, PAR2 agonists may sensitize TRPV4 through the activation of multiple second messenger pathways, such as PKA, PKC, PKD, PLCβ [66]. Proteases generated during inflammation activate PAR2 thus leading to TRPV4-mediated release of SP and CGRP in the spinal cord and TRPV4-induced mechanical hyperalgesia [75].

1.4.4 The TRPM subfamily

Members of the TRPM family fall into three subgroups on the basis of sequence homology: TRPM1/3, TRPM4/5, and TRPM6/7, with TRPM2 and TRPM8 representing structurally distinct channels. In contrast to TRPCs and TRPVs, TRPMs do not contain ankyrin repeats within their NH_2-terminal domain. TRPM channels exhibit highly variable permeability to Ca^{2+} and Mg^{2+}, ranging from Ca^{2+} impermeable (TRPM4 and

TRPM5) to highly Ca^{2+} and Mg^{2+} permeable (TRPM6, TRPM7 and specific splice variants of TRPM3).

1.4.5 The TRPML subfamily

The TRPML family consists of three mammalian members (TRPML1–3) that are relatively small proteins consisting of ~600 amino acid residues. TRPML1 is widely expressed and appears to reside in late endosomes/lysosomes. Recently, TRPML1 has been described as a H^+ channel that may act as a H^+ leak in lysosomes preventing over acidification in these organelles [76].

1.4.6 The TRPP subfamily

The TRPP family is very heterogeneous and can be divided, on structurally criteria, into PKD1-like (TRPP1-like) and PKD2-like (TRPP2-like) proteins. PKD1-like members comprise TRPP1 (previously termed PKD1), PKDREJ, PKD1L1, PKD1L2, and PKD1L3. TRPP1 consists of 11 transmembrane domains, a very longand complex ~3,000 amino acid extracellular domain, and an intracellular COOH-terminal domain that interacts with the COOH-terminal of TRPP2 through a coiled-coil domain. The PKD2-like members structurally resemble other TRP channels. There is considerable evidence that TRPP1 and TRPP2 physically couple to act as a signaling complex at the plasma membrane to which TRPP2 is recruited by TRPP1 [77].

1.4.7 The TRPA subfamily

The TRPA family currently comprises one mammalian member, TRPA1, which is expressed in DRG and TG neurons and in hair cells [78,79]. TRPA1 consists of at least 14 N-terminal ankyrin repeat domain (ARD), an unusual structural feature that may be relevant to the proposed role of the channel as a mechanosensor. TRPA1 receptor is activated by various stimuli including exogenous (natural compound) but also endogenous compound. TRPN is a channel that is closely homologous to TRPA1. It is characterized by 29 ankyrin repeats within the N-terminus. To date, this subfamily comprises only one member in *C. elegans*, *Drosophila*, and zebrafish. TRPN1 probably acts as a mechanotransduction channel that is involved in hearing. Currently available genome information indicates that mammals have no TRPN orthologs.

1.5 The TRPA1 channel

TRPA1 is the only member of the ankyrin subfamily found in mammals. This receptor was originally cloned from human pulmonary fibroblasts [80], and was found selectively expressed in a subpopulation of unmyelinated nociceptors that also express the capsaicin receptor TRPV1, suggesting a significant role in nociception [28,79,81]. The TRPA1 is a non-selective cation channel permeable to both monovalent and divalent ions, including Ca^{2+}, Na^{+}, K^{+}. TRPA1 has a high Ca^{2+} permeability compared to most other TRP channels and a unitary conductance ~70 pS to ~110 pS in the inward and outward directions, respectively, under physiological conditions when the channel is constitutively open [82,83]). In presence of TRPA1 activators the pore of the channel, with a size of 11.0 Å, can undergo dilation increasing Ca^{2+} permeability and allowing larger charged molecules to pass through the channel [84,85].

Like all other TRP proteins, TRPA1 has six predicted transmembrane domains (S1-S6), a pore loop between S5 and S6 and the N- and C-termini located intracellulary. Although there is no apparent voltage sensor in S4, as shown for voltage-gated K^{+} channels, TRPA1 displays some voltage dependency although less pronounced compared to TRPM8 and TRPV1 [86,87]. A distinguish features of TRPA1 receptor is its long N-terminus with 14 to 18 ankyrin repeats which are important for protein-protein interactions and insertion of the channel into the plasma membrane [88] (Figure 5 a,b). The N-terminus contains a large numbers of cysteine residues, some of which can form a network of protein disulfide bridges within or between monomers [89] (Figure 5 c). N-terminal cysteine and lysine residues are key targets for electrophilic TRPA1 activators, but cysteines outside the N-terminus region may also contribute to channel gating [89]. Furthermore, the potent TRPA1 activator Zn^{2+} may bind to cysteine and histidine residues in the C-terminus [90,91]. The N- and C-termini have been suggested to contain binding sites for Ca^{2+} that can both sensitize or desensitize TRPA1 [81,92,93]. Ca^{2+} strikingly modulates TRPA1 activity. Indeed micromolar intracellular Ca^{2+} concentrations ($[Ca^{2+}]_i$) activate TRPA1, and also elevation of extracellular Ca^{2+} concentration can transiently increase the channel activity. It has been suggested that activation may depend on Ca^{2+} binding to an N-terminal EF-hand motif [94,95]. The putative EF-hand motif involved in $[Ca^{2+}]_i$-dependent activation of TRPA1 is located between ARD11 and ARD12 [94,95] (Figure 5 a,b). The importance of this EF-hand site is questionable, since point mutations in this region have only modest effects on $[Ca^{2+}]_i$-dependent activation mechanism, while deletions impair trafficking of the truncated channel to the plasma membrane [82]. Another putative Ca^{2+}-binding domain is composed of a cluster of acidic residues in the distal C-terminus of TRPA1 [93]. Four

conserved residues in human TRPA1, Glu1077, Asp1080, Asp1081 and Asp1082, have strong effects on the Ca^{2+}- and voltage-dependent potentiation and/or inactivation of agonist-induced responses. Truncation of the C-terminus by only 20 residues selectively slowed down the Ca^{2+}-dependent inactivation without affecting other functional parameters. The only direct structural insights on TRPA1 channel are those available from a 16 Å resolution structure of purified, amphipol-stabilized, TRPA1 proteins analyzed by single-particle electron microscopy [96]. This structural model suggests that the critical N-terminal cysteine residues involved in electrophilic activation are located at the interface between neighboring subunits and form a ligand-binding pocket, allowing disulfide bonding between the cysteine residues [89]. Covalent modifications by thiol-reactive compounds within such pockets may alter interactions between subunits and promote conformational changes that translate to modification of the gating mechanism [89,96].

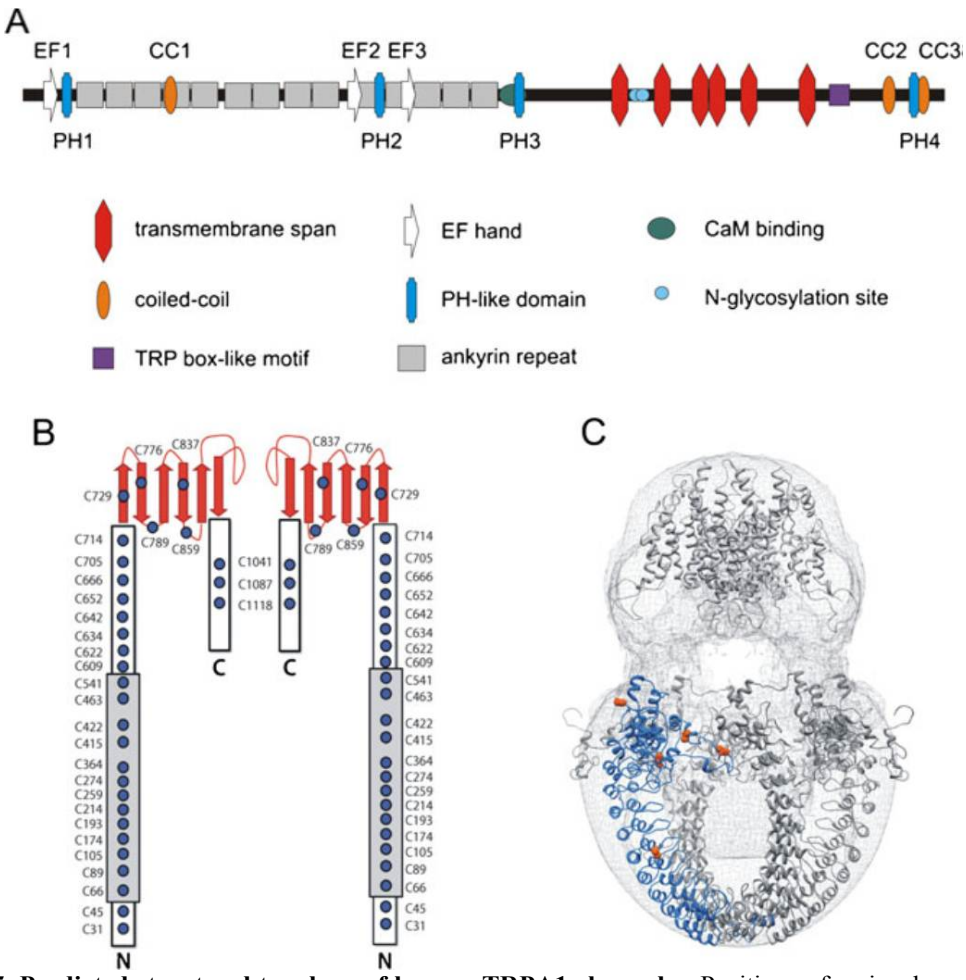

Figure 5. Predicted structural topology of human TRPA1 channel. **a** Positions of major domains and motifs are annotated. **b** Schematic representation of a TRPA1 dimer with annotations of all 31 cysteine residues (blue circles). The position of ankyrin repeat domains is represented by a gray box. **c** Reconstruction of electron microscopy density and N-terminal model of TRPA1 (blue ribbon). The cysteines involved in disulfide bonding are displayed in orange (adapted from Cvetkov, 2011; Nilius 2011).

1.5.1 Localization of TRPA1 channel

Shortly after the identification of TRPA1 receptor in human pulmonary fibroblast [80]and in hairy cells of the auditory system [78] abundant expression of TRPA1 have been localized in a subpopulation of peptidergic primary sensory neurons (with C and Aδ fibers) where it signals nociceptive/painful responses. TRPA1-expressing neurons contain and release the neuropeptides, SP, NKA and CGRP. TRPA1 is mostly found in a subpopulation of TRPV1-positive neurons, but non-TRPV1-containig neurons expressing TRPA1 also exist, including a small population of myelinated Aβ-fibers, which are activated by innocuous mechanical force [97]. By using radial stretch in combination with live-cell calcium imaging different mechano-sensitive or -insensitive sensory neuronal categories were identified [98]. A group of small-diameter stretch-sensitive cells could be further subdivided in a cluster of small-diameter cells, sensitive to hydroxy-α-sanshool (a two pore K^+ channel antagonist) and the TRPV1 agonist, capsaicin, and a second one which comprises large-diameter cells that respond to hydroxy-α-sanshool, but not capsaicin. The former neuron type likely corresponds to high threshold nociceptors and the latter to low threshold proprioceptors. Moreover, stretch insensitive neurons fall into two groups of small-diameter cells. A first group is composed by petidergic neurons sensitive to capsaicin and to the TRPA1 selective agonist, mustard oil, and a second group by a small cohort of menthol-sensitive cells [98]. Thus, TRPA1 expressing neurons which obligatory co-express TRPV1, are those apparently insensitive to mechanical stimulation and that, because they contain neuropeptides, bring about neurogenic inflammation.

More recently extraneuronal localization of TRPA1 has been identified. TRPA1 activation inhibited the repair of the epithelial wound in the stomach, probably by the suppression of cell migration, and suggested the involvement of TRPA1 in the mechanism of gastric epithelial restitution [99]. TRPA1, highly expressed in the bladder epithelium, might be involved in the bladder sensory transduction and the induction process of overactive bladder by bladder outlet obstruction [100].

TRPA1 has been proposed to contribute to different airway inflammatory diseases, including chronic cough, asthma and chronic obstructive pulmonary diseases (COPD) by activating neurogenic and non-neurogenic inflammatory responses. TRPA1 has been detected in non-neuronal airway cells (human small cell lung cancer cells, fibroblasts, epithelial cells and smooth muscle cells) where by increasing intracellular Ca2+ releases proinflammatory cytokines, such as interleukin-8 [101], prevents apoptosis and promotes cell survival, via an extracellular-signal regulated kinases (ERK1/2)-dependent pathway and favors detrimental processes in epithelial airway cells taken from cystic fibrosis

patients. Neurogenic and non-neurogenic inflammatory responses to cigarette smoke, allergen [102] or NAPQI were found to be attenuated by TRPA1 inhibition.

The localization of TRPA1 to nerves that also express TRPV1 and CGRP, and in urothelial cells and interstitial cells, as well as the findings that TRPA1 agonists can modify tone of human urethral preparations, propose a role for TRPA1 in afferent and efferent sensory signaling of the human outflow region [103]. TRPA1 is highly expressed in rat enterochromaffin cells (EC), and TRPA1 agonists, including allyl isothiocyanate and cinnamaldehyde, stimulate EC cell functions, such as increasing intracellular Ca^{2+} levels and 5-HT release. By this mechanism TRPA1 regulates intestinal motility [104]. Finally, and more importantly for the present research proposal there is evidence that TRPA1 expressed in endothelial cells of rat cerebral vessels regulates vascular tone by nitric oxide (NO)- and cyclooxygenase-independent pathways [105]. The relaxing mechanism activated by TRPA1 agonists is mediated by endothelial cell Ca^{2+}-activated K^+ channels and inwardly rectifying K^+ channels in arterial myocytes [105]. TRPA1 is found in melanocytes, mast cells, fibroblasts, odontoblasts [106-109].

1.5.2 TRPA1: more than just a spice receptor

Many different stimuli have been reported to either directly or indirectly activate the TRPA1 receptor channels, including cold, mechanical displacement and exogenous pungent compound and irritants, bradykinin and other endogenous proalgesic agents.

TRPA1 and thermosensation. The molecular basis of thermosensation has made great strides with the discovery that several members belonging to the TRP channel family exhibit highly temperature-sensitive gating and are expressed in cells of the sensory system. Among the TRP channels expressed in sensory neurons, TRPM8, activated by cold temperatures and cooling compounds, such as menthol, plays a major role in cold sensing [110]. TRPA1 was originally reported to be a potential candidate to mediate detection of noxious cold, based on its expression in nociceptive neurons, and on the finding that heterologously expressed TRPA1 in CHO cells is activated by cold temperatures with a lower temperature threshold for activation than TRPM8 [79]. Whether or not TRPA1 is a noxious cold sensor, via either direct or indirect mechanism, is not well explained. On one hand, some studies have shown that when TRPA1 is expressed in heterologous systems, human embryonic kidney (HEK) cells or chinese hamster ovary (CHO) cells, it is activated by cold temperatures, ~17 °C and below that are in the noxious range [79,111,112]. Alternatively, other studies have shown that exogenously expressed TRPA1 is not activated by noxious cold [78,81,113]. A more recently report suggests that cold-

induced activation of TRPA1 in overexpression systems is an indirect effect caused by Ca^{2+} release from intracellular stores by a direct activation of the receptor, mediated by intracellular Ca^{2+}, via an EF-hand domain in its N-terminus domain [95]. These contradictory findings appear to have been resolved by subsequent work, where TRPA1 null mice were still able to sense cold, but that also indicated that the behavioral response to noxious cold was significantly reduced in the absence of TRPA1 [114].Furthermore, mice in which $Na_V1.8$-expressing sensory neurons were eliminated by diphtheria toxin A exhibit a strongly reduced expression of TRPA1 in DRG neurons and lack TRPA1-mediated nociceptive responses to formalin and cold [115]. Thus, noxious cold sensing *in vivo* requires somatosensory neurons that express both $Na_V1.8$ and TRPA1.

TRPA1 and mechanotransduction. TRPA1 receptor has also been proposed to be involved in mechanotransduction adding further diversity to its potential physiological roles. Mice with a deletion of the pore domain of TRPA1 exhibit decreased behavioral responses to intense mechanical force in the noxious range [116], although behavioral deficits to mechanical stimuli were not observed in a similar TRPA1 mutant mouse [117]. A small molecule inhibitor of TRPA1 reverses mechanical hyperalgesia induced by inflammation in mice [118]. No cellular studies have provided clear evidence that TRPA1 is directly gated by mechanical force, although a recent study shows that heterologously-expressed TRPA1 is activated by hypertonic saline, suggesting that TRPA1 is sensitive to osmotic stimuli [119]. However, it should be noted that the nature of osmotic stimuli and how it activates channels in a cell membrane may differ substantially from that of punctuate mechanical force applied to a localized region of the neuronal membrane.

TRPA1 and chemical irritants. The TRPA1 channel is best characterized as a chemosensor activated in response to many chemical agents, produced by plants or some synthetic that cause neurogenic inflammation and pain. It has been established that TRPA1 acts as a detector of thiol-reactive electrophiles and oxidants in addition to non-electrophiles compounds as well as being indirectly regulated by G-protein coupled receptor signaling.

Electrophilic activators. Electrophilic TRPA1 ligands of environmental-, dietary- or endogenous origin modify nucleophilic cysteine and lysine residue(s) in the N-terminus of the channel [120]. Allyl isothiocyanate (AITC) from mustard oil is one of the most efficient electrophilic activators of TRPA1 (Figure 6a). In human TRPA1, electrophilic agonists modify cysteines Cys619, Cys639 and Cys663 (and to a lesser extent K708) [121]. In the mouse TRPA1 homologue the most reactive cysteine residues are Cys415 and Cys422 and Cys622 [122]. Other electrophiles, such as methyl-, isopropyl-, benzyl-, phenylethyl-isothiocyanate, cinnamaldehyde (in cinnamon), iodoacetamide, and 2-

(trimethylammonium) ethyl methane-thiosulfonate bromide (MTSEA; used for cysteine scanning), are capable of reacting with cysteine residues and act as TRPA1 activators [28,81] (Figure 6a).

TRPA1 has been also recognized as the target of a series of endogenous α,β-unsaturated aldehydes, which are produced by lipid peroxidation in response to oxydative stress at sites of inflammation and tissue injury [47,117,123] (Figure 6a). These aldehydes include 4-hydroxy-2-nonenal (4-HNE) which is produced by peroxidation of omega 6-polyunsaturated fatty acids, such as linoleic acid and arachidonic acid [124,125] or 4-oxononenal [126] that has been reported to cause nociceptive behavior via a selective action at TRPA1. 4-HNE is an α,β-unsaturated hydroxyalkenal which is produced in inflammed tissues during peroxidation of membrane phospholipids by reactive oxygen species (ROS). It evokes release of SP and CGRP from nerve endings, causing extravasations of plasma proteins into the surrounding tissue. 4-HNE acts via covalent modification of the cysteine/lysine residues in the TRPA1 N-terminus [123]. More recently, mediators of oxidative and nitrative stress have been identified as activators of the TRPA1 channel. These include the ROS hydrogen peroxide (H_2O_2) [112,127,128], superoxide (O^{2-}), hypochlorite (ClO^-) [128] and the reactive nitrative species (RNS) peroxynitrite ($ONOO^-$) [112]. Nitrooleic acid, a byproduct nitrative stress, is a TRPA1 activator [129]. It has been reported that ROS cause cysteine oxidation or disulfide formation, RNS, like nitric oxide (NO), mediate S-nitrosylation, and reactive carbonyl species (RCS), like electrophilic prostaglandins (PG) and α,β-unsaturated aldehyde, alkylatively modify cysteine activating TRPA1. Cyclopentenone PGs have been reported to produce pain and neurogenic inflammation by TRPA1 stimulation [130,131]. Moreover, the cyclopentenone isoprostane (IP), 8-iso-PGA2, which forms from E-isoprostane that does not require for its synthesis activation of cyclooxygenases, stimulates sensory nerve terminals by targeting TRPA1 [130]. Altogether these findings suggest that TRPA1 is an unspecific sensor for a plethora of stimuli (exogenous and metabolites generated by both oxidative and nitrative stress), that use the TRPA1 channel to alert of inflammation and tissue injury.

Hydrogen sulfide (H_2S), a RNS, is a malodorous gas that functions as an endogenous gasotransmitter in humans and is involved in a wide variety of processes including nociceptive processes [132]. H_2S evokes CGRP release from sensory neurons of isolated rat tracheae through TRPA1 activation.

It has been reported that high concentrations of carbon dioxide (CO_2) evoke a stinging sensation that depends on the activation TG nociceptors that express TRPA1 and innervate the respiratory, nasal, and oral epithelia. CO_2 diffuses into cells and produce

intracellular acidification thereby gating TRPA1 [133]. Alkaline pH also causes pain via activation of TRPA1. Two N-terminal residues, Cys422 and Cys622, are responsible for high pH perception. Pain behaviors evoked by intraplantar injection of ammonium chloride are completely reduced in TRPA1$^{-/-}$ mice [134].

N-acetyl-p-benzoquinoneimine (NAPQI), the metabolite of N-Acetyl-p-aminophenol (paracetamol, acetaminophen, APAP) is another example of TRPA1 electophilic agonist. NAPQI, like other TRPA1 activators, stimulates TRPA1 causing airway neurogenic inflammation. These inflammatory responses evoked by NAPQI can be abolished by TRPA1 antagonists [135].

Although it is now generally accepted that TRPA1 is activated through covalent modification of specific cysteines, the precise mechanism and the chemistry of this covalent modification with unsaturated carbonyl-containing compounds is unclear. Channel activation occurs with chemicals that react with cysteine residues via alkylative conjugate addition [136], but unravelling of the molecular details underlying activation and deactivation of TRPA1 *via* covalent modifications remains an exciting challenge. TRPA1 electrophilic agonists, that are structurally different, are unified in their ability to form covalent adduct with thiol group, a moiety that confers them the ability to activate TRPA1 receptor. A variety of known TRPA1 agonists, including acrolein and other α,β-unsaturated aldehydes, possess an electrophilic carbon or sulphur atom that is subject to nucleophilic attack (Michael addition) [137] by cysteine, lysine or histidine of TRPA1. Indeed, mutagenesis studies have clarified that such reactivity promotes channel gating through covalent modification of residues within the cytoplasmic N-terminal domain of the channel [121-123]. In human TRPA1, crucial residues for channel activation by AITC include a cluster of cysteines (Cys619, Cys639 and Cys663) and Lys708 [121]. The ability to form Michael adducts with cysteine is virtually shared by all α,β-unsaturated aldehydes, including the highly electrophilic compound, 4-oxononenal [126].

Non-electrophilic activators. Beside the huge number of electrophilic activators, TRPA1 can also be modulated by other compounds that are unlikely to induce covalent modifications of the channel proteins. Anesthetic agents can induce an activation and sensitization of TRPA1. Propofol (2,6-diisopropylphenol), a commonly used intravenous anesthetic, elicits intense pain upon injection *via* TRPA1 activation [138]. Lidocaine, inhibits cellular excitability by blocking voltage-gated Na^+ channels, but can activate TRPA1 in a concentration-dependent manner. Lidocaine can also act as an inhibitor of TRPA1, an effect more evident with rodent than human TRPA1. This species-specific difference is probably linked to the pore region (S5 and S6) [139]. Fenamate nonsteroidal anti-inflammatory drugs (NSAIDs) can also activate and sensitize TRPA1. Several non-

electrophilic NSAIDs, including flufenamic, niflumic, and mefenamic acid, as well as flurbiprofen, ketoprofen, diclofenac, and indomethacin, reversibly activate TRPA1.

TRPA1 is a non-covalent sensor of polyunsaturated fatty acids (PUFAs), which contain at least 18 carbon atoms and three unsaturated bonds. Those PUFAs activate TRPA1 to excite primary sensory neurons and enteroendocrine cells. They act non-covalently binding domains located in the N-terminus [140].

Many non-covalent modulators of TRPA1 function in a bimodal fashion, i.e. they activate the channel at low concentration, and inhibit it at higher concentrations. Menthol from *Mentha piperita*, a known TRPM8 activator, is also a bimodal modulator of TRPA1. Low-micromolar concentrations of menthol cause channel activation, whereas higher concentrations lead to a reversible channel inactivation [141]. This is only true for human TRPA1, indeed mouse TRPA1 is blocked by menthol. Similarly, to menthol, the super-cooling synthetic compound icilin activates not only TRPM8 as but also TRPA1 [142,143].

Another non-electophilic TRPA1 agonist is caffeine from *Coffea Arabica*. This compound activates mouse TRPA1 but suppresses its human version. Similarly, nicotine from *Nicotinia tabacum* or its analogue, anabasin from *Nicotiana glauca*, are bimodal TRPA1 modulators. Topical application of nicotine causes irritation of the mucosa and skin due to TRPA1 activation. In contrast, higher concentrations inhibit the channel.

Zinc, an essential biological trace element, is required for the structure or function of over 300 proteins. High concentrations of zinc have cytotoxic effects and can cause pain and inflammation. Surprisingly, zinc activates TRPA1 through a unique mechanism that requires zinc influx through TRPA1 channels and subsequent activation via specific intracellular cysteine and histidine residues. TRPA1 is highly sensitive to intracellular zinc, as low nanomolar concentrations activate TRPA1 and modulate its sensitivity [144].

TRPA1 is also activated by Δ9THC, the psychoactive compound in marijuana. Also, two non-psychoactive cannabinoids, cannabidiol (CBD) and cannabichromene (CBC), are known to modulate TRPA1.

Many TRP channels are activated or modulated downstream of neurotransmitter or growth-factor receptors that stimulate PLC (Figure 6b). *In vitro* studies have shown that TRPA1 can be activated in this manner, raising the possibility that it functions as a ‘‘receptor-operated’’ channel that depolarizes nociceptors in response to proalgesic or proinflammatory agents that activate PLC [111]. One such agent is bradykinin (BK), a proalgesic and proinflammatory nonapeptide produced endogenously in response to tissue injury, inflammation, or ischemia, which binds to PLC coupled bradykinin receptors (BK2) on sensory neurons [145]. BK elicits acute pain through immediate excitation of nociceptors, followed by a longer lasting sensitization to thermal and

mechanical stimuli [146]. Indeed, mice with a mutation in TRPA1 did not develop hyperalgesia after exposure to BK [117]. More interestingly, there are many other proalgesic and proinflammatory agents that activate the PLC pathway, suggesting that may exert they action via TRPA1 receptor [81]. Finally, TRPA1 appears to be sensitized by NGF and PAR2 [147,148] both of which are known to play a role in inflammatory pain.

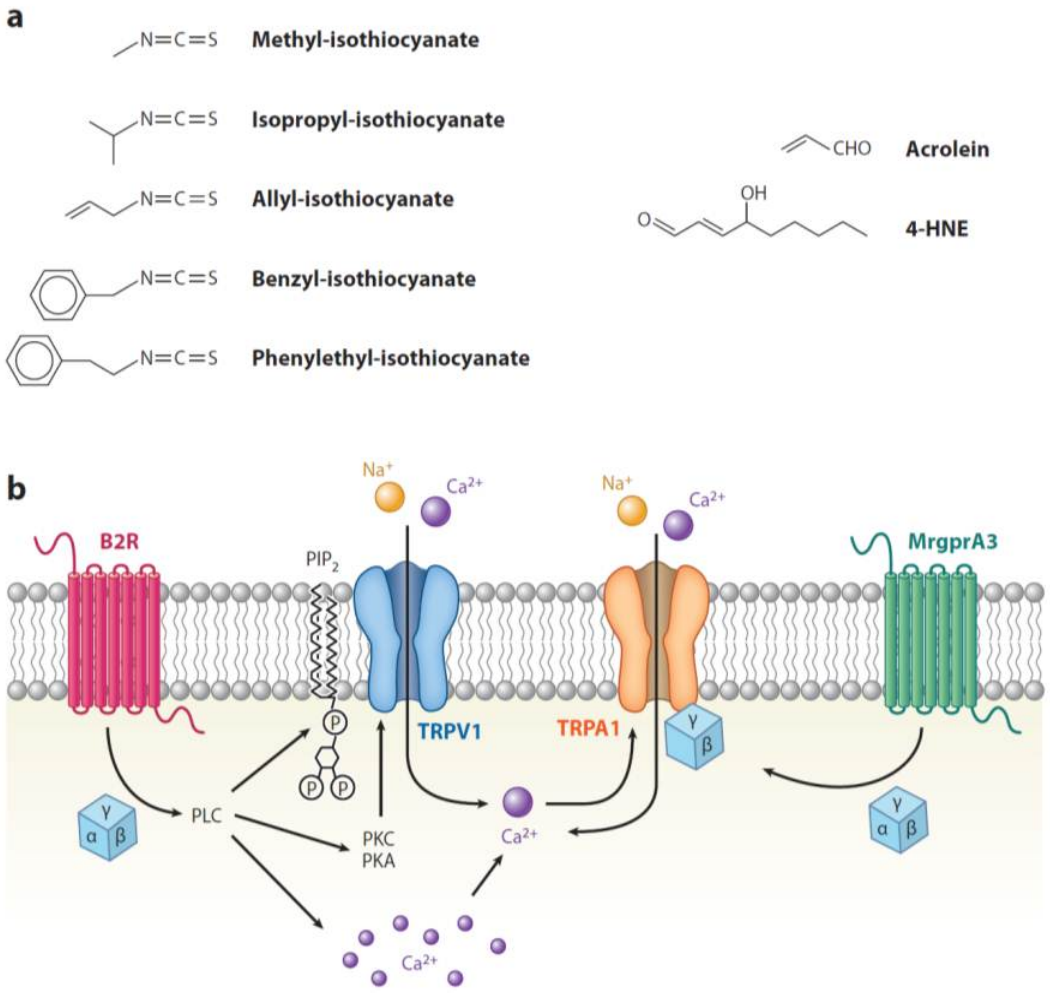

Figure 6. TRPA1, is a detector of chemical irritants. a A variety of compounds activate TRPA1, including exogenous irritants and endogenous products of tissue injury and inflammation. The agents shown here include isothiocyanates and α,β-unsaturated aldehydes, both of which exhibit strong electrophilic reactivity as the functional attribute underlying their ability to activate TRPA1 channels. **b** In addition to direct activation by electrophilic irritants, TRPA1 functions as a receptor-operated channel that can be activated or sensitized by G protein-coupled signaling pathways. Two such mechanisms have been proposed: (i) A GPCR, such as the B2R bradykinin receptor, activates phospholipase C (PLC) to mobilize release of intracellular calcium. Increased cytoplasmic calcium then activates TRPA1. (ii) Activation of a GPCR, such as the MrgprA3 puritogen receptor, promotes the release of free Gβγ, which serves as the downstream cytoplasmic activator of TRPA1. In addition to these proposed mechanisms, TRPA1 can be activated or sensitized by other events that enhance cytoplasmic calcium levels, such as activation of TRPV1 or other calcium-permeable channels. (Adapted from Julius, 2013).

1.5.3 Pharmacology of TRPA1 receptor

In addition to various pain-producing chemicals described as TRPA1 agonists, some molecules have been studied as TRPA1 receptor antagonist: ruthenium red, gentamicin, gadolinium and amiloride. Ruthenium red and gentamicin are very similar,

both are pore blockers that plug into the channel pore, and differ from amiloride and gadolinium, that block by interacting with an extracellular site of the channel that is outside of the electric field of the pore [78]. However, each of these antagonists also blocks other type of TRP channels, as well as other ion channels. More recently has been identified a TRPA1 selective antagonist, HC-030031[149]. The first pharmacological evidence implicating the TRPA1 receptor in mediating pain under inflammatory conditions came from the discovery of this new molecule. Indeed, HC-030031 has been a key compound to determine the role of the channel in the first and second phase of the nociceptive and inflammatory response to formaldehyde [149]. Further studies showed that HC-030031 reduced somatic and visceral nociceptive response [150] or BK-induced mechanical hyperalgesia [118]. Along with TRPA1 deficient mice, this antagonist is currently being used to identify novel roles of TRPA1 in health and disease. Additional TRPA1 antagonists have been more recently identified, including AP18 [118]and Chembridge5861528 [151]. AP18 is a small molecule that blocks TRPA1 through a competitive mechanism displacing the receptor agonists from the binding site. The *in vivo* analgesic activity of AP18 was tested in well-established animal models of inflammation, such as the complete Freund adjuvant (CFA) and the bradykinin-induced mechanical hyperalgesia [118]. Moreover, AP18 is a selective TRPA1 antagonist that inhibits both the mouse and human receptor. Chembridge5861528 is an analogue of HC-030031 and has been shown to display mechanical anti-hyperalgesic activity in vivo in diabetic mice [151].

1.6 TRPA1 and Neuropathic Pain

Neuropathic pain is dependent from a damage or dysfunction of the nervous system and is most frequently due to peripheral nerve injury. The involvement of TRPA1 in different patterns of neuropathic pain has been proposed by recent results obtained in different animal models. Growing evidence is robustly building up the hypothesis that TRPA1 plays a major role in the hypersensitivity to chemical, thermal and mechanical stimuli, which characterizes a variety of models of neuropathic pain, such as nerve injury, diabetic neuropathy, and neuropathy induced by some chemotherapeutic agents (CIPN). Supporting data have been obtained by using both pharmacological and genetic tools.

1.6.1 Chemotherapy-induced peripheral neuropathy

Chemotherapy-induced peripheral neuropathy (CIPN) is a potentially dose limiting side effect of commonly used chemotherapeutic agents like taxanes, vinca-alkaloids,

platinum compounds, bortezomib and thalidomide. Symptoms are predominantly sensory, ranging from a mild tingling sensation to spontaneous burning pain and hypersensitivity to stimuli. These symptoms often affect both hands and feet and may spread into a "glove and stocking" distribution. Sometimes there are motor symptoms like weakness, autonomic neuropathy and incidentally cranial nerve involvement. CIPN leads to a lower quality of life and often causes patients to discontinue chemotherapy [152]. The incidence of CIPN depends on the dose, mainly cumulative, the type of agent, and concomitant use of other neurotoxic agents. Moreover, the development of chemotherapy side effects may be influenced by the age of the patients and preexisting conditions that potentially cause nerve damages, such as diabetes and use of alcohol [152]. CIPN can begin weeks to months after initial treatment and reach a peak at, or after, the end of treatment and it is most frequently associated with axonal degeneration. Usually, this axonopathy occurs weeks to months after exposure to the medication, may continue despite withdrawal of the drug, and may be irreversible. If the degree of axonal degeneration is mild, then complete regeneration may occur. However, if there is injury to the dorsal root ganglion resulting in neuronal apoptosis, then the sensory neuropathy is severe and usually irreversible [153]. The toxic effects of chemotherapy target the structures and functions of the peripheral nervous system, including neuronal cell bodies, axons, myelin sheath, and supporting glial cells. Most toxic neuropathies affect axons, resulting in an axonopathy and causing distal, symmetric, sensory-predominant neuropathy that exhibits a "dying-back" pattern. The most distal portions of axons are usually the first that undergo degeneration, and axonal atrophy advances slowly towards the cell body. These effects lead to sensory disturbances with a symmetrical "glove and stocking" distribution. In its most severe form, it will lead to wallerian (or secondary) degeneration of the surrounding nerve sheath (i.e., demyelination) distal to the injury. Neuronal cell body damage results in neuronopathies and manifests as global nerve failure. Patients will first notice paresthesias, pain, or both, in the toes and feet that with time and continued insult will advance proximally. By the time the fingertips are affected, a tear-drop pattern of sensory loss and dysesthesias appears the abdominal wall, and sensory distortion will have migrated proximally up the leg, approaching or passing the knee. Myalgias are another presentation of neuropathic pain, and patients complain of muscle cramps and aching that are frequently exacerbated by activity. Chemically different chemotherapeutic agents with different anticancer mechanisms, however, share the common ability to induce CIPN. These include platinum-based compounds (*e.g.,* cisplatin and oxaliplatin), taxanes (*e.g.,* paclitaxel), vinca alkaloids (*e.g.,* vincristine), and the first-in-class proteasome inhibitor, bortezomib.

The ability to produce oxidative stress is considered an additional and collective property of chemotherapeutic agents that, if from one hand contributes to their anticancer action, on the other hand seems to be responsible for major adverse reactions, including CIPN. In line with this assumption, it has been reported that oxaliplatin-induced mechanical hyperalgesia and heat- and cold-evoked allodynia in rats are attenuated by antioxidants, including acetyl-L-carnitine, α-lipoic acid or vitamin C, suggesting the contribution of oxidative stress to these painful conditions [154]. Clinical trials have shown some benefits of antioxidant agents in CIPN [155], although further confirmatory investigation is required in this field of investigation. A series of mechanisms has been advocated to explain CIPN, however, the pathway(s) underlying the neuronal hyperexcitability and pain remains unrecognized. In recent years, much attention has been paid to the peculiar interactions of chemotherapeutic agents with ion channels located on the membrane of the sensory nerve fibres. Voltage sensitive channels, and more recently TRP channels, have been the object of intense investigation, mainly because of their prevalent localization in nociceptors. The first report of the involvement of a TRP channel in a rodent model of CIPN was obtained by studying cisplatin. Paradoxically, TRPV1 was found to protect against mechanical allodynia, because channel deletion worsened cisplatin-induced neurotoxicity [156]. Due to its primary localization to sensory neurons, and its nociceptive role as a sensor of oxidative stress [128], TRPA1 nociceptive results to be perfectly suited to contribute to CIPN.

TRPA1 contribution to mechanical hypersensitivity does not seem confined to oxaliplatin, as TRPA1-deficient mice also developed a much-reduced mechanical allodynia after administration of the closely related drug, cisplatin. This early series of events may occur rapidly after oxaliplatin administration, but there is indirect evidence that oxidative stress may last for days after exposure to oxaliplatin. In fact, the antioxidants, acetyl L-carnitine, α-lipoic acid, and vitamin C profoundly reduced oxaliplatin-evoked mechanical hyperalgesia when given on the fifth day after oxaliplatin administration [154]. The role of TRPA1 in models of CIPN, although prevalent, does not seem exclusive. In a mouse model of neuropathy induced by paclitaxel, mechanical hyperalgesia derives in part from the activation of the TRPV4 channel [74]. However, both cold allodynia and the TRPV4-resistant mechanical hyperalgesia evoked by paclitaxel are entirely mediated by TRPA1 [157].

Platinum-derived drugs, paclitaxel, or bortezomib do not directly target TRPA1 and there is evidence that cisplatin and oxaliplatin gate the channel by producing ROS, most likely from cells other than primary sensory neurons [158]. Hypersensitivity, when established, is totally although transiently reverted by the antioxidant, α-lipoic acid or the TRPA1

antagonist, HC-030031 [158,159]. However, hypersensitivity was completely absent if chemotherapeutic agents were administered to TRPA1 deleted mice [158,159]. This finding implies that TRPA1 is necessary and sufficient for establishing a prolonged (10 days) hypersensitivity condition. Treatment with oxaliplatin or bortezomib transiently (1-6 hours) increased plasma concentrations of a marker of oxidative stress [159], suggesting that both events (increased oxidative stress and its ability to target TRPA1) are required to establish the hypersensitivity condition.

1.6.2 Third-generation aromatase inhibitors-induced painful states

Third-generation aromatase inhibitors (AIs) are currently recommended for adjuvant endocrine treatment as primary, sequential, or extended therapy with tamoxifen, for postmenopausal women diagnosed with estrogen receptor-positive breast cancer [96,160,161]. Estrogen is the main hormone involved in the development and growth of breast tumors; oophorectomy was first shown to cause regression of advanced breast cancer, and estrogen deprivation remains a key therapeutic approach. Tamoxifen inhibits the growth of breast tumors by competitive antagonism of estrogen at its receptor site. Its actions are complex and it also has partial estrogen-agonist effects. These partial agonist effects can be beneficial, since they may help prevent bone demineralization in postmenopausal women, but also detrimental, since they are associated with increased risks of uterine cancer and thromboembolism. In addition, they may play a part in the development of tamoxifen resistance. In contrast, AIs markedly suppress plasma estrogen levels in post-menopausal women by inhibiting or inactivating aromatase, the enzyme responsible for the synthesis of estrogens from androgenic substrates (specifically, the synthesis of estrone from the preferred substrate androstenedione and estradiol from testosterone). Unlike tamoxifen, AIs have no partial agonist activity.

AIs are described as first-, second-, and third-generation inhibitors according to the chronologic order of their clinical development, and they are further classified as type 1 or type 2 inhibitors according to their mechanism of action. Type 1 inhibitors are steroidal analogue of androstenedione and bind to the same site on the aromatase molecule, but unlike androstenedione they bind irreversibly. Therefore, they are commonly known as enzyme inactivators. Type 2 inhibitors are non-steroidal and bind reversibly to the heme group of the enzyme by way of a basic nitrogen atom; anastrozole and letrozole, both third-generation inhibitors, bind at their triazole groups. The third-generation AIs, developed in the early 1990s, include the triazoles anastrozole (Arimidex) and letrozole (Femara) and the steroidal agent exemestane (Aromasin). They

are administered orally; anastrozole and letrozole have similar pharmacokinetic properties, with half-lives approximating 48 hours, allowing a once-daily dosing schedule. The half-life of exemestane is 27 hours. Pharmacokinetic interactions between some inhibitors and tamoxifen have been described. The levels of anastrozole and letrozole are reduced (by a mean of 27 percent and 37 percent, respectively) when they are coadministered with tamoxifen, but these reductions are not associated with impaired suppression of plasma estradiol levels.

The use of AIs is associated with a series of relevant side effects which are reported in 30-60% of treated patients [162,163]. Among these, the AI-associated musculoskeletal symptoms (AIMSS) are characterized by morning stiffness and pain of the hands, knees, hips, lower back, and shoulders [164,165]. In addition to musculoskeletal pain, pain symptoms associated with AIs have recently been more accurately described with the inclusion of neuropathic, diffused, and mixed pain [166]. The whole spectrum of painful conditions has been reported to affect up to 40% of patients, and to lead 10-20% of patients to non-adherence or discontinuation of treatment [164,166-170]. Although it has been proposed that estrogen deprivation and several other factors, including a higher level of anxiety, may contribute to the development of AIMSS and related pain symptoms, none of these hypotheses has been confirmed [166,171].

The chemical structure of exemestane includes a system of highly electrophilic conjugated Michael acceptor groups, which might react with the thiol groups of reactive cysteine residues [172]. Michael addition reaction with specific cysteine residues is a major mechanism that results in TRPA1 activation by a large variety of electrophilic compounds [121-123]. Aliphatic and aromatic nitriles can react with cysteine to form thiazoline derivatives and accordingly the tear gas 2-chlorobenzylidene malononitrile (CS) has been identified as a TRPA1 agonist [173]. Exemestane, letrozole and anastrozole may produce neurogenic inflammation, nociception and hyperalgesia by targeting TRPA1 [174].

Aromatase inhibition, while reducing downstream production of estrogens, moderately increases upstream plasma concentrations of androgens, including androstenedione (ASD) [175]. Exemestane, a false aromatase substrate, blocks enzymatic activity by accommodating in the binding pocket that snugly encloses ASD [176]. ASD, which retains some of the reactive chemical features of exemestane, such as the α,β-carbonyl moiety of the A ring and the ketone group at the 17 position, might target TRPA1.

1.7 TRPA1 and Migraine

The original proposal by William Bayliss [177] and later by Sir Thomas Lewis [16] of the existence of a 'nocifensor system', which, made up by a subset of somatosensory neurons, senses tissue injury and immediately orchestrates a local, inflammatory and defensive response, has only recently obtained an all too long awaited neurochemical demonstration. The CGRP receptor antagonist, telcagepant [178], inhibited the neurogenic flare response induced by capsaicin application to the human forearm skin [179]. This mechanism appears to be relevant in migraine headaches. While the proposal that meningeal plasma extravasation (mediated by SP acting at the NK1 receptor) contributes to migraine headache was not confirmed by several clinical trials [180], the component of neurogenic inflammation produced by CGRP released from perivascular trigeminal nerve endings seems to represent the underlying mechanism of migraine headaches. Indeed, various chemically unrelated CGRP receptor antagonists have been shown to ameliorate the pain and associated symptoms of migraine attacks [24,181,182]. As a consequence, stimuli, which acting upon different receptors/channels excite peptidergic nociceptors to release CGRP, may be expected to trigger migraine attacks. Recently, TRPA1 has emerged as a specific target for many migraine triggers, and there is also evidence that some antimigraine medicines have an inhibitory action on channel activity.

1.7.1 TRPA1 is activated by migraine producing agents

It is a common notion for clinicians and a general experience for patients that a series of exogenous stimuli, including environmental agents, foods, medicines and other stimuli, either provoke or favour headache in migraineurs[183-185]. A proportion of migraineurs is particularly sensitive to inhalation of cigarette smoke, which increases the frequency of migraine [185] and cluster headache (a rarer and particularly severe type of primary headache) attacks [186]. Crotonaldehyde [187], acetaldehyde [188], formaldehyde [149], hydrogen peroxide [112], nicotine [189], and acrolein [117] are, among the thousands of components of cigarette smoke, those which have been identified as TRPA1activators. Cigarette smoke exposure in rodents causes a neurogenic inflammatory response in the airways [190] that is entirely mediated by TRPA1 activation [187]. In line with these findings, it has recently been shown that application to the rat nasal mucosa of the TRPA1 agonist, acrolein produces a TRPA1-dependent and CGRP-mediated increase in meningeal blood flow [191]. In clinical settings it is, thus, possible that inhalation of cigarette smoke through its TRPA1-acting components, such as acrolein, crotonaldehyde, formaldehyde, acetaldehyde, hydrogen peroxide, and nicotine, promotes CGRP release, e.g. the process

now recognized to trigger migraine attacks [191,192].Acrolein, which is also present in vehicle exhaust and tear gas, because of its ability to excite TRPA1, could be responsible for the irritant responses evoked by tear gas, which in addition to cough, chest pain and dyspnea, include headache [193]. Additional molecules, identified as TRPA1 agonists, which have been long known as migraine or cluster headache provocative agents [194,195] include ammonium chloride [196] and formalin (formaldehyde) [47,149].

Nitroglycerine and its analogues exert cardioprotective effect through the release of the active vasodilator gaseous compound, nitric oxide (NO). Intra- and extra-cranial vasodilatation is considered one possible mechanism [197] responsible for the common adverse reaction produced by nitroglycerine and congeners [198]. Reversal of nitroglycerine-evoked headache/migraine by sumatriptan [199], presumably mediated by a vasoconstrictor action though serotonin 5-HT1B receptor activation [200,201] but not by a CGRP receptor antagonist [202] strengthens the hypothesis of a major pro-headache role of NO-mediated vasodilatation of cranial arteries. Although not always confirmed [203], nitroglycerine/NO have been reported to release CGRP in vitro [204] and in vivo [205], and more recently NO has been found to act as a TRPA1 agonist [206]. Typically, nitroglycerine evokes an early and transient moderate headache in both migraineurs and healthy controls, while only migraineurs after a 4-5 hours delay develop an almost genuine migraine attack [207]. Thus, vasodilation in vivo [207]and CGRP release in vitro [204] cannot easily account for the postponed migraine onset. However, it is not known whether a TRPA1-dependent mechanism contributes to the neuronal sensitization or other pathways responsible for the ability of NO and NO-donors to trigger migraine attacks.

Umbellulone is the major constituent of the California bay laurel, Umbellularia californica, which is also known as the “headache tree” because of the headache provoking properties of its scent [208]. Cluster headache like attacks may also be triggered by exposure to the scent of Umbellularia californica [209]. Umbellulone, in a manner not immediately predictable from its chemical structure, reacts in a “click-fashion” with the biogenic thiol cysteamine, producing a Michael adduct [210], a prerequisite to exert a TRPA1 agonistic activity. Indeed, umbellulone gated TRPA1, thereby releasing CGRP. These in vitro responses were recapitulated in vivo by intranasal application of umbellulone, which, as for acrolein [191], produced a TRPA1-mediated and CGRP-dependent neurogenic meningeal vasodilation [210]. The reflex pathway or other possible neural mechanisms responsible for acrolein- and umbellulone-evoked meningeal vasodilatation following intranasal exposure to TRPA1 agonists remain to be investigated.

1.7.2 Analgesic and antimigraine drugs act by TRPA1 targeting

Some compounds contained in common butterbur [Petasites hybridus (L.) Gaertn.] [247], the major constituents, petasin and isopetasin [211], are considered responsible for the antimigraine effects of the herbal extract [212]. Clinical evidence [213-215] of beneficial action in migraine prevention has been obtained with a preparation that contains standardized amounts (minimum 15%, corresponding to 7.5 mg) of petasin/isopetasin [211,212]. The collective standardization is due to the instability of petasin, which spontaneously turns into isopetasin. Due to the stability issue, the specific role of each sesquiterpenoid for bioactivity has not been clearly identified. Several hypotheses have been advanced to explain the antimigraine action of petasin/isopetasin, including inhibition of leukotriene synthesis in leukocytes [216] and of voltage sensitive calcium channel in arterial smooth muscle cells [217,218] or antimuscarinic activity [219]. However, none of these actions seem to be relevant for migraine pathophysiology. Despite this mechanistic uncertainty, butterbur extract is currently recommended at high levels of strength for migraine prophylaxis [220]. Petasin and its cross-conjugated isomer, isopetasin, are eremophilane sesquiterpene esters of petasol and angelic acid. Both compounds contain electrophilic double bonds and can potentially interact with bionucleophiles. Nevertheless, given disubstitution at the β-carbon, they do not react with thiols, while giving a negative cysteamine assay [221]. The petasin family of compounds selectively target TRPA1, thus leading to an initial neuronal excitation followed by remarkable desensitization of the afferent and efferent function of peptidergic TRPA1-expressing nociceptors. The antimigraine action of butterbur extracts may derive from the ability of isopetasin to evoke TRPA1-dependent desensitization of nociceptors that mediate neurogenic inflammation.

1.8 Aim of the study

The TRPA1, from its first cloning [80], has gained increasing scientific interest for its role as a sensor of irritating and cell-damaging agents. The identification of TRPA1 as the target of an unprecedented series of chemically different molecules, many of which are generated following oxidative stress, points to the TRPA1-oxidative stress system as a novel pathway to produce neurogenic inflammation and sense pain. Although previous reports have identified the main role of TRPA1 in nociceptive pain models, more recent studies have emphasized the key function of the channel in models of neuropathic pain (particularly in the transition from acute nociception to chronic hypersensitivity) and in models of those peculiar types of pain experienced by migraine or cluster headache patients.

Unlike inflammatory pain, neuropathic pain is not associated with an overt tissue inflammatory condition, but rather is dependent from a damage or dysfunction of the nervous system and is most frequently due to peripheral nerve injury. The involvement of TRPA1 in different patterns of neuropathic pain has been proposed by recent results obtained in different animal models. Growing evidence is robustly building up the hypothesis that TRPA1 plays a major role in the hypersensitivity to chemical, thermal and mechanical stimuli, which characterizes a variety of models of neuropathic pain, such as nerve injury, diabetic neuropathy, and neuropathy induced by some chemotherapeutic agents (CIPN).

The TRPA1 is a nonspecific calcium-permeable channel expressed in primary sensory neurons of the dorsal root, trigeminal and vagal ganglia, where it co-localizes with the TRPV1 channel [82,222]. Whereas the role of TRPA1 in mechano- and cold-transduction remains to better clarify, it has been extensively demonstrated that TRPA1 plays a key role in the detection of chemical irritants. Indeed, TRPA1 is activated by a wide range of pungent and irritant exogenous compounds, also derived from alimentary [111]. Compelling evidence indicates that TRPA1 can be activated by endogenous products generated at sites of inflammation and tissue injury from metabolism, and oxidative stress-derived substances.

The main purpouse of the three years study, was to investigate the role of TRPA1 in different pathological conditions that generate pain.

Firstly, we investigate the role of TRPA1 in pain symptoms associated with the treatment of the third-generation AIs, that include the triazoles anastrozole (Arimidex) and letrozole (Femara), and the steroidal agent exemestane (Aromasin), currently recommended for adjuvant endocrine treatment as primary, sequential, or extended therapy with tamoxifen, for postmenopausal women diagnosed with estrogen receptor-positive breast cancer

[160,161,223]. Among these, the AI-associated musculoskeletal symptoms (AIMSS) are characterized by morning stiffness and pain of the hands, knees, hips, lower back, and shoulders [164,165]. In addition to musculoskeletal pain, pain symptoms associated with AIs have recently been more accurately described with the inclusion of neuropathic, diffused, and mixed pain [166]. The chemical structure of exemestane includes a system of highly electrophilic conjugated Michael acceptor groups, which might react with the thiol groups of reactive cysteine residues [172]. Michael addition reaction with specific cysteine residues is a major mechanism that results in TRPA1 activation by a large variety of electrophilic compounds [121-123]. In addition, aliphatic and aromatic nitriles can react with cysteine to form thiazoline derivatives and accordingly the tear gas 2-chlorobenzylidene malononitrile (CS) has been identified as a TRPA1 agonist [173]. We noticed that both letrozole and anastrozole possess nitrile moieties. Thus, we hypothesized that exemestane, letrozole and anastrozole may produce neurogenic inflammation, nociception and hyperalgesia by targeting TRPA1.

The ability to gate TRPA1 in vitro was confirmed in vivo by the observation that the pain-like behaviors evoked by AIs in mice are abrogated by genetic deletion or pharmacological blockade of the channel [174]. However, AI concentrations required for TRPA1 gating in vitro [174] are 1-2 order of magnitude higher than those found in patient plasma [224]. In addition, an important proportion (30-40%), but not all, of treated patients develop the painful condition [169,171]. These observations suggest that exposure to AIs is necessary, but not sufficient, to produce AIMSS, and that additional factors should cooperate with AIs to promote pain symptoms.

Aromatase inhibition, while reducing downstream production of estrogens, moderately increases upstream plasma concentrations of androgens, including androstenedione (ASD) [175]. Exemestane, a false aromatase substrate, blocks enzymatic activity by accommodating in the binding pocket that snugly encloses ASD [176]. We reasoned that ASD, which retains some of the reactive chemical features of exemestane, such as the α,β-carbonyl moiety of the A ring and the ketone group at the 17 position, might target TRPA1.

We also investigated the role of TRPA1 in another painful condition, in migraine pain. Occupational exposure to, or treatment with, organic nitrates has long been known to provoke headaches [225,226]. These observations have led to the clinical use of glyceryl trinitrate (GTN) as a reliable provocation test for migraine attacks [227-230]. In most subjects, including healthy controls, GTN administration causes a mild headache that develops rapidly and is short-lived. However, after a remarkable time lag (hours) from GTN

exposure, migraineurs develop severe headaches that fulfill the criteria of a typical migraine attack [227-230].

Several mechanisms have been proposed to explain GTN-evoked headaches, including degranulation of meningeal mast cells [231,232], delayed meningeal inflammation sustained by induction of NO synthase and prolonged NO generation, and the release of CGRP [233,234], a primary migraine neuropeptide [235,236]. GTN administration to rodents and humans produces a delayed and prolonged (hours) hyperalgesia that temporally correlates with GTN-induced migraine-like attacks in humans [232,237-239].

TRPA1 inhibition attenuates different types of neuropathic [240] and inflammatory [149,241] pain. TRPA1 may also contribute to migraine, since triggers of headache attacks can target the channel in peptidergic nociceptors [101]. Furthermore, drugs [242,243] or herbal preparations [244] used for migraine treatment inhibit or desensitize TRPA1.

Finally, we have investigated petasin and isopetasin conteined in butterbur [*Petasites hybridus* (L.) Gaertn.] in their ability to selectively target TRPA1. Butterburs (*Petasites*), herbaceous perennial plants belonging to the genus of *Asteraceae*, which includes also *Tanacetum parthenium* L. [245], have been used by folk medicine of northern Eurasia and America for therapeutic purposes, including treatment of fever, respiratory diseases, spasms, and pain [246]. Among the number of compounds contained in common butterbur [247], the major constituents, petasin and isopetasin [211], are considered responsible for the antimigraine effects of the herbal extract [212]. Clinical evidence [213-215] of beneficial action in migraine prevention has been obtained with a preparation that contains standardized amounts (minimum 15%, corresponding to 7.5 mg) of petasin/isopetasin [211,212]. The collective standardization is due to the instability of petasin, which spontaneously turns into isopetasin. Due to the stability issue, the specific role of each sesquiterpenoid for bioactivity has not been clearly identified. Given the role of electrophilic compounds for the paradoxical induction/prevention of headache *via* modulation of the activity of the TRPA1 channel [210,248] we wondered if the butterbur sesquiterpenoids could target the channel.

Chapter II - Steroidal and non-steroidal third-generation aromatase inhibitors induce pain-like symptoms via TRPA1

2.1 Methods

Animals. Animal experiments were carried out in conformity to the European Communities Council (ECC) guidelines for animal care procedures and the Italian legislation (DL 116/92) application of the ECC directive 86/609/EEC. Studies were conducted under the University of Florence research permit number 204/2012-B. Male C57BL/6 (25-30 g) (Harlan Laboratories, Milan, Italy), wild type, *Trpa1*$^{+/+}$, or TRPA1-deficient, *Trpa1*$^{-/-}$, (25-30 g) mice generated by heterozygous on a C57BL/6 background (B6;129P-Trpa1tm1Kykw/J; Jackson Laboratories, Italy) [116], or Sprague-Dawley rats (75-100 g, male, Harlan Laboratories, Milan, Italy) were used. Animals were housed in a temperature- and humidity-controlled *vivarium* (12 hours dark/light cycle, free access to food and water). Behavioral experiments were done in a quiet, temperature-controlled (20 to 22 °C) room between 9 a.m. and 5 p.m., and were performed by an operator blinded to the genotype and the drug treatment. Animals were sacrificed with a high dose of sodium pentobarbital (200 mg/kg, i.p.).

Reagents. Exemestane, letrozole and anastrozole were purchased from Tocris Bioscience (Bristol, UK). The activating peptide (PAR2-AP, SLIGRL-NH2) and its reverse peptide (PAR2-RP, LRGILS-NH2) of the murine PAR2 receptor were synthesized from G. Cirino (University of Naples, Naples, Italy) and dissolved in distilled water. If not otherwise indicated, all other reagents were from Sigma-Aldrich (Milan, Italy). HC-030031 was synthesized as previously described [187].

Cell culture and isolation of primary sensory neurons. Human embryonic kidney (HEK293) cells stably transfected with the cDNA for human TRPA1 (hTRPA1-HEK293), kindly donated by A.H. Morice (University of Hull, Hull, UK) or with the cDNA for human TRPV1 (hTRPV1-HEK293), kindly donated by Martin J. Gunthorpe (GlaxoSmithKline, Harlow, UK), and naive untransfected HEK293 cells (American Type Culture Collection, Manassas, VA, USA) were cultured as previously described [210]. HEK293 cells were transiently transfected with the cDNAs (1 μg) codifying for wild-type

or mutant 3C/K-Q (C619S, C639S, C663S, K708Q) [121,123] human TRPA1 using the jetPRIME transfection reagent (Euroclone, Milan, Italy) according to the manufacturer's protocol.

Primary dorsal root ganglion (DRG) neurons were isolated from Sprague- Dawley rats and C57BL/6 or *Trpa1*$^{+/+}$ and *Trpa1*$^{-/-}$ adult mice, and cultured as previously described [157]. Briefly, ganglia were bilaterally excised under a dissection microscope and enzymatically digested using 2 mg/ml of collagenase type 1A and 1 mg/ml of trypsin, for rat DRG neurons, or 1 mg/ml of papain, for mouse DRG neurons, in Hank's Balanced Salt Solution (HBSS) for 25-35 minutes at 37 °C. Rat and mouse DRG neurons were pelleted and resuspended in Dulbecco's Modified Eagle's Medium (DMEM) supplemented with 10% heat inactivated horse serum or Ham's- F12, respectively, containing 10% heat-inactivated fetal bovine serum (FBS), 100 U/ml of penicillin, 0.1 mg/ml of streptomycin, and 2 mM L-glutamine for mechanical digestion. In this step, ganglia were disrupted by several passages through a series of syringe needles (23-25G). Neurons were then pelleted by centrifugation at 1200 g for 5 minutes, suspended in *medium* enriched with 100 ng/ml mouse-NGF and 2.5 mM cytosine-b-D-arabino-furanoside free base, and then plated on 25 mm glass coverslips coated with poly-L-lysine (8.3 μM) and laminin (5 μM). DRG neurons were cultured for 3-4 days before being used for calcium imaging experiments.

Calcium Imaging Assay. Intracellular calcium was measured in transfected and untransfected HEK293 cells or in DRG neurons, as previously reported [245]. Plated cells were loaded with 5 μM Fura-2AM-ester (Alexis Biochemicals, Lausen, Switzerland) added to the buffer solution (37 °C) containing the following (in mM): 2 CaCl2; 5.4 KCl; 0.4 MgSO4; 135 NaCl; 10 D-glucose; 10 HEPES and 0.1% bovine serum albumin at pH 7.4. After 40 minutes, cells were washed and transferred to a chamber on the stage of a Nikon Eclipse TE-2000U microscope for recording. Cells were excited alternatively at 340 nm and 380 nm to indicate relative intracellular calcium changes by the Ratio340/380 recorded with a dynamic image analysis system (Laboratory Automation 2.0, RCSoftware, Florence, Italy). Cells and neurons were exposed to exemestane, letrozole and anastrozole (1-300 μM), AITC (10-30 μM), menthol (100 μM), icilin (30 μM), or their vehicles (1.5-3 % dimetyl sulfoxide, DMSO). The calcium response to capsaicin (0.1 μM) was used to identify nociceptive neurons. The selective TRPA1 antagonist, HC-030031 (30 μM), and TRPV1 antagonist, capsazepine (10 μM) or their vehicles (3% and 0.1% DMSO, respectively), were applied ten minutes before the stimuli. Results are expressed as or the percentage of increase of Ratio340/380 over the baseline normalized to the maximum effect induced by ionomycin (5 μM) added at the end of each experiment

(% Change in R340/380) or Ratio340/380.

Electrophysiology. Whole-cell patch-clamp recordings were performed on hTRPA1-HEK293, vector-HEK293 cells or rat DRG neurons grown on a poly-L- lysine-coated 13 mm-diameter glass coverslips. Each coverslip was transferred to a recording chamber (1 ml volume) mounted on the platform of an inverted microscope (Olympus CKX41, Milan, Italy) and superfused at a flow rate of 2 ml/min with a standard extracellular solution containing (in mM): 10 HEPES, 10 D-glucose, 147 NaCl, 4 KCl, 1 MgCl2, and 2 CaCl2 (pH adjusted to 7.4 with NaOH). Borosilicate glass electrodes (Harvard Apparatus, Holliston, MA, USA) were pulled with a Sutter Instruments puller (model P-87) to a final tip resistance of 4-7 MΩ. Pipette solution used for HEK293 cells contained (in mM): 134 K-gluconate, 10 KCl, 11 EGTA, 10 HEPES (pH adjusted to 7.4 with KOH). When recordings were performed on rat DRG neurons, 5 mM CaCl2 was present in the extracellular solution and pipette solution contained (in mM): CsCl 120, Mg2ATP 3, BAPTA 10, HEPES-Na 10 (pH adjusted to 7.4 with CsOH). Data were acquired with an Axopatch 200B amplifier (Axon Instruments, CA, USA), stored and analyzed with a pClamp 9.2 software (Axon Instruments, CA, USA). All the experiments were carried out at 20-22°C. Cells were voltage-clamped at –60 mV. Cell membrane capacitance was calculated in each cell throughout the experiment by integrating the capacitive currents elicited by a ± 10 mV voltage pulse. In hTRPA1-HEK293 currents were detected as inward currents activated on cell superfusion with AITC (100 μM), exemestane (50-200 μM), letrozole (50-200 μM) or anastrozole (50-200 μM) in the presence of HC-030031 (50 μM) or its vehicle (0.5% DMSO). TRPV1 currents in rat DRG neurons were detected as inward currents activated by capsaicin (1 μM) in the presence of capsazepine (10 μM) or its vehicle (0.1% DMSO). To evaluate the potentiating effect of H_2O_2 or PAR2-AP on AIs- activated currents, rat DRG neurons were superfused with H_2O_2 or PAR2-AP (both 100 μM) 1 minute before and during the application of exemestane or letrozole (both, 20 μM). Some experiments were performed in the presence of HC-030031 (50 μM) or its vehicle (0.5% DMSO). Peak currents activated by each compound were normalized to cell membrane capacitance and expressed as mean of the current density (pA/pF) in averaged results. Currents were evoked in the voltage-clamp mode at a holding potential of -60 mV; signals were sampled at 1 kHz and low-pass filtered at 10 kHz.

Behavioral experiments. For behavioral experiments, after habituation and baseline of pain sensitivity measurements, mice were randomized into treatment groups. In a first series of experiments, we explored whether the injection (20 μl/paw) of exemestane (1, 5, 10 nmol) or letrozole (10, 20 nmol), or their vehicle (5% DMSO) induced, in C57BL/6 or *Trpa1*$^{+/+}$ and *Trpa1*$^{-/-}$ mice, an acute nociceptive behavior and a delayed mechanical

allodynia. In this set of experiments mechanical allodynia was measured just before (30 minutes) and 0.25, 0.5, 1, 2, 4, and 6 hours post injection. Some C57BL/6 mice were pretreated with HC-030031 (100 mg/kg, i.p.) or capsazepine (10 mg/kg, i.p.) or their respective vehicles (4% DMSO and 4% Tween20 in isotonic solution), 60 minutes and 30 minutes, respectively, before exemestane (10 nmol) or letrozole (20 nmol) i.pl. injection. Mechanical allodynia was measured 60 minutes after AIs i.pl. injection.

In a second set of experiments, nociceptive behavior and mechanical allodynia were assayed before and after systemic administration of exemestane (5 mg/kg, i.p. or 10 mg/kg, i.g.) and letrozole (0.5 mg/kg, i.p. or i.g.), or their vehicles (5% DMSO for i.p. or 0.5% carboxymethylcellulose, CMC, for i.g. administration), in C57BL/6 mice or *Trpa1*$^{+/+}$ and *Trpa1*$^{-/-}$ mice. Mechanical allodynia was measured just before (30 minutes) and 1, 3, 6, 24, 48 hours after injection. Some animals 2 hours after AI administration received HC-030031 (100 mg/kg, i.p.) or its vehicle (4% DMSO and 4% Tween80 in isotonic solution), and mechanical allodynia and the forelimb grip strength were measured 1 and 3 hours after vehicle or HC-030031. In a third series of experiments, *Trpa1*$^{+/+}$ and *Trpa1*$^{-/-}$ mice were treated i.p. once a day for 15 consecutive days with exemestane or letrozole at the dose of 5 mg/kg or 0.5 mg/kg, respectively, or with their vehicle (5% DMSO) and with i.g. exemestane or letrozole at the dose of 10 mg/kg or 0.5 mg/kg, respectively, or with their vehicle (0.5% CMC). Mechanical allodynia and the forelimb grip strength were measured 10 min before and 1, 3, 6 and 24 hours post administration at day 1, 5, 10 and 15.

To test whether PAR2 activation enhances the nocifensor behavior evoked by exemestane and letrozole, in another experimental setting, the PAR2 activating peptide (PAR2-AP), SLIGRL-NH2, (10 µg/10 µl i.pl.) or its reversed inactive form (PAR2- RP), LRGILS-NH2, (10 µg/10 µl i.pl.), were injected in the right hind paw. Ten minutes after i.pl. PAR2-AP or PAR2-RP injection, mice received exemestane (10 nmol/10 µl i.pl.) or letrozole (20 nmol/10 µl, i.pl.), or their vehicle (5% DMSO), in the plantar surface in the same paw injected with PAR2-AP or PAR2-RP, and the acute nociceptive behavior was recorded. In another series of experiments H_2O_2 (0.5 µmol/10 µl, i.pl.) or its vehicle were injected and the acute nocifensor behavior to H_2O_2, which did not last longer than 5 min, was recorded for 10 min. Ten min after vehicle/H_2O_2, exemestane (10 nmol/10 µl i.pl.) or letrozole (20 nmol/10 µl, i.pl.) were injected in the same paw injected with H_2O_2 or vehicle and the acute nociceptive behavior in response to AIs was recorded. Three hours after systemic administration of exemestane (5 mg/kg, i.p.) or letrozole (0.5 mg/kg, i.p.) mice were locally injected with H_2O_2 (0.5 µmol/20 µl, i.pl.) or its vehicle and both acute nocifensor behavior and mechanical allodynia were recorded.

Acute Nocifensive Response. AITC (10 nmol/paw), exemestane (10 nmol/paw), letrozole (20 nmol/paw) or their vehicles (5% DMSO), H_2O_2 (0.5 μmol/paw) or its vehicle (isotonic solution) and PAR2-AP or PAR2-RP (10 μg/paw) (10 or 20 μl) were injected into the paw of C57BL/6, *Trpa1*$^{+/+}$ and *Trpa1*$^{-/-}$ mice, and immediately after injection animals were placed in a plexiglas chamber. The total time spent licking and lifting the injected hind paw was recorded for 5 minutes as previously described [130].

Mechanical Stimulation (Von Frey Hair Test). Mechanical threshold was measured in C57BL/6, *Trpa1*$^{+/+}$ and *Trpa1*$^{-/-}$ mice after both local (i.pl.) administration of AITC (10 nmol/paw), exemestane (10 nmol/paw), letrozole (20 nmol/paw) or their vehicles (5% DMSO), H_2O_2 (0.5 μmol/paw) or its vehicle (isotonic solution), and systemic (i.p.) administration of exemestane (5 mg/kg, i.p.) or letrozole (0.5 mg/kg, i.p.) at different time points by using the up-and-down paradigm [249]. Mechanical nociceptive threshold was determined before (basal level threshold) and after different treatments. The 50% mechanical paw withdrawal threshold response (in g) was then calculated from these scores, as previously described [249,250].

Forelimb Grip Strength Test. The grip strength test was performed with a grip strength meter (Ugo Basile, Varese, Italy), as previously reported [251]. Mice were allowed to grasp a triangular ring attached to a force transducer and gently pulled away by the base of the tail until the grip was broken. The test was repeated 4 times and the mean peak force values (g) were calculated for each animal. The grip strength was measured in C57BL/6, *Trpa1*$^{+/+}$ and *Trpa1*$^{-/-}$ mice 10 min before and 1, 3, 6 and 24 hours post AI administration.

Paw Oedema. AITC (10 nmol/paw), exemestane (10 nmol/paw), letrozole (20 nmol/paw) or their vehicles (5% DMSO) (all 20 μl) were injected into the paw of C57BL/6, *Trpa1*$^{+/+}$ and *Trpa1*$^{-/-}$ mice and paw thickness was measured to determine the development and severity of oedema in the hind paws. Some animals received HC-030031 (100 mg/kg, i.p.), a combination of L-733,060 and CGRP8-37 (both, 2 μmol/kg, i.v.), or their vehicles (4% DMSO and 4% Tween20 in isotonic solution for HC-030031, and isotonic solution for L-733,060 and CGRP8-37) prior to stimuli. An engineer's micrometer, with 0.01 mm accuracy (Harvard Apparatus, Kent, UK) was used to measure the paw thickness in millimeters (mm), before and after (60 and 120 minutes) the i.pl. injection with tested agents by an investigator blinded to treatments. Data were expressed as the increase in mm in paw thickness.

CGRP-Like Immunoreactivity (LI) assay. For neuropeptide release experiments, 0.4 mm slices of rat and *Trpa1*$^{+/+}$ or *Trpa1*$^{-/-}$ mouse spinal cords were superfused with an aerated (95% O2 and 5% CO2) Krebs solution containing (in mM): 119 NaCl, 25 NaHCO3, 1.2 KH2PO4, 1.5 MgSO4, 2.5 CaCl2, 4.7 KCl, 11 D-glucose; the solution was

maintained at 37°C, and was added with 0.1% bovine serum albumin, and, to minimize peptide degradation, with the angiotensin converting enzyme inhibitor, captopril (1 μM), and the neutral endopeptidase inhibitor, phosphoramidon (1 μM). Tissues were stimulated with exemestane, letrozole or anastrozole (all 100 μM) or their vehicles (0.05% DMSO) dissolved in the Krebs solution. Some tissues were pre-exposed to capsaicin (10 μM, 20 minutes) or pretreated with HC-030031 (50 μM). Fractions (4 ml) of superfusate were collected at 10-minute intervals before, during, and after administration of the *stimulus* and then freeze-dried, reconstituted with assay buffer, and analyzed for CGRP-like immunoreactivity (LI) by an ELISA assay kit (Bertin Pharma, Montigny le Bretonneux, France). CGRP-LI was calculated by subtracting the mean *pre-stimulus* value from those obtained during or after stimulation. Detection limits of the assays were 5 pg/ml. Results are expressed as femtomoles of peptide per g of tissue per 10 minutes.

In another set of experiments, exemestane (5 nmol/50 μl) and letrozole (10 nmol/50 μl) or their vehicle (1% DMSO) were i.a. injected in anesthetized (sodium pentobarbital, 50 mg/kg i.p.) rats. Ten minutes after injection, rats were sacrificed and the knee joint was dissected [241]. CGRP-LI was measured in the synovial fluid lavage added with captopril (1 μM) and phosphoramidon (1 μM) by using the ELISA assay kit as previously described [241]. Detection limits of the assays were 5 pg/ml. Results are expressed as femtomoles of peptide per g of tissue per 20 minutes in the spinal cord experiments or pg/ml in the rat synovial fluid.

Assay of Exemestane and Letrozole by Liquid Chromatography-Mass Spectrometry. Blood samples (100 μl) were obtained by venepuncture of the tail vein from each mouse at different time points (0.25, 0.5, 1, 3, 6 and 24 hours) after i.g. administration of exemestane (10 mg/kg) or letrozole (0.5 mg/kg). Blood samples were dropped on a filter paper (903® Whatman GmbH, Dassel, Germany) to obtain dried blood spots (DBS) [252] which were punched, obtaining a 6.0 mm diameter disk, containing approximately 6 μl of blood. DBS, transferred into a 2 ml Eppendorf vial were extracted with 200 μl of methanol: water (95:5, *v/v*) containing 0.1% acetic acid and the appropriate internal standard (for letrozole and exemestane quantification, extracting solutions contained 5 μg/l of anastrozole or 2 μg/l of letrozole, respectively) and after shaking with an orbital shaker for 25 min at 37°C, solutions were dried under a gentle nitrogen stream. Residues were reconstituted with 40 μl water containing 0.1% of acetic acid.

Samples were measured using a 1290 Infinity liquid chromatograph (LC, Agilent Technologies, Waldbronn, Germany) coupled to a QTRAP 5500 (AB SCIEX, Toronto, Canada) equipped with the Turbo Ion Spray source operating in positive ion mode. The

capillary voltage was set to 5 kV. Heated turbo gas (400°C, air) at a flow rate of 10.0 l/min was used. The transitions (quantifier and qualifier) recorded in Multiple Reaction Monitoring (MRM) mode were: 286.1>217.1 and 286.1>190.1 for letrozole, 294.1>225.1 and 294.1>210.1 for anastrozole and 297.1>121.0 and 297.1>93.1 for exemestane. The LC column was a Gemini C6-Phenyl (100 x 2 mm, 3 µm) with the corresponding 4x2 mm SecurityGuardTM cartridge (Phenomenex, Torrance, CA), operated at 0.3 ml/min. Eluent A (water + 0.1% acetic acid) and B (acetonitrile) were used. The gradient elution program was as follows: 20% B maintained for 2 min, then to 90% B in 7 min, back to 20% B in 1 min and re- equilibrated for a 20 min total run time. Anastrozole, exemestane and letrozole retention times were 6.12, 6.31 and 7.45 min, respectively. Four µl of the extracted sample were injected for LC-MS/MS assays. System control and data acquisition were done by Analyst 1.5.1 software and calibration curves were calculated using the non- weighted linear least-square regression of Analyst Quantitation program (AB SCIEX, Toronto, Canada).

Calibration curves were constructed for both exemestane and letrozole, using the appropriate internal standard. Whole blood from control mouse was spiked with different concentrations of exemestane (from 2 to 100 µg/l) or letrozole (from 10 to 200 µg/l). A 20 µl volume for each fortified blood sample was spotted on filter paper (DBS) and then treated as described in sample preparation. Each calibration curve was prepared in duplicate. Satisfying linearity was obtained for the two analytes (letrozole, r=0.996; exemestane, r=0.998). Each analytical batch included a double blank sample (without internal standard), a blank sample (with internal standard), five or six standard concentrations for calibration curve, and a set of treated mouse samples (each prepared in duplicate). LC-MS grade acetic acid, methanol, water and acetonitrile were supplied by Sigma Aldrich (Milan, Italy).

Statistical Analysis Data represent mean ± SEM or confidence interval (CI). Statistical analysis was performed by the unpaired two-tailed Student's t-test for comparisons between two groups, the ANOVA, followed by the Bonferroni post-hoc test for comparisons between multiple groups. Agonist potency was expressed as half maximal effective concentration (EC50), that is, the molar concentration of agonist producing 50% of the maximum measured effect, and 95% confidence interval (CI). $P<0.05$ was considered statistically significant (GraphPadPrism version 5.00, San Diego, CA).

2.2 Results

2.2.1 Aromatase inhibitors selectively activate TRPA1 channels

To explore whether AIs gate the human TRPA1 channel, we first used cells stably transfected with human TRPA1 cDNA (hTRPA1-HEK293). In hTRPA1- HEK293 cells, which respond to the selective TRPA1 agonist AITC (30 μM), but not in untransfected HEK293 cells, the three AIs, exemestane, letrozole, and anastrozole evoked concentration-dependent calcium responses that were inhibited by the selective TRPA1 antagonist, HC-030031 (30 μM) [253] (Figure 1a,b,c). EC50 of AIs ranged between 58 and 134 μM (Figure 1b). The calcium response was abated in a calcium- free medium, thus supporting the hypothesis that the increase in intracellular calcium originates from extracellular sources (Supplementary Figure 1a). In HEK293 cells stably transfected with human TRPV1 cDNA (hTRPV1-HEK293) all AIs (100 μM) were ineffective (Supplementary Figure 1b). Key aminoacid residues are required for channel activation by electrophilic TRPA1 agonists [47,121,123]. Notably, HEK293 cells expressing a mutated TRPA1 channel (3C/K-Q), which presents substitutions of three cysteine with serine (C619S, C639S, C663S) and one lysine with glutamine (K708Q) residues, were insensitive to both AITC [121,123] and all three AIs, while maintaining sensitivity to the non-electrophilic agonists, menthol [129] or icilin [47] (Figure 1d and Supplementary Figure 1c). This finding supports the hypothesis that the ability of AIs to target TRPA1 derives from their electrophilic nature. Electrophysiology experiments recapitulated findings obtained by means of the calcium assay. Exemestane, letrozole, and anastrozole selectively activated a concentration-dependent inward current in hTRPA1-HEK293 cells, a response that was abated by HC-030031 (Supplementary Figure 1d). AIs did not evoke any current in untransfected HEK293 cells (Supplementary Figure 1d).

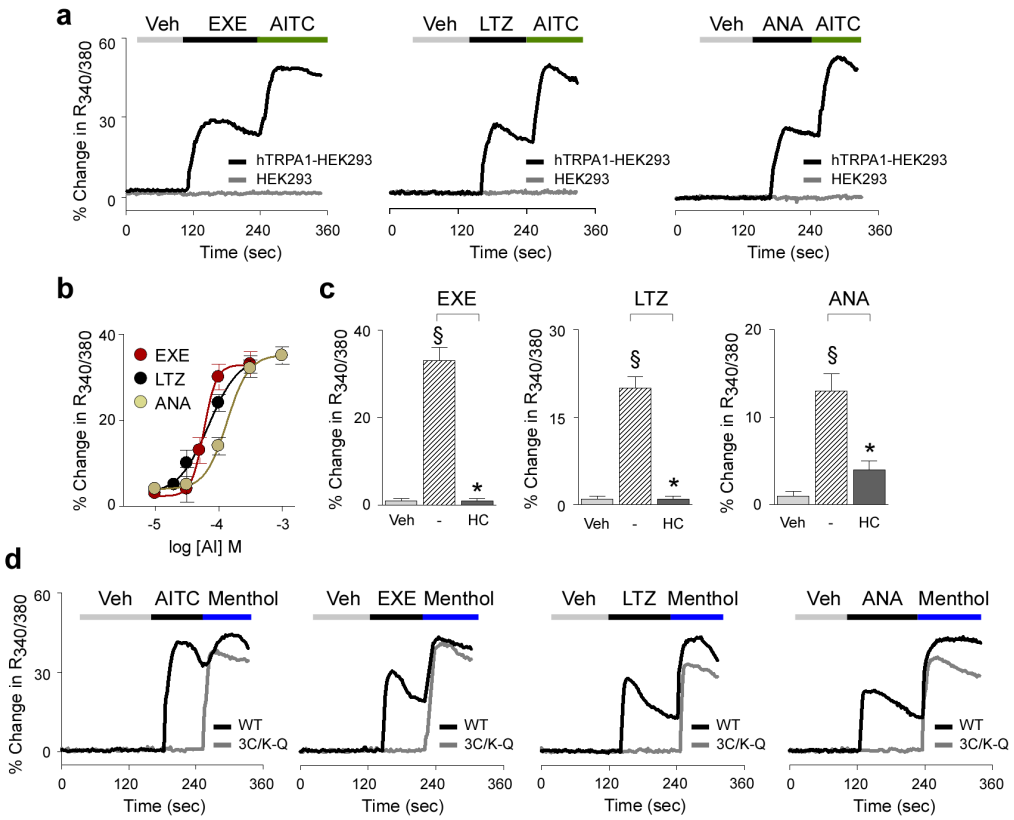

Figure 1. Exemestane (EXE), letrozole (LTZ) and anastrozole (ANA) selectively activate the human TRPA1 channel. a Representative traces of intracellular calcium response evoked by the aromatase inhibitors (AIs), EXE (100 µM), LTZ (100 µM) and ANA (100 µM), in HEK293 cells transfected with the cDNA for human TRPA1 (hTRPA1-HEK293) which respond to the selective TRPA1 agonist, allyl isothiocyanate (AITC; 30 µM). AITC (30 µM), EXE, LTZ, and ANA (all 100 µM) fail to produce any calcium response in untransfected-HEK293 cells (HEK293). **b** Concentration-response curves to EXE, LTZ and ANA, yielded EC50 (95% confidence interval) of 58 (46-72) µM, 69 (43-109) µM, and 134 (96-186) µM, respectively. **c** AI-evoked calcium response in hTRPA1-HEK293 is abolished by the selective TRPA1 antagonist, HC-030031 (HC; 30 µM). **d** Representative traces of cells transfected with the cDNA codifying for the mutant hTRPA1 channel (3C/K-Q), which are insensitive to AITC (30 µM) or AIs (100 µM), but respond to the non-electrophilic agonist, menthol (100 µM), whereas HEK293 cells transfected with the cDNA codifying for wild type hTRPA1 (WT) respond to all the drugs. Veh is the vehicle of AIs; dash (-) indicates the vehicle of HC. Each point or column represents the mean ± s.e.m. of at least 25 cells from 3-6 independent experiments. §P<0.05 *vs.* Veh, *P<0.05 *vs*. EXE, LTZ or ANA group; ANOVA and Bonferroni *post hoc* test.

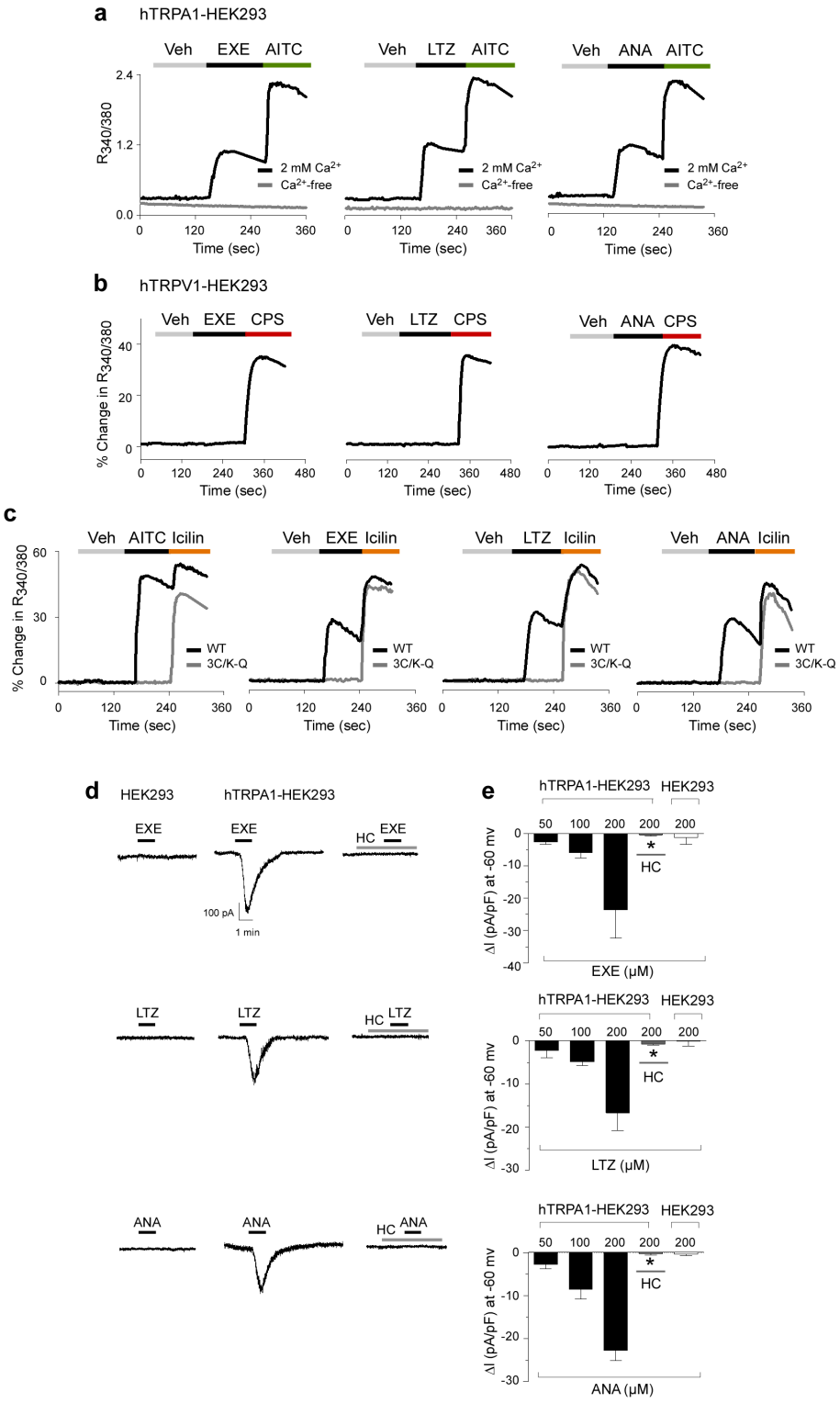

Supplementary Figure 1. Exemestane (EXE), letrozole (LTZ) and anastrozole (ANA) elicit a calcium influx and an inward current by selectively stimulating the human TRPA1 channel. a Representative traces of calcium mobilization evoked by EXE (100 μM), LTZ (100 μM), ANA (100 μM) in HEK293 cells stably transfected with the cDNA codifying for human TRPA1 (hTRPA1-HEK293) which also respond to allyl isothiocyanate (AITC; 30 μM). These effects are abated in a Ca^{2+}-free medium. Due to the absence of Ca^{2+} in the medium, results are expressed as $Ratio_{340/380}$ and not as % of increase of $Ratio_{340/380}$ normalized to ionomycin. **b** AIs (all 100 μM) fail to evoke any calcium response in HEK293 cells stably transfected with the cDNA codifying for human TRPV1 (hTRPV1-HEK293), which respond to the selective TRPV1 agonist, capsaicin (CPS; 0.1 μM). **c** Representative traces of cells transfected with the cDNA codifying for the mutant hTRPA1 channel (3C/K-Q), which are insensitive to AITC (30 μM) or AIs (100 μM), but respond to the non-electrophilic agonist, icilin (30 μM), whereas HEK293 cells transfected with the cDNA codifying for the wild type hTRPA1 (WT) respond to all the drugs. Veh is the vehicle of AIs. **d** Representative traces and **e** pooled data obtained by whole-cell patch-clamp recordings in hTRPA1-HEK293 cells. Exposure to EXE, LTZ or ANA elicits a concentration-dependent inward current at -60 mV

in hTRPA1-HEK293, but not in untransfected (HEK293) cells. The selective TRPA1 antagonist, HC-030031 (HC; 50 μM), abolishes currents evoked by all the AIs. Results are mean ± s.e.m. of at least 5 cells tested for each experimental condition. **P*<0.05 *vs*. EXE, LTZ or ANA; ANOVA and Bonferroni *post hoc* test.

Next, to verify whether exemestane, letrozole and anastrozole stimulate nociceptive sensory neurons *via* TRPA1 activation, we used primary culture of both rat and mouse dorsal root ganglion (DRG) neurons. Similar to AITC [123], all AIs produced a concentration-dependent calcium response (Figure 2a,b) in a proportion (about 30%) of cells that responded to the selective TRPV1 agonist, capsaicin (0.1 μM). All cells responding to AIs, but none of the non-responding cells, invariably responded to a subsequent high concentration of AITC (30 μM) (Figure 2a), further documenting TRPA1 as the target of AIs. In rat DRG neurons, EC50 ranged between 78 and 135 μM (Figure 2b). Calcium responses evoked by the three AIs were abated by HC-030031 (30 μM), but were unaffected by the selective TRPV1 antagonist, capsazepine (10 μM) (Figure 2c). Notably, AITC and all AIs produced a calcium response in capsaicin-sensitive DRG neurons isolated from wild type (*Trpa1*$^{+/+}$) mice, an effect that was absent in neurons obtained from TRPA1-deficient (*Trpa1*$^{-/-}$) mice (Typical traces Figure 2d and pooled data Figure 2e).

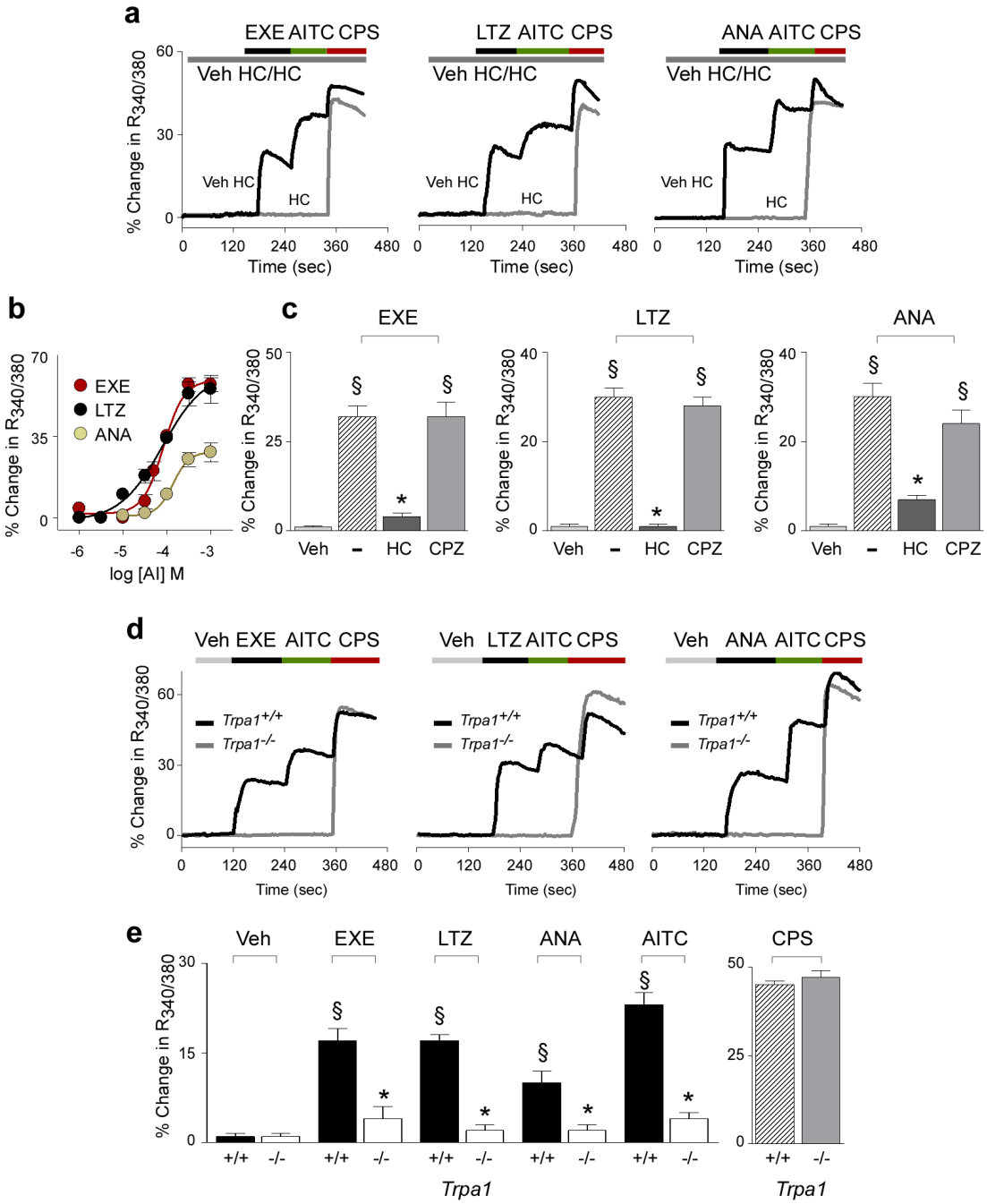

Figure 2. Exemestane (EXE), letrozole (LTZ) and anastrozole (ANA) selectively activate the native TRPA1 channel expressed in rodent dorsal root ganglion (DRG) neurons. a Representative traces of calcium response evoked by EXE (100 µM), LTZ (100 µM), ANA (300 µM) in cultured rat DRG neurons which also respond to allyl isothiocyanate (AITC; 30 µM) and capsaicin (CPS; 0.1 µM). Calcium responses evoked by AIs and AITC are abolished by the selective TRPA1 antagonist, HC- 030031 (HC; 30 µM), which does not affect response to CPS. **b** Concentration-response curves of EXE, LTZ, and ANA, yielded EC50 (95% confidence interval) of 82 (61-108) µM, 78 (39-152) µM, and 135 (78-231) µM, respectively. **c** Calcium responses induced by AIs are inhibited by HC and unaffected by the TRPV1 antagonist, capsazepine (CPZ; 10 µM). §P<0.05 *vs.* Veh, *P<0.05 *vs.* EXE, LTZ or ANA; ANOVA and Bonferroni *post hoc* test. **d** Representative traces and **e** pooled data of the calcium response evoked by EXE, LTZ, ANA (all 100 µM) or AITC (30 µM), in neurons isolated from *Trpa1*$^{+/+}$ mice. Neurons isolated from *Trpa1*$^{-/-}$ mice do not respond to AITC, EXE, LTZ and ANA, whereas they do respond normally to CPS (0.1 µM). In DRG neurons isolated from both *Trpa1*$^{+/+}$ and *Trpa1*$^{-/-}$ mice, calcium response is evaluated only in capsaicin responding neurons. §P<0.05 *vs.* Veh, *P<0.05 *vs.* EXE, LTZ, ANA or AITC-*Trpa1*$^{+/+}$, ANOVA and Bonferroni *post hoc* test. Veh is the vehicle of AIs; dash (-) indicates the combination of the vehicles of HC and CPZ. Each point or column represents the mean ± s.e.m. of at least 25 neurons obtained from 3-7 independent experiments.

2.2.2 AIs activate nociceptive and hyperalgesic TRPA1-dependent pathways

It has been well documented that local exposure to TRPA1 agonists in experimental animals is associated with an immediate nociceptive response, lasting for a few minutes, and a delayed more prolonged mechanical allodynia [117,123]. To investigate whether AIs activate such a nociceptive and hyperalgesic TRPA1- dependent pathway, we used one steroidal (exemestane) and one non-steroidal (letrozole) AI. Given the chemical similarity and the hypothesized analogous mechanism of the two non-steroidal AIs, to minimize the number of animals used, anastrozole was not investigated in the following *in vivo* experiments. Intraplantar (i.pl.) injection (20 µl/paw) of exemestane (1, 5, and 10 nmol) (Supplementary Figure 2a) or letrozole (10, 20 nmol) (Supplementary Figure 2e) evoked an acute (0-5 min) nociceptive response and a delayed (15-120 min for exemestane and 15-240 min for letrozole) mechanical allodynia in C57BL/6 mice (Supplementary Figure 2c,g). Both the nociceptive response and mechanical allodynia evoked by AIs were confined to the treated paw (Supplementary Figure 2c,g) and were almost completely prevented by intraperitoneal (i.p.) pretreatment with HC-030031 (100 mg/kg), but not with capsazepine (4 mg/kg) (Supplementary Figure 2b,d,f,h). Furthermore, similar to results obtained in C57BL/6 mice, local injection (i.pl.) of exemestane or letrozole in *Trpa1*$^{+/+}$ mice evoked an early nociceptive response and a delayed mechanical allodynia (Supplementary Figure 2i,j). *Trpa1*$^{-/-}$ mice did not develop such responses (Supplementary Figure 2i,j). Thus, by using both pharmacological and genetic tools, we demonstrated that local administration of both steroidal and non-steroidal AIs produces a typical TRPA1-dependent behavior, characterized by acute nociception and delayed mechanical allodynia.

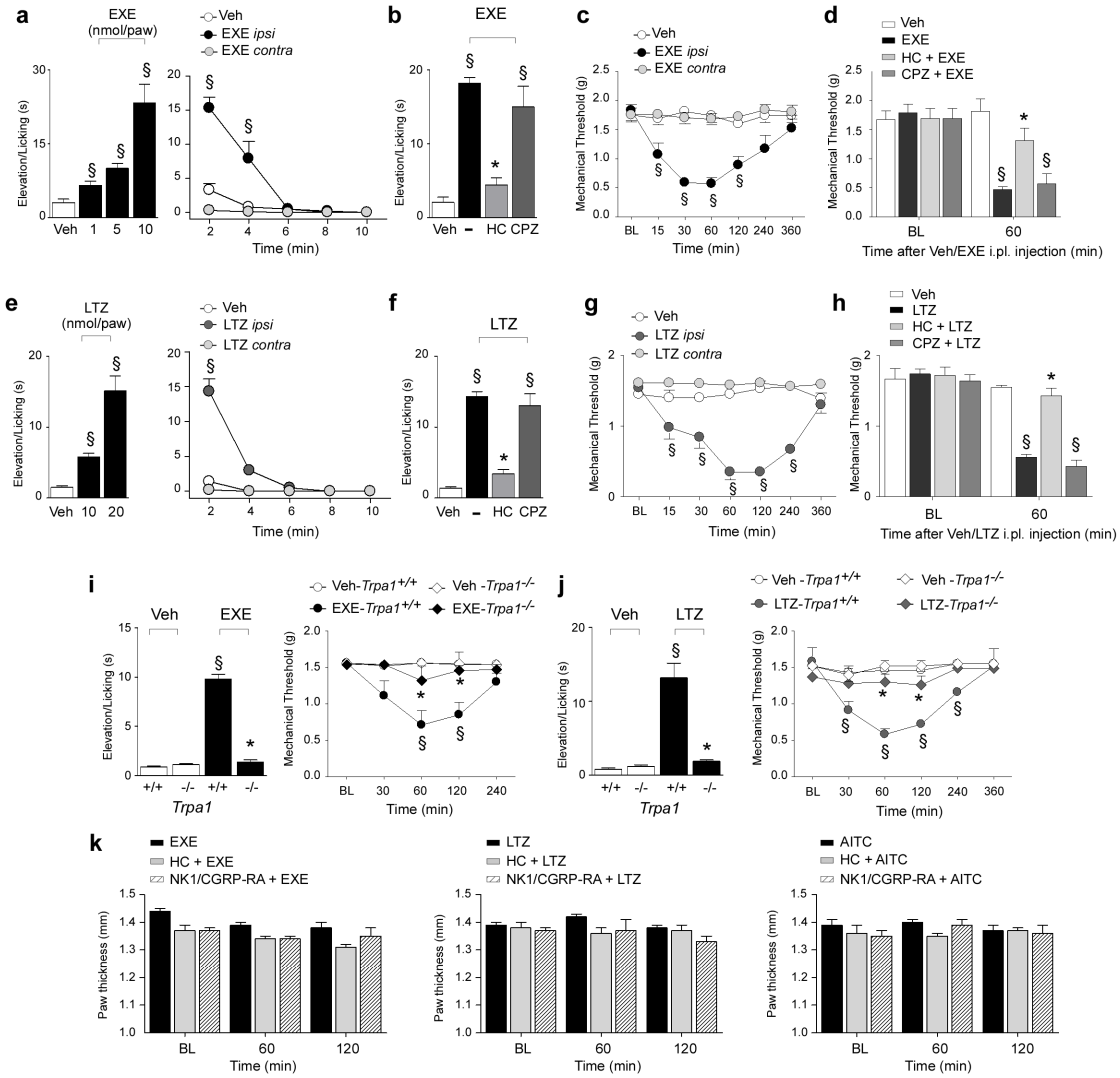

Supplementary Figure 2. **Local administration of exemestane (EXE) or letrozole (LTZ) induces acute nociception and mechanical allodynia *via* TRPA1 activation**. **a** Intraplantar (i.pl., 20 µl) injection of EXE (1-10 nmol) or (**e**) LTZ (10-20 nmol) in C57BL/6 mice induces pain-related behavior that lasts 5 minutes and is attenuated **b**,**f** by intraperitoneal (i.p.) HC-030031 (HC, 100 mg/kg), but not capsazepine (CPZ, 4 mg/kg, i.p.). **c** EXE (10 nmol) and **g** LTZ (20 nmol) produce mechanical allodynia that starts 15 minutes and lasts 120 or 240 minutes, respectively, after the i.pl. injection. **d**,**h** The mechanical allodynia induced by EXE- and LTZ (60 minutes after i.pl. injection) is prevented by systemic HC, but not by CPZ. Results represent mean ± s.e.m. of at least 5 mice for each group. Veh is the vehicle of EXE or LTZ, dash (-) indicates the combination of the vehicles of HC and CPZ. $^{§}P<0.05$ *vs.* Veh or BL values, $^{*}P<0.05$ *vs.* EXE, LTZ; ANOVA followed by Bonferroni *post hoc* test. **i,j** EXE (10 nmol) or LTZ (20 nmol) (both i.pl., 20 µl) produce acute nociception and mechanical allodynia in *Trpa1*$^{+/+}$ mice, which are markedly reduced in *Trpa1*$^{-/-}$ mice. Results are mean ± s.e.m. of at least 5 mice for each group. Veh is the vehicle of EXE or LTZ. $^{§}P<0.05$ *vs.* Veh, $^{*}P<0.05$ *vs.* EXE- or LTZ- *Trpa1*$^{+/+}$; ANOVA and Bonferroni *post hoc* test. **k** Injection (20 µl, i.pl.) of EXE (10 nmol), LTZ (20 nmol) or allyl isothiocyanate (AITC, 10 nmol) in the ipsilateral side (right paw) does not induce paw edema in the contralateral side (left paw). In all conditions baseline levels (BL) were recorded 30 minutes before EXE, LTZ or AITC administration.

2.2.3 AIs produce neurogenic oedema by releasing sensory neuropeptides

TRPA1 is expressed by peptidergic nociceptors, and its stimulation is associated with proinflammatory neuropeptide release and the ensuing neurogenic inflammatory responses [123,187]. First, we explored whether AIs are able to directly promote the release of CGRP (one of the proinflammatory neuropeptides, which are usually co- released upon stimulation of peptidergic nociceptors) [15,254] *via* a TRPA1-dependent pathway. AIs

increased CGRP outflow from slices of rat dorsal spinal cord (an anatomical area enriched with central terminals of nociceptors). This effect was substantially attenuated in rat slices pretreated with a desensitizing concentration of capsaicin (10 μM, 20 min) or in the presence of HC-030031 (Figure 3a). The increase in CGRP outflow observed in slices obtained from *Trpa1*$^{+/+}$ mice was markedly reduced in slices obtained from *Trpa1*$^{-/-}$ mice (Figure 3b).

These neurochemical data were corroborated by functional experiments. Injection (i.pl.) of the TRPA1 agonist, AITC (10 nmol/paw), induced paw edema that peaked at 60 min after injection. The response was abated by treatment with HC- 030031 (100 mg/kg, i.p.) or a combination of the SP neurokinin-1 (NK-1) receptor antagonist, L-733,060, and the CGRP receptor antagonist, CGRP8-37 (both, 2 μmol/kg, intravenous, i.v.) (Figure 3c). Similarly, we found that i.pl. administration of exemestane (10 nmol/paw) and letrozole (20 nmol/paw) caused paw edema that peaked at 60 minutes and faded 120 minutes after injection (Figure 3c, insets). Treatment with HC-030031 (100 mg/kg, i.p.) or a combination of L-733,060 and CGRP8-37 (both, 2 μmol/kg, i.v.), markedly reduced the AI-evoked edema (Figure 3c). No edema was found in the paw contralateral to that injected with AIs (Supplementary Figure 2k). Importantly, the edema produced in *Trpa1*$^{+/+}$ mice by exemestane and letrozole was markedly attenuated in *Trpa1*$^{-/-}$ mice (Figure 3d). Next, to directly evaluate the ability of AIs to release CGRP from peripheral terminals of peptidergic nociceptors, AIs were administered to the rat knee joint. Intraarticular (i.a., 50 μl) injection of exemestane (5 nmol) or letrozole (10 nmol) increased CGRP levels in the synovial fluid, an effect that was markedly attenuated by pretreatment with HC- 030031 (100 mg/kg, i.p.) (Figure 3e). Neurochemical and functional data indicate that AIs by TRPA1 activation release sensory neuropeptides from sensory nerve endings, and by this mechanism promote neurogenic inflammatory responses in the innervated peripheral tissue.

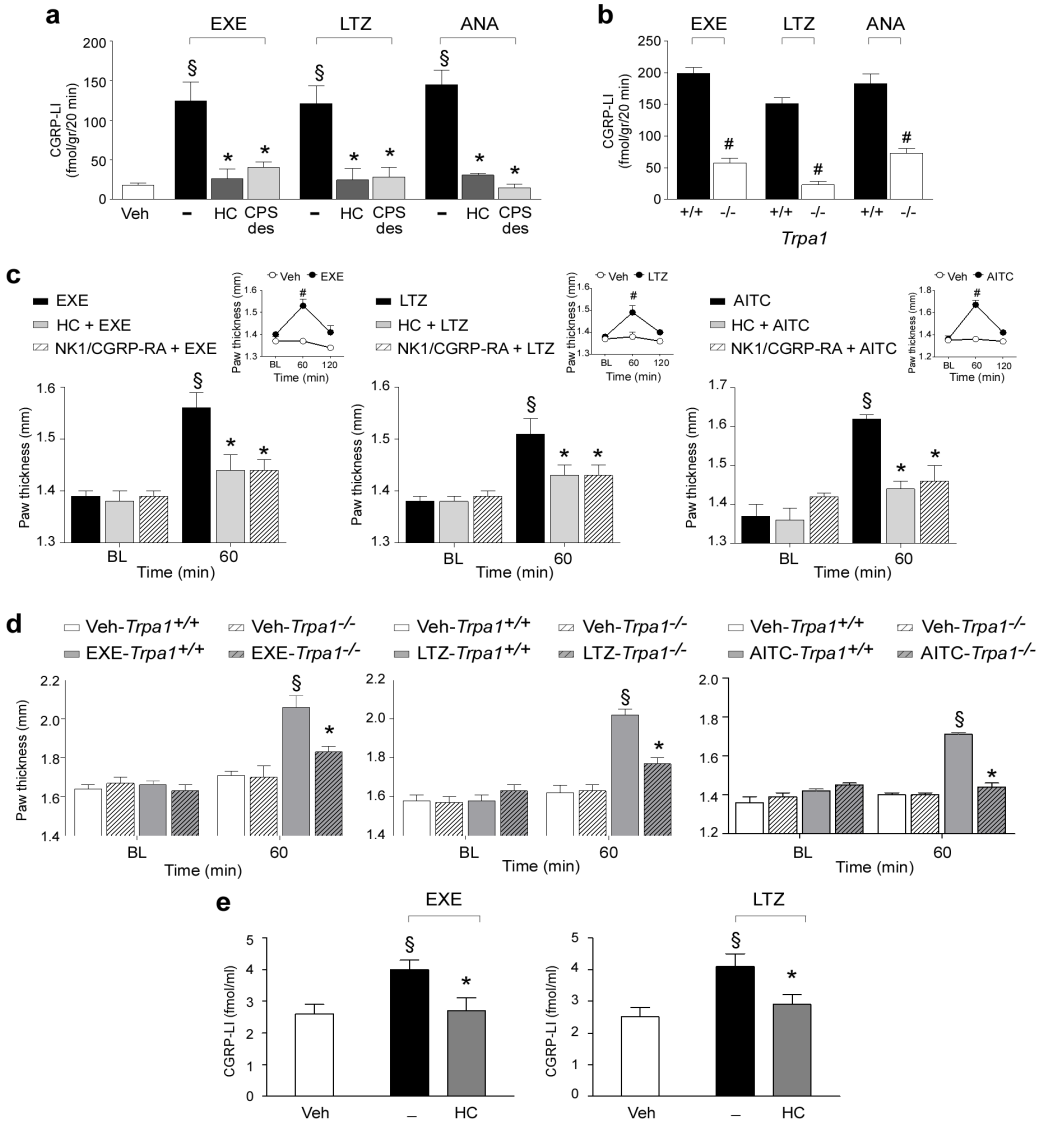

Figure 3. Aromatase inhibitors release calcitonin gene-related peptide (CGRP) and produce neurogenic edema. a Exemestane (EXE), letrozole (LTZ) and anastrozole (ANA) (all 100 μM) increase the CGRP-like immunoreactivity (CGRP-LI) outflow from slices of rat dorsal spinal cord. This effect is prevented by HC-030031 (HC; 30 μM) or after exposure to capsaicin (10 μM, 20 minutes; CPS- des). **b** EXE, LTZ and ANA (all 100 μM) increase the CGRP-LI outflow from spinal cord slices obtained from *Trpa1*$^{+/+}$, but not from *Trpa1*$^{-/-}$ mice. Results are mean ± s.e.m. of at least 4 independent experiments. Veh is the vehicle of EXE, LTZ and ANA, dash (-) indicates the vehicle of HC and CPS.
§*P*<0.05 *vs*. Veh, **P*<0.05 *vs.* EXE, LTZ or ANA; ANOVA followed by Bonferroni *post hoc* test.
#*P*<0.05 *vs.* EXE-, LTZ-, ANA-*Trpa1*$^{+/+}$, Student's T test. **c** In C57BL/6 mice intraplantar (i.pl.) injection (20 μl) of EXE (10 nmol), LTZ (20 nmol) or allyl isothiocyanate (AITC; 10 nmol) induces paw edema, which peaks at 60 minutes and fades 120 minutes after injection (**c**, upper insets), and is attenuated by pretreatment with HC (100 mg/kg intraperitoneal, i.p.) or the combination of the selective antagonists of the neurokinin-1 receptor, (NK1-RA), L-733,060, and of the CGRP receptor (CGRP-RA), CGRP8-37, (both, 2 μmol/kg, intravenous). **d** Paw edema induced by EXE, LTZ and AITC (i.pl.) in *Trpa1*$^{+/+}$ mice is markedly reduced in *Trpa1*$^{-/-}$ mice. BL, baseline level. Results are mean ± s.e.m. of at least 5 mice for each group. Veh is the vehicle of EXE, LTZ and AITC. #*P*<0.05 *vs*. Veh, Student's T test; §*P*<0.05 *vs.* BL values, **P*<0.05 *vs.* EXE, LTZ, AITC or EXE-, LTZ-, AITC-*Trpa1*$^{+/+}$; ANOVA followed by Bonferroni *post hoc* test. **e** Injection (50 μl) of EXE (5 nmol) or LTZ (10 nmol) in the rat knee increases CGRP-LI levels in the synovial fluid, an effect that is markedly attenuated by pretreatment with HC (100 mg/kg, i.p.). Results are mean ± s.e.m. of at least 5 mice for each group. Veh is the vehicle of EXE and LTZ, dash (-) indicates the vehicle of HC. §*P*<0.05 *vs.* Veh, **P*<0.05 *vs.* EXE, LTZ; ANOVA followed by Bonferroni *post hoc* test.

2.2.4 Systemic AIs induce prolonged pain-like effects by targeting TRPA1

AIs are given to patients by a systemic route of administration. Therefore, we explored in mice whether intraperitoneal (i.p.) or intragastric (i.g.) administration of exemestane and letrozole could produce pain-like effects *via* TRPA1 activation. For i.p. administration experiments, doses, corresponding to those used in humans, were selected according to the mouse to human conversion factor indicated by the National Institute of Health [255]. Exemestane (5 mg/kg, i.p.) or letrozole (0.5 mg/kg, i.p) injection did not produce any visible nociceptive behavior (Supplementary Figure 3a and Supplementary Figure 4a, insets) in mice. However, 3 hours after exemestane or letrozole administration, mice developed a prolonged (3 hours) mechanical allodynia (Supplementary Figure 3a and Supplementary Figure 4a) and a reduction in forelimb grip strength (Supplementary Figure 3c and Supplementary Figure 4c), a test used in its clinical version for the study of musculoskeletal pain in patients [256]. When mechanical allodynia by exemestane or letrozole was at its maximum, systemic HC-030031 administration (100 mg/kg, i.p.) transiently reverted both responses (Supplementary Figure 3b,d and Supplementary Figure 4b,d). Furthermore, mechanical allodynia and the reduction in forelimb grip strength produced by exemestane and letrozole in *Trpa1*$^{+/+}$ mice were markedly reduced in *Trpa1*$^{-/-}$ mice (Supplementary Figure 3e,f and Supplementary Figure 4e,f). In experiments where AIs were given by intragastric (i.g.) gavage, doses were adjusted considering the oral bioavailability in humans, which is 99% for letrozole [257], and 40% (with food) for exemestane [258]. First, we found that after i.g. administration of exemestane (10 mg/kg) or letrozole (0.5 mg/kg) their peak plasma levels (13.2 ± 1.7 ng/ml, n=5; and 60.5 ± 12.1 ng/ml, n=5, respectively) (Supplementary Figure 5) approximated the maximum plasma concentrations found in humans [257,259]. Second, results similar to those obtained after i.p. administration were reported when AIs were given by i.g. gavage. First, exemestane (10 mg/kg, i.g.) or letrozole (0.5 mg/kg, i.g.) ingestion was not associated with any spontaneous nocifensor behavior (Figure 4a and 5a, insets). Second, exemestane or letrozole produced, with a similar time-course, mechanical allodynia and a marked reduction in forelimb grip strength (Figure 4a,c and Figure 5a,c). Pretreatment with HC-030031 or deletion of TRPA1 (*Trpa1*$^{-/-}$ mice) significantly attenuated both responses (Figure 4b,d,e,f and Figure 5b,d,e,f). Furthermore, since in clinical practice patients are treated with AIs on a daily basis over very long periods of time (up to 5 years), we asked whether exemestane or letrozole maintain the ability to evoke a TRPA1-dependent mechanical hypersensitivity and decreased grip strength upon repeated administration. In *Trpa1*$^{+/+}$ mice, treatment with systemic exemestane (5 mg/kg, i.p.) or letrozole (0.5 mg/kg i.p) (both once a day for 15 consecutive days) produced at day 1, 5, 10 and 15 a transient

(from 1 to 6 hours) and reproducible mechanical allodynia (Supplementary Figure 3e and Supplementary Figure 4e). Importantly, in *Trpa1*$^{-/-}$ the proalgesic action of AIs was markedly attenuated (Supplementary Figure S3e and Supplementary Figure S4e). In addition, the decrease in the grip strength was maintained, without undergoing desensitization, over the entire time period of daily i.p. administration of exemestane or letrozole (Supplementary Figure S3f and Supplementary Figure S4f). Both these effects of AIs were significantly reduced in *Trpa1*$^{-/-}$ mice (Supplementary Figure 3f and Supplementary Figure 4f). Similar results were obtained after i.g. administration of exemestane or letrozole (once a day for 15 consecutive days at the dose of 10 mg/kg i.g. or 0.5 mg/kg i.g., respectively). Both mechanical allodynia and decreased grip strength were observed, without signs of desensitization, over the 15 days of observation in *Trpa1*$^{+/+}$ mice, but were markedly reduced in *Trpa1*$^{-/-}$ mice (Figure 4e,f and Figure 5e,f). Altogether, the present data demonstrate that both steroidal and non- steroidal third-generation AIs induce a series of pain-like effects predominantly *via* a TRPA1-dependent mechanism, effects that over time do not undergo desensitization, thus mimicking the chronic clinical condition.

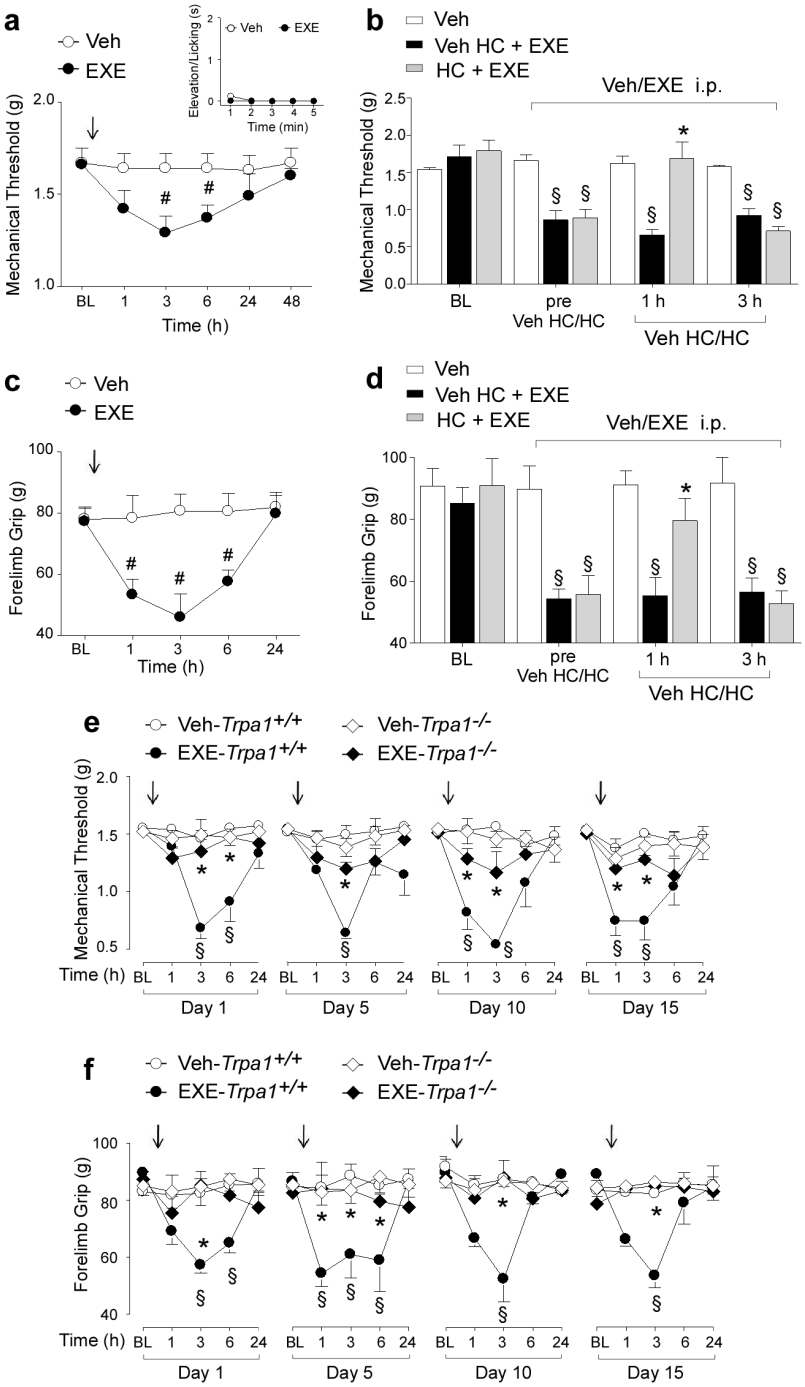

Supplementary Figure 3. Intraperitoneal exemestane (EXE) induces TRPA1-dependent prolonged mechanical allodynia and reduction in forelimb grip strength in mice. In C57BL/6 mice intraperitoneal (i.p.) administration of EXE (5 mg/kg) induces **a** mechanical allodynia and (**c**) a reduction in forelimb grip strength that last 3-6 hours after administration. EXE does not produce any acute nocifensor behavior as measured by the indicated test (**a,** inset). **b,d** Three hours after EXE administration, HC-030031 (HC; 100 mg/kg i.p.) reverts both mechanical allodynia and reduction in forelimb grip strength. Inhibition is no longer visible 3 hours after its administration. Veh is the vehicle of EXE. $^{\#}P<0.05$ *vs.* Veh; Student's T test **a,c** and $^{\S}P<0.05$ *vs.* Veh and $^{*}P<0.05$ *vs.* Veh HC-EXE; ANOVA followed by Bonferroni *post hoc* test **b,d**. **e,f** EXE (once a day for 15 consecutive days, 5 mg/kg i.p.) induces reproducible mechanical allodynia and decrease in grip strength at day 1, 5, 10 and 15 in *Trpa1*$^{+/+}$mice. Arrows indicate Veh or EXE administration. Both these effects are markedly reduced in *Trpa1*$^{-/-}$ mice. $^{\S}P<0.05$ *vs.* Veh-*Trpa1*$^{+/+}$, $^{*}P<0.05$ *vs* EXE-*Trpa1*$^{+/+}$; ANOVA followed by Bonferroni *post hoc* test. Results are mean ± s.e.m. of at least 5 mice for each group. In all conditions baseline levels (BL) were recorded 30 minutes before EXE administration.

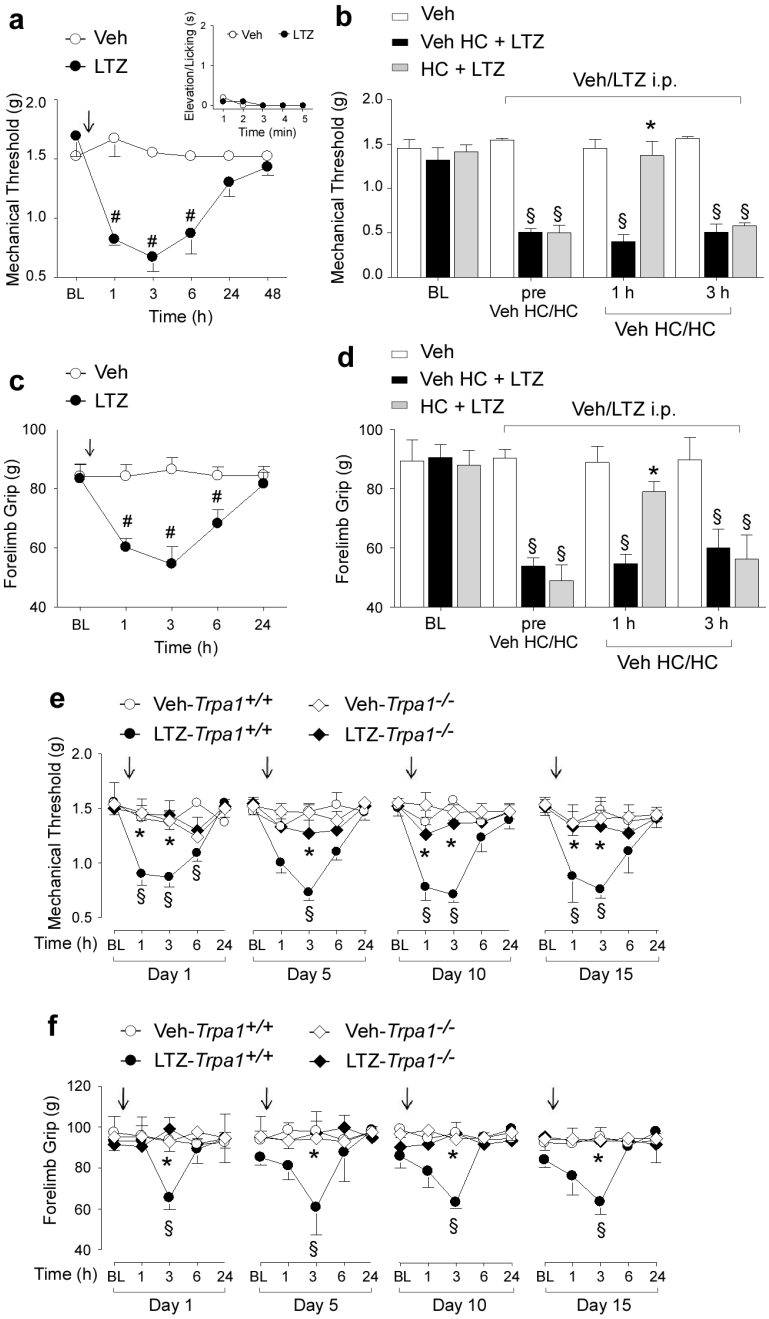

Supplementary Figure 4. Intraperitoneal letrozole (LTZ) induces TRPA1-dependent prolonged mechanical allodynia and reduction in forelimb grip strength in mice. Intraperitoneal (i.p.) administration of LTZ (0.5 mg/kg) induces **a** mechanical allodynia and (**c**) a reduction in forelimb grip strength that last 3-6 hours after administration in C57BL/6 mice. LTZ does not produce any acute nocifensor behavior as measured by the indicated test (**a,** inset). **b,d** Three hours after LTZ administration HC-030031 (HC; 100 mg/kg i.p.) reverts both mechanical allodynia and reduction in forelimb grip strength. Inhibition by HC is no longer visible 3 hours after its administration. Veh is the vehicle of LTZ. $^{\#}P<0.05$ *vs.* Veh; Student's T test **a,c** and $^{\S}P<0.05$ *vs.* Veh and $^{*}P<0.05$ *vs.* Veh HC-LTZ; ANOVA followed by Bonferroni *post hoc* test **b,d**. **e,f** LTZ (once a day for 15 consecutive days, 0.5 mg/kg i.p.) induces reproducible mechanical allodynia and decrease in grip strength at day 1, 5, 10 and 15 in *Trpa1*$^{+/+}$mice. Arrows indicate Veh or LTZ administration. Both these effects are markedly reduced in *Trpa1*$^{-/-}$ mice. $^{\S}P<0.05$ *vs.* Veh-*Trpa1*$^{+/+}$, $^{*}P<0.05$ *vs.* LTZ-*Trpa1*$^{+/+}$; ANOVA followed by Bonferroni *post hoc* test. Data are mean ± s.e.m. of at least 5 mice for each group. In all conditions baseline levels (BL) were recorded 30 minutes before LTZ administration.

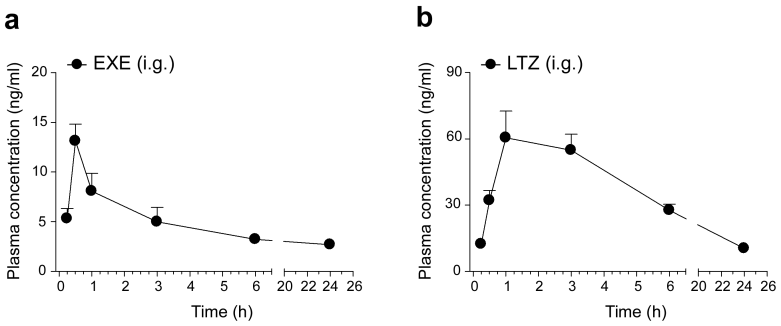

Supplementary Figure 5. Concentration-time profiles of exemestane (EXE) and letrozole (LTZ) in mouse plasma. Plasma concentrations measured at 0.25, 0.5, 1, 3, 6 and 24 hours after the intragastric (i.g.) administration of a single dose of EXE (10 mg/kg) or LTZ (0.5 mg/kg). Data are mean ± s.e.m. of at least 5 mice in each group.

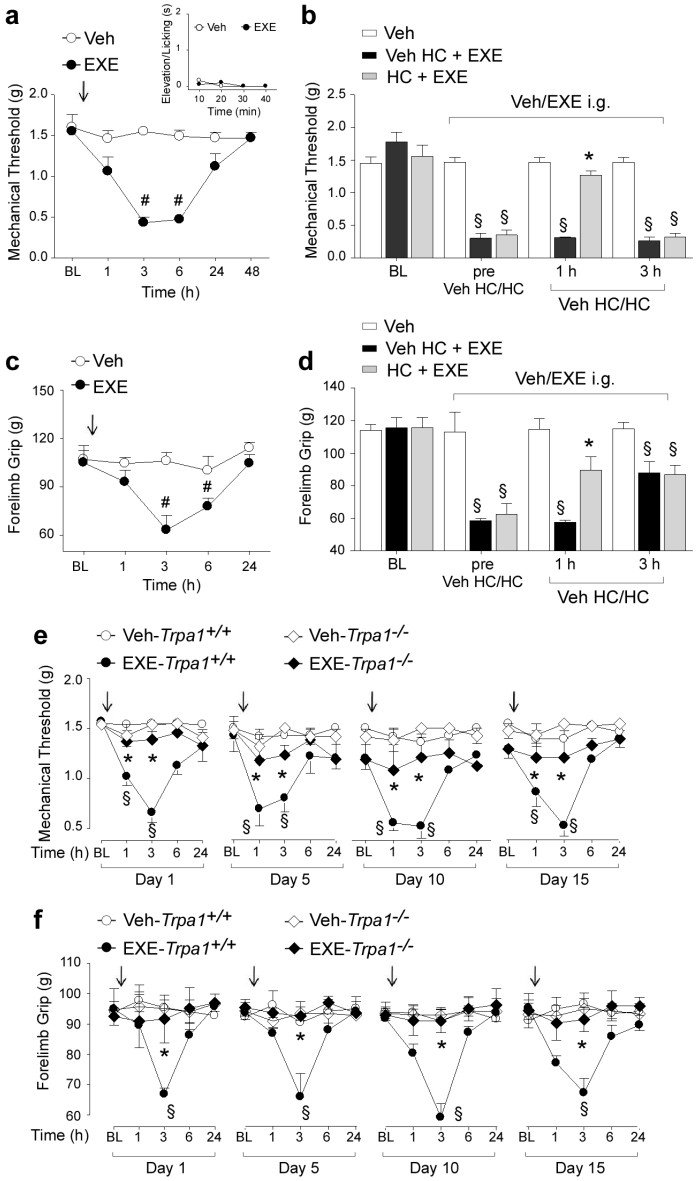

Figure 4. Intragastric exemestane (EXE) induces TRPA1-dependent prolonged mechanical allodynia and reduction in forelimb grip strength in mice. In C57BL/6 mice intragastric (i.g.) administration of EXE (10 mg/kg) induces **a** mechanical allodynia and **c** a reduction in forelimb grip strength that last 3-6 hours after administration. EXE does not produce any acute nocifensor behavior as measured by the indicated test (**a,** inset). **b,d** Three hours after EXE administration, HC-030031 (HC; 100 mg/kg i.p.) reverts both mechanical allodynia and the reduction in forelimb grip strength. HC inhibition is no longer visible 3

hours after its administration. Veh is the vehicle of EXE. #*P*<0.05 *vs.* Veh; Student's T test **a,c** and §*P*<0.05 *vs.* Veh and **P*<0.05 *vs.* Veh HC-EXE; ANOVA followed by Bonferroni *post hoc* test **b,d**. **e,f** EXE (once a day for 15 consecutive days, 10 mg/kg i.g.) induces reproducible mechanical allodynia and decrease in forelimb grip strength at day 1, 5, 10 and 15 in *Trpa1*$^{+/+}$ mice. Arrows indicate Veh or EXE administration. Both these effects are markedly reduced in *Trpa1*$^{-/-}$ mice. §*P*<0.05 *vs.* Veh-*Trpa1*$^{+/+}$, **P*<0.05 *vs.* EXE-*Trpa1*$^{+/+}$; ANOVA followed by Bonferroni *post hoc* test. Results are mean ± s.e.m. of at least 5 mice for each group. In all conditions, baseline (BL) levels were recorded 30 minutes before EXE administration.

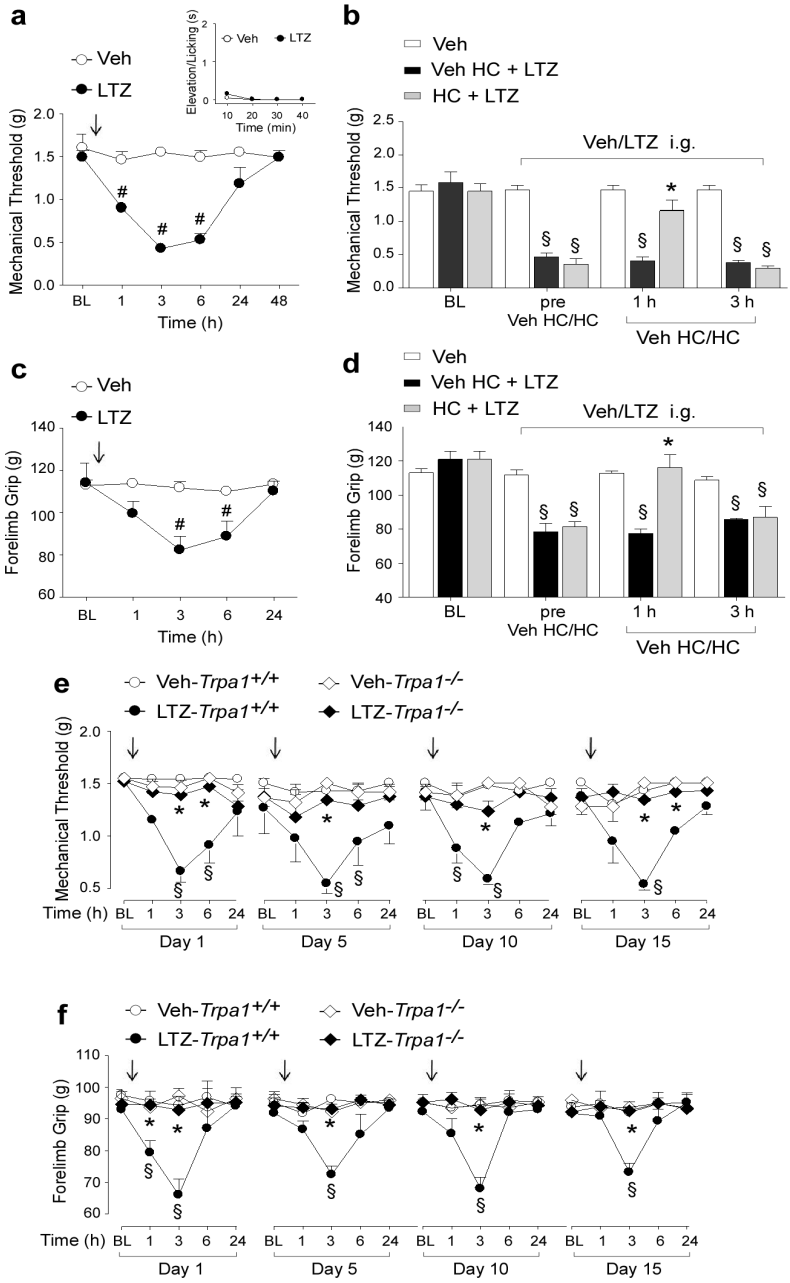

Figure 5. Intragastric letrozole (LTZ) induces TRPA1-dependent prolonged mechanical allodynia and reduction in forelimb grip strength in mice. In C57BL/6 mice intragastric (i.g.) administration of LTZ (0.5 mg/kg) induces **a** mechanical allodynia and **c** reduction in forelimb grip strength that last 3-6 hours after administration. LTZ does not produce any acute nocifensor behavior as measured by the indicated test (a, inset). (b,d) Three hours after LTZ administration, HC-030031 (HC; 100 mg/kg i.p.) reverts both mechanical allodynia and the reduction in forelimb grip strength. HC inhibition is no longer visible 3 hours after its administration. Veh is the vehicle of LTZ. #P<0.05 vs. Veh; Student's T test **a,c** and §P<0.05 vs. Veh and *P<0.05 vs. Veh HC-LTZ; ANOVA followed by Bonferroni post hoc test **b,d**. **e,f** LTZ (once a day for 15 consecutive days, 0.5 mg/kg i.g.) induces reproducible mechanical allodynia and decrease in forelimb grip strength at day 1, 5, 10 and 15 in *Trpa1*$^{+/+}$ mice. Arrows indicate Veh or LTZ administration. Both effects are markedly reduced in *Trpa1*$^{-/-}$ mice. §P<0.05 vs. Veh-*Trpa1*$^{+/+}$, *P<0.05 vs. LTZ-*Trpa1*$^{+/+}$; ANOVA followed by Bonferroni post hoc test. Results are mean ± s.e.m. of at least 5 mice for each group. In all conditions baseline (BL) levels were recorded 30 minutes before LTZ administration.

2.2.5 AI-evoked TRPA1 activation is enhanced by proinflammatory stimuli

Although it affects a large proportion of subjects, not all patients treated with AIs develop AIMSS. One possible explanation for the peculiar susceptibility to AIMSS of some patients is that, if TRPA1 activation is a necessary prerequisite, *per se* it is not sufficient, and additional proalgesic factors must contribute to the development of pain symptoms. It has been reported that stimulation of proalgesic pathways exaggerates TRPA1-dependent responses *in vitro* and *in vivo* [147,260]. One example of such potentiating action has been reported for the proteinase-activated receptor-2 (PAR2), whose subthreshold activation results in an exaggerated response to the TRPA1 agonist, AITC [147]. PAR2 undergoes activation upon a unique proteolytic mechanism by cleavage of its tethered ligand domain by trypsin and other proteases, thus mediating inflammation and hyperalgesia [261]. On this basis, and following a previously reported protocol [147], we explored, by *in vivo* functional experiments in C57BL/6 mice, whether PAR2 activation exaggerates TRPA1-dependent hypersensitivity induced by AIs. Prior (10 minutes) injection (i.pl.) of the PAR2 activating peptide (AP) (PAR2-AP, 1 μg/paw), but not the reverse peptide (RP) (PAR2-RP, 1 μg/paw, inactive on PAR2), markedly enhanced the duration of licks and flinches of the hind paw produced by local injection (i.pl.) of exemestane (1 nmol/paw) and letrozole (10 nmol/paw) (Figure 6a). The injected dose of PAR2-AP, as well as PAR2-RP, did not cause *per se* any visible acute nocifensor response (Figure 6a). The exaggerated responses to the combination of PAR2-AP and exemestane or letrozole were inhibited by HC-030031 (100 mg/kg, i.p.) (Figure 6a).

We also tested the ability of a recognized endogenous TRPA1 agonist, H_2O_2 [112,127] to increase the nocifensor response of exemestane or letrozole. In addition, we explored the ability of AIs to increase either nociception or mechanical allodynia to H_2O_2. H_2O_2 (0.5 μmol/paw) injection produced a transient nocifensor behavior that terminated within 5 min (Figure 6b, inset). We found that 10 min after H_2O_2 injection (when baseline levels of nociception were restored) administration of exemestane (1 nmol/paw) and letrozole (10 nmol/paw) evoked nociceptive responses markedly increased as compared to vehicle-pretreated mice (Figure 6b). The exaggerated responses to AIs were inhibited by HC-030031 (Figure 6b). Thus, both homologous activation of the channel by the TRPA1 agonist H_2O_2, or heterologous stimulation of a classical proinflammatory pathway, such as PAR2, converge in a final common pathway, which results in the potentiation of the AI-evoked and TRPA1-dependent proalgesic mechanism. In the attempt to understand the mechanism underlying the *in vivo* potentiation between PAR2 or H_2O_2 and AIs, cultured DRG neurons were challenged with combinations of these same agents. First, in *in vitro* electrophysiological experiments, we found that AITC, exemestane and letrozole (all 100

μM) produced inward currents in cultured DRG neurons, effects that were abated in the presence of HC-030031 (50 μM). However, HC-030031 did not affect the inward current produced by capsaicin (Figure 6c). Second, we showed that pre-exposure to subthreshold concentrations of PAR2-AP or H_2O_2 enhanced currents evoked by subthreshold concentrations of either exemestane or letrozole (both 20 μM) (Typical traces Figure 6d and pooled data Figure 6e). Third, HC-030031 inhibited the exaggerated responses (Figure 6e).

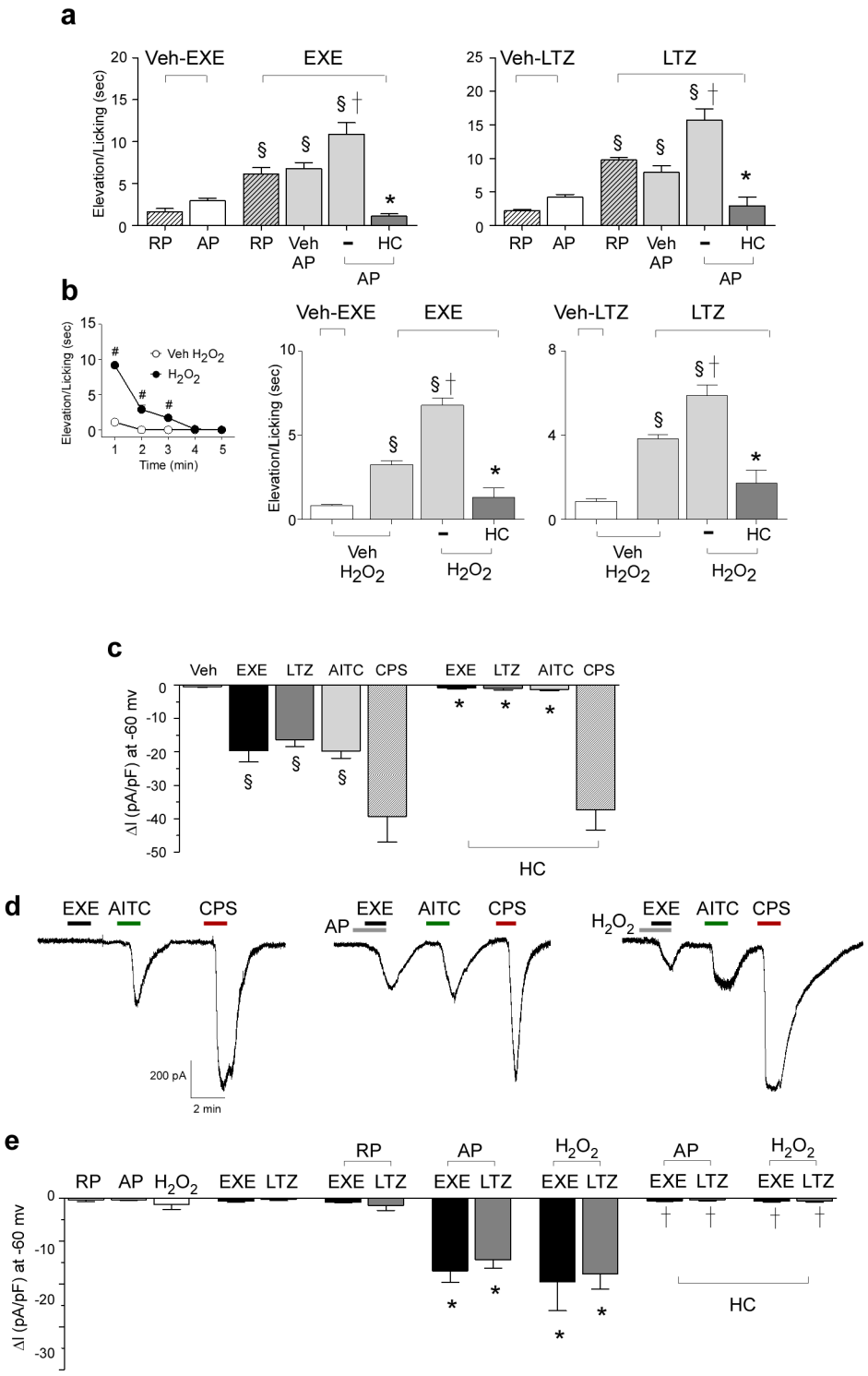

Figure 6. TRPA1-activation by exemestane (EXE) and letrozole (LTZ) is enhanced by proinflammatory stimuli. a Intraplantar (i.pl.; 10 µl) pretreatment (10 minutes) with the proteinase-activated receptor 2 (PAR2) activating peptide (AP; 1 µg), but not with the inactive PAR2 reverse peptide (RP; 1 µg), enhances nocifensor behavior produced by EXE (1 nmol/10 µl, i.pl.) or LTZ (10 nmol/10 µl, i.pl.). AP and RP alone cause negligible nociception. The potentiated responses to EXE or LTZ are markedly attenuated by HC-030031 (HC; 100 mg/kg, i.p.). **b** H_2O_2 (0.5 µmol/10 µl, i.pl.) injection produces a transient nocifensor behavior, lasting only 5 minutes (**b**, inset). Pretreatment (10 minutes before AI administration) with H_2O_2 (0.5 µmol/10 µl, i.pl.) increases nocifensor behavior produced by EXE (1 nmol/10 µl, i.pl.) or LTZ (10 nmol/10 µl, i.pl.). HC (100 mg/kg, i.p.) inhibits the exaggerated responses to both EXE and LTZ. Dash (-) indicates the vehicle of HC. Points or columns are mean ± s.e.m. of at least 5 mice for each group. §P<0.05 *vs.* RP or AP or Veh H_2O_2; †P<0.05 *vs.* Veh AP/EXE or Veh AP/LTZ or Veh H_2O_2/EXE or Veh H2O2/LTZ; *P<0.05 *vs.* AP/EXE or AP/LTZ or H_2O_2/EXE or H_2O_2/LTZ*;* ANOVA followed by Bonferroni *post hoc* test. #P<0.05 *vs.* Veh H_2O_2, Student's T test. **c** An active concentration of EXE or LTZ (both 100 µM) evokes inward currents in rat dorsal root ganglion (DRG) neurons, which also respond to allyl isothiocyanate (AITC; 100 µM) and capsaicin (CPS; 1 µM). Inward currents evoked by EXE, LTZ or AITC are inhibited in the presence of HC (50 µM), which does not affect CPS-evoked currents. Typical traces **d** and pooled data **e** showing that pre-exposure to AP (100 µM) or H_2O_2 (100 µM) exaggerates currents evoked by a subthreshold concentration of EXE and LTZ (both 20 µM). The inactive RP does not affect responses to EXE or LTZ (both 20 µM). The potentiated responses to EXE or LTZ are markedly attenuated by HC (50 µM). Veh is the vehicle of EXE, LTZ and AITC. Results are mean ± s.e.m. of at least 5 independent experiments. §P<0.05 *vs.* Veh, *P<0.05 *vs.* EXE, LTZ or AITC and †P<0.05 *vs.* EXE- or LTZ-AP and EXE- or LTZ- H_2O_2; ANOVA followed by Bonferroni *post hoc* test.

2.3 Discussion

In the present study, we provide for the first time evidence that third-generation steroidal and non-steroidal AIs, proven to be very effective drugs in the treatment of hormone receptor-positive breast cancer [160,161] selectively target the TRPA1 channel. This conclusion derives from a series of experiments in cells expressing the recombinant human TRPA1 or in rodent DRG neurons expressing the native channel. Indeed, calcium responses and currents evoked by AIs are confined to TRPA1- expressing cells, and are selectively abolished by HC-030031, or absent in neurons obtained from TRPA1-deficient mice. Exemestane exhibits a chemical structure with a system of highly electrophilic conjugated Michael acceptor groups [172]. A variety of known TRPA1 agonists, including acrolein and other α,β-unsaturated aldehydes, possess an electrophilic carbon or sulfur atom that is subject to nucleophilic attack (Michael addition) by cysteine and lysine residues [262]. Nitriles also exhibit electrophilic properties, which may result in TRPA1 gating [263]. Non-steroidal letrozole and anastrozole possess nitrile moieties that underscore their potential ability to activate TRPA1. We show that key cysteine and lysine residues, required for channel activation by electrophilic agonists [47,121,123] are also required for TRPA1 activation by AIs. Thus, the three AIs, most likely because of their electrophilic nature, selectively target TRPA1, whereas TRPV1, TRPV2, TRPV3 and TRPV4, all co-expressed with TRPA1 [79,98], and other channels or receptors in DRG neurons, do not seem to play a relevant role in the direct excitation of nociceptors by AIs. TRPA1-expressing neurons activated by AIs also responded to capsaicin, a selective TRPV1 agonist. As TRPV1 is considered a specific marker of nociceptors [264], AIs may be assumed to activate pain-like responses. *In vivo* stimulation of the irritant TRPA1 receptor in rodents produces an early nociceptive behavior, followed by a delayed and prolonged mechanical allodynia [117,123,149]. Subcutaneous exemestane and letrozole recapitulated the two effects produced by TRPA1 agonists, and produced such responses in a TRPA1-dependent way. Magnetic resonance imaging of painful wrists in patients treated with AIs has shown signs of inflammatory tenosynovitis poorly reverted by common anti- inflammatory treatments [254]. Systemic increases in plasma cytokines have not been found in patients with AIMSS and, therefore, do not appear to represent the underlying mechanism for such inflammatory conditions [166,265]. This implies that pathways different from cytokine-dependent inflammation operate in joints of patients treated with AIs. As TRPA1 is expressed by a subpopulation of peptidergic nociceptors, which mediate neurogenic inflammation [15,79] we anticipated that AIs, by targeting

TRPA1, release proinflammatory neuropeptides, thereby causing neurogenic plasma extravasation. Pharmacological and genetic findings indicate that AIs produce a specific type of edema, which is neurogenic in nature. The conclusion is corroborated by the direct neurochemical observation that exemestane and letrozole evoke TRPA1-dependent CGRP release from peripheral endings of primary sensory neurons. The neurogenic component, mediated by TRPA1-activation and sensory neuropeptide release, may thus represent an important mechanism contributing to the cytokine-independent inflammation observed in AI users. When AIs were given to mice by systemic (intraperitoneal or intragastric) administration, no acute nocifensive response was observed, but, after ~1 hour delay they produced a prolonged condition (up to 6 hours) of mechanical allodynia and a decrease in forelimb grip strength. Also, in this case, pharmacological and genetic results indicate that AI-evoked pain-like responses are principally TRPA1-dependent. In clinical practice, AIs are used for a 3- or 5-year period, and the pain condition associated to their use is often persistent [266]. Although the present experimental conditions cannot fully mimic the clinical setting in cancer patients, our findings suggest that the TRPA1-dependent ability of AIs to produce mechanical allodynia and to decrease forelimb grip strength is maintained and does not undergo desensitization in mice over a time period of 15 days, which broadly corresponds to a 1-year time in humans. Despite a general good tolerability [169], AIs produce some types of pain, including AIMSS and neuropathic, diffuse and mixed pain in 10-20% of the treated patients [166]. The reason why only some of the patients exposed to AIs develop these severe pain conditions, which may lead to non-adherence or therapy discontinuation, is unknown.

Here, we reveal the key role of TRPA1 as the main mediator of exemestane- and letrozole-evoked nociceptor stimulation. However, it is likely that additional factors contribute to determine the development of AIMSS and related pain symptoms, particularly in those susceptible patients who suffer from the more severe form of this adverse reaction. *In vitro* and *in vivo* experiments with the co-administration of AIs and pro-algesic stimuli, such as PAR2-AP, an agonist of the pro-inflammatory receptor, PAR2, and the TRPA1 agonist, H_2O_2 [112], indicate that additional factors may cooperate to increase the sensitivity to AIs of TRPA1 expressing nociceptors. Enhancement by PAR2 activation of the proalgesic activity of exemestane and letrozole is fully consistent and closely mimic previous observations that PAR2 activation increases the pro-algesic response evoked by TRPA1 agonists [147]. Findings that a combination of AIs and H_2O_2

exaggerates TRPA1-mediated *in vitro* and *in vivo* responses suggest that increased levels of oxidative stress byproducts, known to be generated under inflammatory conditions [267] may facilitate the development of AIMSS and related pain symptoms. Our present investigation on the cooperation between AIs and proinflammatory mediators has been limited to PAR2 and H_2O_2. However, it is possible that additional pro-inflammatory and pro-algesic mediators can activate similar cooperating pathways. AI concentrations required for TRPA1 activation are higher than those found in the plasma of treated subjects [268,269]. However, it should be noted that all three AIs have a large volume of distribution, indicating a high tissue distribution [257,259]. The present findings that in mice plasma levels of both AIs were comparable to those found in humans [257,259] strengthen the hypothesis that compartmentalization of AIs in mice is similar to that reported in humans [257,259]. Thus, under standard drug regimens, concentrations sufficient to activate TRPA1 or to potentiate TRPA1-mediated responses evoked in cooperation with inflammatory mediators may be reached in tissues neighboring sensory nerve terminals. Altogether, the present results indicate that AIs *per se* or, most likely, in cooperation with other proinflammatory mediators, promote TRPA1-dependent neurogenic inflammation, mechanical hypersensitivity, and decreased forelimb grip force in rodents. This novel pathway may represent the main underlying mechanism responsible for pain and inflammatory symptoms associated with AI treatment. The other important proposal deriving from the present findings is that antagonists of the TRPA1 channel may be beneficial in the prevention and treatment of such painful conditions.

This work has been published in Nature Communications

Fusi C, Materazzi M, Benemei S, Coppi E, Trevisan G, Marone IM, Minocci D, De Logu F, Tuccinardi T, Di Tommaso MR, Susini T, Moneti G, Pieraccini G, Geppetti P, Nassini R (2014). "Steroidal and non-steroidal third-generation aromatase inhibitors induce pain-like symptoms via TRPA1" Nat Commun 5(5736):5736.

Chapter III - TRPA1 mediates aromatase inhibitor-evoked pain by the aromatase substrate androstenedione

3.1 Methods

Animals. *In vivo* experiments and tissue collection were carried out according to the European Union (EU) guidelines and Italian legislation (DLgs 26/2014, EU Directive application 2010/63/EU) for animal care procedures, and under University of Florence research permits #204/2012-B and #194/2015-PR. C57BL/6 mice (male, 20-25 g, 5 weeks; Envigo, Milan, Italy; N=284), littermate wild type (*Trpa1*$^{+/+}$, N=22) and TRPA1-deficient (*Trpa1*$^{-/-}$; N=22) mice (25-30 g, 5-8 weeks), generated by heterozygotes on a C57BL/6 background (B6.129P-*Trpa1*$^{tm1Kykw/J}$; Jackson Laboratories, Bar Harbor, ME, USA) (19), TRPV1-deficient mice (*Trpv1*$^{-/-}$; B6.129X1-*Trpv1*$^{tm1Jul/J}$; N=8) backcrossed with C57BL/6 mice (*Trpv1*$^{+/+}$; N=8) for at least 10 generations (Jackson Laboratories, Bar Harbor, ME, USA; 25-30 g, 5-8 weeks) or Sprague-Dawley rats (male, 75-100 g, Envigo, Milan, Italy; N=24) were used. Animals were housed in a temperature- and humidity-controlled *vivarium* (12-hour dark/light cycle, free access to food and water). Behavioral experiments were done in a quiet, temperature-controlled (20 to 22 °C) room between 9 a.m. and 5 p.m., and were performed by an operator blinded to genotype and drug treatment. Animals were euthanized with inhaled CO_2 plus 10-50% O_2.

Reagents. The activating peptide of the human protease activated receptor 2 (hPAR2-AP) was synthesized by G. Cirino (University of Naples, Naples, Italy), and dissolved in distilled water. HC-030031 was synthesized as previously described (20). Letrozole, L-733,060, and $CGRP_{8-37}$ were from Tocris Bioscience (Bristol, UK). If not otherwise indicated, all other reagents were from Sigma-Aldrich (Milan, Italy). For *in vitro* experiments, all compounds were dissolved in 100% DMSO at 10 mM concentration.

Cell culture and isolation of primary sensory neurons. Naive untransfected HEK293

cells (American Type Culture Collection, Manassas, VA, USA; ATCC® CRL-1573™) were cultured according to the manufacturer's instructions. HEK293 cells were transiently transfected with the cDNAs (1 μg) codifying for wild type (wt-hTRPA1) or mutant 3C/K-Q (C619S, C639S, C663S, K708Q) (donated by D. Julius, University of California, San Francisco, CA, USA) [121] human TRPA1 (hTRPA13C/K-Q-HEK293) using the jetPRIME transfection reagent (Euroclone, Milan, Italy) according to the manufacturer's protocol. HEK293 cells stably transfected with cDNA for human TRPA1 (hTRPA1-HEK293, donated by A.H. Morice, University of Hull, Hull, UK), or with cDNA for human TRPV1 (hTRPV1-HEK293, donated by M. J. Gunthorpe, GlaxoSmithKline, Harlow, UK), or with cDNA for human TRPV4 (hTRPV4-HEK293, donated by N.W. Bunnett, Monash Institute of Pharmaceutical Sciences, Parkville, Australia), or with cDNA for both human TRPA1 and human TRPV1 (hTRPA1/V1-HEK293, hTRPA1/V1-HEK293, donated by A.H. Morice, University of Hull, Hull, UK) were cultured as previously described [274]. Human lung fibroblasts (IMR90; American Type Culture Collection, Manassas, VA, USA; ATCC® CCL-186™), which express the native TRPA1 channel, were cultured in DMEM supplemented with 10% FBS, 2 mM glutamine, 100 U penicillin and 100 μg/ml streptomycin. Cells were plated on glass coated (poly-L-lysine, 8.3 μM) coverslips and cultured for 2-3 days before being used for recordings. For all cell lines, the cells were used when received without further authentication. Primary DRG neurons were isolated from adult Sprague-Dawley rats and C57BL/6 or *Trpa1*$^{+/+}$ and *Trpa1*$^{-/-}$ mice, and cultured as previously described [174].

Cellular Recordings. Intracellular calcium was measured as previously reported [174]. Results are expressed as the percentage of increase of $Ratio_{340/380}$ over the baseline normalized to the maximum effect induced by ionomycin (5 μM) (% Change in $R_{340/380}$) or as the percentage of responding neurons, identified by KCl (50 mM). Whole-cell patch-clamp recordings were performed as reported elsewhere [174]. Peak currents were normalized to cell membrane capacitance and expressed as mean of the current density (pA/pF) in averaged results. Currents were evoked in the voltage-clamp mode at a holding potential of -60 mV; signals were sampled at 1 kHz and low-pass filtered at 10 kHz. Capsaicin (0.1 or 1 μM) has been used to identify TRPV1-expressing nociceptors.

Behavioral experiments. For behavioral experiments, after habituation, mice (C57BL/6, *Trpa1*$^{+/+}$ and *Trpa1*$^{-/-}$, *Trpv1*$^{+/+}$ and *Trpv1*$^{-/-}$) were randomized into treatment groups, consistent with experimental design. First, we evaluated the acute nocifensive response and mechanical allodynia evoked by ASD, H_2O_2 (20 μl, intraplantar, i.pl.), letrozole (0.5

mg/kg, intragastric, i.g.), or their vehicles [5% DMSO, isotonic saline or 0.5% carboxymethylcellulose (CMC)], respectively. α-lipoic acid (100 mg/kg, i.g.), or its vehicle (0.5% CMC, i.g.), was administered 2 hours after letrozole (i.g.). Mechanical allodynia evoked by the combination of different doses of letrozole (i.g.), ASD (20 µl i.pl.), H_2O_2 (, 20 µl, i.pl.), or their vehicles was studied in C57BL/6, *Trpa1*$^{+/+}$ and *Trp1*$^{-/-}$ mice, with the timing of the various pharmacological interventions based on the timing of the responses to different stimuli. Mechanical allodynia and reduction in grip strength have been studied in C57BL/6 mice, *Trpa1*$^{+/+}$ and *Trpa1*$^{-/-}$ mice treated with systemic D,L-buthionine sulfoximine (BSO) (intraperitoneal, i.p.), ASD (i.p.) and letrozole (i.g.), or their vehicles (isotonic saline, 4% DMSO and 4% Tween 80 and 0.5% CMC, respectively), alone or in combination, with the timing of the various pharmacological interventions based on the timing of the responses to different stimuli.

Acute nocifensive response. Immediately after i.pl. injection of the different compounds, C57BL/6, *Trpa1*$^{+/+}$ and *Trpa1*$^{-/-}$ mice were placed in a Plexiglas chamber, and the total time spent licking and lifting the injected hind paw was recorded for 5 minutes, as previously described [130].

Mechanical stimulation (von Frey hair test). Mechanical threshold was measured in C57BL/6, *Trpa1*$^{+/+}$ and *Trpa1*$^{-/-}$, *Trpv1*$^{+/+}$ and *Trpv1*$^{-/-}$ mice before (basal level threshold) and after the various i.pl. or systemic treatments by using the up-and-down paradigm [250]. The 50% mechanical paw withdrawal threshold response (in g) was then calculated as previously described [249,251]

Forelimb grip strength test. The grip strength test was performed with a grip strength meter (Ugo Basile, Varese, Italy), as previously reported [174,251]. The grip strength was measured in C57BL/6, *Trpa1*$^{+/+}$ and *Trpa1*$^{-/-}$, *Trpv1*$^{+/+}$ and *Trpv1*$^{-/-}$ mice before and after the various treatments.

H_2O_2 levels assay. Sciatic nerves collected from euthanized C57BL/6 mice after various treatments were homogenized in 50 mM phosphate buffer (pH 7.4) containing 5 mM of sodium azide at 4°C for 60 seconds, centrifuged at 12,000xg for 20 minutes at 4°C, and the supernatant was used to determine the H_2O_2 content. H_2O_2 levels were detected by using the phenol red-HRPO method [241] corrected by protein content and expressed as µmol/mg of proteins [270].

Immunostaining. C57BL/6 mice were anesthetized with a mixture (i.p.) of ketamine (90 mg/kg) and xylazine (3 mg/kg), and transcardially perfused with phosphate buffer saline followed by 4% paraformaldehyde. The sciatic nerve with the surrounding tissue was

removed and embedded in paraffin. Immunofluorescence staining for 4-hydroxynonenal adducts and TRPA1 was performed as previously reported [240].

Plasma protein extravasation. BSO was given 30 minutes before letrozole, and ASD immediately after letrozole; mice were anesthetized 15 minutes after letrozole as previously described [123]. HC-030031 (100 mg/kg, i.p.) or its vehicle (4% DMSO plus 4% Tween80, i.p.), or a combination of L-733,060 and $CGRP_{8-37}$, (NK_1/CGRP-RA; both 2 μmol/kg, i.v.) or its vehicle (isotonic saline), were administered 60 minutes or 15 minutes before ASD, respectively. The extravasated dye was extracted from synovial tissue of the knee joint by overnight incubation in formamide, and assayed by spectrophotometry at 620 nm, as previously reported [187].

Synovial fluid lavage. The synovial fluid was collected from anesthetized mice treated with the combination of BSO (i.p.), letrozole (i.g.) and ASD (i.p.), or their vehicles (isotonic saline, 0.5% CMC and 4% DMSO plus 4% Tween80, respectively). BSO was given 30 minutes before letrozole and ASD immediately after letrozole. Synovial fluid was collected by instilling 3 times 0.1 ml of Hank's Buffer plus 10 mM HEPES and 10 mM EDTA in the knee 15 minutes after letrozole. The neutrophil count was performed using standard morphological criteria on Diff-Quick stained cytospins. Data are expressed as total number of neutrophils in 100 μl of solution.

GRP-Like Immunoreactivity assay. Slices (0.4 mm) of rat spinal cords were superfused with ASD or vehicle. Tissues were pre-exposed to capsaicin (10 μM, 20 minutes), superfused with a calcium-free buffer containing EDTA (1 mM), and pretreated with HC-030031 (50 μM) or capsazepine (10 μM). Superfusate fractions (4 ml) were collected at 10-minute intervals before, during, and after stimulus administration, freeze-dried, reconstituted with assay buffer, and analyzed for CGRP-like immunoreactivity (LI) as previously described [174]. CGRP-LI was calculated by subtracting the mean prestimulus value from those obtained during or after stimulation. Results are expressed as femtomoles of peptide per gram of tissue. Stimuli did not cross-react with CGRP antiserum.

ASD and letrozole level determination. ASD levels were measured in mouse serum by using the Active® ASD Radioimmunoassay (Beckman Coulter, CA, USA), a competitive RIA with a sensitivity of 0.1 nmol/L. Radiometric detection was performed using a 2470 WIZARD Automatic Gamma Counter (Perkin Elmer, IL, USA). Letrozole levels were measured by LC-MS/MS. Briefly, plasma samples (50 μl) were obtained from the blood collected at different time points (1 and 3 hours) after i.g. administration of letrozole (0.1

and 0.5 mg/kg). At 50 µl of plasma sample, 200 pg of d4-letrozole was added. The sample was vortex-mixed for 10 seconds, then 50 µl of $ZnSO_4$ (90 mg/ml) diluted 1:4 with methanol was added, vortex-mixed for 30 seconds, and centrifuged at 12,000 rpm for 10 minutes. Supernatant (50 µl) was injected in On-line column-switching SPE (CS-SPE). The CS-SPE consists of two high-performance-liquid chromatography (HPLC) systems connected by a six-port switching valve. In the first step, analytes of interest are retained on column 1 (trapping column, SPE Strata C18 20um, 20 x 2 mm, Phenomenex, Torrance, CA, USA), whereas the matrix components can be washed off. In the second step, column 1 is switched in back-flush to column 2 (analytical column, LUNA, 3 um, C18 20 x 2 mm, Mercury MS Penomenex, Torrance, CA, USA). The mobile phases were the same for the trapping column and the analytical column, eluent A water with 0.1% formic acid and eluent B methanol. Samples were measured with a Perkin Elmer Sciex (Thornhill, Canada) API 365 triple quadrupole mass spectrometer equipped with a Turbo IonSpray source, operating in positive ion mode, interfaced with a HPLC Perkin Elmer pump series 200. The capillary voltage was set to 5.5 kV. Heated turbo gas (450° C, air) at a flow rate of 10 l/minutes was used. The ion transitions recorded in Multiple Reaction Monitoring (MRM) were m/z 286.2→217.2 for letrozole and 290.2→221.2 for d4-letrozole. A calibration curve was constructed for letrozole using the appropriate internal standard (d4-letrozole). Plasma samples (50 µl) from control mice were spiked with different concentrations of letrozole (from 2 to 16 ng/ml). A satisfying linearity was obtained for letrozole (r^2=0.994).

Data Analysis. Data represent mean±SEM. Statistical analysis was performed by the unpaired two-tailed Student's t-test for comparisons between two groups, and the ANOVA, followed by the Bonferroni *post-hoc* test, for comparisons between multiple groups (GraphPadPrism version 5.00, San Diego, CA, USA). Agonist potency was expressed as half maximal effective concentration (EC_{50}); that is, the molar concentration of an agonist producing 50% of the maximum measured effect. $P<0.05$ was considered statistically significant.

3.2 Results

3.2.1 ASD selectively activates the recombinant and native human TRPA1 by targeting key electrophilic amino acid residues

In hTRPA1-HEK293 cells, but not in untransfected HEK293 cells, ASD evoked calcium responses in a concentration-dependent manner (EC_{50}, 49 μM) (Figure 1A and Supplementary Figure 1B). Responses to both ASD and the TRPA1 agonist, AITC, were abrogated by HC-030031 (Figure 1B). Consistently, hTRPA1-HEK293 cells superfused with ASD elicited concentration-dependent inward currents (Supplementary Figure 1E), an effect blocked by HC-030031 (Figure 1C) and absent in untransfected HEK293 cells (Figure 1D). In hTRPV1-HEK293 and hTRPV4-HEK293, activated by the selective TRPV1 agonist, capsaicin, or the selective TRPV4 agonist, GSK1016790A, respectively, ASD failed to evoke calcium responses or inward currents (Figure 1E and 1F). Notably, hTRPA13C/K-Q-HEK293 did not respond to AITC or ASD, while they did respond to the non-electrophilic TRPA1 agonist, menthol (Figure 1G and Supplementary Figure 1D) [174]. In IMR90 cells, which constitutively express the TRPA1 channel [80] and do not respond to capsaicin, indicating the absence of a functional TRPV1 channel (Figure 1H), ASD produced concentration-dependent (EC_{50}, 37 μM) calcium responses that were fully and selectively inhibited by HC-030031 (Figure 1H and Supplementary Figure 1C). Similar results were obtained in electrophysiology experiments, where ASD activated TRPA1-mediated inward currents that were entirely and selectively abolished by HC-030031 (Figure 1I). TRPA1 selectivity of HC-030031 in inhibiting ASD-evoked responses was supported by failure to affect responses produced by hPAR2-AP or KCl in hTRPA1-HEK293 or IMR90 (Figure 1A-D, 1H, 1I). Next, we wondered whether the other aromatase substrate, testosterone, or steroid hormones upstream to aromatase that maintain the α,β-carbonyl moiety of the A ring (progesterone, 17-hydroxy-progesterone), or the ketone group at the 17 position (dehydroepiandrostenedione), or other steroid hormones that retain the α,β-carbonyl moiety of the A ring (aldosterone, cortisol, corticosterone, deoxycorticosterone, 11-deoxycortisol), were able to activate hTRPA1-HEK293 cells. No hormone evoked a measurable response (Supplementary Figure 1E).

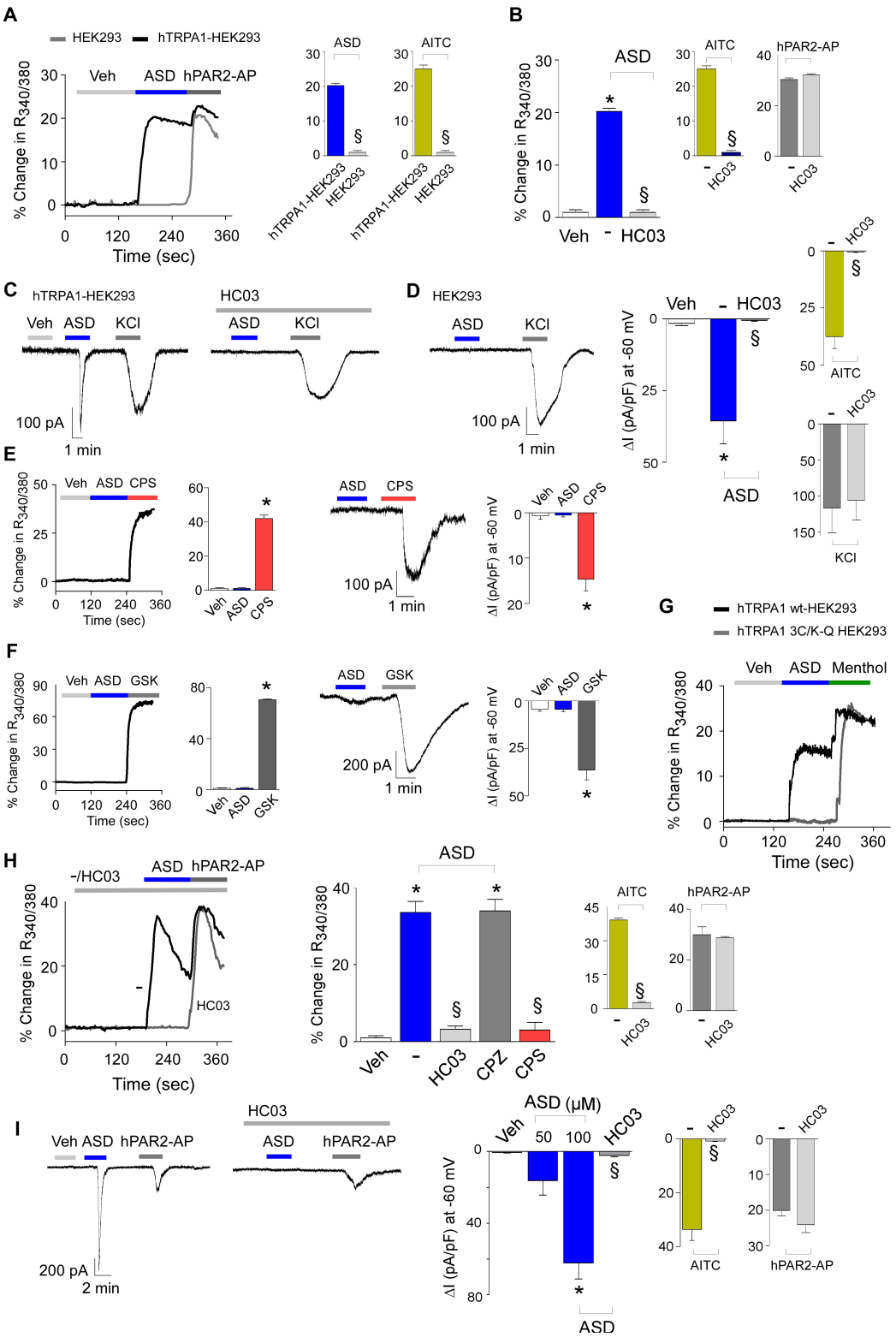

Figure 1. ASD selectively activates the recombinant and native human TRPA1 by targeting key electrophilic amino acid residues. ASD selectively activates the human TRPA1 channel. **A**, calcium response evoked by ASD (100 μM), AITC (5 μM) and hPAR2-AP (100 μM) in hTRPA1-HEK293 and in HEK293 cells. **B**, HC-030031 (HC03; 30 μM) abates the response to both ASD and AITC, but not to hPAR2-AP. **C** and **D**, ASD (50 μM) or AITC (100 μM), elicit inward currents in hTRPA1-HEK293, but not in HEK293 cells. HC03 (50 μM) does not affect responses to KCl (50 mM), but abolishes responses to either ASD or AITC. **E** and **F**, ASD (100 μM) is ineffective in hTRPV1-HEK293, activated by capsaicin (CPS; 0.1 μM), and in hTRPV4-HEK293, activated by GSK1016790A (GSK; 0.1 μM). **G**, hTRPA1 3C/K-Q HEK293 are insensitive to ASD (100 μM), but respond to menthol (100 μM), whereas wt-hTRPA1 respond to both compounds. **H**, IMR90 respond to ASD (100 μM) and AITC (1 μM), but not to CPS (5

μM). Responses to AITC and ASD, but not to hPAR2-AP (100 μM), are inhibited by HC03 (30 μM), but not by capsazepine (CPZ, 10 μM). **I**, In IMR90 fibroblasts ASD (100 μM) and AITC (100 μM), but not hPAR2-AP (100 μM), evoke inward currents, which are abated by HC03 (50 μM). Veh is the vehicle of ASD; (-) indicates the vehicle of antagonists. Each point/column is the mean±SEM of at least n=25 cells from 3-6 independent experiments for calcium recordings or of at least n=6 cells from 4-8 independent experiments for electrophysiological recordings. *P<0.05 *vs*. Veh, §P<0.05 *vs*. ASD or AITC. ANOVA and Bonferroni *post hoc* test.

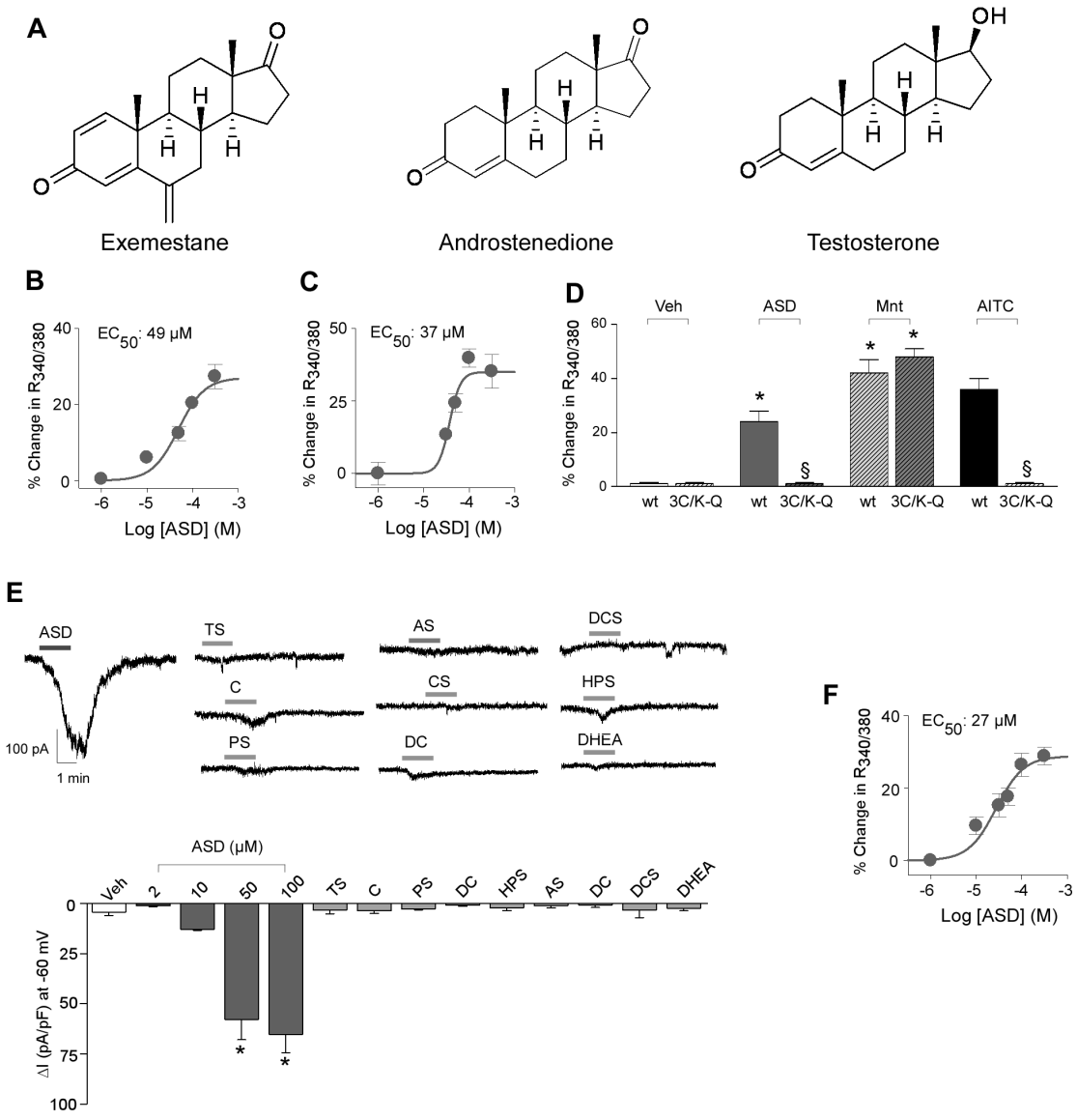

Supplementary Figure 1. Chemical structure of letrozole and androstenedione and additional *in vitro* data. A, Chemical structure of exemestane, androstenedione and testosterone. **B** and **C**, Concentration-response curves and EC_{50s} of calcium responses evoked by androstenedione (ASD) in hTRPA1-HEK293 and IMR90 fibroblasts. **D**, Calcium responses evoked by ASD (100 μM), AITC (30 μM), menthol (Mnt; 100 μM) or their vehicles (Veh) in HEK293 cells expressing the mutant hTRPA1 channel (3C/K-Q) and the wild type (wt) hTRPA1. **E**, Aldosterone, cortisol, 11-deoxycortisol, corticosterone, deoxycorticosterone, progesterone, 17α-hydroxy-progesterone, testosterone and dehydroepiandrostenedione (all 50 μM) fail to evoke inward currents in hTRPA1-HEK293 cells. ASD elicits inward currents in a concentration-dependent manner in hTRPA1-HEK293 cells. **F**, Concentration-response curves and EC_{50} of the calcium response evoked by ASD in rat DRG neurons. Veh indicates the vehicle of steroid hormones or the vehicle of TRPA1 agonists (1% DMSO). Each point or column represents the mean±SEM of at least 25 cells obtained from 3-7 independent calcium recordings. Results are mean±SEM of at least 4-8 independent electrophysiological recordings. *P<0.05 *vs.* Veh, §P<0.05 *vs*.

ASD or AITC. ANOVA and Bonferroni *post hoc* test.

3.2.2 ASD excites DRG neurons by a prominent role of TRPA1 and, surprisingly, with the contribution of TRPV1

ASD evoked concentration-dependent (EC_{50} = 27 μM) calcium responses in a subset of rat DRG neurons, identified by their ability to respond to KCl, AITC and capsaicin as nociceptors [130] (Figure 2A and Supplementary Figure 1F). Capsaicin-sensitive neurons that did not respond to AITC were also unresponsive to ASD (Figure 2A). The percentages of ASD-responding and AITC-responding neurons out of the KCl-responding neurons were similar (Figure 2B). Superimposable findings were obtained by electrophysiological recording (Figure 3A). Surprisingly, the remarkable ASD selectivity for TRPA1 was challenged by experiments in rat DRG neurons. The selective TRPV1 antagonist, capsazepine, reduced both the calcium response and the inward currents evoked by ASD, and it abated the residual response observed in the presence of HC-030031 (Figure 2C and 2D and Figure 3A). The calcium response to ASD was, however, unaffected by the selective TRPV4 antagonist, HC-067047 (Figure 2D). Results obtained in rat DRG neurons were replicated in mouse DRG neurons. Cells obtained from *Trpa1*$^{-/-}$ mice exhibited a residual calcium response to ASD that, being consistently unaffected by HC-030031, was abated by capsazepine (Figure 2E). The percentages of ASD-responding and AITC-responding neurons out of the KCl-responding neurons were similar (Figure 2F) in DRG neurons isolated from *Trpa1*$^{+/+}$ mice. The percentage of neurons from *Trpa1*$^{-/-}$ mice that exhibited a residual calcium response to ASD did not exceed the percentage obtained in neurons from *Trpa1*$^{+/+}$ mice (Figure 2F).

To confirm the contribution of TRPV1 in the overall response to ASD, we used hTRPA1/V1-HEK293 cells [274], where the calcium response evoked by ASD was reduced by both HC-030031 and capsazepine, and was abated solely by the combination of the two antagonists, while responses to AITC and capsaicin were fully attenuated by respective antagonists (Figure 2G). Thus, TRPV1, when co-expressed with TRPA1, as constitutively happens in DRG neurons, appears to contribute to the response to ASD.

CGRP release from slices of the rat dorsal spinal cord, an anatomical site enriched with terminals of TRPA1-positive peptidergic nociceptors, illustrates the ability of ASD to activate such neurons [174]. The increased CGRP-LI outflow by ASD was abated by the removal of extracellular calcium, previous desensitization to capsaicin, or in the presence of HC-030031, but only partially reduced by capsazepine (Figure 2H). Thus, ASD elicits CGRP release from a subset of TRPV1-positive neurons *via* a neurosecretory process,

mediated by TRPA1.

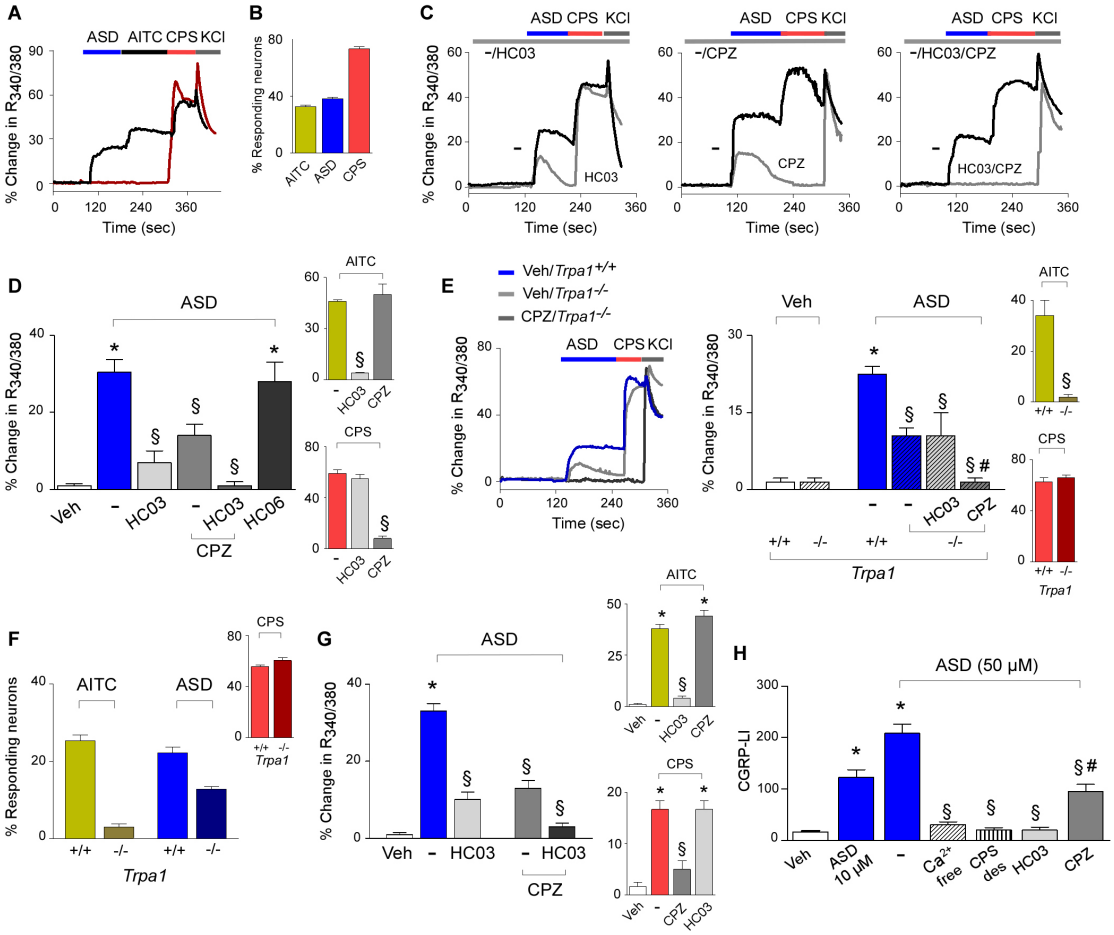

Figure 2. ASD excites DRG neurons by a prominent role of TRPA1 and, surprisingly, with the contribution of TRPV1. ASD activates the native TRPA1 channel expressed in rodent DRG neurons. **A**, typical tracings of calcium responses in rat DRG neurons that respond to ASD (100 µM), AITC (30 µM) and capsaicin (CPS; 0.1 µM) (black line), or solely to CPS (red line). **B**, percentage of DRG neurons (sensitive to 50 mM KCl) that respond to ASD, AITC or CPS. **C** and **D**, in rat DRG neurons concentrations of HC-030031 (HC03; 30 µM) and capsazepine (CPZ; 10 µM) that selectively and completely attenuated AITC and CPS responses, respectively, partially inhibit the response to ASD that, however, is abated by their combination (HC03/CPZ). HC-067047 (HC06; 10 µM) does not affect the response to ASD. **E**, ASD produces a calcium response in CPS-sensitive DRG neurons isolated from *Trpa1*$^{+/+}$ mice. The residual response to ASD in neurons from *Trpa1*$^{-/-}$ mice is abated by CPZ. **F**, percentage of *Trpa1*$^{+/+}$ or *Trpa1*$^{-/-}$ DRG neurons responsive to AITC, ASD and CPS. G, in hTRPA1/V1-HEK293 cells the calcium response to ASD is partially inhibited by HC03 or CPZ and abated by their combination (HC03/CPZ). Calcium responses to AITC (5 µM) and CPS (1 µM) are abolished by HC03 and CPZ, respectively. Each point/column represents the mean±SEM of at least n=25 neurons from 3-7 independent experiments. *P<0.05 *vs*. Veh or Veh-*Trpa1*$^{+/+}$, §P<0.05 *vs*. ASD, CPS, AITC or ASD-*Trpa1*$^{+/+}$, $^{\#}$P<0.05 *vs*. ASD-*Trpa1*$^{-/-}$. H, CGRP-LI outflow elicited by ASD (10-50 µM) from rat dorsal spinal cord slices is prevented by pre-exposure to CPS (10 µM, 20 min; CPS-des) or by calcium removal (Ca^{2+}-free) and is attenuated by HC03 (50 µM) and only partially reduced by CPZ (10 µM). Each column represents the mean±SEM of at least 4 independent experiments running in duplicate. *P<0.05 *vs*. Veh, §P<0.05 *vs*. ASD 50 µM, $^{\#}$P<0.05 *vs*. HC03. Veh is the vehicle of ASD; (-) indicates the vehicle of antagonists. ANOVA and Bonferroni *post hoc* test.

3.2.3 ASD cooperates with letrozole and H_2O_2 to excite nociceptors in vitro

To explore whether ASD cooperates with AIs and proinflammatory mediators to excite nociceptors *via* a TRPA1-dependent final common pathway, we used letrozole, the most prescribed AI in clinical practice [271]. As a prototypical proinflammatory mediator, we selected the ROS H_2O_2, because oxidative stress is increased by breast cancer [281] and letrozole [272]. In addition, the effect of letrozole (0.5 mg/kg, i.g.), at a dose that was previously shown to produce *per se* mechanical allodynia, was partially reduced by the antioxidant, α-lipoic acid (Supplementary Figure 2). These observations suggest that the TRPA1-dependent letrozole-evoked mechanical hypersensitivity [174] is partially due to ROS generation, which cooperates with the anticancer drug to target TRPA1.

From the concentration-response curves of ASD, letrozole, and H_2O_2 (Figure 3A-C), we selected subthreshold concentrations that were unable to elicit measurable inward currents in rat DRG neurons, and combined a *per se* inactive concentration of ASD with inactive concentrations of letrozole or H_2O_2 (ASD/letrozole or ASD/H_2O_2). Interestingly, we found that each combination evoked inward currents, which were abated by TRPA1 antagonism and reduced by TRPV1 antagonism (Figure 3D). Finally, we identified an inactive combination of letrozole and H_2O_2 (Figure 3E), and we found that adding an inactive ASD concentration to it triggered an inward current that was abated by HC-030031 and only partially reduced by capsazepine (Figure 3E).

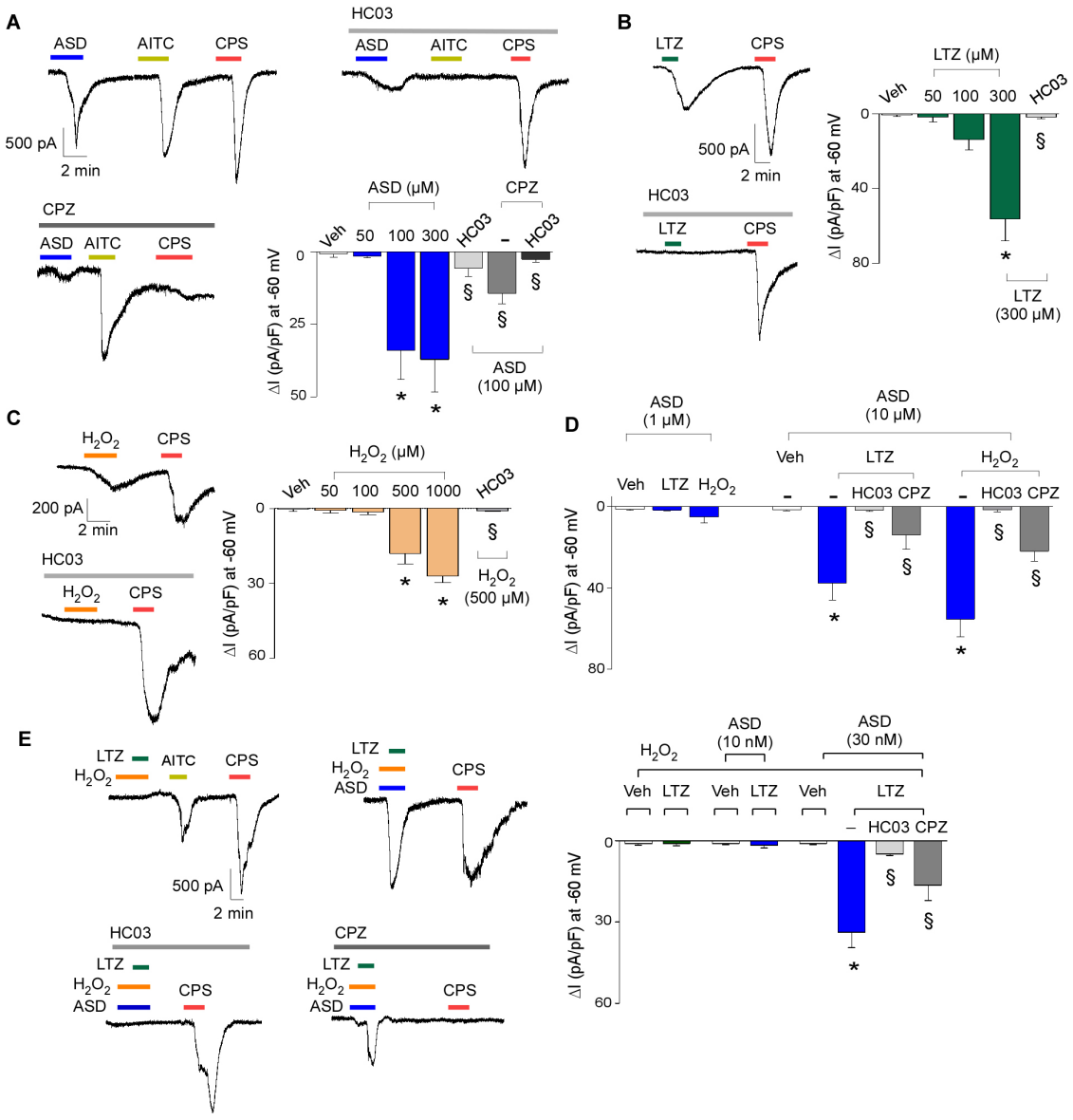

Figure 3. ASD cooperates with letrozole and H_2O_2 to excite nociceptors in vitro. ASD potentiates TRPA1-mediated inward currents in the presence of subthreshold letrozole and/or proinflammatory stimuli in rat DRG neurons. **A**, ASD and AITC (100 μM) evoke inward currents (whole-cell patch-clamp recordings) in capsaicin (CPS; 1 μM)-sensitive rat DRG neurons. ASD-evoked currents are partially reduced by HC-030031 (HC03; 50 μM) or capsazepine (CPZ; 10 μM), which abated currents evoked by AITC or CPS, respectively. The combination of HC03 and CPZ abated the ASD-evoked currents. **B** and **C**, letrozole (LTZ) and H_2O_2 evoke concentration-dependent inward currents that are abolished by HC03 (50 μM). **D**, inward currents elicited by a combination of ineffective concentrations of ASD (10 μM)/LTZ (50 μM) or ASD (10 μM)/H_2O_2 (50 μM) are abolished by HC03 and reduced by CPZ. The combination with a lower concentration of ASD (1 μM) is ineffective. E, addition of a much lower concentration of ASD (30 nM) to the ineffective combination of LTZ (50 μM)/H_2O_2 (50 μM) elicits inward currents, which are abated by HC03 and reduced by CPZ. Veh is the vehicle of ASD, LTZ or H_2O_2; (-) indicates the vehicle of antagonists. Results are mean±SEM of at least 4 independent experiments. *P<0.05 *vs*. Veh; §P<0.05 *vs*. LTZ, H_2O_2, ASD. ANOVA and Bonferroni *post hoc* test.

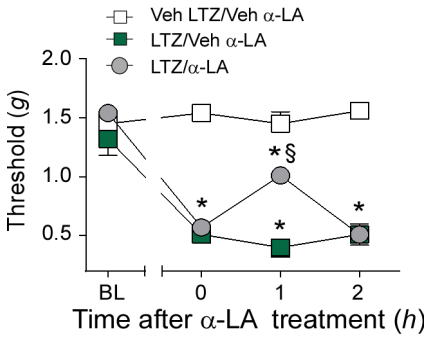

Supplementary Figure 2. Systemic administration of letrozole induces pain-like responses partially reduced by the antioxidant α-lipoic acid. In C57BL/6 mice, intragastric (i.g.) administration of letrozole (LTZ; 0.5 mg/kg) induces mechanical allodynia, partially reduced by the antioxidant α-lipoic acid (α-LA; 100 mg/kg, i.g.) administered 3 hours after LTZ. BL, baseline threshold. Veh LTZ and Vehα-LA are the vehicles of LTZ or α-LA, respectively. Results are mean±SEM of at least 5 mice for each group. *P<0.05 *vs.* Veh LTZ/veh α-LA; §P<0.05 *vs.* LTZ/veh α-LA, ANOVA and Bonferroni *post hoc* test.

3.2.4 ASD cooperates with letrozole and H_2O_2 to produce local TRPA1-dependent mechanical allodynia

Previous *in vitro* findings were translated to an *in vivo* setting. Injection of ASD (1-10 nmol/paw) into the mouse paw did not evoke any acute nociceptive behavior (data not shown). However, 30 minutes after the injection, and for the following 2 hours, ASD produced a dose-dependent mechanical allodynia (Figure 4A and 4B) that was partially and completely abrogated by capsazepine and HC-030031, respectively (Figure 4B). H_2O_2 injected in the mouse paw produced a dose-dependent mechanical allodynia that was entirely dependent on TRPA1 (Figure 4C). Similar to previous findings [174], systemic letrozole (0.1-0.5 mg/kg, i.g.) evoked a dose-dependent, delayed (1-6 hours) mechanical allodynia that was abated by HC-030031 and unaffected by capsazepine (Figure 4D). The combined administration of allodynia-evoking doses of ASD and letrozole produced an exaggerated pain-like response (Supplementary Figure 3A).

Next, we found doses of ASD and letrozole, or H_2O_2 and ASD, which, although *per se* ineffective, when given in combination, lowered the threshold for eliciting mechanical allodynia (Supplementary Figure 3B and 3C). Finally, we identified ineffective combinations of ASD/letrozole, letrozole/H_2O_2, or H_2O_2/ASD that, when given simultaneously (letrozole/ASD/H_2O_2), caused mechanical allodynia (Figure 4E). This response was partially reduced by capsazepine, completely reverted by HC-030031 (Figure 4F), and absent in *Trpa1*$^{-/-}$ (Figure 4G).

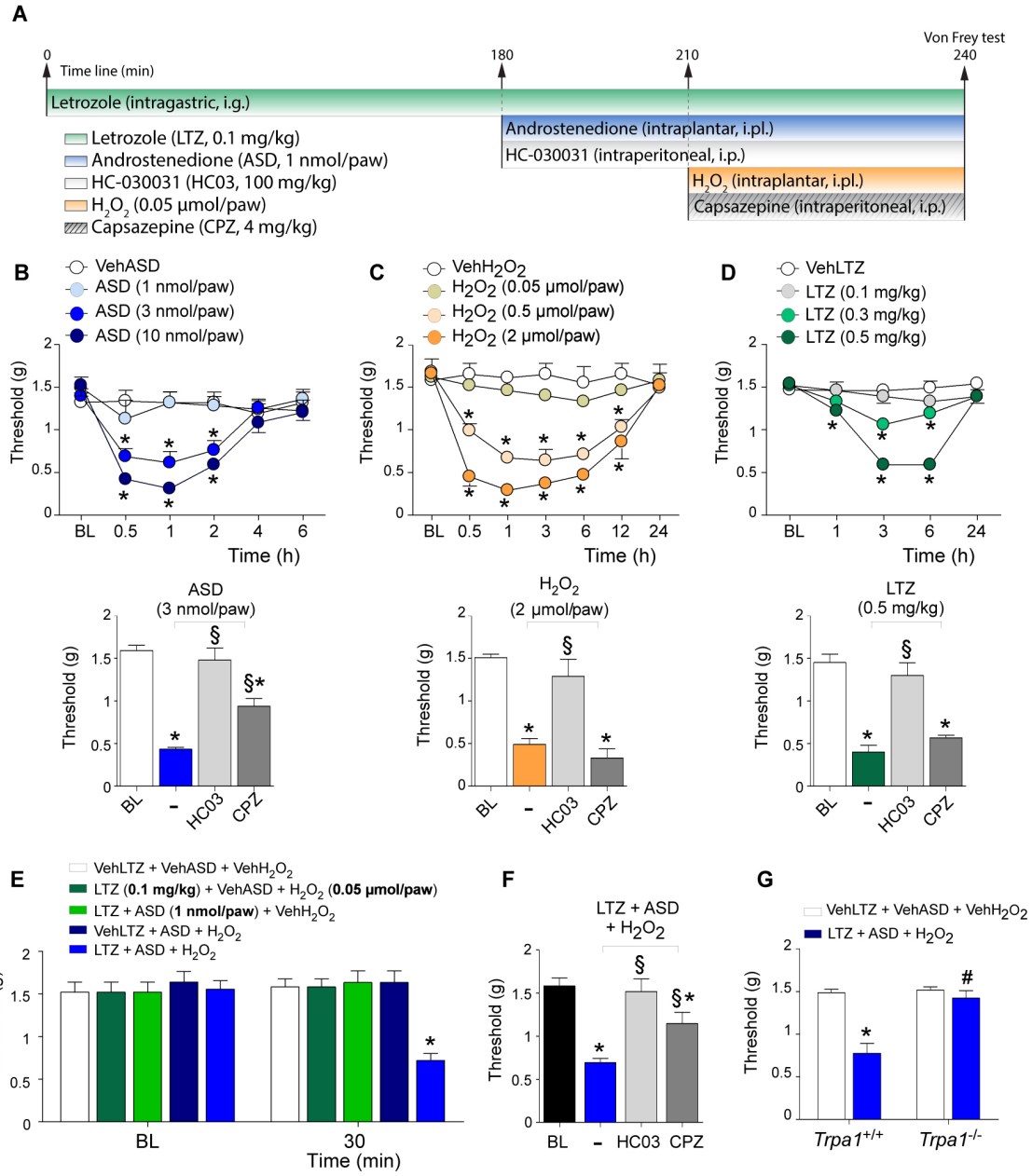

Figure 4. ASD cooperates with letrozole and H_2O_2 to produce local TRPA1-dependent mechanical allodynia. ASD cooperates with letrozole and H_2O_2 to produce TRPA1-dependent local mechanical allodynia. **A**, diagram illustrating the treatment schedule before behavioral tests. **B-D**, In C57BL/6 mice, injection (20 µl) of ASD or H_2O_2 and administration of LTZ induce a dose and time-dependent mechanical allodynia that is reversed completely by HC03, and partially by CPZ. **E** and **F**, The combination of ineffective doses of LTZ, ASD and H_2O_2 evokes mechanical allodynia that is completely prevented by HC03, partially reduced by CPZ, and (G) absent in *Trpa1*$^{-/-}$ mice. BL, baseline threshold. VehASD, VehLTZ and Veh H_2O_2 are the vehicle of ASD, LTZ and H_2O_2, respectively; (-) is the vehicle of antagonists. Results are mean ± SEM of at least n=5 mice for each group. *P<0.05 *vs.* BL; §P<0.05 *vs.* (-); $^{\#}$P<0.05 *vs.* *Trpa1*$^{+/+}$. ANOVA and Bonferroni *post hoc* test.

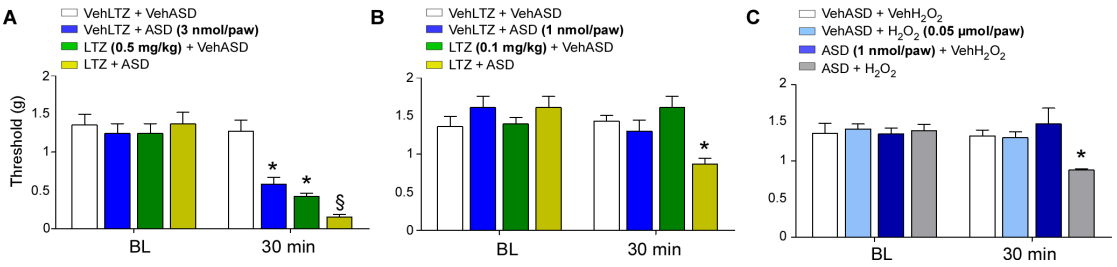

Supplementary Figure 3. A, Intraplantar (i.pl.) administration (20 µl) of androstenedione (ASD, 3 nmol/paw) or intragastric (i.g.) letrozole (LTZ, 0.5 mg/kg) produce mechanical allodynia and their combined administration (ASD is injected 180 min after LTZ) potentiates mechanical allodynia. **B**, Administration of an ineffective dose of ASD (1 nmol/paw) 180 min after an ineffective dose of LTZ (0.1 mg/kg, i.g.) induces mechanical allodynia. **C**, Combined administration of *per se* ineffective doses of ASD (1 nmol/paw, i.pl.) and of H_2O_2 (0.05 µmol/paw, i.pl., 30 min after ASD) induces mechanical allodynia. Behavioral tests were performed 240 min after LTZ or 30 min after H_2O_2. BL, baseline threshold. VehASD, VehLTZ, $VehH_2O_2$ are the vehicles of ASD, LTZ and H_2O_2. Results are mean±SEM of at least 5 mice for each group. *P<0.05 *vs.* VehLTZ + VehASD; §P<0.05 *vs.*, LTZ + VehASD or VehLTZ + ASD. ANOVA and Bonferroni *post hoc* test.

3.2.5 ASD cooperates with letrozole and H_2O_2 to produce systemic TRPA1-dependent AIMSS-like behaviors and neurogenic inflammation

In mice, letrozole (0.5 mg/kg, i.g.) has been reported to evoke TRPA1-dependent mechanical allodynia and a decrease in grip strength, two effects reminiscent of AIMSS [174]. The same dose of letrozole (0.5 mg/kg, i.g.) [174] increased H_2O_2 in the sciatic nerve tissue and slightly augmented ASD serum levels (Figure 5A and 5C). BSO, by inhibiting γ-glutamylcysteine synthetase, causes systemic depletion of glutathione, and the ensuing increase in ROS (35). BSO (800 mg/kg, i.p.) increased mechanical allodynia and decreased forelimb grip strength through a TRPA1-dependent mechanism (Supplementary Figure 4A), while, at the dose of 400 mg/kg, it slightly increased H_2O_2 in the sciatic nerve tissue (Figure 5C) without affecting pain-like behaviors (Supplementary Figure 4A). Finally, systemic administration of ASD (2 µg/kg, i.p.) caused, in mice, mechanical allodynia and reduced forelimb grip strength *via* TRPA1, with a partial contribution of TRPV1 (Supplementary Figure 4B). ASD (2 µg/kg, i.p.) also increased H_2O_2 levels in the sciatic nerve (Figure 5C). To better understand the contribution of ASD and oxidative stress to the AIMSS-like behaviors, a low dose of ASD (0.2 µg/kg, i.p.) that failed to affect H_2O_2 generation (Figure 5C), as well as mechanical allodynia and forelimb grip strength, (Supplementary Figure 4B) was used. This same dose slightly increased hormone plasma concentration to levels comparable to those produced by a dose of letrozole (0.5 mg/kg, i.g.) that caused pain-like behaviors (Figure 5A and Figure 4D). In mice, 1 hour after oral administration of letrozole (0.1 and

0.5 mg/kg), drug concentrations in plasma were 13.5 ± 2.0 ng/ml (n = 4) and 55.3 ± 4.8 ng/ml (n = 4), respectively, whereas 3 hours after dosing, plasma concentrations were 8.41 ± 1.0 ng/ml (n = 4) and 45.4 ± 6.11 ng/ml (n = 4), respectively. Notably, the plasma concentration of 0.5 mg/kg letrozole measured at 1 hour after dosing was similar to that found previously [174]. Systemic BSO (400 mg/kg, i.p.), letrozole (0.1 mg/kg, i.g.) and ASD (0.2 μg/kg, i.p.), which *per se*, or in combinations (letrozole/ASD, BSO/ASD or BSO/letrozole), did not affect behavioral responses, when given simultaneously caused remarkable mechanical allodynia and decreased forelimb grip strength (Figure 5D and 5E). The triple combination of BSO, letrozole, and ASD increased H_2O_2 levels in the sciatic nerve (Figure 5C). However, the increase equals that evoked by BSO (400 mg/kg) alone. Finally, the remarkable increase in 4-hydroxynonenal staining in the sciatic nerve allowed us to localize the oxidative stress generation within the neural structure (Figure 5H). Behavioral responses evoked by the triple combination were partially and totally reverted by capsazepine and HC-030031, respectively (Figure 5D and 5E), and were absent in *Trpa1*$^{-/-}$ mice, but unaffected in *Trpv1*$^{-/-}$ mice (Figure 5F and 5G). Finally, the combination of BSO (400 mg/kg, i.p.), letrozole (0.1 mg/kg, i.g.) and ASD (0.2 μg/kg, i.p.), which produced AIMSS-like behaviors, increased Evans blue dye extravasation in the synovial tissue and the number of neutrophils in the synovial fluid of mouse knee joint (Figure 5I and 5J). Both responses were reduced by pretreatment with HC-030031 or a combination of L733,060 and $CGRP_{8-37}$ (both 2 μmol/kg, i.v.) (Figure 5I and 5J). These findings indicate that the letrozole/ASD/BSO combination *via* TRPA1 promotes two typical neurogenic inflammatory responses, such as plasma protein and neutrophil extravasation [273].

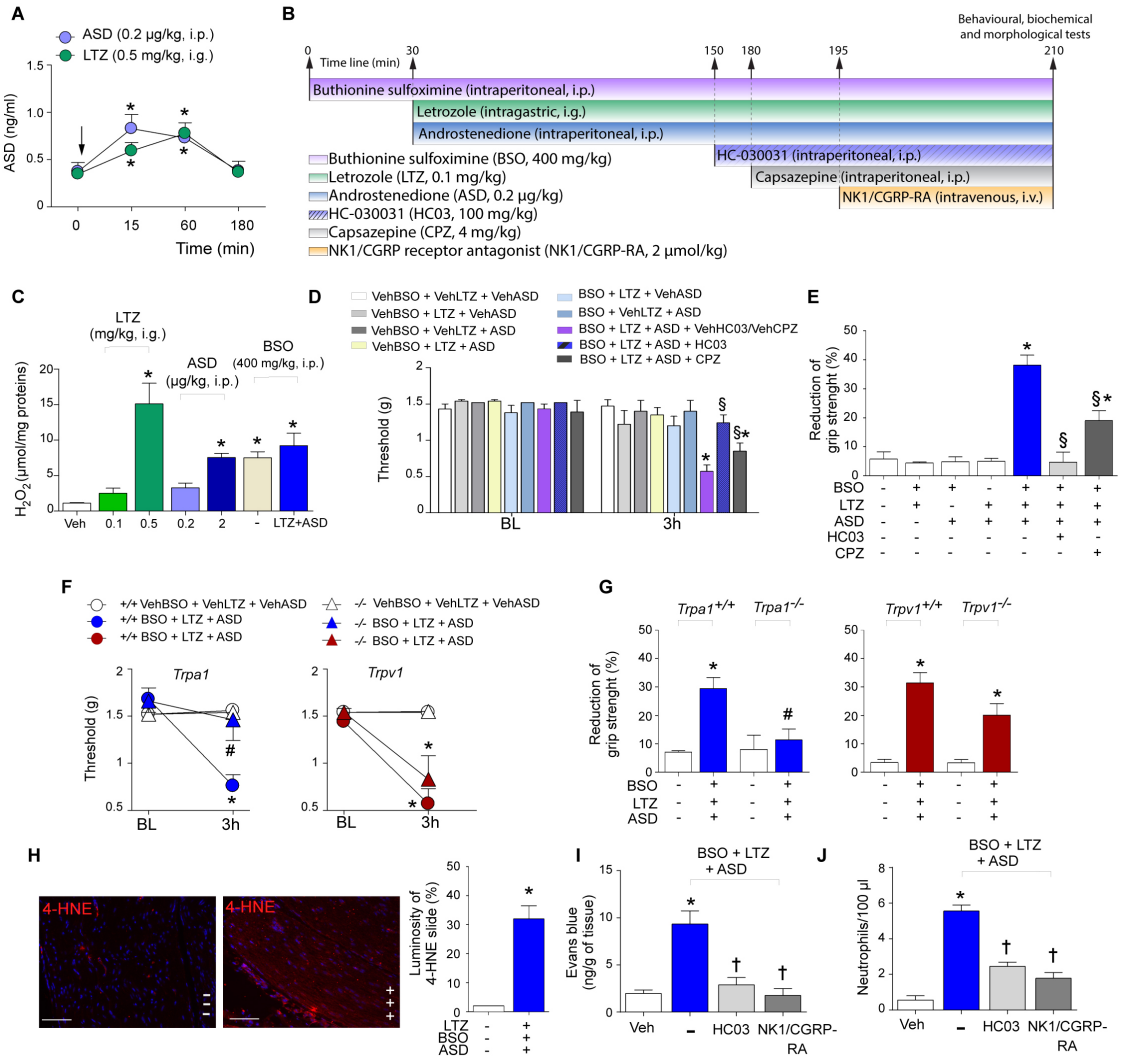

Figure 5. ASD cooperates with letrozole and H_2O_2 to produce systemic TRPA1-dependent AIMSS-like behaviors and neurogenic inflammation. Androstenedione cooperates with letrozole and H_2O_2 to evoke systemic TRPA1-dependent AIMSS-like behaviors. **A**, ASD serum levels are similarly increased by systemic administration (↓) of ASD or letrozole (LTZ). **B**, diagram illustrating the treatment schedule before behavioral tests. **C**, LTZ or ASD increase H_2O_2 in homogenates of mouse sciatic nerve. Addition of ineffective doses of LTZ and ASD does not further increase H_2O_2 levels produced by BSO alone. **D** and **E**, ASD, LTZ and BSO alone or in dual combinations (ASD/LTZ; ASD/BSO; LTZ/BSO) do not increase mechanical allodynia or decrease grip strength. However, their combination (BSO/LTZ/ASD) increases mechanical allodynia and decreases grip strength. Both responses are reverted by HC03 and attenuated by CPZ. **F** and **G**, changes in mechanical allodynia and grip strength induced by BSO/LTZ/ASD observed in *Trpa1*$^{+/+}$mice are similar to those observed in *Trpv1*$^{+/+}$ and abrogated in *Trpa1*$^{-/-}$ mice, but not in *Trpv1*$^{-/-}$ mice. **H**, BSO/LTZ/ASD (+++), but not their vehicles (---) increase 4-hydroxynonenal (4-HNE) staining within the sciatic nerve. **I** and **J**, HC03 or the combination of L-733,060 and $CGRP_{8-37}$ (NK1/CGRP-RA) attenuate increases in Evans blue dye extravasation in the knee joint synovial tissue, and in neutrophil number in synovial fluid evoked by BSO/LTZ/ASD. BL, baseline threshold. Scale bar, 100 µm. Veh is the vehicle of LTZ, ASD and BSO; VehASD, VehLTZ and VehBSO are the vehicle of ASD, LTZ and BSO, respectively; VehHC03/CPZ (D) and (-) (I, J) are the vehicle of antagonists. Results are mean±SEM of at least n=5 mice for each group. *P<0.05 *vs.* Veh (B), time 0 (C) or white columns or circle (D-J); §P<0.05 *vs.* Veh HC03/CPZ; $^{\#}$P<0.05 *vs.* *Trpa1*$^{+/+}$; †P<0.05 *vs.* (-). ANOVA and Bonferroni *post hoc* test.

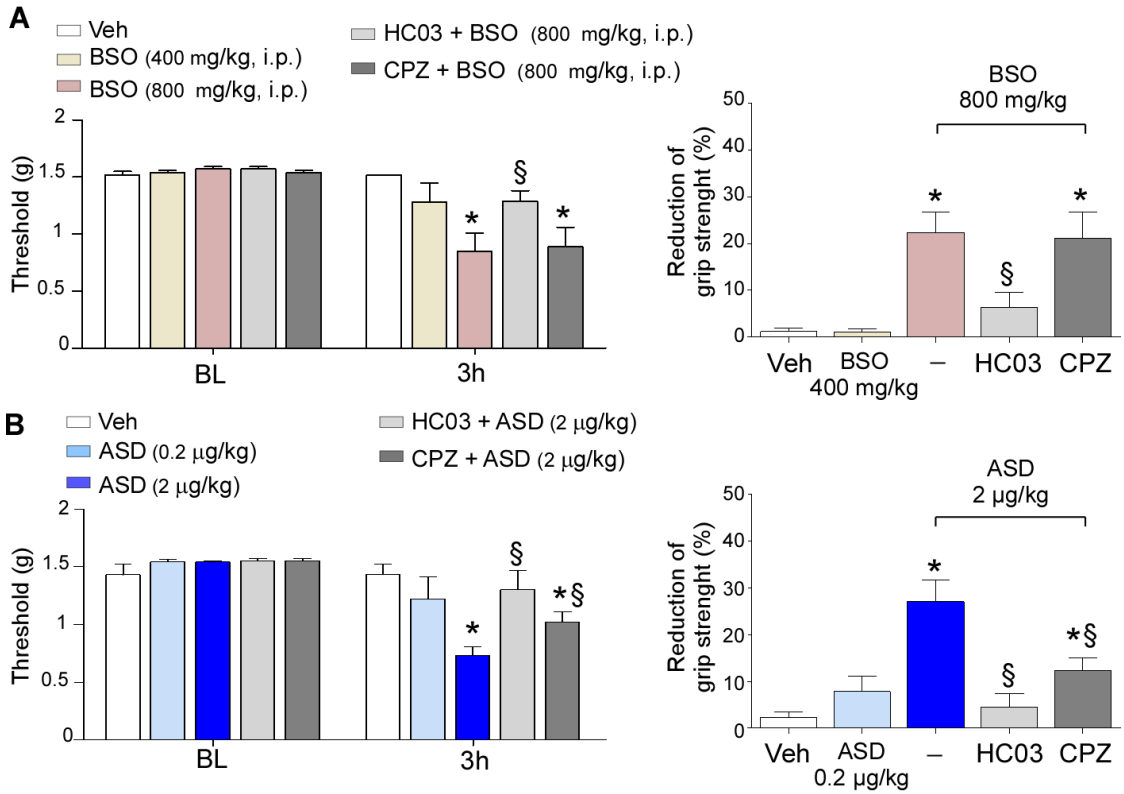

Supplementary Figure 4. Pain-like responses evoked by systemic co-administration of ineffective doses of androstenedione with ineffective doses of both letrozole and BSO. A, Buthionine sulfoximine (BSO, 800 mg/kg, intraperitoneal, i.p.) induces mechanical allodynia and decreases grip strength. Both responses are markedly reduced by HC-030031 (HC03, 100 mg/kg, i.p., 60 min before the behavioral tests) and are unaffected by capsazepine (CPZ, 4 mg/kg, i.p., 30 min before the behavioral tests). **B**, Androstenedione (ASD, 2 μg/kg, i.p.) induces mechanical allodynia and decreases grip strength. Both responses are abated by HC03 (100 mg/kg, i.p., 60 min before the behavioral tests) and reduced by CPZ (4 mg/kg, i.p., 30 min before the behavioral tests). BL, baseline threshold. Veh is the vehicle of BSO or ASD. Results are mean±SEM of at least 5 mice for each group. *P<0.05 *vs.* veh; §P<0.05 *vs.* BSO (800 mg/kg) or ASD (2 μg/kg). ANOVA and Bonferroni post *hoc test*.

3.3 Discussion

We found that ASD, unique among several steroid hormones, activates TRPA1, thereby promoting AIMSS-like responses. ASD behaves as a TRPA1 agonist across species, as it engages both the recombinant and native human channel and the rat and mouse channel. TRPA1 activation by ASD, similar to other electrophilic agonists [248], requires the presence of three cysteine (C619, C639, C663) and one lysine (K708) key residues. Furthermore, ASD exhibits a peculiar selectivity profile. Whereas in cells expressing only one channel (transfected HEK293 cells, IMR90 human fibroblasts) [80,101], ASD is a selective TRPA1 agonist, surprisingly, in rodent DRG neurons, which express multiple TRP channels, TRPV1 contributes to TRPA1-dependent ASD-evoked responses. Notably, DRG neurons from *Trpa1*$^{-/-}$ mice maintained a residual responsiveness to ASD which was abolished by capsazepine. One possible explanation for this unexpected finding is that the TRPA1 protein remaining after the homologous recombination, while lacking the domain required for channel activation by most agonists [83], including ASD itself, maintains the domain essential for TRPV1-dependent ASD activity. TRPV1 contribution to TRPA1-mediated responses evoked by ASD or other chemicals [274] was confirmed in cells expressing the recombinant forms of both the TRPA1 and TRPV1 (hTRPA1/V1-HEK293) channels. Formation of heterotetramers [222,275], or intracellular calcium movement initiated by TRPA1 gating that results in a secondary TRPV1 activation [276], may explain how ASD heterologously interregulates channel activities [277,278]. Notwithstanding, this peculiar selectivity pattern was not replicated *in vivo* as TRPA1 inhibition was sufficient to totally prevent ASD actions. Tenosynovitis and joint swelling are symptoms reported by patients treated with AIs [170]. However, association with proinflammatory markers, including cytokines, such as interleukin-6, has been excluded [265]. The ability of ASD to release sensory neuropeptides or, in combination with letrozole and BSO, to provoke TRPA1-dependent SP/CGRP release, edema and neutrophil infiltration in the knee joint, suggests that neurogenic inflammation mediates the inflammatory component of AIMSS. The recent observation that, due to their electrophilic and reactive properties, exemestane, anastrozole and letrozole target TRPA1, thus evoking pain-like responses and neurogenic inflammation, supported the hypothesis that channel activation in peptidergic nociceptors promotes AIMSS [174]. However, while the three AIs target TRPA1 with remarkable selectivity, they exhibit low potency at both human and rodent channels [174]. Notably, the peak plasma concentration of letrozole measured in mice in the present study after the 0.5 mg/kg dose (~194 nM) is

close to the maximum concentration reported in human plasma after a single therapeutic dose (2.5 mg) (~128 nM) [279]. It must be underlined that the plasma concentrations found in mice and humans are 50-400 times lower than the threshold concentrations of letrozole able to gate *in vitro* the mouse, rat or human TRPA1 (>10 μM). This gap between plasma levels and threshold concentrations at TRPA1 argues against the hypothesis that AIs *per se* cause AIMSS. Elevated tissue concentrations due to high AI volumes of distribution [257] may still be insufficient for effective channel gating. Lack of evidence associating increased AI plasma levels with pain symptoms [279] further weakens the hypothesis that AIMSS results from an exclusive AI action. Similarly, attempts to associate serum ASD concentrations with AIMSS have failed [175]. Thus, a direct cause-and-effect relationship between plasma levels of AIs or ASD and AIMSS has not been shown. TRPA1 is amenable to sensitization by a variety of endogenous proinflammatory and proalgesic mediators [280], and we previously reported that H_2O_2 or PAR2 stimulation exaggerated TRPA1-dependent responses evoked by AIs [174]. The present novel finding that the aromatase substrate, ASD, activates TRPA1 proposes a novel paradigm to explain AIMSS generation. Multiple factors, concomitantly occurring in breast cancer patients treated with AIs, may cooperate to engage TRPA1, thus causing AIMSS-like behaviors. Letrozole (and probably other AIs) is the essential, although *per se* ineffective, initiating stimulus. Letrozole slightly augments ROS [272] and ASD concentrations [175]. Breast cancer [281] or incidental inflammatory processes [282] may boost oxidative stress, thus increasing the possibility of the simultaneous presence of the three TRPA1 stimulants. However, the current hypothesis does not exclude that additional agents, able to activate or sensitize the TRPA1, may act along with AIs and ASD to reach the threshold for AIMSS generation. The present study, while showing that TRPV1 signaling negligibly contributes to ASD-evoked AIMSS-like behaviors, robustly underscores the paramount role of TRPA1. Thus, TRPA1 blockade by both new compounds currently under clinical scrutiny and old medicines recently identified as TRPA1 antagonists [243] may represent a new frontier to treat or prevent AIMSS.

This work has been published in Cancer Research

De Logu F, Tonello R, Materazzi S, Nassini R, Fusi C, Coppi E, Li Puma S, Marone IM, Sadofsky LR, Morice AH, Susini T, Terreni A, Moneti G, Di Tommaso M, Geppetti P, Benemei S (2016). "TRPA1 Mediates Aromatase Inhibitor-Evoked Pain by the Aromatase Substrate Androstenedione" Cancer Res. 76(23):7024-7035.

Chapter IV - TRPA1/NOX in the soma of trigeminal ganglion neurons mediates migraine-related pain of glyceryl trinitrate in mice

4.1 Methods

Animals. *In vivo* experiments were in accordance with the European Union Directive 2010/63/EU guidelines, the Italian legislation (DLgs 26/2014), and the University of Florence research permit #194/2015-PR. The following mouse strains were used: C57BL/6 (male, 20-25 g, 5-6 weeks; Envigo); littermate wild type (wt, *Trpa1*$^{+/+}$) and TRPA1-deficient (*Trpa1*$^{-/-}$) mice (25-30 g, 5-8 weeks) [116]; wt (*Trpv4*$^{+/+}$) and TRPV4-deficient (*Trpv4*$^{-/-}$) mice (25-30 g, 5-8 weeks) [313]; and TRPV1-deficient mice (*Trpv1*$^{-/-}$; B6.129X1-*Trpv1*$^{tm1Jul/J}$) backcrossed with C57BL/6 mice (*Trpv1*$^{+/+}$) for at least 10 generations (Jackson Laboratories, 25-30 g, 5-8 weeks). To selectively delete *Trpa1* gene in primary sensory neurons, 129S-Trpa1$^{tm2Kykw/J}$ mice (*floxed TRPA1, Trpa1*$^{fl/fl}$, Stock No: 008649; Jackson Laboratories), which possess loxP sites on either side of the S5/S6 transmembrane domains of the *Trpa1* gene, were crossed with hemizygous *Advillin-Cre* male mice [283,284]. The progeny was genotyped by standard PCR for *Trpa1* (PCR Protocol 008650) and *Advillin-Cre* [283]. Mice negative for *Advillin-Cre* (*Adv-Cre*$^{-}$;*Trpa1*$^{fl/fl}$) were used as control. Successful *Advillin-Cre* driven deletion of TRPA1 mRNA was confirmed by RT-qPCR [285]. Mice were housed in a temperature- and humidity-controlled *vivarium* (12 h dark/light cycle, free access to food and water, 10 animals per cage). Mice were acclimatized in a quiet, temperature-controlled room (20-22°C) for 1 h before behavioral studies of nociception between 9 a.m. and 5 p.m.

Animal studies were reported in compliance with the ARRIVE guidelines. The sample sizes chosen for animal groups were adequately powered to observe the effects based on both our experience in similar experimental settings and data published by others. Allocation concealment was performed using a randomization procedure

(http://www.randomizer.org/). Experiments were performed by an operator blinded to genotype and drug treatments. Each experiment was repeated two to three times. Animals were anaesthetized with intraperitoneal (i.p.) ketamine (90 mg/kg) and xylazine (3 mg/kg) and euthanized with inhaled CO_2 plus 10-50% O_2.

Reagents. Glyceryl trinitrate (GTN 50 mg/50 ml, Bioindustria L.I.M. S.p.A.) or its vehicle (5% glucose and 1.5% propylene glycol in sterile water) were used. HC-030031 [2-(1,3-dimethyl-2,6-dioxo-1,2,3,6-tetrahydro-7H-purin-7-yl)-N-(4-isopropylphenyl) acetamide] was synthesized as previously described [130]. If not otherwise indicated, reagents were obtained from Sigma-Aldrich. The vehicle, except for GTN or where expressly indicated, was 4% dimethyl sulfoxide (DMSO) plus 4% tween 80 in isotonic saline, NaCl 0.9%.

Mechanical allodynia, eye wiping test and nociceptive behavior. For behavioral experiments, C57BL/6, *Trpa1*$^{+/+}$ and *Trpa1*$^{-/-}$, *Trpv1*$^{+/+}$ and *Trpv1*$^{-/-}$, *Trpv4*$^{+/+}$ and *Trpv4*$^{-/-}$ or *Adv-Cre*; *Trpa1*$^{fl/fl}$ and *Adv-Cre*$^{-}$; *Trpa1*$^{fl/fl}$ were used. Mechanical allodynia was evaluated by applying the von Frey filaments to the periorbital region over the rostral portion of the eye (periorbital mechanical allodynia, PMA) [286] or to the posterior hind paw of mice, before (basal threshold) and for 24 h after GTN (1, 5 and 10 mg/kg) or vehicle. Mechanical threshold was measured by the up-and-down paradigm [250]. The selective TRPA1 antagonist HC-030031 (100 mg/kg, i.p.) or its vehicle were administered 0.5 h before or 1, 2.5, 4 and 5 h after GTN (10 mg/kg, i.p.) or 1 h after GTN (1 mg/kg, i.p.). A967079, [(1E,3E)-1-(4-Fluorophenyl)-2-methyl-1-penten-3-one oxime] (100 mg/kg, i.p.), capsazepine (4 mg/kg, i.p.), HC-067047 [2-methyl-1-[3-(4-morpholinyl) propyl]-5-phenyl-N-[3-(trifluoromethyl) phenyl]-1Hpyrrole-3-carboxamide] (10 mg/kg, i.p.), disulfiram (100 mg/kg, i.p.) or their vehicles were administered 0.5 h before and 1 h after GTN (10 mg/kg i.p.). The NO scavenger, 2-(4-carboxyphenyl)-4,4,5,5-tetramethylimidazoline-1-oxyl-3-oxide (cPTIO) (0.6 mg/kg, i.p.), or its vehicle (0.9% NaCl) was administered 0.5 h before and 1 h after GTN (10 mg/kg i.p.). Alpha-lipoic acid (αLA, 100 mg/kg, i.p.) or its vehicle were administered 0.5 h before and 1, 2, 3, 4 h after GTN (10 mg/kg i.p.). Phenyl-N-t-butyl-nitrone (PBN, 100 mg/kg, i.p.) or its vehicle (0.9% NaCl) were administered 0.5 h before and 1 and 4 h after GTN (10 mg/kg i.p.). N-acetyl cysteine (NAC, 250 mg/kg, i.p.) or L-carnosine (250 mg/kg, i.p.), scavengers for α,β-unsaturated aldehydes, or their vehicle (0.9% NaCl) were administered 0.5 h before and 4 h after GTN (10 mg/kg, i.p.).

The NOX inhibitors [287], apocynin (100 mg/kg, i.p., unselective), gp91ds-tat peptide

(Tocris Bioscience) (gp91, 10 mg/kg, i.p., NOX2 selective), ML171 [2-acetylphenothiazine] (60 mg/kg, i.p., NOX1 selective), GKT137831 [2-(2-chlorophenyl)-4-[3-(dimethylamino)phenyl]-5-methyl-1H-pyrazolo[4,3-c]pyridine-3,6(2H,5H)-dione] (Tocris Bioscience) (60 mg/kg, i.p., NOX1/4 selective) or vehicles (0.9% NaCl for gp91ds-tat peptide) was administered 0.5 h before and 1 h after GTN (10 mg/kg i.p.). A mixture of gp91 and ML171 or GKT137831 was administered 1, 3 and 5 h after GTN (10 mg/kg i.p.). $CGRP_{8-37}$ (Tocris Bioscience) (2 μmol/kg, i.p.) [135] or BIBN4096BS (Tocris Bioscience) (Olcegepant; 1 mg/kg, i.p.) [288] or vehicle was administered 0.5 h before or 1.5 h after GTN (10 mg/kg, i.p.). In different experiments, C57BL/6 mice treated with GTN (10 mg/kg, i.p.) or vehicle were subcutaneously (s.c., 10 μl/site) administered into the periorbital area over the rostral portion of the eye with

The following antagonists were administered to C57BL/6 mice treated with GTN (10 mg/kg, i.p.) or vehicle by subcutaneous injection (10 μl/site, s.c.) into the periorbital area over the rostral portion of the eye: HC-030031 (100 μg) [240], cPTIO (60 μg) [289], disulfiram (10 μg), αLA (10 μg) [240], NAC (20 μg) [290], $CGRP_{8-37}$ (10 nmol), BIBN4096BS (4 nmol) or their vehicles (2% DMSO in 0.9% NaCl for HC-030031, αLA, disulfiram and BIBN4096BS or 0.9% NaCl for cPTIO, NAC and $CGRP_{8-37}$, respectively). The following antagonists were administered to C57BL/6 mice treated with GTN (10 mg/kg, i.p.) or vehicle by intrathecal injection (5 μl/site, i.th. in the lumbar region): HC-030031, A967079 (both 10 μg), cPTIO (30 μg), NAC (50 μg), $CGRP_{8-37}$ (5 nmol) [291], BIBN4096BS (1 μg) [292] or vehicles. Antagonists were given either 0.5 h before or 1.5 h or 4.5 h after GTN treatment.

C57BL/6, *Trpa1*$^{+/+}$ and *Trpa1*$^{-/-}$ mice were injected (10 μl/site, s.c.) with the selective TRPA1 agonist, allyl isothiocyanate (AITC, 10 nmol in 2.5% DMSO in 0.9% NaCl), GTN (10 μg/site), S-nitroso-N-acetylpenicillamine (SNAP, 40 μg/site in 2.5% DMSO in 0.9% NaCl), CGRP (0.5-5 μg/site in 0.9% NaCl) or their vehicles, and PMA was assessed (Elliott *et al.*, 2012) before and for 6 h after treatment. The effect of HC-030031 (50 μg/10 μl, s.c., 0.5 h before and 1 h after GTN/SNAP and 100 mg/kg, i.p., 0.5 h before GTN/SNAP), disulfiram (100 mg/kg, i.p., 0.5 h before GTN/SNAP), cPTIO (100 mg/kg, i.p., 0.5 h before GTN/SNAP) and their vehicles, were investigated.

Additional C57BL/6 mice received resiniferatoxin (RTX, 50 μg/kg, s.c.) or its vehicle (10% ethanol and 10% tween 80 in 0.9% NaCl) [293]. When the eye wiping test responses (evaluated as the number of eye wipes recorded for 10 min [293] to capsaicin (1 nmol/5 μl) was abolished, GTN (10 mg/kg, i.p.)-evoked PMA and H_2O_2 levels were evaluated.

TRPA1 antisense (5'-TATCGCTCCACATTGCTAC-3')- or mismatch control (5'-ATTCGCCTCACATTGTCAC-3')-oligonucleotide (TRPA1 AS/MM-ODN) was administered to C57BL/6 mice by i.th. injection (5 nmol/5 µl) (Bonet *et al.*, 2013) for 4 consecutive days. At day 5, the efficiency of TRPA1 silencing was tested by eye wiping (AITC, 10 nmol/5 µl) and the TRPA1 mRNA content in TGs, and PMA evoked by GTN (10 mg/kg, i.p.) and H_2O_2 levels were evaluated.

Adv-Cre^{+};*Trpa1*$^{fl/fl}$ and Adv-Cre^{-};*Trpa1*$^{fl/fl}$ received GTN (10 mg/kg, i.p.) or its vehicle and PMA and H_2O_2 levels in TGs collected 2 h after GTN/vehicle, were evaluated. Eye wiping was assayed after ocular instillation of capsaicin (1 nmol/5 µl). All the drugs, at the maximum used doses, did not evoke any direct nociceptive/allodynic responses or locomotor impairment.

Cell culture and isolation of primary sensory neurons. HEK293 cells (American Type Culture Collection; ATCC® CRL-1573™), cultured according to the manufacturer's instructions, were transiently transfected with the cDNAs (1 µg) codifying for wild type (Wt) (hTRPA1-HEK293) or mutant 3C/K-Q human TRPA1 (C619S, C639S, C663S, K708Q; 3C/K-Q hTRPA1-HEK293) [121] using the jetPRIME transfection reagent (Poliyplus-transfection® SA) according to the manufacturer's protocol. Primary TG neurons were isolated from C57BL/6 or *Trpa1*$^{+/+}$ and *Trpa1*$^{-/-}$ mice, and cultured as previously described [101]. To obtain trigeminal neuronal and satellite glial cells (SGCs)-mixed cultures or SGCs-enriched cultures the protocol reported previously [294] was used.

Calcium Imaging Assay. Intracellular calcium mobilization, $[Ca^{2+}]_i$, was measured in transfected HEK293 cells and in TG neurons, as previously reported [101]. TG neurons were challenged with GTN (10-300 µM), SNAP (30 µM), AITC (10 µM) or their vehicles. Capsaicin (0.1 µM) was used to identify capsaicin-sensitive neurons. Some experiments were performed in the presence of HC-030031 (50 µM), capsazepine (10 µM), HC-067047 (30 µM), cPTIO (100 µM) and disulfiram (1 µM). Buffer solution containing 0.5% DMSO was used as vehicle for SNAP and all inhibitors/scavenger. Wt or mutant hTRPA1-HEK293 cells were challenged with GTN (100 µM), menthol (100 µM) or their vehicle.

H_2O_2 assay. H_2O_2 was determined by using the Amplex Red® assay (Invitrogen), in C57BL/6 mice, in TGs before or after (0.5-6 h) GTN (10 mg/kg, i.p.), and 2 h after GTN/Veh in mice pretreated (0.5 h before GTN) with cPTIO (0.6 mg/kg, i.p.) and disulfiram (100 mg/kg, i.p.) or treated (1 h after GTN) with HC-030031 (100 mg/kg, i.p.) and αLA (100 mg/kg i.p.), or desensitized with RTX or silenced with TRPA1 AS/MM-

ODN; in dorsal horn of brain stem before and after (1 and 2 h) GTN; in *Trpa1*$^{+/+}$ and *Trpa1*$^{-/-}$, and in *Adv-Cre*;*Trpa1*$^{fl/fl}$ and *Adv-Cre*$^{-}$;*Trpa1*$^{fl/fl}$ mice. Increase in H_2O_2 release was quantified in trigeminal neuron-SGCs mixed and SGCs-enriched primary culture after challenge with GTN (10, 50 and 100 μM), AITC (30 μM), SNAP (100 μM) or their vehicle (0.3% DMSO for AITC and SNAP) in the presence of HC-030031 (50 μM) or its vehicle (0.5% DMSO in Krebs-Ringer phosphate buffer), or in a Ca^{2+}-free KRP buffer containing EDTA (1 mM) or after a pre-exposure to a high concentration of capsaicin (10 μM, 20 min) [295]. Detailed method is reported in supplementary materials.

Immunofluorescence. Anesthetized C57BL/6 and *Trpa1*$^{+/+}$ and *Trpa1*$^{-/-}$ mice treated with GTN (10 mg/kg, i.p.) or its vehicle were transcardially perfused with PBS, followed by 4% paraformaldehyde. TGs and brainstem were removed, postfixed for 24 h, and paraffin- embedded or cryoprotected (4°C, overnight) in 30% sucrose. Cryosections (10 μm) of brainstem and formalin fixed paraffin-embedded sections (5 μm) of TGs were incubated with the following primary antibodies: 4-HNE (ab48506, 1:40, HNEJ-2, Abcam), TRPA1 (ab58844, 1:400, Abcam), NOX1 (SAB2501686, 1:250), NOX2 (ab80897, 1:200, Abcam), NOX4 (ab109225, 1:200, Abcam), glutamine synthetase (GS, G2781, 1:400) (1 h, RT) diluted in PBS and 2.5% normal goat serum (NGS). Sections were then incubated with fluorescent secondary antibodies: polyclonal Alexa Fluor 488, and polyclonal Alexa Fluor 594 (1:600, Invitrogen) (2 h, RT) and coverslipped. The analysis of negative controls (non-immune serum) was simultaneously performed to exclude the presence of non-specific immunofluorescent staining, cross-immunostaining, or fluorescence bleed-through. Tissues were visualized and digital images were captured using an Olympus BX51 (Olympus srl). 4-HNE staining in TG was evaluated as the fluorescence intensity measured by an image processing software (ImageJ 1.32J, National Institutes of Health). Data are expressed as mean fluorescence intensity (% of basal). 4-HNE staining was determined in TGs collected from C57BL/6 mice before (basal level, BL) or after (0.5-6 h) GTN (10 mg/kg, i.p.) and 4 h after GTN/vehicle administration in C57BL/6 mice pretreated with cPTIO (0.6 mg/kg, i.p. given 0.5 h before GTN) or NAC (250 mg/kg, i.p., given 0.5 h before GTN) or treated with HC-030031 or αLA (both 100 mg/kg i.p., given 3 h after GTN) and in *Trpa1*$^{+/+}$ and *Trpa1*$^{-/-}$ mice, and in dorsal horn of brain stem collected from C57BL/6 mice before and after (1 and 2 h) GTN.

Mouse trigeminal neuron-SGCs mixed and SGCs-enriched cultures were cultured for 2-3 days, fixed in ice-cold methanol/acetone (5 min, 20°C), washed with PBS and blocked with NGS (10%) (1 h, RT). The cells were then incubated with the primary antibodies

(NeuN, 1:600, and GS, 1:300) (1 h, RT), with fluorescent secondary antibodies (1:600, polyclonal Alexa Fluor 488, and polyclonal Alexa Fluor 594, Invitrogen) (2 h, RT), mounted and digital images were captured using an Olympus BX51.

Proximity ligation assay (PLA). Colocalization of TRPA1 and NOX2 in mouse TG was obtained using an *in situ* PLA detection kit (Duolink, Olink Biosciences Inc.) as previously described [296]. In TG sections (5 μm) fluorescence images were obtained using Olympus BX51 and a 100X oil-immersion objective. Negative control was performed by omitting primary antibodies or PLA probes.

Real-Time PCR. RNA was extracted from TG of C57BL/6 mice after TRPA1 AS/MM-ODN (i.th.) and of *Adv-Cre*; $Trpa1^{fl/fl}$ and $Adv\text{-}Cre^{-}$; $Trpa1^{fl/fl}$. The standard Trizol® extraction method was used. Detailed method is reported in supplementary materials.

Blood flow experiments. Cutaneous blood flow was assessed using a laser doppler flowmeter (Perimed Instruments) in anaesthetized in C57BL/6, $Trpa1^{+/+}$ and $Trpa1^{-/-}$ mice. Cutaneous blood flow was monitored by a probe (cutaneous type) fixed to the shaved periorbital area, before and after the systemic administration of GTN (10 mg/kg, i.p.) or its vehicle. Before (0.5 h) GTN injection, mice were treated with i.p. HC-030031, disulfiram (both, 100 mg/kg) and BIBN4096BS (1 mg/kg) or their vehicles and cutaneous blood flow was monitored for at least 0.5 h. Baseline blood flow was calculated by the mean flow value measured during a 5-min period before the stimulus. The increase in cutaneous blood flow was calculated as the percentage change over the baseline.

Statistical Analysis. Statistical analysis was performed by the unpaired two-tailed Student's t-test for comparisons between two groups and the one- or two- way ANOVA followed by the post-hoc Bonferroni's test for comparisons of multiple groups. $P<0.05$ was considered statistically significant (GraphPad Prism version 5.00).

4.2 Results

4.2.1 GTN evokes NO-mediated TRPA1-independent vasodilatation and TRPA1-dependent allodynia

Administration of GTN (1-10 mg/kg, i.p.) to C57BL/6 mice induced a dose-dependent and prolonged periorbital mechanical allodynia (PMA) (Figure 1A). GTN (10 mg/kg, i.p.) also produced an early and transient (0-10 min) cutaneous increase in blood flow in the periorbital skin (Figure 1B). GTN (10 mg/kg) induced a similar PMA in *Trpa1*$^{+/+}$ mice, whereas *Trpa1*$^{-/-}$ mice were fully protected (Figure 1C). The increase in cutaneous blood flow evoked by GTN (10 mg/kg) in *Trpa1*$^{+/+}$ mice was maintained in *Trpa1*$^{-/-}$ mice (Figure 1E). Genetic deletion of TRPV1 or TRPV4 channels did not affect GTN-evoked PMA (Supplementary Figure 1A and B). Systemic GTN (10 mg/kg) also induced sustained mechanical allodynia in the hind paw of C57BL/6 and *Trpa1*$^{+/+}$, but not *Trpa1*$^{-/-}$ mice (Supplementary Figure 1C and D). This response, which indicates a general proalgesic action of GTN, was not further investigated.

The TRPA1 antagonists, HC-030031 [297], given (i.p.) 0.5 h before and 1-5 h after GTN, transiently and completely reversed PMA at all time points (Figure 1F). TRPA1 contribution to GTN-induced PMA was independent of the GTN dose, since *Trpa1* deletion abolished and HC-030031 (1 h after GTN) reversed PMA induced by the lowest dose of GTN (1 mg/kg) (Figure 1D and Supplementary Figure 1E). Another channel antagonist, A967079 [240], given 0.5 h before and 1 h after GTN (10 mg/kg) also transiently reversed allodynia (Supplementary Figure 1F). Antagonists of TRPV1 (capsazepine) and TRPV4 (HC-067047), given either 0.5 h before or 1 h after GTN, were ineffective (Supplementary Figure 1G and H).

Mitochondrial ALDH2 is known to generate NO from GTN [298]. To determine the contribution of NO to GTN-evoked PMA, mice were treated with the ALDH2 inhibitor, disulfiram, or the specific NO scavenger, cPTIO. Both disulfiram and cPTIO, when administered (i.p.) 0.5 h before, but not 1 hour after, GTN, attenuated GTN-evoked PMA (Figure 1G). The ability of disulfiram and cPTIO to prevent PMA if given before GTN indicates that NO mediates the onset of GTN-evoked PMA. However, failure of disulfiram and cPTIO to reverse established PMA suggests that additional mechanisms are required to sustain PMA. Pretreatment with disulfiram, but not with HC-030031 (both

i.p., 0.5 h before GTN), attenuated the increase in periorbital blood flow evoked by GTN (10 mg/kg) (Figure 1H).

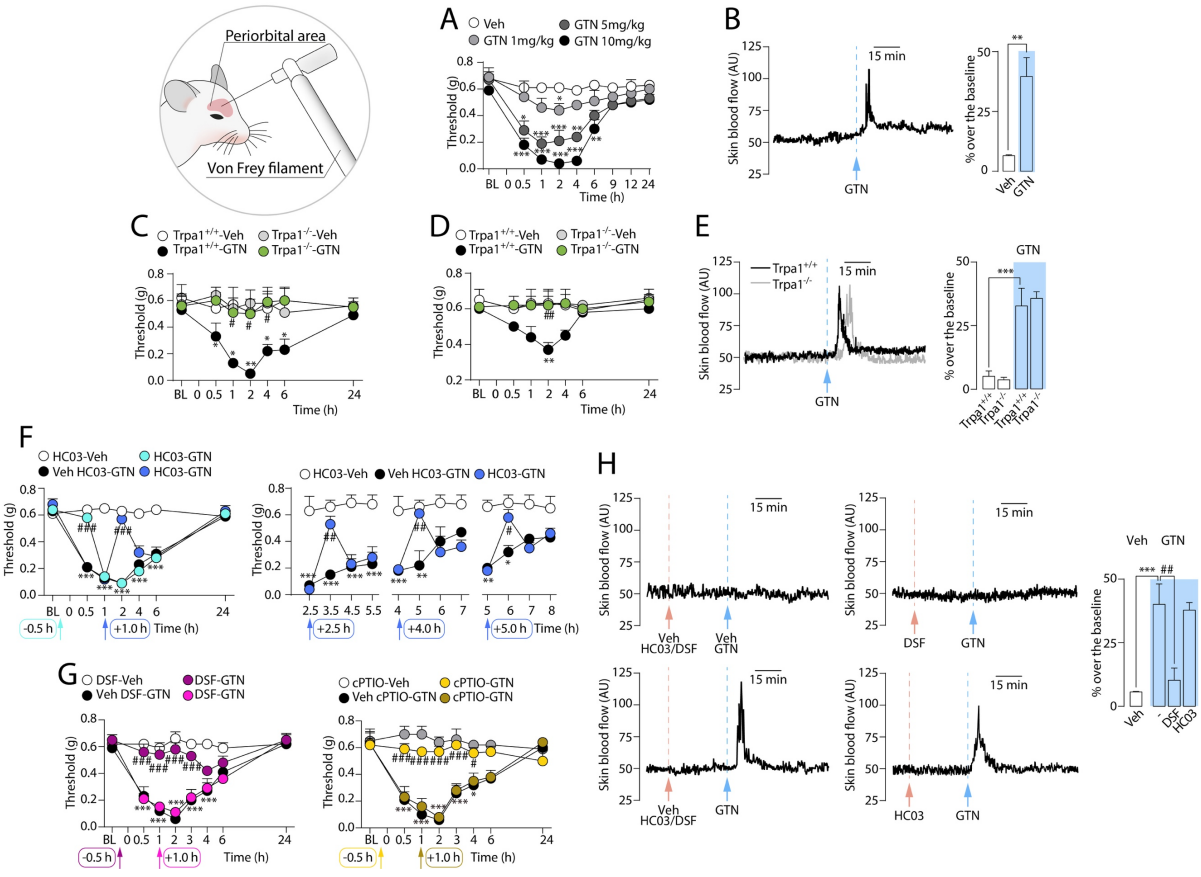

Figure 1. GTN induces periorbital mechanical allodynia (PMA) *via* a TRPA1-dependent mechanism. **A,** Dose- and time-dependent PMA evoked by i.p. GTN in C57BL/6 mice. **B**, Representative traces and pooled data of the increases in cutaneous blood flow evoked by GTN (10 mg/kg, i.p.). PMA evoked by **C** low (1 mg/kg, i.p.) and **D** high (10 mg/kg, i.p.) dose of GTN, in *Trpa1*$^{+/+}$ and *Trpa1*$^{-/-}$ mice. **E**, Representative traces and pooled data of the increases in cutaneous blood flow evoked by GTN (10 mg/kg, i.p.) in *Trpa1*$^{+/+}$ and *Trpa1*$^{-/-}$ mice. **F**, TRPA1 antagonism by HC-030031 (HC03; 100 mg/kg, i.p.) transiently reverses GTN-evoked (10 mg/kg, i.p.) PMA in C57BL/6 mice. **G**, Pretreatment with disulfiram (DSF, ALDH2 inhibitor) or cPTIO (NO scavenger) abates PMA evoked by GTN (10 mg/kg, i.p.) in C57BL/6 mice. **H**, Representative traces and pooled data of the increases in cutaneous blood flow evoked by GTN (10 mg/kg, i.p.) or its vehicle. DSF but not HC03, both given 0.5 h before GTN abolishes the increase in blood flow induced by GTN (10 mg/kg, i.p.). Veh is the vehicle of GTN. BL, baseline mechanical threshold. Arrows indicate times of drug administration. Error bars indicate mean ± SEM, 4-6 mice per group. **P*< 0.05, ***P*< 0.01, ****P*< 0.001 *vs*. Veh, *Trpa1*$^{+/+}$ -Veh, *Trpv1*$^{+/+}$-Veh, *Trpv4*$^{+/+}$-Veh, HC03-Veh, A96-Veh and $^{\#}$*P*< 0.05, $^{\#\#}$*P*< 0.01, $^{\#\#\#}$*P*< 0.001 *vs*. *Trpa1*$^{+/+}$-GTN or Veh HC03-GTN or Veh A96-GTN; two-way ANOVA with Bonferroni post-hoc correction.

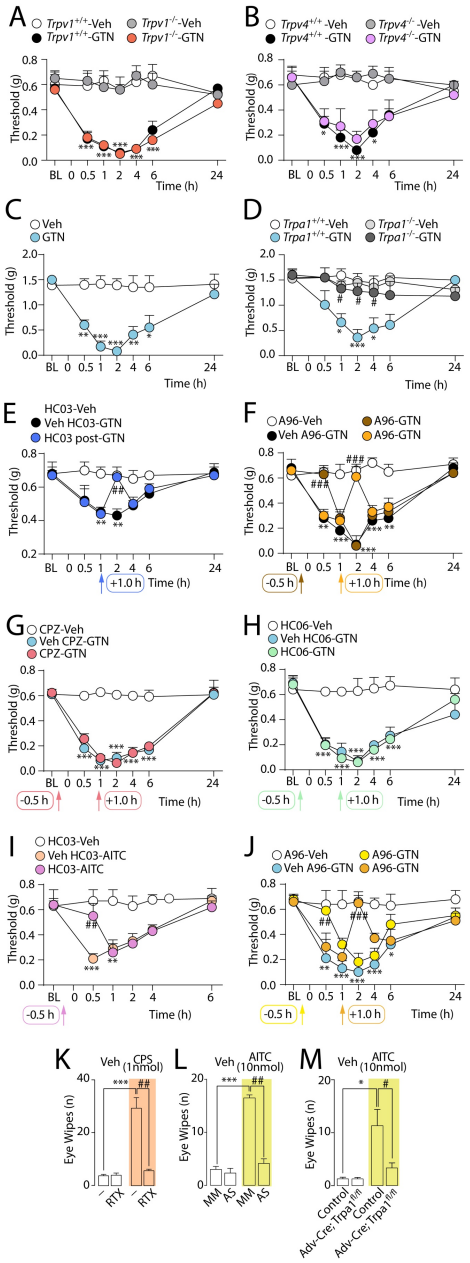

Supplementary Figure 1. Time-course of mechanical allodynia evoked by intraperitoneal (i.p.) GTN (10 mg/kg) and assessed within the posterior hind paw in **A** C57BL/6 mice or **B** *Trpa1*$^{+/+}$ and *Trpa1*$^{-/-}$ mice. **C-F**, Periorbital mechanical allodynia (PMA) evoked by GTN (10 mg/kg, i.p.) in C57BL/6 mice is unaffected in *Trpv1*$^{-/-}$ or in *Trpav4*$^{-/-}$ mice or by capsazepine (CPZ, 4 mg/kg, i.p.) or HC-067047 (HC06, 10 mg/kg, i.p.). **G**, PMA evoked by intraperitoneal (i.p.) GTN (1 mg/kg) injection is inhibited by HC-030031 (HC03; 100 mg/kg, i.p). **H**, GTN-evoked PMA is inhibited by A967079 (A96; 100 mg/kg, i.p). **I**, Time–dependent PMA evoked by subcutaneous (s.c.) injection (10 µl/site) into the periorbital area of allyl isothiocyanate (AITC; 100 nmol) is inhibited by s.c. HC-030031 (HC03; 100 µg/site). **K**, Eye wiping response evoked by ocular instillation (5 µl/drop eye) of capsaicin (CPS) in resiniferatoxin (RTX) desensitized C57BL/6 mice. **L**, Eye wiping response evoked by ocular instillation (5 µl/drop eye) of AITC in C57BL/6 mice treated (i.th.) with TRPA1 antisense (AS) or mismatch (MM) oligonucleotide. **M**, Eye wiping response evoked by ocular instillation (5 µl/drop eye) of AITC in *Advillin-Cre*; *Trpa1*$^{fl/fl}$ (*Adv-Cre;Trpa1*$^{fl/fl}$) or *Advillin-Cre*$^{-}$; *Trpa1*$^{fl/fl}$ (Control) mice. Veh is the vehicle of GTN or CPS or AITC. BL, baseline threshold. Arrows indicate time of drug administration. Error bars indicate mean ± SEM, 4-6 mice per group. **P*< 0.05, ***P*< 0.01, ****P*< 0.001 *vs*. HC03-Veh, *Trpa1*$^{+/+}$-Veh, CPZ-Veh, HC06-Veh, A96-Veh, Control-Veh. $^{\#}$*P*< 0.05, $^{\#\#}$*P*< 0.01, $^{\#\#\#}$*P*< 0.001 *vs*. *Trpa1*$^{+/+}$-GTN, Veh HC03-AITC, Veh A96-GTN, Control-GTN. One-way or Two-way ANOVA with Bonferroni post-hoc correction.

4.2.2 NO but not GTN directly targets TRPA1

To determine whether TRPA1 is directly gated by GTN and/or NO, responses to different NO donors were investigated *in vitro*. GTN caused a concentration-dependent increase in $[Ca^{2+}]_i$ in TG neurons from C57BL/6 and *Trpa1*$^{+/+}$, but not from *Trpa1*$^{-/-}$ mice (Figure 2A and B). HC-030031, but not capsazepine or HC-067047, abolished responses (Figure 2A). Key intracellular cysteine and lysine residues of TRPA1 interact with oxidants and electrophilic agents [121]. Whereas GTN increased $[Ca^{2+}]_i$ in hTRPA1-HEK293, HEK293 cells expressing a mutant 3C/K-Q/hTRPA1 were unresponsive (Figure 2C). Disulfiram or cPTIO did not affect GTN signals in neurons from C57BL/6 mice (Figure 2D). In contrast, both HC-030031 and cPTIO inhibited the Ca^{2+}-response to

SNAP (Figure 2D). Thus, GTN activates TRPA1 by targeting specific cysteine and lysine residues, but its *in vitro* action, conversely to SNAP, is not mediated through NO release. Results obtained *in vivo* by local administration of NO donors recapitulated the *in vitro* findings. Injection (s.c.) in the periorbital area of the TRPA1 agonist, AITC, evoked PMA that was reversed by local (s.c.) pretreatment with HC-030031 (Supplementary Figure 1I). Local (s.c.) NO-donors, GTN or SNAP, induced PMA in *Trpa1*$^{+/+}$, but not *Trpa1*$^{-/-}$ mice (Figure 2E and I). Both local (s.c.) (Figure 2F and J) or systemic (i.p.) HC-030031 (Figure 2G and K) reversed PMA by local GTN or SNAP. Systemic (i.p.) cPTIO and disulfiram did not affect PMA evoked by local (s.c.) GTN (Figure 2H). However, cPTIO (i.p.) attenuated PMA evoked by local (s.c.) SNAP (Figure 2L). Thus, GTN evokes allodynia by mechanisms that depend from the route of administration. Local GTN directly regulates TRPA1 gating, whereas systemic GTN indirectly regulates TRPA1 by a process that involves ALDH2-mediated liberation of NO.

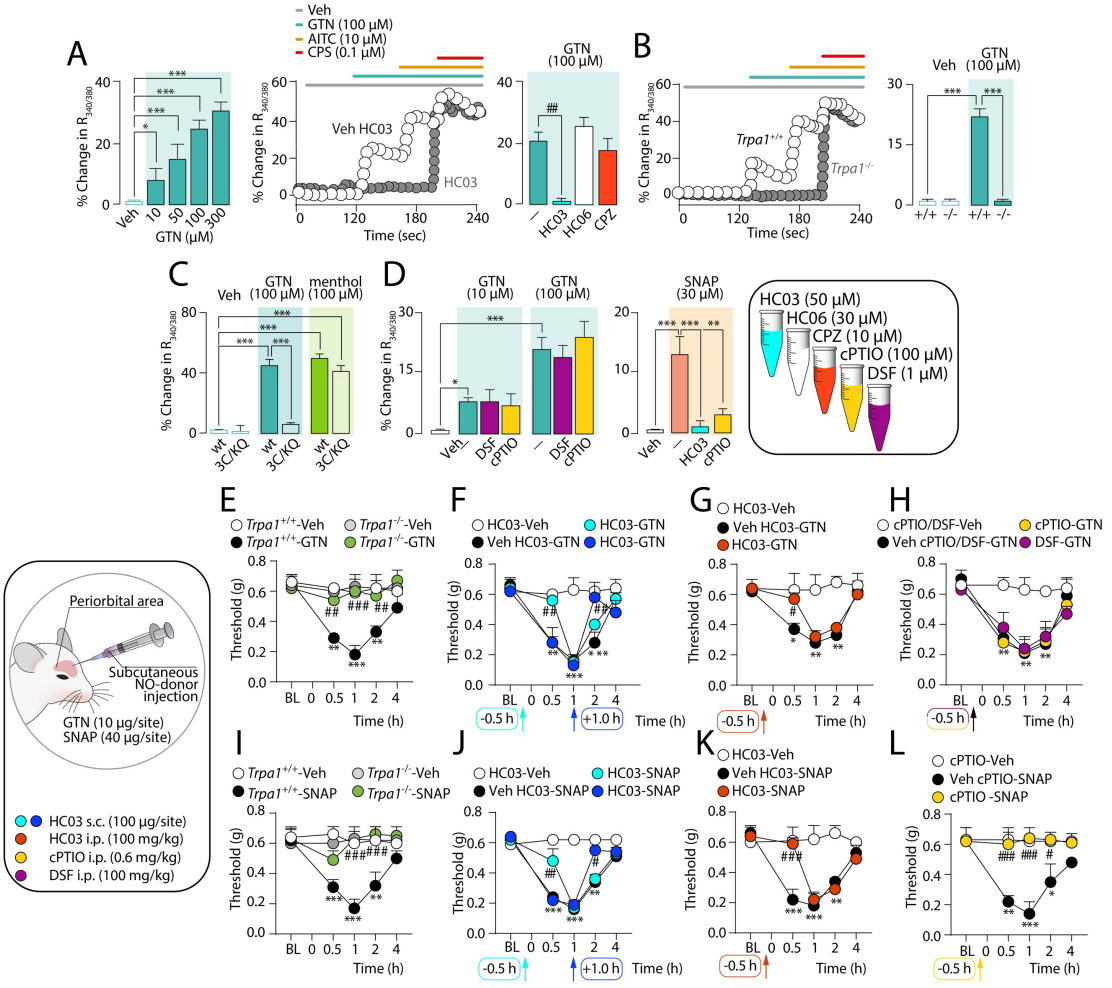

Figure 2. GTN-evoked periorbital mechanical allodynia (PMA) is mediated by NO. A, Ca^{2+}-response to GTN in mouse trigeminal ganglion (TG) neurons, which also respond to AITC or capsaicin (CPS), is attenuated by HC-030031 (HC03), but not by HC-067047 (HC06, TRPV4 antagonist) or capsazepine (CPZ, TRPV1 antagonist), and **B** abated by TRPA1 deletion. **C**, GTN-evoked Ca^{2+}-response in TG neurons is unaffected by DSF or cPTIO while SNAP-evoked Ca^{2+}-response is abated by cPTIO and HC03. **D**, Ca^{2+}-response to GTN or menthol in HEK293-cells expressing wild type (wt) or mutant (3C/K-Q) human

TRPA1. Error bars indicate mean ± SEM of n > 15 neurons or 25 cells **A-D**. *P< 0.05, **P< 0.01, ***P< 0.001; One-way ANOVA with Bonferroni post-hoc correction. GTN or SNAP (NO donor) (s.c., 10 µl) evokes time-dependent PMA that is abated in **E,I** *Trpa1*$^{-/-}$ mice and by **F,J** s.c. or **G,K** i.p. HC03. **H**, DSF or cPTIO (i.p.) do not affect PMA evoke by local GTN. (**L**) cPTIO (i.p.) prevents PMA evoked by local SNAP. Veh is the vehicle of GTN or SNAP. BL, baseline mechanical threshold. Arrows indicate time of drug administration. Error bars indicate mean ± SEM, 4-6 mice per group **E-L**. *P< 0.05, **P<0.01, ***P< 0.001 *vs*. DSF-Veh, cPTIO-Veh, *Trpa*1$^{+/+}$-Veh, HC03-Veh, DSF/cPTIO-Veh and $^{\#}P$< 0.05, $^{\#\#}P$< 0.01, $^{\#\#\#}P$< 0.001 *vs*. Veh DSF-GTN, Veh cPTIO-GTN, *Trpa1*$^{+/+}$-GTN, Veh *Trpa1*$^{+/+}$-SNAP, Veh HC03-GTN, Veh HC03-SNAP, Veh DSF/cPTIO-GTN, Veh cPTIO-SNAP; two-way ANOVA with Bonferroni post-hoc correction.

4.2.3 Oxidative stress and TRPA1 sustain GTN-evoked mechanical allodynia

cPTIO or disulfiram prevented GTN-evoked allodynia when administered before, but were ineffective when given after GTN. Thus, NO is necessary to initiate the hypersensitivity condition, but is not sufficient for its maintenance. Since GTN stimulates oxidative stress [299], we hypothesized that NO, liberated from GTN, initiates the process that subsequently sustains TRPA1-dependent PMA *via* ROS generation. The ROS scavenger αLA reversed PMA only when given (i.p.) 1 h after, but not 0.5 h before GTN (Figure 3A and B). Another ROS scavenger, PBN, also reversed allodynia with a similar time course (Figure 3C).

GTN-evoked PMA persisted for ~8 h, but αLA or PBN were unable to reverse PMA 3-4 h post-GTN (Figure 3B and C), indicating that mediators other than ROS are required to sustain hypersensitivity beyond 3-4 h. 4-HNE is a major electrophilic aldehyde that is generated by free radical attack of ω-6 polyunsaturated fatty acids [300], and is a TRPA1 agonist [123]. In contrast to ROS, which are short-lived, the biological activity of 4-HNE may last for hours [301]. NAC and L-carnosine efficiently scavenge α,β-unsaturated aldehydes, including 4-HNE. NAC or L-carnosine (i.p., pre-GTN) did not attenuate the first phase of GTN-evoked PMA, but strongly inhibited later phases (4-8 h) (Figure 3D and E), indicating that carbonylic derivatives more stable than ROS, sustain the final phase of PMA.

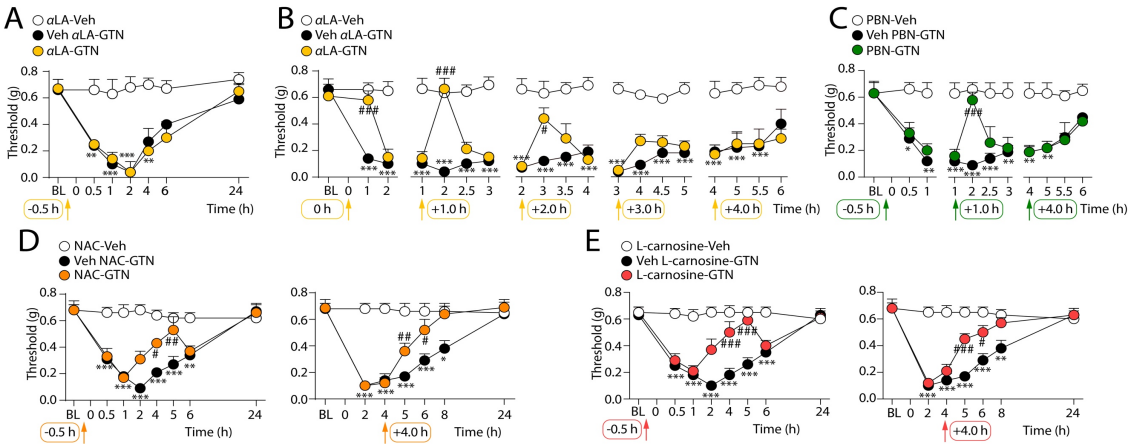

Figure 3. Prolonged periorbital mechanical allodynia (PMA) induced by GTN is mediated by oxidative stress. A-C, PMA evoked by GTN (10 mg/kg, i.p.) in C57BL/6 mice is inhibited by scavengers for reactive oxygen species, αLA (100 mg/kg, i.p.) or PBN (100 mg/kg, i.p.), when given after, but not before, GTN. **D,E**, The late phase of GTN-evoked PMA is reduced by treatment with NAC (250 mg/kg, i.p.) or L-carnosine (200 mg/kg, i.p.) given before and after GTN. Veh is the vehicle of GTN. BL, baseline mechanical threshold. Arrows indicate time of drug administration. Data are presented as mean ± SEM of 4-6 mice per group. **P*< 0.05, ***P*< 0.01, ****P*< 0.001 *vs*. αLA-Veh or PBN-Veh or NAC-Veh or L-carnosine-Veh. $^{\#}P$< 0.05, $^{\#\#}P$< 0.01, $^{\#\#\#}P$< 0.001 *vs*. Veh αLA-GTN or Veh PBN-GTN or Veh NAC-GTN or Veh L-carnosine-GTN; two-way ANOVA with Bonferroni post-hoc correction.

4.2.4 Systemic GTN does not produce periorbital allodynia by a local mechanism

Local injections of AITC, GTN or SNAP caused TRPA1-dependent PMA, suggesting the involvement of TRPA1 on cutaneous nerve terminals. However, PMA evoked by systemic GTN was unaffected by local treatment with HC-030031 (post-GTN), disulfiram and cPTIO (pre-GTN), or αLA and NAC (post-GTN) (Figure 4A-E). These findings, excluding that systemic GTN activates TRPA1 on cutaneous afferent nerve fibers to induce PMA, point to the involvement of central sites. Centrally administered HC-030031 or A967079 (pre- or post-GTN, i.th.) attenuated PMA-evoked by systemic GTN (Figure 4F and Supplementary Figure 1J). Disulfiram or cPTIO (pre-, but not post-GTN), αLA (post-, but not pre-GTN) and NAC (pre- or post-GTN) (all i.th.) (Figure 4G-J) also attenuated PMA.

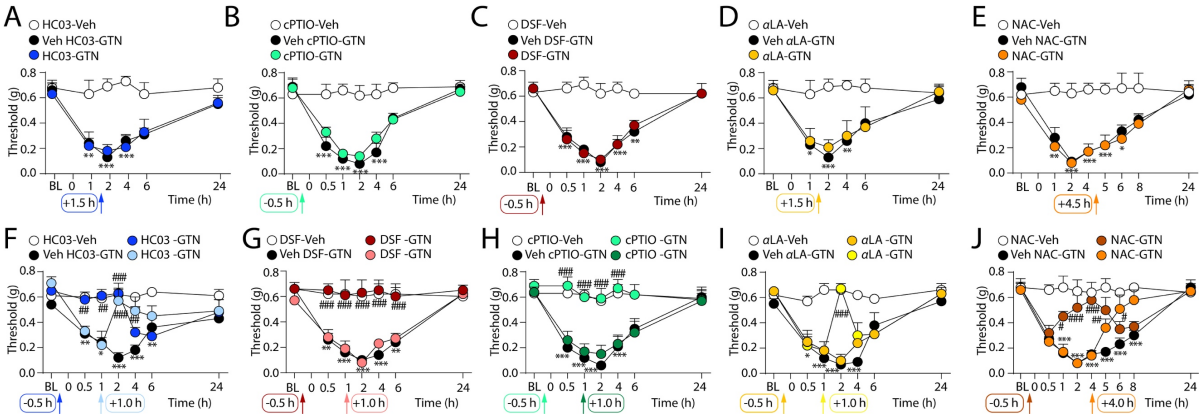

Figure 4. GTN-evoked periorbital mechanical allodynia (PMA) originates from trigeminal ganglion (TG) in C57BL/6 mice. A-E, PMA evoked by systemic GTN (10 mg/kg, i.p.) is unaffected by local administration (10 µl, s.c.) of HC-030031 (HC03; 50 µg), cPTIO (60 µg), disulfiram (DSF; 10 µg), αLA (5 µg) or NAC (20 µg). **F-J**, PMA evoked by systemic GTN (10 mg/kg, i.p.) is attenuated by intrathecal administration (5 µl, i.th.) of HC03 (10 µg, 0.5 h before or 1 h after GTN), DSF (5 µg, 0.5 h before GTN) and cPTIO (30 µg, 0.5 h before GTN), αLA (10 µg, 1 h after GTN), or NAC (50 µg, 0.5 h before or 4 h after GTN). Veh is the vehicle of GTN. BL, baseline mechanical threshold. Arrows indicate time of drug administration. Error bars indicate mean ± SEM, 4-6 mice per group. **P*< 0.05, ***P*< 0.01, ****P*< 0.001 *vs*. HC03- Veh, cPTIO-Veh, DSF-Veh, αLA-Veh, NAC-Veh. $^{\#}P$< 0.05, $^{\#\#}P$< 0.01, $^{\#\#\#}P$< 0.001 *vs*. Veh HC-03-GTN, Veh cPTIO-GTN, Veh DSF-GTN, Veh αLA- GTN, Veh NAC-GTN; two-way ANOVA with Bonferroni post-hoc correction.

4.2.5 GTN/NO targets TRPA1 in the soma of TG neurons to generate oxidative stress

The ability of intrathecal drugs to attenuate GTN-evoked, ROS- and 4-HNE-dependent activation of TRPA1 and the ensuing allodynia suggests the involvement of anatomical areas, which are contained by the dura mater membrane, namely the dorsal horns of the brainstem and the soma of nociceptors in the TG. To determine whether systemic GTN induces oxidative stress in these locations, we measured two markers of oxidative and carbonylic stress, H_2O_2 and 4-HNE, respectively. GTN, which failed to increase H_2O_2 and 4-HNE in brain stem, caused a rapid and transient increase in H_2O_2 (1-3 h) and a gradual and sustained increase in 4-HNE (4-6 h) in the TGs (Figure 5A and B). cPTIO and disulfiram (both pre-GTN) and αLA (post-GTN) blunted the H_2O_2 increase (at 2 h) (Figure 5C). cPTIO (pre-GTN), αLA (post-GTN) and NAC (pre-GTN) blunted the 4-HNE signal (at 4 h) (Figure 5D). Unexpectedly, HC-030031 and *Trpa1* deletion also attenuated GTN-induced increases in H_2O_2 or 4-HNE (Figure 5 C-E). These data suggest that oxidative stress generation, which seems to mediate GTN-evoked PMA, is initiated by NO-induced activation of TRPA1 within the TG.

Sensory neurons and satellite glial cells (SGCs) are present in the TG (Figure 6A). To determine which cell type generates GTN/NO-evoked oxidative stress, C57BL/6 mice were treated with RTX, which is known to defunctionalize TRPV1-expressing neurons that co-express TRPA1 [293]. RTX treatment, which suppressed capsaicin-induced eye

wiping (Supplementary Figure 1K), attenuated both GTN-evoked PMA and H_2O_2 generation (Figure 6B), supporting a role of TRPV1/TRPA1-positive neurons in these responses. GTN stimulated release of H_2O_2 from mixed cultures of TG neurons/SGCs (Figure 6C), but not from cultures of SGCs (Figure 6D). Removal of extracellular Ca^{2+} or pre-exposure to a high capsaicin concentration, which, similar to RTX, desensitizes TRPV1/TRPA1-positive neurons [243], attenuated GTN-evoked increase in H_2O_2 in mixed cultures of TG neurons/SGCs (Figure 6C). GTN, AITC and SNAP increased H_2O_2 release from TG neurons/SGCs mixed cultures in a HC-030031-dependent manner (Figure 6C). Intrathecal administration of TRPA1 AS-ODN down-regulated TRPA1 mRNA expression in TG neurons (Figure 6E) and reduced AITC-evoked eye wiping (Supplementary Figure 1L). TRPA1 AS-ODN attenuated GTN-evoked PMA and H_2O_2 increase in TGs (Figure 6E). Further evidence for the role of neuronal TRPA1 in GTN-evoked oxidative stress and allodynia was obtained by studying *Advillin-Cre*$^{+}$*;Trpa1*$^{fl/fl}$ mice, which lack TRPA1 in peripheral sensory neurons and do not respond to AITC-evoked eye wiping (Supplementary Figure 1M). GTN failed to evoke PMA or H_2O_2 generation in TGs in *Advillin-Cre*$^{+}$*;Trpa1*$^{fl/fl}$ mice (Figure 6F), thus supporting that GTN/NO initiates a TRPA1-dependent and oxidative stress-mediated mechanism that perpetuates nociceptor activation by an autocrine pathway that is confined to the TG.

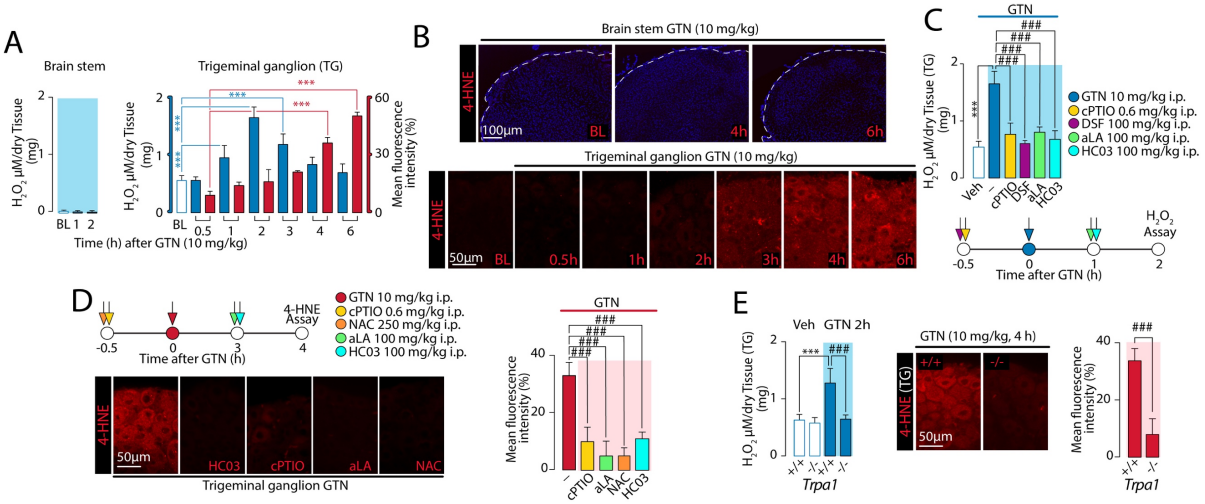

Figure 5. GTN generates oxidative stress in trigeminal ganglion (TG), *via* NO and TRPA1. GTN increases **A**, H_2O_2 levels and **B**, 4-HNE staining in TG, but not in brain stem of C57BL/6 mice. **C**, H_2O_2 increase in TGs 2 h after GTN is reduced by systemic cPTIO, disulfiram (DSF), αLA or HC-030031 (HC03). **D**, Representative images and pooled data of 4-HNE staining in TGs 4 h after GTN administration in C57BL/6 mice pretreated (0.5 hbefore) with cPTIO or NAC, or treated (3 h after) with HC03 and αLA. (**e**) GTN increases H_2O_2 levels and 4-HNE staining in TGs from *Trpa1*$^{+/+}$, but not *Trpa1*$^{-/-}$ mice. BL, baseline level of H_2O_2 or 4-HNE. Dash (-) indicates the combination of the vehicle of the various treatments. Error bars indicate mean ± SEM, n > 4-6 mice per group. ***P< 0.001; $^{###}P$< 0.001; one-way or two-way ANOVA with Bonferroni post-hoc correction for multiple comparison, and Student's t-test for comparisons between two groups.

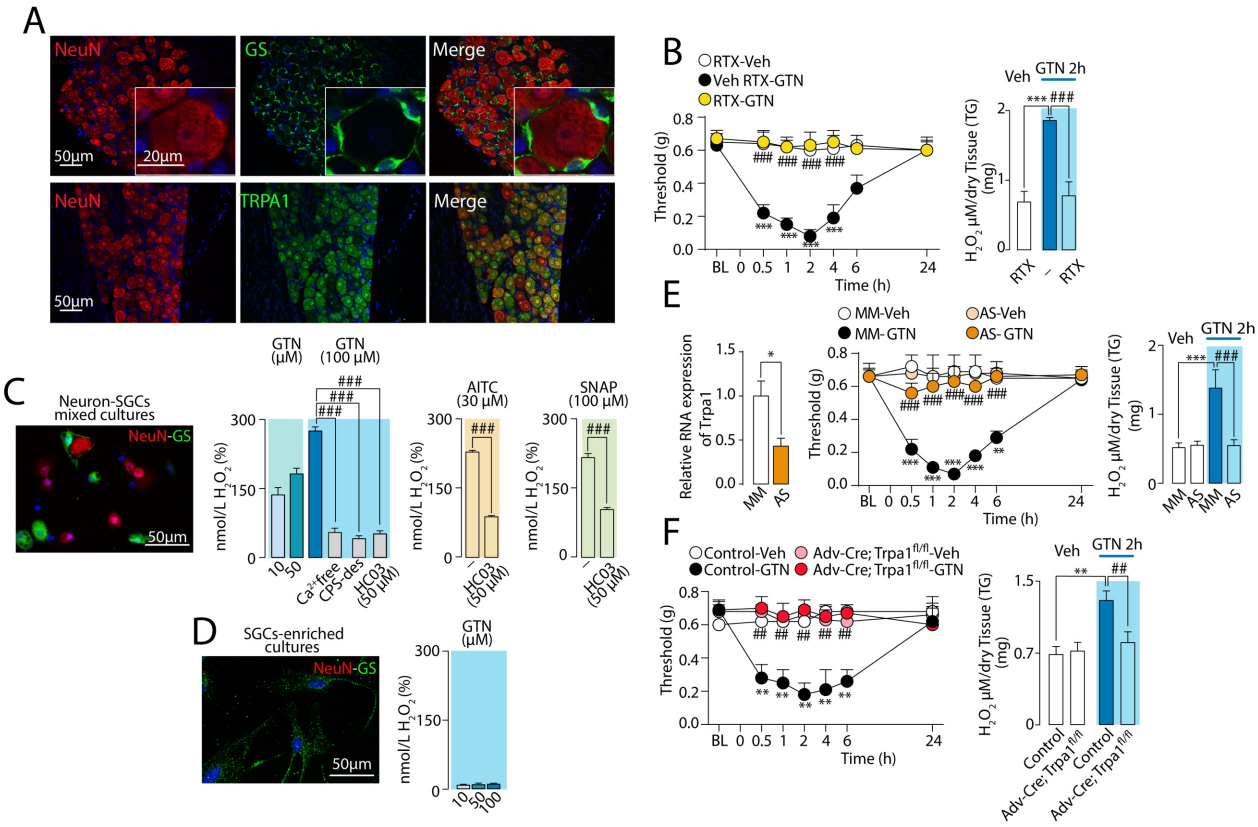

Figure 6. GTN targets neuronal TRPA1 to generate periorbital oxidative stress and mechanical allodynia (PMA). A, Neuronal (NeuN), satellite glial cells (SGCs) (glutamine synthetase, GS) and TRPA1 staining in trigeminal ganglion (TG). **B**, Neuronal defunctionalization with resiniferatoxin (RTX) prevents GTN-evoked PMA and H_2O_2 increase in TGs in C57BL/6 mice. **C**, H_2O_2 release elicited by GTN from TG neurons-SGCs mixed cultures (see staining for NeuN/GS) is inhibited by extracellular Ca^{2+} removal (Ca^{2+} free), pre-exposure to capsaicin (CPS-des) or HC-030031 (HC03), which also inhibits H_2O_2 release elicited by AITC or SNAP. **D**, In SGCs-enriched cultures (see staining for GS, but not NeuN) GTN does not release H_2O_2. **E**, Intrathecal TRPA1 antisense (AS), but not mismatch (MM) oligonucleotide, inhibits TRPA1 mRNA expression, GTN-evoked PMA and H_2O_2 increase in TGs. **F**, GTN-evoked PMA and H_2O_2 increase in TGs are reduced in *Advillin-Cre*; *Trpa1*$^{fl/fl}$ (*Adv-Cre;Trpa1*$^{fl/fl}$) mice. Veh is the vehicle of GTN. BL, baseline mechanical threshold. Dash (-) indicates the vehicle of HC03. Error bars indicate mean ± SEM, n > 4-6 mice per group. *P< 0.05, **P< 0.01, ***P< 0.001 *vs*. RTX-Veh, MM-Veh and control-Veh. $^{\#\#}P$< 0.01, $^{\#\#\#}P$< 0.001 *vs*. Veh RTX-GTN, MM-GTN and control-GTN; one-way or two-way ANOVA with Bonferroni post-hoc correction for multiple comparison, and Student's t-test for comparisons between two groups.

4.2.6 TRPA1 and NOXs in the soma of TG nociceptors maintain GTN-evoked allodynia

To explore the mechanism by which oxidative stress sustains GTN-evoked allodynia within TG neurons we detected immunoreactive NOX1, NOX2, and NOX4 that were expressed by mouse TG neurons but not SGCs (Supplementary Figure 2A), confirming previous studies [302]. NOX isoforms were coexpressed with immunoreactive TRPA1 (Figure 7A). The non-selective NOX inhibitor, apocynin (i.p., after, but not before GTN) reversed GTN-evoked allodynia (Figure 7B). Selective NOX2 (gp91ds-tat) or NOX1 (ML171) inhibitors (i.p., after, but not before GTN), attenuated allodynia, and

their combination abolished GTN-evoked PMA (Figure 7C). The NOX4 inhibitor, GKT137831, reduced, and the combination of GKT137831 and gp91ds-tat, abolished GTN-evoked allodynia (Supplementary Figure 2B and C). However, since GKT137831 also inhibits NOX1, the role of NOX4 remains uncertain. Furthermore, a proximity ligation assay showed that NOX2 and TRPA1 are closely located in TG neuronal cell bodies (Figure 7D), suggesting that their interaction could underlie efficient ROS release. Similar to αLA, the effect of the combination of the two NOX1/NOX2 inhibitors declined over time to disappear 3-4 h after GTN (Figure 7E). Thus, the soma of TRPA1-expressing TG neurons possesses the biochemical machinery required to initiate and sustain GTN-evoked oxidative stress.

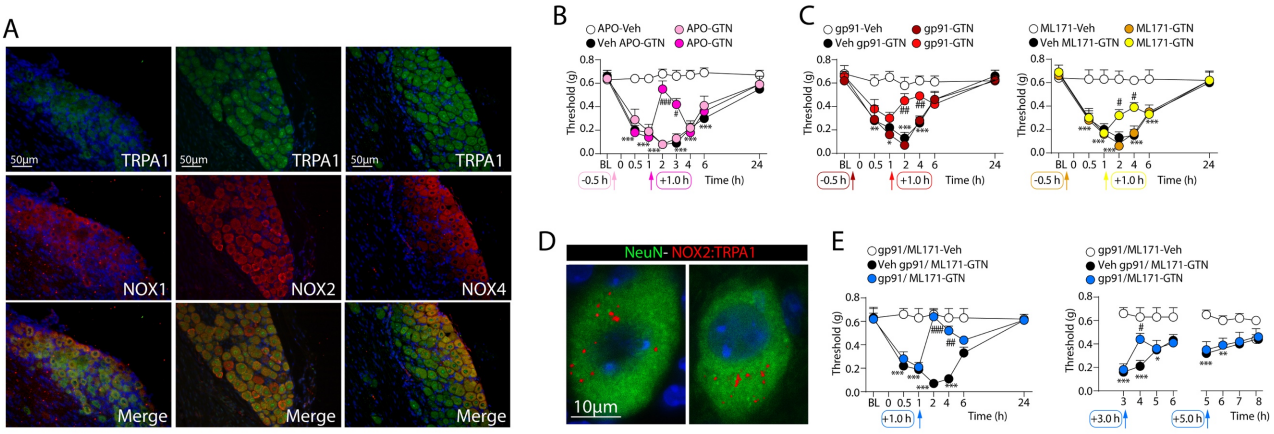

Figure 7. GTN evokes periorbital mechanical allodynia (PMA) *via* NADPH oxidase dependent mechanism. A, Representative images of TRPA1, NOX1, NOX2 and NOX4 staining in mouse trigeminal ganglion (TG). PMA evoked by GTN (10 mg/kg, i.p.) in C57BL/6 mice treated with the **B** unselective NOX inhibitor, apocynin (APO; 100 mg/kg i.p.), or the selective **C** NOX2 (gp91ds-tat peptide, gp91; 10 mg/kg, i.p.) or **D** NOX1 (ML171; 60 mg/kg i.p.) inhibitor. **D**, *In situ* proximity ligation assays (PLAs) for TRPA1:NOX2 in mouse TG labeled by a neuronal marker (NeuN). **E**, The combination of NOX1/NOX2 inhibitors (gp91/ML171) transiently attenuates PMA evoked by GTN (10 mg/kg, i.p.) in C57BL/6 mice. Veh is the vehicle of GTN. BL, baseline mechanical threshold. Arrows indicate time of drug administration. Error bars indicate mean ± SEM, 4-6 mice per group. **P*< 0.05, ***P*< 0.01, ****P*< 0.001 *vs*. APO-Veh, gp91-Veh, ML171-Veh, gp91/ML171-Veh. $^{\#}P$< 0.05, $^{\#\#}P$< 0.01, $^{\#\#\#}P$< 0.001 *vs*. Veh APO-GTN, Veh gp91-GTN, Veh ML171-GTN, Veh gp91/ML171-GTN; two-way ANOVA with Bonferroni post-hoc correction.

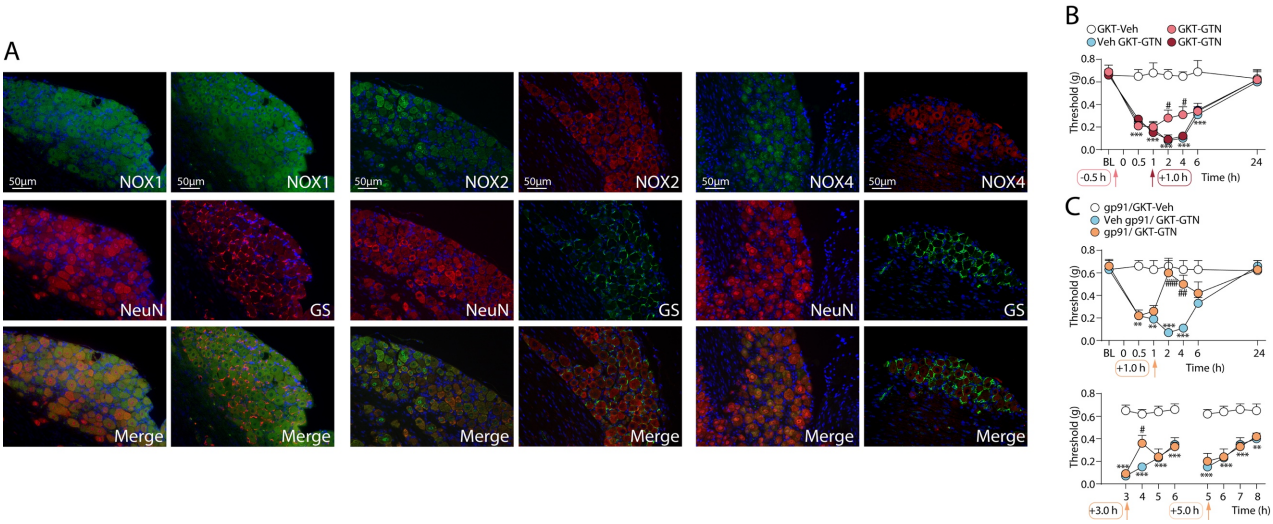

Supplementary Figure 2. A, Representative images of staining for NOX1, NOX2 and NOX4 and neuronal (NeuN) or satellite glial cells (glutamine sinthethase, GS) in mouse trigeminal ganglion (TG) from C57BL/6 mice. (Scale bars: 100 µm). **B,C**, Periorbital mechanical allodynia (PMA) evoked by GTN (10 mg/kg, i.p.) in C57BL/6 mice is reduced by NOX1/4 inhibitor, GKT137831 (GKT, 60 mg/kg, i.p.) alone, and completely abated by the combination of NOX1/4 and the NOX2 selective, gp91ds-tat peptide (gp91, 10 mg/kg, i.p.), inhibitors. Veh is the vehicle of GTN. BL, baseline threshold. Arrows indicate time of drug administration. Error bars indicate mean ±SEM, 4-6 mice per group. **P*< 0.05, ****P*< 0.001 *vs*. GKT-Veh, gp91/GKT-Veh. $^{\#}P$< 0.05, $^{\#\#}P$< 0.01, $^{\#\#\#}P$< 0.001 *vs*. Veh GKT-GTN and Veh gp91/GKT-GTN. Two-way ANOVA with Bonferroni post-hoc correction.

4.2.7 CGRP contributes only in part to GTN-evoked allodynia

As CGRP is a key mediator of migraine headaches [235,236] the contribution of CGRP to GTN-induced vasodilation and PMA was explored. Two different CGRP receptor antagonists, $CGRP_{8-37}$ and BIBN4096BS (olcegepant) given (i.p.) after, but not before GTN partially inhibited PMA (Figure 8A). $CGRP_{8-37}$ or BIBN4096BS administered centrally (i.th.) either before or after GTN did not affect GTN-evoked PMA (Figure 8B). CGRP injection (s.c., 0.5-5 µg/10µl) in the periorbital area induced a dose-dependent and sustained (4 h) PMA (Figure 8C). Pretreatment (s.c.) with $CGRP_{8-37}$ or BIBN4096BS prevented CGRP (5 µg/10µl)-induced PMA (Figure 8D). Local administration of $CGRP_{8-37}$ or BIBN4096BS after, but not before GTN partially attenuated PMA in a manner similar to that produced by their systemic administration (Figure 8E). GTN-evoked increase in cutaneous blood flow was unaffected by BIBN4096BS pretreatment (Figure 8F). Thus, the early vasodilation evoked by GTN is unrelated to CGRP.

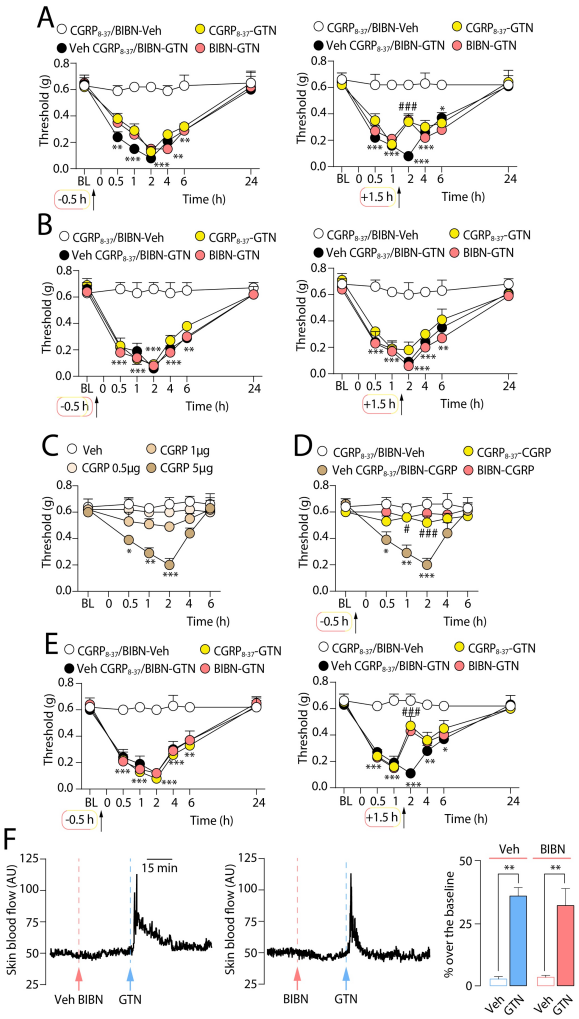

Figure 8. CGRP released from periorbital nerve terminals contributes to GTN evoked periorbital mechanical allodynia (PMA). A, PMA evoked by GTN (10 mg/kg, i.p.) in C57BL/6 mice is inhibited by i.p. administration of CGRP receptor antagonists, $CGRP_{8-37}$ (4 µmol/kg) or BIBN4096BS (BIBN; 1 mg/kg), when given after, but not before, GTN. **B**, Intrathecal administration of $CGRP_{8-37}$ (5 nmol/site) or BIBN (1 µg/site) does not affect GTN-evoked PMA. **C**, CGRP (0.5-5 µg/10 µl site, s.c.) evokes a dose- and time-dependent PMA. **D**, $CGRP_{8-37}$ (10 nmol/site) or BIBN (4 nmol/site) given 0.5 h before CGRP (5 µg/site) prevent CGRP-evoked PMA. **E**, Locally administered (10 µl, s.c.) $CGRP_{8-37}$ (10 nmol/site) or BIBN (4 nmol/site) reduce PMA when given after, but not before GTN. Veh is the vehicle of GTN or CGRP. BL, baseline mechanical threshold. Arrows indicate time of drug administration. Data are presented as mean ± SEM of 4-6 mice per group. **P*< 0.05, ***P*< 0.01, ****P*< 0.001 *vs.* $CGRP_{8-37}$/BIBN-Veh or Veh. $^{\#}P$< 0.05, $^{\#\#\#}P$< 0.001 *vs.* Veh $CGRP_{8-37}$/BIBN-GTN or Veh $CGRP_{8-37}$/BIBN-CGRP; two-way ANOVA with Bonferroni post-hoc correction. **F**, Representative traces and pooled data of the increases in cutaneous blood flow evoked by GTN (10 mg/kg, i.p.) or its vehicle. BIBN (1 mg/kg, i.p.), given 0.5 h before GTN does not affect the early increase in blood flow. Data are presented as mean ± SEM of 4-6 mice per group. **P*< 0.05, ***P*< 0.01 *vs.* Veh. $^{\#}P$< 0.05 *vs.* GTN; Student's t-test.

4.3 Discussion

GTN ability to provoke migraine-like attacks has been used to model the disease and understand its pathophysiology [199,227,229]. The prolonged allodynia evoked in rodents by GTN administration has been proposed to recapitulate the delayed migraine-like attacks after exposure to GTN in humans [232,237,238]. Here, we found that the delayed and prolonged GTN-evoked PMA in mice is entirely TRPA1-dependent, as two chemically unrelated TRPA1 antagonists, but not TRPV1 or TRPV4 antagonists, transiently, but completely, reversed PMA, and *Trpa1* deletion, but not *Trpv1* or *Trpv4* deletion, prevented the development of PMA. A recent report that GTN potentiation of formalin-evoked periorbital allodynia in rats is partly attenuated by TRPA1 antagonism is in line with our findings [303].

Mice received a high dose of GTN (10 mg/kg), which has been largely used in previous reports [237,238,304]. However, genetic deletion or pharmacological blockade of TRPA1 suppressed also PMA evoked by a low dose of GTN (1 mg/kg), which is 25 times greater than the dose (40 μg/kg, i.v.) commonly used in humans [199,227,230]. However, after correction for the mouse to man conversion factor (12 to 1) [255], these two doses are quite similar, thus supporting the translational relevance of TRPA1 role in GTN-evoked allodynia in mice.

NO activation of TRPA1, either directly, or indirectly *via* its byproducts, through nitrosylation of cysteinyl residues, represents an important posttranslational mechanism of channel regulation [206]. NO donors activate TRPA1 in cultured TG neurons and hTRPA1-HEK293 cells by distinct mechanisms. As *in vitro* cPTIO inhibited Ca^{2+}-responses by SNAP, but not Ca^{2+}-responses by GTN, NO does not seem required for TRPA1activation by GTN. It is possible that NO is released with insufficient velocity or in insufficient amounts to elicit TRPA1 gating, while the channel is engaged directly by GTN which binds to the same key cysteine/lysine residues required for channel activation by electrophilic and oxidant molecules [121,305].

GTN induces PMA that, depending from the route of administration, shows distinct anatomical pathways, mechanisms and time courses. The initial ALDH2-mediated conversion of GTN to NO seems to occur distant [298] from the site where NO targets TRPA1 as disulfiram and cPTIO blocked PMA elicited by systemic, but not local administration of GTN. Thus, while local GTN causes allodynia by direct TRPA1 targeting, systemic GTN does not. Evidence that NO must have spent some time in the extracellular environment before leading to S-nitrosothiol formation [306] supports this

explanation. Furthermore, the observation that cPTIO and disulfiram prevent allodynia when administered before but not after systemic GTN implies that NO is initially necessary, but is not subsequently sufficient, to sustain the allodynia. Attenuation by HC-030031 or A967079 of GTN-evoked allodynia was a transient phenomenon, probably due to the limited half-lives of the antagonists. These findings suggest that to maintain allodynia TRPA1 must be engaged continuously by one or more mediators generated by GTN/NO and whose identity and source are unknown.

GTN generates oxidative stress [299]. The observation that pretreatment with αLA or PBN did not prevent GTN-evoked hypersensitivity indicates that ROS do not initiate PMA. However, the finding that ROS scavengers attenuated allodynia from for 3-4 h after GTN reveals ROS contribution to a first phase, whereas additional TRPA1 agonists must contribute to the late phase of PMA. Carbonylic byproducts of oxidative stress, including 4-HNE, have half-lives longer than ROS [301], and are known to target TRPA1 [123]. PMA attenuation by NAC and L-carnosine, which efficiently quenches aldehydes, indicates that 4-HNE and/or related aldehydes engage TRPA1 to mediate the terminal phase of PMA, from 3-4 to 8 h after GTN.

Failure of local and efficacy of intrathecal antioxidants and TRPA1 antagonists to block PMA indicate that systemic GTN/NO does not target TRPA1 on nociceptor peripheral terminals and suggests the involvement of TRPA1 in a central site, including the soma of nociceptors in TGs and brainstem dorsal horns. Assessment of GTN-induced oxidative stress showed no change in the dorsal brain stem, whereas a marked increase in H_2O_2 and 4-HNE levels were found in TGs. Remarkably, the time course of H_2O_2 formation (1-3 h) paralleled the ability of ROS scavengers to attenuate PMA, and the time course of increased 4-HNE staining (3-6 h) paralleled the ability of aldehyde scavengers to inhibit PMA. These findings strengthen the hypothesis that ROS and aldehydes generated within the TGs provide the initial and final contribution to PMA, respectively.

Primary sensory neurons and associated SGCs are most abundant cell types in TG. The observation that RTX, which defunctionalizes TRPV1/TRPA1 expressing nociceptors [293], attenuated GTN-evoked H_2O_2 generation *in vivo*, suggests that TG neurons rather than SGCs generate oxidative stress. As pharmacological blockade of TRPA1, global TRPA1 deletion, neuronal TRPA1 knockdown and selective deletion of TRPA1 in primary sensory neurons all abrogated GTN-evoked increase in H_2O_2/HNE, TRPA1 expressed by TG sensory neurons is a critical mediator of oxidative stress-dependent PMA. Although various TRP channels can promote ROS release [307], to our knowledge this is the first

evidence that TRPA1 expressed by cell bodies of primary sensory neurons increase the tissue burden of oxidative stress.

Sensory neurons express several NOX isoforms that may mediate the GTN/NO/TRPA1 signal [302]. TG neurons, but not SGCs, co-express TRPA1 and NOX1, NOX2 and NOX4, and the NOX inhibitor apocynin reverses GTN-evoked mechanical allodynia, thus suggesting that NOXs expressed by TG neurons and located downstream from TRPA1 generate the pro-allodynic oxidative burden. NOX1 and NOX2 isoforms provide a major contribution, since the combination of selective NOX1 and NOX2 inhibitors afforded complete inhibition of allodynia. Notably, similar to αLA, the capacity of NOX inhibitors to suppress allodynia faded with time, and was absent when the drugs were administered 3-4 h after GTN.

The beneficial action of CGRP/CGRP receptor blockade by small molecules or monoclonal antibodies indicate that CGRP is a major mediator of migraine headaches [236,308]. The observation that two different CGRP receptor antagonists, by systemic or local, but not central, administration reduced GTN-evoked PMA suggests that CGRP acts at a peripheral site. One possible explanation is that excitation of the NO/TRPA1/NOX pathway in the soma of TG neurons generates antidromic action potentials, which ultimately invade cutaneous nerve terminals to promote local CGRP release. This hypothesis is supported by the recent observation that an anti-CGRP monoclonal antibody, which does not cross the blood brain barrier, reduced rat PMA induced by sodium nitroprusside plus sumatriptan [309]. Our findings that CGRP provides a limited contribution to the allodynia in mice may explain the failure of BIBN4096BS to reduce GNT-evoked migraine-like pain in migraineurs [202].

Notably, we report that the early periorbital vasodilation elicited by GTN is entirely due to ADH2-dependent NO formation, but neither TRPA1 nor CGRP are involved. Thus, vasodilatation and allodynia are temporally and mechanistically distinct. While vasodilatation is probably due to a direct NO action in the vascular smooth muscle, allodynia is a neuronal phenomenon mediated by TRPA1 activation and the ensuing oxidative stress.

Our present results suggest that (Supplementary Figure 3) systemic GTN is converted by ALDH2 to NO that causes a transient vasodilatation unrelated to TRPA1 and most probably due to a direct action of the gaseous mediator on smooth muscle guanylyl cyclase. NO and/or its byproducts also target TRPA1/NOXs in the soma of TG neurons to increase ROS/RCS, thereby sustaining mechanical allodynia. The peculiar localization

of TGs, which although outside the blood brain barrier, are contained within the meningeal membranes, make them accessible to both systemic and intrathecal drugs. The TRPA1 channel that triggers the oxidative burst is expressed by the same sensory neurons that potentially mediate the allodynia. Thus, it is not possible to discriminate whether TRPA1, in addition to generating the proalgesic oxidative stress, is the final mediator of the hypersensitivity. Nevertheless, since TRPA1 is a major sensor of oxidative and carbonylic stress [123,127,130], it is possible that TRPA1 is the target of the ROS/4-HNE, which are generated by its own initial activation by GTN/NO. TRPA1 antagonists, which are currently in clinical development, or established anti-migraine drugs, which have recently been identified as selective channel inhibitors [243,310] may be used to test whether a mechanism similar to the present one mediates the delayed attack evoked by GTN in migraineurs.

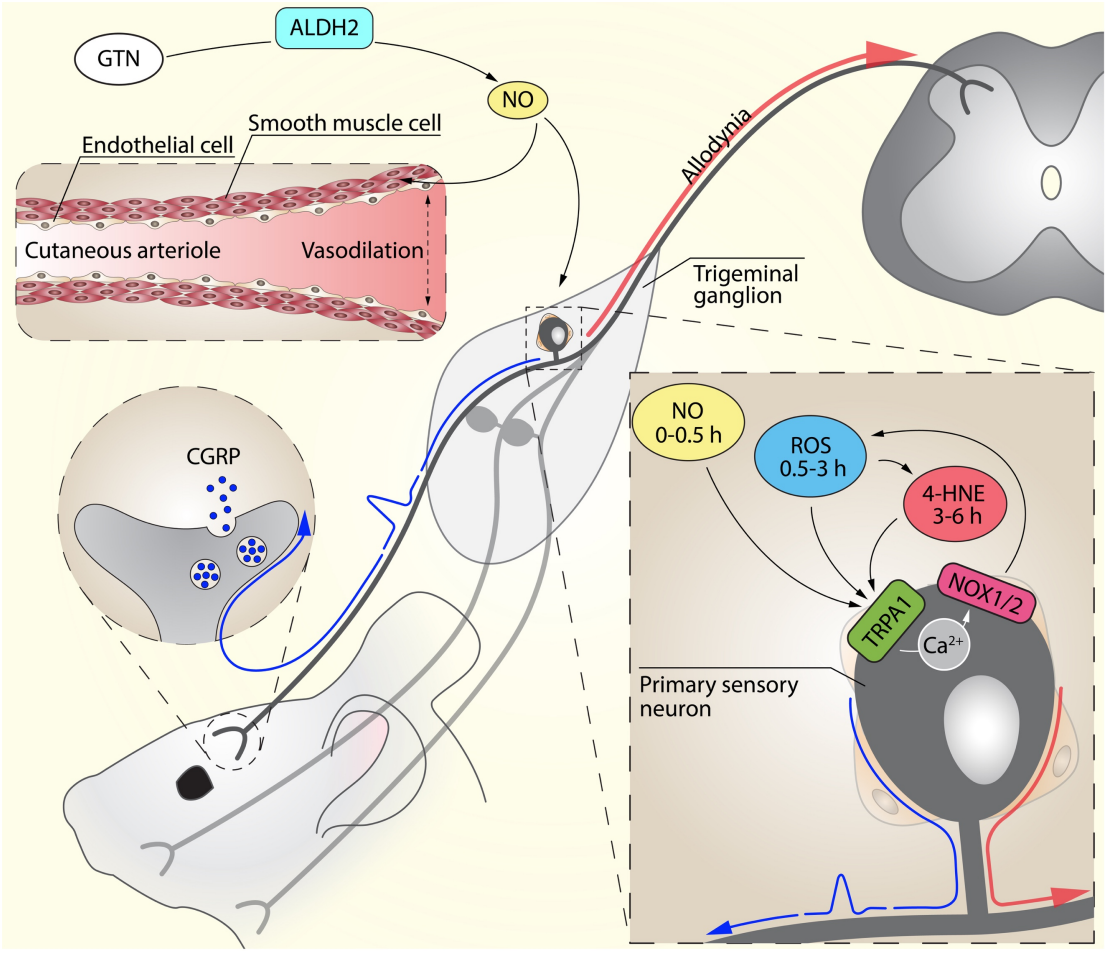

Supplementary Figure 3. GTN given systemically is converted to nitric oxide (NO) by aldehyde dehydrogenase-2 (ALDH2) at sites distant to the trigeminal ganglion (TG). NO diffusing into vascular smooth muscle cells increases periorbital cutaneous blood flow by a TRPA1- and CGRP-independent mechanism. NO, or its derivatives, also targets TRPA1 that by a Ca^{2+}-dependent mechanism and NOX1/NOX2-mediated pathway, increases reactive oxygen (H_2O_2) and carbonylic (4-hydroxynenal, HNE) species that by an apparently autocrine mechanism sustain periorbital mechanical allodynia. Activation of the NO/TRPA1/NOX pathway in the soma of TG neurons results in the generation of antidromically-

propagated action potentials, which ultimately invade cutaneous nerve terminals to promote local CGRP release that contributes to allodynia.

This work has been submitted to Brain

Marone IM, De Logu F, Nassini R, De Carvalho Goncalves M, Benemei S, Ferreira J, Jain P, Li Puma S, Bunnett NW, Geppetti P, Materazzi S (2017). "TRPA1/NOX in the soma of trigeminal ganglion neurons mediates migraine-related pain of glyceryl trinitrate in mice".

Chapter V- The antimigraine butterbur ingredient, isopetasin, desensitizes peptidergic nociceptors *via* the TRPA1 channel

5.1 Methods

Animals. *In vivo* experiments and tissue collection were carried out according to the European Union (EU) guidelines and Italian legislation (DLgs 26/2014, EU Directive application 2010/63/EU) for animal care procedures, and under University of Florence research permits #204/2012-B and #194/2015-PR. In addition, the number of animals and intensity of noxious stimuli used were the minimum necessary to demonstrate consistent effects of the treatments used. Animal studies are reported in compliance with the ARRIVE guidelines [311,312]. C57BL/6 mice (male, 20-25 g, 5 weeks; Envigo, Milan, Italy; N=208), littermate wild type (*Trpa1*$^{+/+}$, N=30) and TRPA1-deficient (*Trpa1*$^{-/-}$; N=30) mice (25-30 g, 5-8 weeks), generated by heterozygotes on a C57BL/6 background (B6.129P-*Trpa1*$^{tm1Kykw/J}$; Jackson Laboratories, Bar Harbor, ME, USA), wild type (*Trpv4*$^{+/+}$; N=15) and TRPV4-deficient (*Trpv4*$^{-/-}$; N=15) mice (25-30 g, 5-8 weeks), generated by heterozygotes on a C57BL/6 background [313] and TRPV1-deficient mice (*Trpv1*$^{-/-}$; B6.129X1-*Trpv1*$^{tm1Jul/J}$; N=15) backcrossed with C57BL/6 mice (*Trpv1*$^{+/+}$; N=15) for at least 10 generations (Jackson Laboratories, Bar Harbor, ME, USA; 25-30 g, 5-8 weeks); 25-30 g, 5-8 weeks) or Sprague-Dawley rats (male, 75-100 g, Envigo, Milan, Italy; N=73) were used. Animals were housed in a controlled-temperature environment, 10 *per* cage (mice) or five per cage (rats), with wood shaving bedding and nesting material, maintained at 22 ± 1°C. Animals were housed with a 12 h light/dark cycle (lights on at 07:00 a.m.) and fed with rodent chow (Global Diet 2018, Harlan, Lombardy, Italy) and tap water *ad libitum*. Animals were allowed to acclimatize to their housing environment for at least 7 days prior to experimentation and to the experimental room for 1 h before experiments. Behavioural experiments were done in a quiet, temperature-

controlled (20 to 22 °C) room between 9 a.m. and 5 p.m., and were performed by an operator blinded to genotype and drug treatment. Animals were euthanized with inhaled CO_2 plus 10-50% O_2 under a valid institutional animal protocol.

Cell culture and isolation of primary sensory neurons. Naïve untransfected HEK293 cells (American Type Culture Collection, Manassas, VA, USA; ATCC® CRL-1573™) were cultured according to the manufacturer's instructions. HEK293 cells were transiently transfected with the cDNAs (1 μg) codifying for wild type (wt-hTRPA1) or mutant 3C/K-Q human TRPA1 (C619S, C639S, C663S, K708Q; 3C/K-Q hTRPA1-HEK293) (both donated by D. Julius, University of California, San Francisco, CA, USA) [121] using the jetPRIME transfection reagent (Poliyplus-transfection® SA, Strasburg, France) according to the manufacturer's protocol. HEK293 cells stably transfected with cDNA for human TRPA1 (hTRPA1-HEK293, donated by A.H. Morice, University of Hull, Hull, UK), or with cDNA for human TRPV1 (hTRPV1-HEK293, donated by M. J. Gunthorpe, GlaxoSmithKline, Harlow, UK), or with cDNA for human TRPV4 (hTRPV4-HEK293, donated by N.W. Bunnett, Monash Institute of Pharmaceutical Sciences, Parkville, Australia) were cultured as previously described [243]. Human fetal lung fibroblasts (IMR90; American Type Culture Collection, Manassas, VA, USA; ATCC® CCL-186™), which express the native TRPA1 channel, were cultured in DMEM supplemented with 10% FBS, 2 mM glutamine, 100 U penicillin and 100 μg · ml^{-1} streptomycin. Cells were plated on glass coated (poly-L-lysine, 8.3 μM) coverslips and cultured for 2-3 days before being used for recordings. For all cell lines, the cells were used as received without further authentication.

Primary trigeminal ganglion (TG) neurons were isolated from adult Sprague-Dawley rats and C57BL/6 or *Trpa1*$^{+/+}$ and *Trpa1*$^{-/-}$ mice, and cultured as previously described [245]. Briefly, TG were bilaterally excised under a dissection microscope and transferred to HBSS containing 1 mg·ml^{-1} of trypsin plus 2mg·ml^{-1} of collagenase type 1A or papain, for rat or mouse ganglia, respectively, for enzymic digestion (30 min, 37°C). Ganglia were then transferred to warmed DMEM containing: 10% FBS, 10% horse serum, 2 mM L-glutamine, 100 U·ml^{-1} penicillin and 100 mg·ml^{-1} streptomycin and dissociated into single cells by several passages through a series of syringe needles (23–25 G). Medium and ganglia cells were filtered to remove debris and centrifuged. The pellet was suspended in DMEM with added 100 ng·ml^{-1} mouse-NGF and 2.5 mM cytosine-D-arabinofuranoside free base. Neurons were then plated on glass coverslips coated with poly-L-lysine (8.3 μM) and laminin (5 μM).

Cellular Recordings. Mobilization of intracellular calcium ($[Ca^{2+}]_i$) was measured in untrasfected or transfected HEK293 cells, in IMR90 and in primary sensory neurons, as previously reported [245]. Plated cells were loaded with 5 μM Fura-2 AM-ester (Alexis Biochemicals; Lausen, Switzerland) added to the buffer solution (37°C) containing the following (in mM): 2 $CaCl_2$; 5.4 KCl; 0.4 $MgSO_4$; 135 NaCl; 10 D-glucose; 10 HEPES and 0.1% bovine serum albumin at pH 7.4. After loading (40 min, 37°C), cells were washed and transferred to a chamber on the stage of a Olympus IX81 microscope for recording. Cells were excited alternately at 340 and 380 nm to indicate relative intracellular calcium changes by the $Ratio_{340/380}$ ($R_{340/380}$) and recorded with a dynamic image analysis system (XCellence Imaging software; Olympus srl, Milan, Italy). Results are expressed as the percentage of increase of $R_{340/380}$ over the baseline normalized to the maximum effect induced by ionomycin (5 μM) (% Change in $R_{340/380}$).

Whole-cell patch-clamp recordings were performed in untransfected and transfected HEK293 cells and in primary sensory neurons plated on coated coverslips as previously reported [245]. Briefly, coverslips were transferred to a recording chamber (1 ml volume), mounted on the platform of an inverted microscope (Olympus CKX41, Milan, Italy) and superfused at a flow rate of 2 $ml \cdot min^{-1}$ with a standard extracellular solution containing (in mM): 10 HEPES, 10 D-glucose, 147 NaCl, 4 KCl, 1 $MgCl_2$, and 2 $CaCl_2$ (pH adjusted to 7.4 with NaOH). Borosilicate glass electrodes (Harvard Apparatus, Holliston, MA, USA) were pulled with a Sutter Instruments puller (model P-87) to a final tip resistance of 4–7 MΩ. Pipette solution used for HEK293 cells contained (in mM): 134 K-gluconate, 10 KCl, 11 EGTA, 10 HEPES (pH adjusted to 7.4 with KOH). When recordings were performed on rat neurons, 5 mM $CaCl_2$ was present in the extracellular solution and pipette solution contained (in mM): 120 CsCl, 3 Mg_2ATP, 10 BAPTA, 10 HEPES-Na (pH adjusted to 7.4 with CsOH). Data were acquired with an Axopatch 200B amplifier (Axon Instruments, CA, USA), stored and analysed with a pClamp 9.2 software (Axon Instruments, CA, USA). All the experiments were carried out at room temperature (20-22°C). Cell membrane capacitance was calculated in each cell throughout the experiment by integrating the capacitive currents elicited by a ± 10 mV voltage pulse. Currents were detected as inward currents activated on cell superfusion with the various stimuli in the voltage-clamp mode at a holding potential of -60 mV. Peak currents activated in each experimental condition were normalized to cell membrane capacitance and expressed as mean of the current density (pA/pF) in averaged results. Signals were sampled at 1 kHz and low-pass filtered at 10 kHz.

Cells and neurons were challenged with isopetasin (0.1 μM-3 mM), isopetasol (0.1 μM-3 mM) and angelic acid (0.1 μM-3 mM) to assess their ability to promote a cellular response. To induce TRPA1 channel-dependent responses, cells and neurons were challenged with the selective agonist, AITC (1-10 μM). GSK1016790A (0.05-0.1 μM) was used to induce a selective TRPV4 response. Buffer solution containing DMSO 0.5% was used as vehicle. Capsaicin (0.1-1 μM) was used to induce a TRPV1 selective response and to identify capsaicin-sensitive neurons. The activating peptide for human proteinase-activated receptor 2 (hPAR2-AP; 100 μM) or KCl (50 mM) have been used to elicit a TRP-independent cellular response. Some experiments have been performed in the presence of selective antagonist for TRPA1, HC-030031 (50 μM), for TRPV1, capsazepine (10 μM), for TRPV4, HC-067047 (30 μM) or their respective vehicles (0.5% or 0.1% or 0.3% DMSO).

Organ (rat urinary bladder) bath assays. Contractile response studies were performed on rat urinary bladder strips. Briefly, urinary bladder was excised from rat and longitudinal strips were suspended at a resting tension of 1 g in 10-ml organ bath bathed in aerated (95% O_2 and 5% CO_2) Krebs–Henseleit solution containing (in mM): 119 NaCl, 25 $NaHCO_3$, 1.2 KH_2PO_4, 1.5 $MgSO_4$, 2.5 $CaCl_2$, 4.7 KCl, and 11 D-glucose, maintained at 37°C. After 45 min of equilibration, tissues were contracted twice with Carbachol (l μM), with a 45-min washing out period between the first and second administration. Tissues were challenged with isopetasin (10-300 μM), AITC (100 μM), GSK1016790A (10 μM) and capsaicin (0.3 μM) or their vehicles. In some experiments, tissues were pretreated with the TRPA1 antagonist, HC-030031 (50 μM), the TRPV1 antagonist, capsazepine (10 μM), the TRPV4 antagonist, HC-067047 (30 μM) or a combination of NK1 and NK2 receptor antagonists, L-733,060 and SR48968, respectively (both 1 μM). Some tissue preparations were desensitized by exposure to capsaicin (10 μM for 20 min, twice). Similarly, some preparations were exposed to isopetasin (100-300 μM for 20 min, twice) before the challenge with various stimuli. Motor activity of tissue preparation was recorded isometrically on a force transducer (Harvard Apparatus, Ltd, Kent, UK). Responses were expressed as percentage (%) of the maximum contraction induced by carbachol (CCh, 1 μM).

CGRP-Like Immunoreactivity (CGRP-LI) assay. For CGRP-LI outflow experiments, 0.4-mm slices of mouse spinal cord were superfused with an aerated (95% O_2 and 5% CO_2) Krebs-Henseleit solution containing 0.1% bovine serum albumin plus the angiotensin-converting enzyme inhibitor, captopril (1 μM) and the neutral endopeptidase

inhibitor, phosphoramidon (1 μM) to minimize peptide degradation. Tissues were stimulated with isopetasin (10-100 μM) or its vehicle (1% DMSO) dissolved in modified Krebs-Henseleit solution and superfused for 10 min. Some tissues were pre-exposed to capsaicin (10 μM, 30 min) or superfused with a calcium-free buffer containing EDTA (1 mM). Other tissues were pre-exposed to a high concentration of isopetasin (300 μM, 30 min) and then, after a prolonged washing (40 min), stimulated with AITC (100 μM), capsaicin (0.3 μM), GSK1016790A (10 μM) or KCl (40 mM). Fractions (4 ml) of superfusate were collected at 10-min intervals before, during, and after administration of the stimulus and then freeze-dried, reconstituted with assay buffer, and analysed for CGRP-LI by using a commercial enzyme-linked immunosorbent assay kit (Bertin Pharma, Montigny le Bretonneux, France). CGRP-LI was calculated by subtracting the mean prestimulus value from those obtained during or after stimulation. Detection limits of the assays were 5 $pg \cdot ml^{-1}$. Results were expressed as femtomoles of peptide *per* gram of tissue. Stimuli did not cross-react with CGRP antiserum.

Behavioral experiments (face rubbing). For behavioural experiments, after habituation, C57BL/6, *Trpa1*$^{+/+}$ and *Trpa1*$^{-/-}$, *Trpv1*$^{+/+}$ and *Trpv1*$^{-/-}$, *Trpv4*$^{+/+}$ and *Trpv4*$^{-/-}$ mice were randomized to treatment groups, consistent with experimental design. Each experiment was repeated two to three times (using two or three animals in each experimental session). For the *in vivo* experiments the first outcome assessed was acute spontaneous nociception evoked by the subcutaneous (s.c.) injection (10 μl), into the right mouse whiskerpad (perinasal area), of AITC (10-100 nmol), capsaicin (0.5-3 nmol), GSK1016790A (1-5 nmol), isopetasin (5-50 nmol) or their vehicle (2.5 % DMSO). Nociception was assessed by measuring, in blinded to the treatment, the time (seconds) that the animal spent face rubbing the injected area with its paws [314]. The nociceptive effects of s.c. injection (10 μl) of isopetasin (50 nmol) and AITC (50 nmol) or capsaicin (3 nmol) or GSK1016790A (2.5 nmol) were also tested in *Trpa1*$^{+/+}$ and *Trpa1*$^{-/-}$, *Trpv1*$^{+/+}$ or *Trpv1*$^{-/-}$, *Trpv4*$^{+/+}$ or *Trpv4*$^{-/-}$ mice, respectively. To assess the pharmacological target of isopetasin C57BL/6 mice received isopetasin (50 nmol in 10 μl, s.c.) 60 min after intraperitoneal (i.p.) treatment with the selective TRPA1 antagonist, HC-030031 (100 $mg \cdot kg^{-1}$) or 30 min after the selective TRPV1 antagonist, capsazepine (4 $mg \cdot kg^{-1}$) or 60 min after the selective TRPV4 antagonist, HC-067047 (100 $mg \cdot kg^{-1}$) or their vehicle (4% DMSO plus 4% tween 80 in isotonic saline). Then, the preventive effect of isopetasine on nociceptive responses evoked by known TRPA1, TRPV1 and TRPV4 agonists was measured. Isopetasine (5 $mg \cdot kg^{-1}$) was administered intragastrically (i.g.) *quod diem* for 5 days and each day, 60

min later, AITC (50 nmol) or capsaicin (3 nmol) or GSK1016790A (2.5 nmol) or their vehicle were administered (10 µl, s.c.) and behavioural test performed, as above mentioned. The dose of isopetasin for preventive purposes was calculated according to the National Institute of Health conversion formula in order to administer to animals a dose similar to that has been proved efficacious for migraine prevention in humans [255].

Dural Blood Flow. Rats were anesthetized (urethane, 1.4 g in 10 ml·kg^{-1}, i.p.) and the head fixed in a stereotaxic frame. A cranial window (4 x 6 mm) was opened into the parietal bone to expose the *dura mater*. Changes in rat middle meningeal artery blood flow were recorded with a Laser Doppler Flowmeter (Perimed Instruments, Milan, Italy). The probe (needle type, tip diameter 0.8 mm) was fixed near a branch of the middle meningeal artery (1 mm from the dural outer layer). The window was filled with synthetic interstitial fluid. In a first set of experiments, dural blood flow was monitored for 30 min after administration of isopetasin (5 mg in 10 ml·kg^{-1}, i.p.) or its vehicle (0.5% CMC, 10 ml·kg^{-1}, i.g.). In a second set of experiments, dural blood flow was measured after the administration of acrolein (50 nmol, intranasal, i.n.), ethanol (140 µl·kg-1, intravenous, i.v.), sodium nitroprusside (1 mM, 100 µl, topical to the exposed dura mater) or their vehicles (isotonic saline) in rats treated for 5 days with isopetasine (5 mg · kg^{-1}, i.g.) or its vehicle (0.5% CMC, 10 ml·kg^{-1}, i.g.) 60 min after the treatment. Baseline flow was calculated by the mean flow value measured during a 5-min period prior to stimulus. The increase in blood flow was calculated as change (%) over the baseline.

Data and Statistical Analysis. The data and statistical analysis in this study comply with the recommendations on experimental design and analysis in pharmacology [315]. Data are reported as mean±SEM. Statistical analysis was performed by the unpaired two-tailed Student's t-test for comparisons between two groups, and the ANOVA, followed by the Bonferroni *post-hoc* test, for comparisons between multiple groups (GraphPadPrism version 5.00, San Diego, CA, USA). Agonist potency was expressed as half maximal effective concentration (EC_{50}), that is, the molar concentration of an agonist producing 50% of the maximum measured effect. $P<0.05$ was considered statistically significant.

Materials. Isopetasin and isopetasol were isolated from a sample of *Petasites hybridus* collected in the Swiss Alps and dissolved in 100% DMSO at 10 mM concentration and then diluted in aqueous solution. For systemic treatment isopetasin (5 mg in 10 ml·kg^{-1}) was dissolved in 0.5% carboxymethylcellulose solution (CMC) and administered intragastrically. HC-030031 was synthesized as previously described [187]. If not otherwise indicated, all other reagents were from Sigma-Aldrich (Milan, Italy) and dissolved in

appropriate vehicle solutions. For *in vitro* experiments, all compounds were dissolved in 100% DMSO at 10 mM concentration and diluted in the various aqueous buffers.

5.2 Results

5.2.1 Isopetasin targets the human TRPA1

In hTRPA1-HEK293, isopetasin and isopetasol, but not angelic acid, produced concentration-dependent increases in $[Ca^{2+}]_i$ (EC_{50s} 10 μM and 100 μM, respectively), responses that were attenuated by the selective TRPA1 antagonist, HC-030031 (Figure 1A and Supplementary Figure 1C). hTRPV1-HEK293 and hTRPV4-HEK293 cells that were activated by capsaicin or GSK1016790A (TRPV1 and TRPV4 agonist, respectively) did not respond to isopetasin (Figure 1C, D). In whole-cell patch-clamp recordings, isopetasin elicited inward currents in hTRPA1-HEK293 cells that were abated by HC-030031 (Figure 1B). Isopetasin did not evoke any current in hTRPV1-HEK293 and hTRPV4-HEK293 cells (Figure 1C, D). Isopetasin and isopetasol did not induce any cellular response in naïve HEK293 cells (Supplementary Figure 1B, D). 3C/K-Q hTRPA1-HEK293 cells, which express a TRPA1 which lacks three cysteine and one lysine residues, responded to the non-electrophilic agonist, menthol, as wild type hTRPA1-HEK293, but failed to respond to isopetasin (50 μM) (Figure 1E). In human foetal lung fibroblasts (IMR90), which constitutively express the TRPA1 channel [80], isopetasin concentration-dependently increases $[Ca^{2+}]_i$, (EC_{50} 8 μM), a response that was abated by HC-030031 (Figure 1F and Supplementary Figure 1E). Calcium responses elicited by hPAR2-AP and ion currents evoked by KCl were not affected by HC-030031 indicating selectivity (Figure 1A, B, F and Supplementary Figure 1B-D).

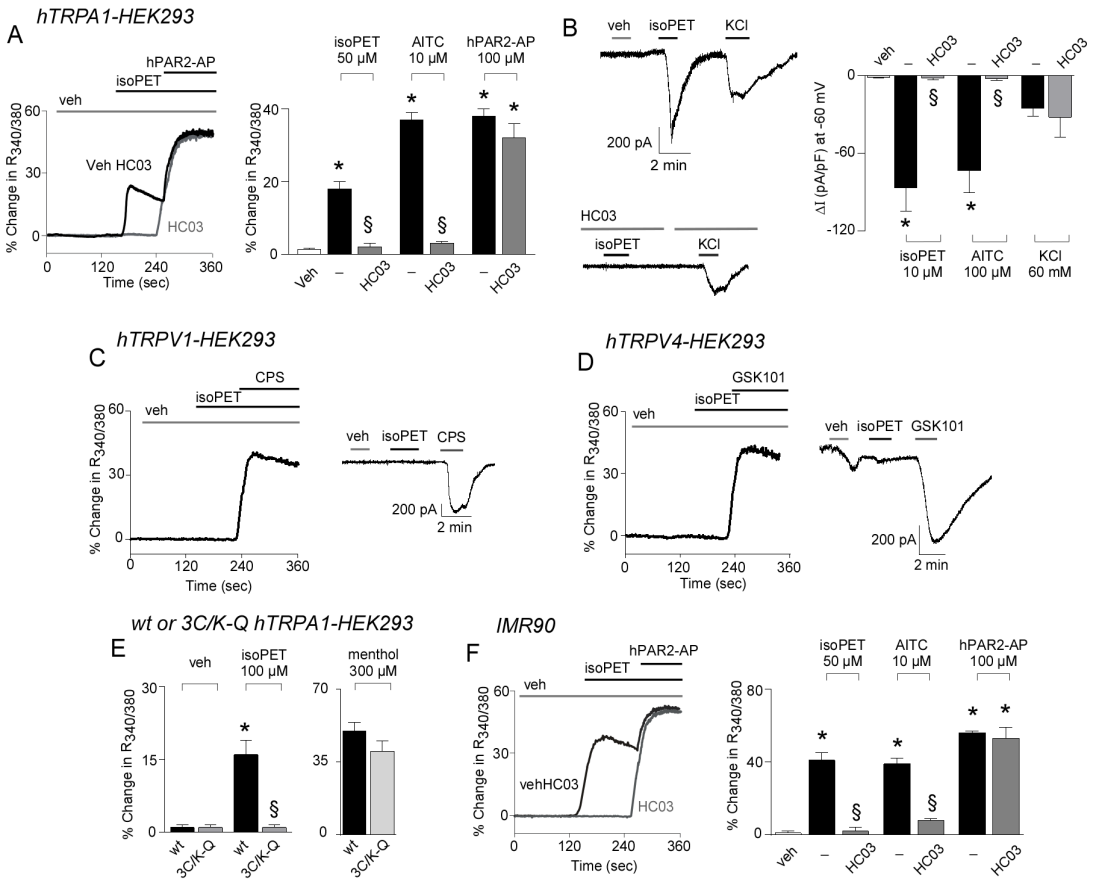

Figure 1. **Isopetasin targets the human TRPA1. A**, Representative traces and pooled-data of $[Ca^{2+}]_i$ response evoked by isoPET (50 µM) in HEK293 cells transfected with the cDNA of human TRPA1 (hTRPA1-HEK293; black line and columns). $[Ca^{2+}]_i$ response evoked by isoPET (50 µM) and the selective TRPA1 agonist, allyl isothiocyanate (AITC; 10 µM) are abolished by the selective TRPA1 antagonist, HC-030031 (HC03; 30 µM; grey line and columns), which does not affect the response evoked by the activating peptide for human proteinase activated receptor 2 (hPAR2 AP, 100 µM). **B**, Representative traces and pooled data of the whole cell patch-clamp inward currents evoked by isoPET (10 µM), AITC (100 µM) and KCl (60 mM) in hTRPA1-HEK293. HC03 abates the response to both isoPET and AITC without affecting the KCl response. **C, D** Representative traces of $[Ca^{2+}]_i$ responses and whole cell patch-clamp inward currents in HEK293 cells transfected with the cDNA of human TRPV1 (hTRPV1-HEK293) **C** or with the cDNA of human TRPV4 (hTRPV4-HEK293) **D** show that isoPET (50 µM in $[Ca^{2+}]_i$ imaging or 10 µM in electrophysiological experiments) does not activate either TRPV1 or TRPV4, which are activated by their respective agonist, capsaicin (CPS; 1 µM) and GSK1016790A (GSK101; 100 nM), respectively. **E,** Pooled data of $[Ca^{2+}]_i$ responses evoked by isoPET (100 µM) and menthol (300 µM) in wild-type (*wt*) and mutant (3C/K-Q; *Mut*) hTRPA1-HEK293 transfected cells. **F**, Representative traces and pooled-data of $[Ca^{2+}]_i$ response induced by isoPET in human fetal lung fibroblasts (IMR90). HC03 (grey line and column) inhibits the $[Ca^{2+}]_i$ response activated by isoPET (50 µM) but not that evoked by hPAR2-AP (100 µM). Veh is the vehicle of isoPET. Each column represents the mean ± SEM of n > 25 cells from 3-6 independent experiments for $[Ca^{2+}]_i$ recording or n > 5 cells from 4-8 independent experiments for electrophysiological recording. Dash indicates combined vehicles of treatments. *$P < 0.05$ *vs*. veh, §$P < 0.05$ *vs*. isoPET; ANOVA followed by Bonferroni test.

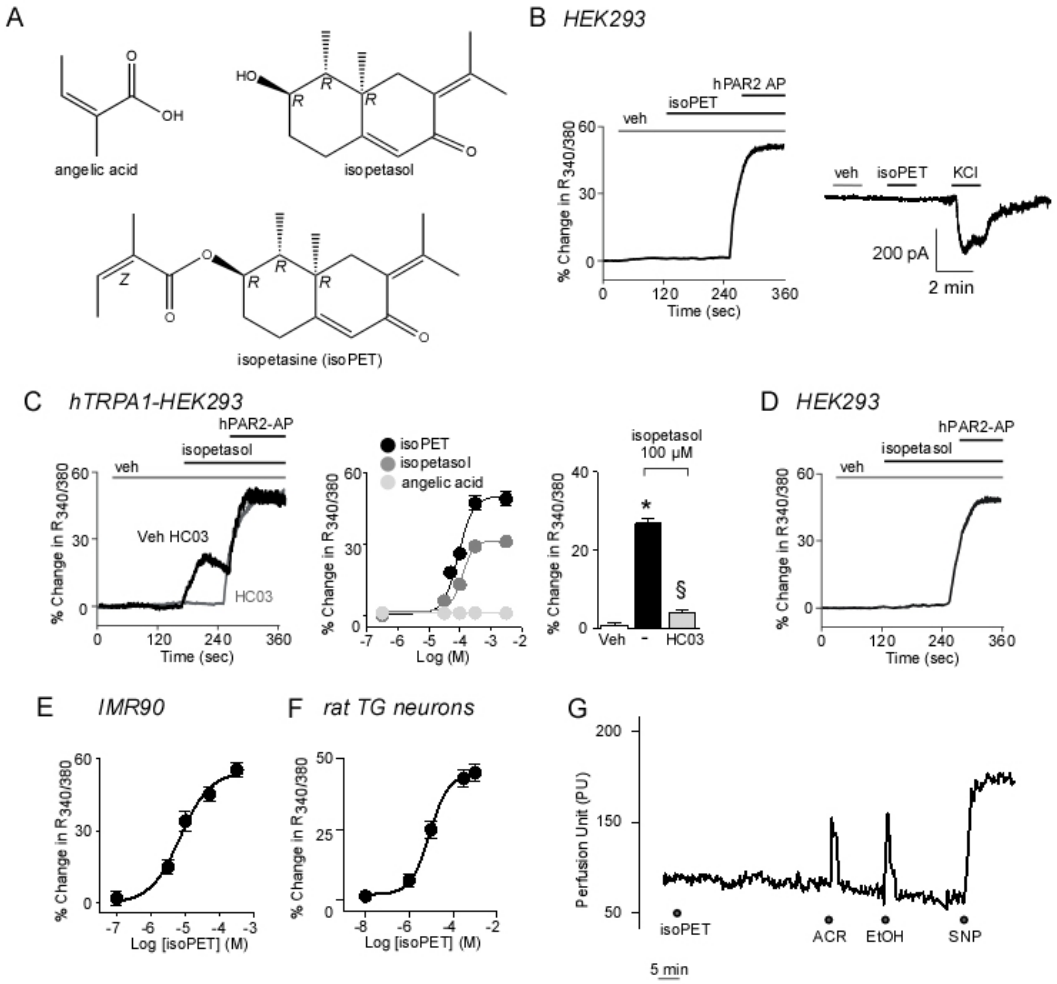

Supplementary Figure 1. A, Chemical structure of isopetasol, angelic acid and isopetasin (isoPET). **B**, Challenge with isoPET (50 µM) does not elicit calcium response nor ion currents in untrasfected HEK293 cells which instead responded to the activating peptide for human proteinase activated receptor 2 (hPAR2-AP, 100 µM) or KCl (100 µM). **C**, Representative traces, concentration response curve and pooled data of the calcium response evoked by isopetasol in HEK293 cells transfected with the cDNA codifying for human TRPA1 (hTRPA1-HEK293). isoPET induces a similar concentration response curve in hTRPA1-HEK293 cells with a higher maximum effect at the highest concentration used. Angelic acid does not produce calcium response at any of the concentrations tested (0.5µM – 3 mM). The calcium response evoked by isopetasol (100 µM) is abolished in the presence of the selective TRPA1 antagonist HC-030031 (HC03; 30 µM) and is absent in **D** untransfected HEK293 cells. Concentration response curves of the calcium response evoked by isoPET in human fetal lung fibroblasts, IMR90 **E**, and in rat cultured trigeminal ganglion (TG) neurons **F**. veh is the vehicle of isopetasol. Each column or point represents the mean ± SEM of n > 20 cells/neurons from 3-6 independent experiments. Dash indicates vehicle of HC03. *$P < 0.05$ *vs*. veh, $^{§}P < 0.05$ *vs*. isopetasol; ANOVA followed by Bonferroni test. **G**, Representative trace of the effect in dural blood flow evoked by intraperitoneal isoPET (5 $mg \cdot kg^{-1}$), intranasal acrolein (ACR, 50 nmol in 50 µl), intravenous ethanol (EtOH, 140 $\mu l \cdot kg^{-1}$) or dural application (100 µl) of sodium nitroprusside (SNP; 10 mM,) in rat.

5.2.2 Isopetasin selectively activates the rodent and human TRPA1 channel

Exposure of cultured rat TG neurons to isopetasin evoked a concentration-dependent (EC_{50} 10 µM) $[Ca^{2+}]_i$ increase in neurons that responded to capsaicin (Figure 2A and Supplementary Figure 1F). Responses to isopetasin were abrogated by HC-030031, but not by selective TRPV1 (capsazepine) or TRPV4 (HC-067047) antagonists

(Figure 2A). Notably, while isopetasin, AITC and capsaicin activated TG neurons from *Trpa1*$^{+/+}$ mice, neurons from *Trpa1*$^{-/-}$ mice responded only to capsaicin (Figure 2C). In capsaicin-sensitive rat TG neurons, isopetasin evoked inward currents that were selectively abrogated by HC-030031, but unaffected by capsazepine and HC-067047 (Figure 2B). Thus, calcium and electrophysiology data indicated that TRPA1 is necessary and sufficient for rodent nociceptors and human cells to respond to isopetasin.

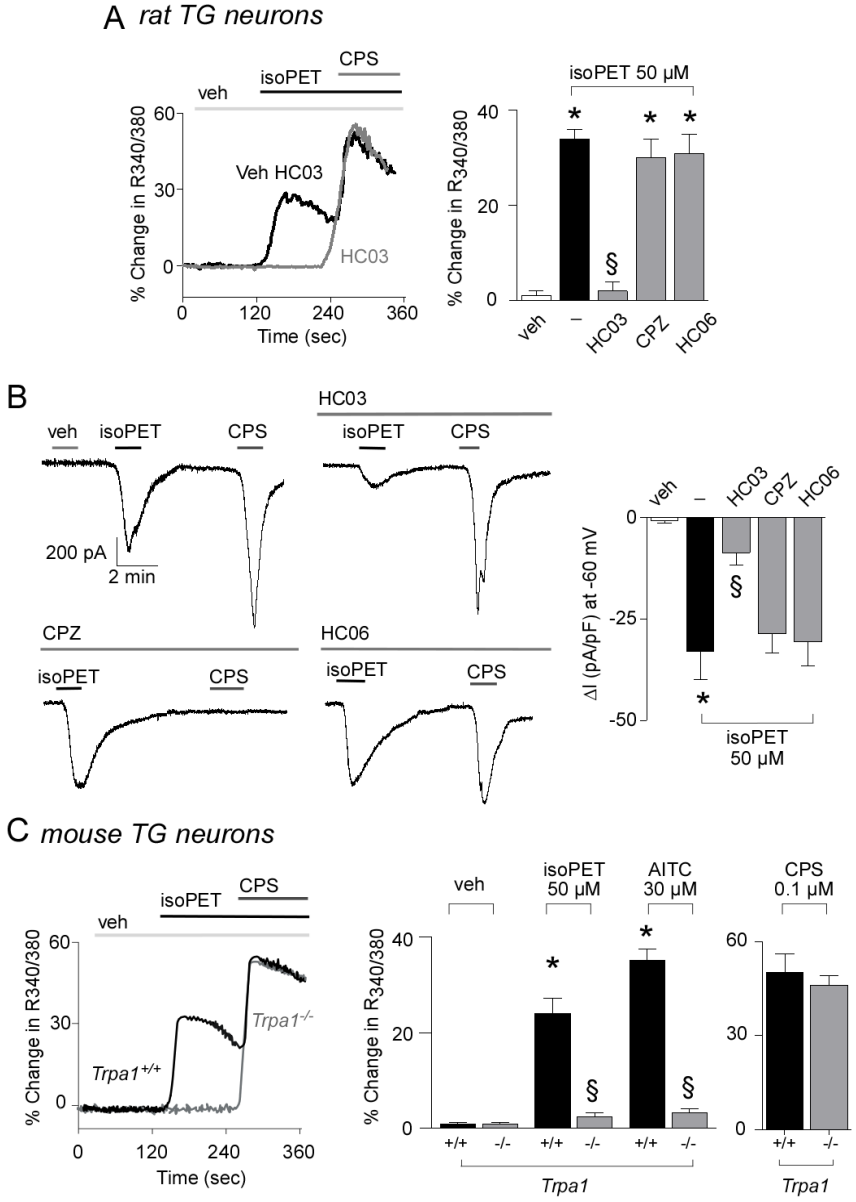

Figure 2. Isopetasin selectively activates the rodent and human TRPA1 channel. A, B, Representative traces and pooled data of $[Ca^{2+}]_i$ responses **A** and whole cell patch-clamp inward currents **B** evoked by isoPET (50 µM, black line and columns) in cultured rat TG neurons responding to capsaicin (CPS; 0.1 µM **A** and 1 µM **B**). Both $[Ca^{2+}]_i$ responses and ion currents elicited by isoPET are abolished in the presence of the selective TRPA1 antagonist, HC-030031 (HC03; 30 µM **A** and 50 µM **B**), and unaffected in the presence of the selective antagonist for TRPV1, capsazepine (CPZ; 10 µM), or TRPV4, HC-067047 (HC06; 30 µM). **C**, Representative traces and pooled data of the $[Ca^{2+}]_i$ response evoked by isoPET (50 µM) or AITC (30 µM) in cultured TG neurons from *Trpa1*$^{+/+}$ mice (black line and columns); both responses are absent in neurons from *Trpa1*$^{-/-}$ mice (grey line and columns). Responses to capsaicin (CPS; 0.1 µM) are unchanged. Veh is the vehicle of isoPET. Each column represents the mean ± SEM of n > 20 neurons from

3-6 independent experiments for $[Ca^{2+}]_i$ recordings or of at least n > 5 cells from 4-8 independent experiments for electrophysiological recordings. Dash indicates combined vehicles of treatments. $*P < 0.05$ *vs*. veh, $^{§}P < 0.05$ *vs*. isoPET; ANOVA followed by Bonferroni test.

5.2.3 Isopetasin excites and desensitizes rodent peptidergic nociceptors

In cultured rat TG neurons, currents evoked by AITC or capsaicin were unaffected by pre-exposure to AITC, but underwent remarkable desensitization after pre-exposure to isopetasin (Figure 3A). Isopetasin-evoked CGRP release from mouse dorsal spinal cord slices was abolished in tissues desensitized to capsaicin or in the absence of extracellular Ca^{2+} (Figure 3D), indicating that isopetasin evokes a neurosecretory process from TRPV1-expressing neurons. The role of TRPA1 in neuronal excitation and the ensuing neurosecretion by isopetasin was demonstrated by its failure to evoke any release in spinal cord slices from *Trpa1*$^{-/-}$ mice (Figure 3E). Notably, exposure to an elevated concentration of isopetasin attenuated the release of CGRP produced by AITC, capsaicin and the unspecific depolarizing agent KCl (Figure 3F), indicating unselective neuronal desensitization.

Terminals of peptidergic primary sensory neurons are widely expressed in most tissues and organs. The rat urinary bladder is enriched by a dense network of SP-containing nerve fibers, whose stimulation results in SP release from intramural sensory nerve endings that *via* NK1/NK2 receptor stimulation, contracts the urinary bladder smooth muscle (Steinhoff *et al.*, 2014). Isopetasin caused a concentration-dependent contraction of isolated strips of the rat urinary bladder, a response attenuated by desensitization to capsaicin, NK1 and NK2 receptor (L-733,060 and SR48968, respectively) antagonism and HC-030031, but not by capsazepine or HC-067047 (Figure 3B). Thus, isopetasin-evoked contractions resulted from SP release from peptidergic sensory nerve terminals *via* TRPA1 activation. Exposure of urinary bladder strips to a high dose of isopetasin markedly attenuated contractions evoked by AITC and capsaicin, but not by carbachol, suggesting neuronal desensitization that, however, preserved the contractility of the bladder smooth muscle (Figure 3C).

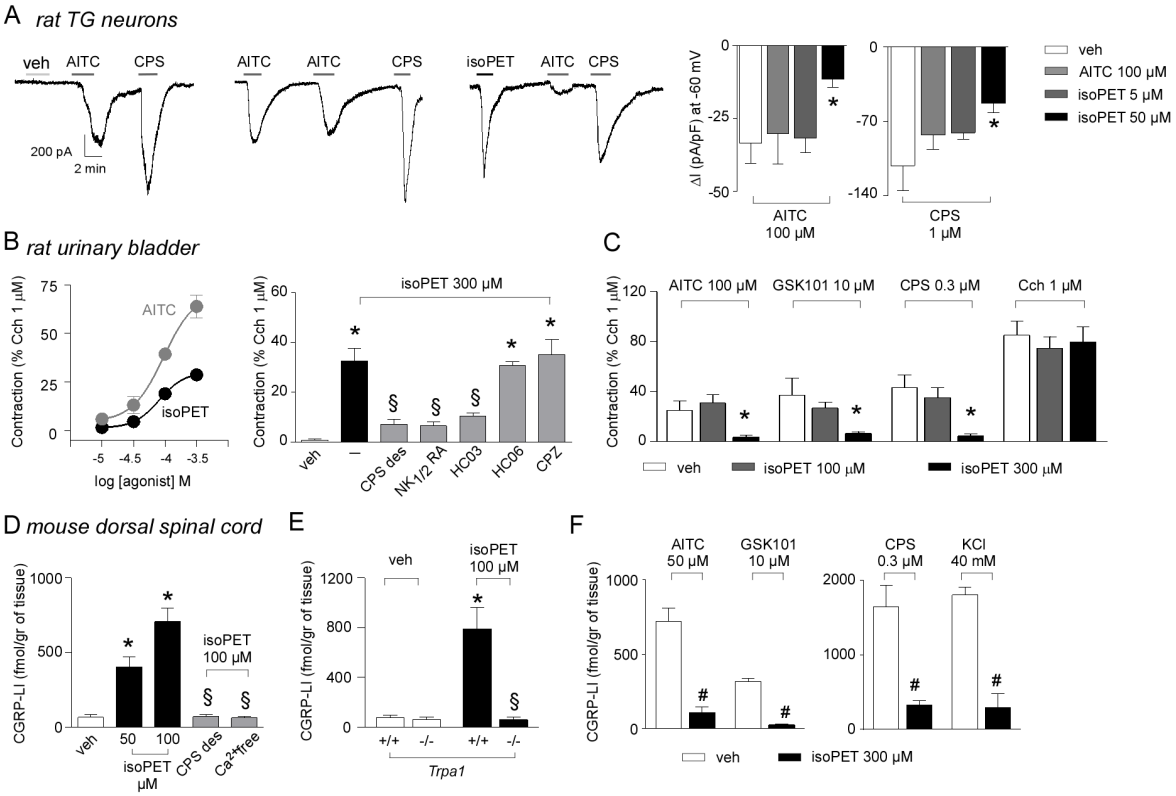

Figure 3. Isopetasin excites and desensitizes rodent peptidergic nociceptors. A, Representative traces and pooled-data of whole-cell patch-clamp inward currents through rat trigeminal ganglion (TG) neurons showing that the initial challenge with isoPET (50 μM), instead of allyl isothiocyanate (AITC; 100 μM), or its vehicle (veh), produces neuronal desensitization with a reduced response to the subsequent exposure to AITC (100 μM), and capsaicin (CPS; 1 μM). Each column represents the mean ± SEM of n > 6 independent experiments. **B**, Concentration response curve of the contractile response evoked by AITC and isoPET in rat urinary bladder strips. At the highest concentration used, isoPET (300 μM) evokes a contractile response that is selectively abated by the selective TRPA1 antagonist HC-030031 (HC03; 50 μM) and unaffected by the selective TRPV1 antagonist capsazepine (CPZ; 10 μM) or the selective TRPV4 antagonist, HC-067047 (HC06; 30 μM). The isoPET-contraction is also abolished by a combination of NK1 and NK2 receptor antagonists (NK1/2 RA; L-733,060 and SR48968, both 1 μM), and after exposure (20 min, twice) to a high concentration of capsaicin (CPS; 10 μM) that induces neuronal desensitization. **C**, Exposure (20 min, twice) to the highest concentration of isoPET (300 μM) markedly reduces the contractile response evoked by a selective TRPA1, TRPV4 or TRPV1 agonist, AITC (100 μM), GSK1016790A (GSK101; 10 μM) or CPS (0.3 μM), but does not affect the response to carbachol (CCh; 1 μM). **D**, isoPET increases the calcitonin gene-related peptide-Like Immunoreactivity (CGRP-LI) outflow from mouse dorsal spinal cord slices in a concentration-dependent manner. Effect of isoPET (100 μM) is abolished by calcium removal (Ca^{2+}-free), capsaicin desensitization (CPS-des). **E**, isoPET (100 μM) increases CGRP-LI outflow from spinal cord slices from *Trpa1*$^{+/+}$ mice, but not from *Trpa1*$^{-/-}$ mice. **F**, Exposure to a high concentration of isoPET (300 μM, 30 min) abates CGRP-LI release evoked by AITC (50 μM), GSK101 (10 μM), CPS (0.3 μM) or KCl (40 mM). Each column represents the mean ± SEM of n = 4 independent experiments. Dash indicates combined vehicles of the treatments. **P* < 0.05 *vs*. veh; $^{\S}P$ < 0.05 *vs*. isoPET ANOVA followed by Bonferroni test. $^{\#}P$ < 0.05 *vs*. isoPET, Student's t-test.

5.2.4 Isopetasin inhibits nociception and neurogenic dural vasodilatation *via* TRPA1

Subcutaneous (s.c.) injection into the upper mouse whiskerpad of irritant agents produces a typical nocifensor behaviour described as facial rubbing [314]. Injection (s.c.) of AITC into the upper mouse whiskerpad evoked a transient (<15 min) and dose-dependent facial rubbing that was abated by HC-030031 (Figure 4A). Similarly, facial rubbing

produced by capsaicin was attenuated by capsazepine (Figure 4B), while facial rubbing evoked by GSK1016790A was inhibited by the TRPV4 antagonist, HC-067047 (Figure 4C). Isopetasin produced facial rubbing that recapitulated the features of AITC response, being abrogated by HC-030031, and unaffected by capsazepine or HC-067047 (Figure 4D). Moreover, similar to AITC, isopetasin failed to provoke any facial rubbing in *Trpa1*$^{-/-}$ mice (Figure 4E). Isopetasin evoked facial rubbing in *Trpv1*$^{-/-}$ and *Trpv4*$^{-/-}$ mice similar to that observed in their respective wild type littermates (Figure 4F).

One i.g. administration of isopetasin did not affect the ability of local AITC, capsaicin or GSK1016790A to evoke facial rubbing (Figure 5A). However, after isopetasin administrations for 3 consecutive days rubbing responses to AITC and GSK1016790A were reduced, whereas that to capsaicin was unaffected (Figure 5A). Following isopetasin administration for 5 consecutive days, responses to AITC, GSK1016790A and also capsaicin were attenuated (Figure 5A). This indicates that longer-term repeated isopetasin i.g. administration leads to a desensitization of nocifensive behavior specifically evoked by activators of TRPV1, TRPV4 and TRPA1. With more direct relevance for headaches and migraine, we next intended to test whether this would also affect CGRP-mediated dilation of meningeal arteries, which we subsequently assessed in rats. Firstly, i.p. administration of isopetasin did not produce any detectable change in meningeal perfusion (Supplementary Figure 1G). Secondly, after isopetasin administrations for 5 consecutive days, increases in blood flow produced by the TRPA1 agonist, acrolein [117,191], and the TRPV1 agonist, ethanol [50,316] were reduced (Figure 5B). In contrast, the response to the direct vasodilator sodium nitroprusside remained unchanged (Figure 5B).

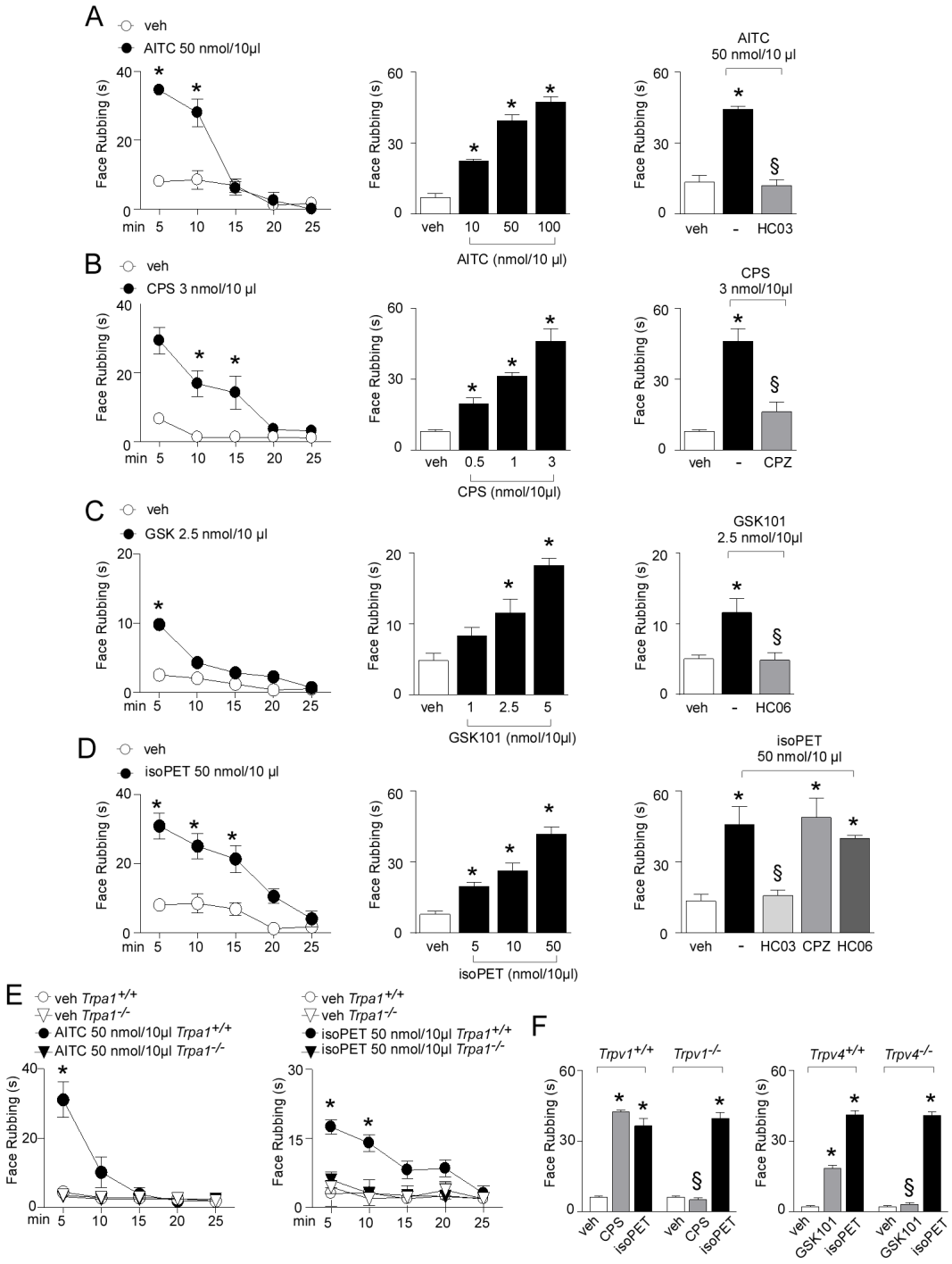

Figure 4. Isopetasin inhibits nociception and neurogenic dural vasodilatation via TRPA1. A, Time course of facial-rubbing in C57C57BL/6/BL6 mice after subcutaneous (s.c.) injection (10 µl) of the selective TRPA1 agonist, allyl isothiocyanate (AITC; 10 nmol) or its vehicle (veh) into the whiskerpad. Time that mice spent rubbing is plotted for each 5-min block over 25 min. The irritant pain evoked by AITC, quantified as the total time spent rubbing in the first 10 min, is dose-dependent and abolished in mice pretreated with the selective TRPA1 antagonist HC-030031 (HC03; 100 mg·kg^{-1} intraperitoneal, i.p., 1 h before). Similar to AITC, the s.c. injection of **B** the selective TRPV1 agonist, capsaicin (CPS), or **C** the selective TRPV4 agonist, GSK1016790A (GSK101), shows dose-dependent irritant pain behaviors which are abated by pretreatment with their respective antagonist, capsazepine (CPZ; 4 mg·kg^{-1}, i.p. 30 min before) or HC-067047 (HC06; 10 mg·kg^{-1}, i.p., 30 min before). **D**, Local injection (10 µl, s.c.) of isoPET into the whiskerpad of C57BL/6 mice elicits dose-dependent irritant behaviours. The effect evoked by isoPET (50 nmol) is abated in HC03 pretreated mice but unaffected in HC06 or CPZ pretreated mice. **E**, Time course of the facial-rubbing activity evoked by both AITC (50 nmol in 10 µl, s.c.) and isoPET (50 nmol in 10 µl, s.c.), or their respective veh in *Trpa1*$^{+/+}$ mice. No effect is observed in injected *Trpa1*$^{-/-}$ mice.

F, isoPET injection (50 nmol in 10 µl, s.c.) into the whiskerpad of *Trpv1*$^{+/+}$ and *Trpv1*$^{-/-}$ mice elicits a similar irritant effect, while CPS (3 nmol in 10 µl, s.c.) produces an irritant response only in *Trpv1*$^{+/+}$ mice. Similarly, *Trpv4*$^{+/+}$ and *Trpv4*$^{-/-}$ show a similar irritant response to isoPET while GSK101 (2.5 nmol in 10 µl, s.c.) produces an irritant response only in *Trpv4*$^{+/+}$ mice. Values are mean ± SEM of at least 5 mice. $^{*}P < 0.05$ *vs*. veh, $^{§}P < 0.05$ *vs*. AITC or CPS or GSK101 or isoPET, ANOVA followed by Bonferroni test. $^{\#}P < 0.05$ *vs*. *Trpa1*$^{+/+}$ or *Trpv1*$^{+/+}$ or *Trpv4*$^{+/+}$, Student's t-test.

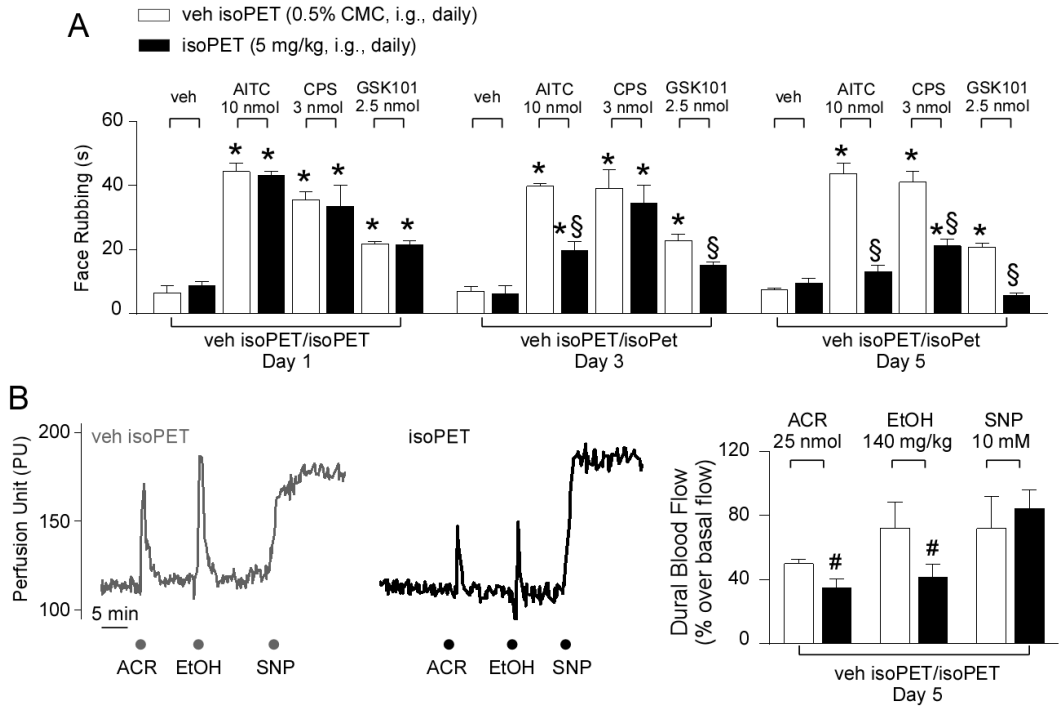

Figure 5. Chronic isopetasin (isoPET) administration desensitizes sensory nerve endings. A, Daily intragastric (i.g.) administration of isoPET (5 mg·kg^{-1}) in naïve C57BL/6 mice gradually reduces the nociceptive response evoked by the subcutaneous injection (10 µl) of allyl isothiocyanate (AITC; 10 nmol), capsaicin (CPS; 3 nmol) or GSK1016790A (GSK101; 2.5 nmol) in mouse whiskerpad and measured as the facial-rubbing activity observed in the first 15 min after the injection. Veh is the vehicle of the various stimuli. Values are mean ± SEM of at least 5 mice per group. $^{*}P < 0.05$ *vs*. veh, $^{§}P < 0.05$ *vs*. veh-isoPET, ANOVA followed by Bonferroni test. **B**, Representative traces and pooled data of the increases in dural blood flow evoked by intranasal acrolein (ACR, 50 nmol in 50 µl), intravenous ethanol (EtOH, 140 µl·kg^{-1}) or dural application (100 µl) of sodium nitroprusside (SNP; 10 mM,) in rat treated for 5 days with systemic isoPET (5 mg·kg^{-1}, i.g. per day) or its vehicle (0.5 % CMC 10 ml/·kg^{-1}, i.g. per day). isoPET chronic treatment significantly reduces responses to ACR and EtOH, but not to SNP. $^{\#}P < 0.05$ *vs*. veh-isoPET, Student's t-test.

5.3 Discussion

Pharmacological and genetic data presented here show that isopetasin activates the universal irritant receptor ion channel, TRPA1. Mouse, rat and human (native and recombinant) TRPA1 are gated with similar efficacy and potency by isopetasin, suggesting that responses evoked by the drug *in vivo* in rodents could be reproduced in humans. Furthermore, failure to activate TRPV1 and TRPV4 channels indicates that nociceptor activation by isopetasin is caused by selective TRPA1 targeting. As it failed to evoke calcium responses in the mutant transfected cells (3C/K-Q hTRPA1-HEK293), the molecular mechanism responsible for channel activation by isopetasin must be similar to that proposed for electrophilic and reactive agonists that gate TRPA1 *via* the involvement of specific cysteine/lysine residues [121], stimulated TRPA1 with similar potency, although with less efficacy than isopetasin. Thus, the hemiterpene moiety of angelic acid is not critical for activity, while the eremophilane sesquiterpenoid framework of isopetasol is essential for channel gating.

TRPA1-expressing peripheral sensory neurons exert a dual function in as much as they both signal nociceptive stimuli to the brain and, by releasing the neuropeptides SP and CGRP, mediate neurogenic inflammation responses in the vasculature and other organs [243,317]. In the rat urinary bladder, AITC, by targeting intramural nerve terminal TRPA1, elicits neurogenic SP-mediated smooth muscle contractions [318]. Isopetasin produced an effect similar to that of AITC in terms of mechanism of action. However, the efficacy of isopetasin was much lower than that of AITC, indicating that the herbal compound may act as a partial channel agonist. Isopetasin, similarly to parthenolide [245], caused desensitization of peptidergic primary sensory neurons either limited to TRPA1 or involving other TRP channel stimulants and non-TRP depolarizing agents. Transition from homologous to heterologous desensitization seems to depend on the concentration and time of exposure to isopetasin. Pre-exposure to isopetasin of cultured TG neurons or their central terminals in the dorsal brainstem reduced AITC-evoked currents or CGRP release, respectively. Defunctionalization of sensory nerve terminals by isopetasin was not limited to trigeminal innervation, as observed in nerve terminals of the rat urinary bladder. In this preparation, neurogenic SP-mediated smooth muscle contractions evoked by AITC and capsaicin [318] were markedly reduced by pre-exposure to isopetasin. Inhibition of neurogenic inflammation by isopetasin in extra-trigeminal innervation may help explain the reported beneficial effects of butterbur in painful and inflammatory conditions, such as arthritis [319] and allergic rhinitis [320,321].

Data obtained *in vitro* were recapitulated by *in vivo* experiments. The facial rubbing evoked by subcutaneous AITC was characterized as a genuine TRPA1-mediated effect, while capsaicin or GSK1016790A were effective via TRPV1 and TRPV4, respectively. To mimic the clinical use of butterbur in migraine treatment, isopetasin was given *via* intragastric administration. Results showed a time-dependent increase in the desensitizing effect of intragastric isopetasin that initially involves solely TRPA1, and thereafter encompasses also TRPV4 and TRPV1. In fact, while after a single isopetasin dose the rubbing responses to AITC, capsaicin and GSK1016790A were unaffected, significant inhibition of AITC- or GSK1016790A-mediated responses was observed following a 3-day cycle of isopetasin administration. After a 5-day cycle, the capsaicin-mediated nociceptive response was also attenuated, suggesting that a more prolonged treatment schedule provided nerve terminal defunctionalization that involves several "pain-TRPs", which might be a beneficial feature in an herbal medicine with a benign safety profile.

Clinical studies with small molecules that selectively block the CGRP receptor for the acute and preventive treatment of the migraine attack [24,181,322] or, more recently, with anti-CGRP monoclonal antibodies as preventive antimigraine medicines [323], have strengthened the hypothesis of a pivotal role of this neuropeptide in the mechanism of migraine headaches. Although the precise CGRP-dependent pathway that results in the pain and associated symptoms of migraine attack has not been completely identified, peptidergic neurons of the trigeminal ganglion appear to play a major role in migraine pain mechanism [322]. CGRP released from sensory nerve terminals in rodents and other mammals, including humans, dilates arterial vessels [179], including meningeal arteries [191,316]. Thus, CGRP-mediated meningeal vasodilatation following stimulation of TG neurons is considered a good approximation of the neurochemical events that occur during the migraine attack. Previous studies have shown that meningeal vasodilation evoked by administration of either acrolein (intranasal) or ethanol (i.p.) is mediated by CGRP released from perivascular trigeminal nerve endings triggered by TRPA1 and TRPV1 activation, respectively [191,316]. The present observation that the 5-day intragastric administration of isopetasin attenuated the increase in rat dural blood flow evoked by both acrolein and ethanol suggests that isopetasin, possibly by TRPA1 targeting, desensitizes trigeminal nociceptors' ability to release the migraine mediator, CGRP. This novel property of isopetasin may add on to mechanisms previously described [216-219] to explain the action of chronically administered butterbur to prevent migraine [213-215].

Migraine therapy consists of different classes of drugs. While acute treatment of attacks

is confined to analgesics, non-steroidal antiinflammatory drugs and triptans attack prevention is primarily based on β-blockers, anti-epileptics, anti-depressants and serotonin antagonists. It is possible that in the near future small molecule CGRP receptor antagonists (gepants) and anti-CGRP or anti-CGRP receptor monoclonal antibodies will be for migraine acute treatment used or prophylaxis, respectively. Present findings support the view that some drugs and herbal medicines currently prescribed for the acute or prophylactic treatment of migraine can be grouped into a novel class of therapeutics, namely TRPA1 inhibitors. These comprise compounds that target the channel with different modalities. The universally used acetaminophen (paracetamol) *via* its reactive metabolite, N-acetylbenzoquinoneimine, activates [135] and then desensitizes [242] TRPA1. The well-established, but still widely and successfully prescribed pyrazolone derivatives [324], dipyrone (metamizole) [310]and propyphenazone, are selective TRPA1 antagonists [243] The active component of feverfew, parthenolide, moderately stimulates TRPA1 both *in vitro* and *in vivo*, causing channel desensitization and neuronal defunctionalization [245]. Butterbur is indicated as per the American Headache Society guidelines with a level A recommendation for migraine prophylaxis [220]. Present findings add the butterbur constituent, isopetasin [247], to the list of TRPA1-tropic agents, which, like parthenolide, stimulate the channel, thereby causing defunctionalization of peptidergic trigeminal nerve terminals, and attenuating their ability to release CGRP and signal pain. Successful treatment and prevention of migraine by targeting of TRPA1 ion channels and the ensuing peptidergic sensory neuron defunctionalization by parthenolide and isopetasin, provides a solid basis for future basic and translational-medical investigations of TRPA1-tropic approaches for migraine.

This work has been published in British Journal of Pharmacology

Benemei S, De Logu F, Li Puma S, Marone IM, Coppi E, Ugolini F, Liedtke W, Pollastro F, Appendino G, Geppetti P, Materazzi S, Nassini R (2017). "The anti-migraine component of butterbur extracts, isopetasin, desensitizes peptidergic nociceptors by acting on TRPA1 cation channel" Br J Pharmacol. 174(17):2897-2911.

Chapter VI – Conclusions

The TRPA1 expressed by primary sensory neurons exhibits the distinctive property to detect and to be sensitized by a series of endogenous molecules, which play a major role in inflammation and tissue injury. These molecules are by products of oxidative and nitrative stress which affect and damage a vast array of molecules, but only recently have been identified as a major pathway, that by TRPA1, signal pain and neurogenic inflammation. The other unique feature of the oxidative and nitrative stress/TRPA1 mechanism is that it seems involved in different types of pain, as inflammatory pain, neuropathic pain and migraine headache.

In the first work our research focused on uncovering the mechanisms underlying painful states induced by third-generation AIs, the steroidal exemestane and non- steroidal azole derivatives, letrozole and anastrozole. The use of AIs is associated with a series of relevant side effects which are reported in 30-60% of treated patients [162,163]. Among these, the AI-associated musculoskeletal symptoms (AIMSS) characterized by morning stiffness and pain of the hands, knees, hips, lower back, and shoulders [164,165]. In addition to musculoskeletal pain, pain symptoms associated with AIs have recently been more accurately described with the inclusion of neuropathic, diffused, and mixed pain [166].

The chemical structure of exemestane includes a system of highly electrophilic conjugated Michael acceptor groups, which might react with the thiol groups of reactive cysteine residues [172]. Michael addition reaction with specific cysteine residues is a major mechanism that results in TRPA1 activation by a large variety of electrophilic compounds [121-123]. Aliphatic and aromatic nitriles can react with cysteine to form thiazoline derivatives and accordingly the tear gas 2-chlorobenzylidene malononitrile (CS) has been identified as a TRPA1 agonist [173]. We noticed that both letrozole and anastrozole possess nitrile moieties.

In this study, we provide for the first time evidence that AIs directly stimulate TRPA1, and *via* this pathway provoke neurogenic inflammatory edema, acute nociception, mechanical allodynia, and reduced grip strength, indicating a new mechanism through which AIs induce cytokine-independent inflammation and pain. AI concentrations required for TRPA1 activation are higher than those found in the plasma of treated

subjects [224,269] however, it should be noted that all three AIs have a large volume of distribution, indicating a high tissue distribution [257,259]. The present findings that in mice plasma levels of both AIs were comparable to those found in humans [257,259] strengthen the hypothesis that compartmentalization of AIs in mice is similar to that reported in humans [257,259]. Thus, under standard drug regimens, concentrations sufficient to activate TRPA1 or to potentiate TRPA1-mediated responses evoked in cooperation with inflammatory mediators may be reached in tissues neighboring sensory nerve terminals.

In the second part, we found that ASD, unique among several steroid hormones, activates TRPA1, thereby promoting AIMSS-like responses. ASD behaves as a TRPA1 agonist across species, as it engages both the recombinant and native human channel and the rat and mouse channel. TRPA1 activation by ASD, similar to other electrophilic agonists [248], requires the presence of three cysteine (C619, C639, C663) and one lysine (K708) key residues. Furthermore, ASD exhibits a peculiar selectivity profile. Tenosynovitis and joint swelling are symptoms reported by patients treated with AIs [170]. However, association with proinflammatory markers, including cytokines, such as interleukin-6, has been excluded [265]. The ability of ASD to release sensory neuropeptides or, in combination with letrozole and BSO, to provoke TRPA1-dependent SP/CGRP release, edema and neutrophil infiltration in the knee joint, suggests that neurogenic inflammation mediates the inflammatory component of AIMSS. The recent observation that, due to their electrophilic and reactive properties, exemestane, anastrozole and letrozole target TRPA1, thus evoking pain-like responses and neurogenic inflammation, supported the hypothesis that channel activation in peptidergic nociceptors promotes AIMSS [174].

The present novel finding that the aromatase substrate, ASD, activates TRPA1 proposes a novel paradigm to explain AIMSS generation. Multiple factors, concomitantly occurring in breast cancer patients treated with AIs, may cooperate to engage TRPA1, thus causing AIMSS-like behaviors. Letrozole (and probably other AIs) is the essential, although *per se* ineffective, initiating stimulus. Letrozole slightly augments ROS [272] and ASD concentrations [175]. Breast cancer [281] or incidental inflammatory processes [282] may boost oxidative stress, thus increasing the possibility of the simultaneous presence of the three TRPA1 stimulants. However, the current hypothesis does not exclude that additional agents, able to activate or sensitize the TRPA1, may act along with AIs and ASD to reach the threshold for AIMSS generation.

During the three years study, our research also focused on uncovering the mechanisms underlying painful states induced by migraine attacks. Migraine is a common and

disabling neurovascular disorder, with heritability estimates as high as 50% and with a likely polygenic multifactorial inheritance [325]. Migraine is characterized by attacks of often throbbing and frequently unilateral severe headache, which are usually associated with nausea, vomiting, and/or sensitivity to light (photophobia), sound (phonophobia), or odours (osmophobia), and aggravated by movement. The last update of the World Health Organization, Global Burden of Disease, states that migraine alone is responsible for almost 3% of disability attributable to a specific disease worldwide. In particular, migraine ranks first among neurological disorders, seventh among non-communicable diseases and eighth among most burdensome diseases [326].

GTN through the release of the active vasodilator gaseous compound, nitric oxide (NO), provokes migraine-like attacks. Despite extensive studies in healthy subjects and migraine patients, the molecular mechanisms by which GTN causes delayed migraine attacks has remained elusive. The prolonged allodynia evoked in rodents by GTN administration has been proposed to recapitulate the delayed events underlying migraine attacks after exposure to GTN in humans [232,237,238]. The major finding of the present study is that the delayed and prolonged GTN-evoked allodynia in mice is entirely TRPA1-dependent. Two lines of evidence support this proposal: genetic deletion and pharmacological blockade of TRPA1.

NO activation of TRPA1, either directly or indirectly *via* its byproducts through nitrosylation of cysteinyl residues, represents an important post translational mechanism of channel regulation [206]. We observed that NO donors activated TRPA1 in cultured of trigeminal neurons and in human transfected cells (hTRPA1-HEK293) by diverse mechanisms. Thus, under *in vitro* circumstances, the conversion of GTN to NO is not required for GTN to activate TRPA1. It is possible that NO is released with insufficient velocity or in insufficient amounts to elicit TRPA1 gating, while the channel is engaged directly by GTN which binds to the same key cysteine/lysine residues required for channel activation by electrophilic and oxidant molecules [121,305]. NO, liberated from GTN by aldehyde dehydrogenase-2, activated TRPA1 in the soma of trigeminal ganglion neurons (TG) to promote NADPH oxidase-1 (NOX1)/NOX2-mediated oxidative stress that sustains allodynia. Although outside the blood brain barrier, TG are contained within the meningeal membranes, and are thus accessible to drugs given both systemically and intrathecally. Furthermore, our results reveal the existence of an autocrine pathway within TG nociceptors that is initiated by NO released from GTN by aldehyde dehydrogenase-2. In this pathway, NO or its byproducts, engages TRPA1 in TG nociceptors, leading to

activation of NOX1/NOX2, which generates ROS and the ensuing aldehyde end-products. The TRPA1 channel that triggers the oxidative burst is expressed by the same sensory neurons that potentially mediate the allodynia. Thus, it is not possible to discriminate whether TRPA1, in addition to generating the proalgesic oxidative stress, is the final mediator of the hypersensitivity. Nevertheless, since TRPA1 is a major sensor of oxidative and carbonylic stress [123,127,130], it is possible that TRPA1 is the target of the ROS/4-HNE, which are generated by its own initial activation by GTN/NO. Also, GTN caused in the mouse periorbital area an early calcitonin gene-related peptide (CGRP)-independent and a delayed and prolonged CGRP-dependent vasodilatation.

CGRP provides a limited contribution to the allodynia in mice may explain the failure of BIBN4096BS to reduce GNT-evoked migraine-like pain in migraineurs [202].

TRPA1 antagonists, which are currently in clinical development, or established anti-migraine drugs, which have recently been identified as selective channel inhibitors [243,310] may be used to test whether a mechanism similar to the present one mediates the delayed attack evoked by GTN in migraineurs.

Finally, we explored the effect of petasin and isopetasin conteined in butterbur [*Petasites hybridus* (L.) Gaertn.]. Butterburs (*Petasites*), herbaceous perennial plants belonging to the genus of *Asteraceae*, which includes also *Tanacetum parthenium* L. [245], have been used by folk medicine of northern Eurasia and America for therapeutic purposes, including treatment of fever, respiratory diseases, spasms, and pain [246]. Among the number of compounds contained in common butterbur [*Petasites hybridus* (L.) Gaertn.] [247], the major constituents, petasin and isopetasin [211], are considered responsible for the antimigraine effects of the herbal extract [212].

Pharmacological and genetic data presented show that isopetasin activates the universal irritant receptor ion channel, TRPA1. Mouse, rat and human (native and recombinant) TRPA1 are gated with similar efficacy and potency by isopetasin, suggesting that responses evoked by the drug *in vivo* in rodents could be reproduced in humans. Furthermore, failure to activate TRPV1 and TRPV4 channels indicates that nociceptor activation by isopetasin is caused by selective TRPA1 targeting. As it failed to evoke calcium responses in the mutant transfected cells (3C/K-Q hTRPA1-HEK293), the molecular mechanism responsible for channel activation by isopetasin must be similar to that proposed for electrophilic and reactive agonists that gate TRPA1 *via* the involvement of specific cysteine/lysine residues [121], stimulated TRPA1 with similar potency, although with less efficacy than isopetasin. Thus, the hemiterpene moiety of angelic acid is not

critical for activity, while the eremophilane sesquiterpenoid framework of isopetasol is essential for channel gating. Present findings add the butterbur constituent, isopetasin [247], to the list of TRPA1-tropic agents, which, stimulate the channel, thereby causing defunctionalization of peptidergic trigeminal nerve terminals, and attenuating their ability to release CGRP and signal pain. Successful treatment and prevention of migraine by targeting of TRPA1 ion channels and the ensuing peptidergic sensory neuron defunctionalization by parthenolide and isopetasin, provides a solid basis for future basic and translational-medical investigations of TRPA1-tropic approaches for migraine.

Thus, TRPA1 can be considered as a novel and major general pain mechanism and TRPA1 antagonists may represent novel analgesic for a long waited advancement for the treatment of various types of pain.

References

1. Turk DC & Okifuji A. Pain Terms and Taxonomies Pain. *Bonica's Management of Pain* 3rd ed. Baltimore, 17-25 (2001).
2. Miranda C, Zanotti G, Pagliardini S, Ponzetto C, Pierotti MA, Greco A. Gain of function mutations of RTK conserved residues display differential effects. *Oncogene. 2002 Nov 28;21(54):8334-9.*, (2002).
3. van Hecke O, Torrance N, Smith BH. Chronic pain epidemiology - where do lifestyle factors fit in? *Br J Pain. 2013 Nov;7(4):209-17.,* (2013).
4. Julius D & Basbaum AI. Molecular mechanisms of nociception. *Nature. 2001 Sep 13;413(6852):203-10.*, (2001).
5. Koltzenburg M & Scadding J. Neuropathic pain. *Curr Opin Neurol. 2001 Oct;14(5):641-7.*, (2001).
6. Bennett R. The rational management of fibromyalgia patients. *Rheum Dis Clin North Am. 2002 May;28(2):181-99.,* (2002).
7. Sarkar S, Aziz Q, Woof CJ, Hobson AR, Thompson DG. Contribution of central sensitisation to the development of non-cardiac chest. *Lancet 2000 Sep 30;356 (9236):1154-9.*,(2000).
8. Bolay H*,* Reuter U, Dunn AK, Huang Z, Boas DA, Moskowitz MA. Intrinsic brain activity triggers trigeminal meningeal afferents in a migraine. *Nat Med 2002 Feb;8(2):136-42.*, (2002).
9. Rainville P, Duncan GH, Price DD, Carrier B, Bushnell MC. Pain affect encoded in human anterior cingulate but not somatosensory cortex. *Science. 1997 Aug 15;277(5328):968-71.*, (1997).
10. Mantyh PW, Clohisy DR, Koltzenburg M, Hunt SP. Molecular mechanisms of cancer pain. *Nat Rev Cancer. 2002 Mar;2(3):201-9.,* (2002).
11. Sherrington CS. *The Integrative Action of the Nervous System* (Scribner, New York, 1906).
12. Basbaum A, Bautista DM, Scherrer G, Julius D. Cellular and molecular mechanisms of pain. *Cell 2009 Oct 16;139(2):284.,* (2009).
13. Hunt, S., A, P. & G, E. - Induction of c-fos-like protein in spinal cord neurons following sensory. - *Nature. 1987 Aug 13-19;328(6131):632-4.*, (1987).
14. Snider WD & McMahon SB. Tackling pain at the source: new ideas about nociceptors. *Neuron. 1998 Apr;20(4):629-32.*, (1998).
15. Geppetti, P. & Holzer, P. *Neurogenic inflammation*, (CRC Press, Boca Raton, 1996).
16. Lewis T. The nocifensor system of nerves and its reactions. *Br Med J* (1937).
17. Szolcsanyi J. Capsaicin and nociception. *Acta Physiol Hung. 1987;69(3-4):323-32.*, (1987).
18. Amadesi S*,* Moreau J, Tognetto M, Trevisani M, Naline E, Advenier C *et al.* NK1 receptor stimulation causes contraction and inositol phosphate increase in. *Am J Respir Crit Care Med. 2001 Apr;163(5):1206-11.*, (2001).
19. Geppetti P*,* Bertrand C, Baker J, Yamawaki I, Piedimonte G, Nadel JA. Ruthenium red, but not capsazepine reduces plasma extravasation by cigarette. *Br J Pharmacol. 1993 Mar;108(3)646-650.,* (1993).
20. Myers A, Goldie RG, Hay DW. A novel role for tachykinin neurokinin-3 receptors in regulation of human. *Am J Respir Crit Care Med. 2005 Feb 1;171(3):212-6.,* (2005).
21. Geppetti P*,* Del Bianco E*,* Cecconi R, Tramontana M, Romani A, Theodorsson E. Capsaicin releases calcitonin gene-related peptide from the human iris and. *Regul Pept. 1992 Sep 3;41(1):83-92.,* (1992).

22. Goadsby P, Edvinsson L, Ekmann R. Vasoactive peptide release in the extracerebral circulation of humans during. *Ann Neurol 1990 Aug;28(2):183-7.,* (1990).
23. Doods H, Hallermayer G, Wu D, Entzeroth M, Rudolf K, Engel W, *et al*. Pharmacological profile of BIBN4096BS, the first selective small molecule CGRP. *Br J Pharmacol. 2000 Feb;129(3):420-3.,* (2000).
24. Olesen J*,* Diener HC, Husstedt IW, Goadsby PJ, Hall D, Meier U, *et al.* Calcitonin gene-related peptide receptor antagonist BIBN 4096 BS for the acute treatment of migraine. *N. Engl. J. Med. 350(11):1104-111.,* (2004).
25. Minke, B. Drosophila mutant with a transducer defect. *Biophys Struct Mech. 1977 Apr 21;3(1):59-64.*, (1997).
26. Montell C & Rubin GM. Molecular characterization of the Drosophila trp locus: a putative integral. *Neuron. 1989 Apr;2(4):1313-23.*, (1989).
27. Vriens J, Watanabe H, Janssens A, Droogmans G, Voets T, Nilius B. Cell swelling, heat, and chemical agonists use distinct pathways for the. *Proc Natl Acad Sci U S A. 2004 Jan 6;101(1):396-401.,* (2004).
28. Nilius, B. Transient receptor potential (TRP) cation channels: rewarding unique proteins. *Bull Mem Acad R Med Belg. 2007;162(3-4):244-53.,* (2007).
29. Denis V & Cyert MS. Internal Ca(2+) release in yeast is triggered by hypertonic shock and mediated by. *J Cell Biol. 2002 Jan 7;156(1):29-34.,* (2002).
30. de Bono M, Tobin DM, Davis MW, Avery L, Bargmann CI. Social feeding in Caenorhabditis elegans is induced by neurons that detect. *Nature. 2002 Oct 31;419(6910):899-903.*, (2002).
31. Kiselyov K, van Rossum DB, Patterson RL. TRPC channels in pheromone sensing. *Vitam Horm. 2010;83:197-213.,* (2010).
32. Zhang Y, Hoon MA, Chandrashekar J, Muller KL, Cook B, Wu D, *et al.* Coding of sweet, bitter, and umami tastes: different receptor cells sharing. *Cell. 2003 Feb 7;112(3):293-301.*, (2003).
33. Clapham DE. TRP channels as cellular sensors. *Nature 2003 426, 517-524.*, (2003).
34. Montell C, Birnbaumer L, Flockerzi V, Bindels RJ, Bruford EA, Caterina MJ, *et al.* A unified nomenclature for the superfamily of TRP cation channels. *Mol Cell. 2002 Feb;9(2):229-31.*, (2002).
35. Clapham DE, Runnels LW, Strubing C. The TRP ion channel family. *Nat Rev Neurosci. 2001 Jun;2(6):387-96.*, (2001).
36. Sedgwick SG & Smerdon SJ. The ankyrin repeat: a diversity of interactions on a common structural framework. *Trends Biochem Sci. 1999 Aug;24(8):311-6.*, (1999).
37. Ramsey IS, Delling M, Clapham DE. An introduction to TRP channels. *Annu Rev Physiol. 2006;68:619-47.*, (2006).
38. Clapham D, Montell C, Schullz G, Julius D. International Union of Pharmacology. XLIII. Compendium of voltage-gated ion. *Pharmacol Rev. 2003 Dec;55(4):591-6.*, (2005).
39. Maroto R, Raso A, Wood TG, Kurosky A, Martinac B, Hamill OP. TRPC1 forms the stretch-activated cation channel in vertebrate cells. *Nat Cell Biol. 2005 Feb;7(2):179-8.,* (2005).
40. Vriens J, Owsianik G, Fisslthaler B, Suzuki M, Janssens A, Voets T, *et al.* Modulation of the Ca2 permeable cation channel TRPV4 by cytochrome P450. *Circ Res. 2005 Oct 28;97(9):908-15.,* (2005).

41. Vennekens R, Hoenderop JG, Prenen J, Stuiver M, Willems PH, Droogmans G, *et al.* Permeation and gating properties of the novel epithelial Ca(2+) channel. *J Biol Chem. 2000 Feb 11;275(6):3963-9.*, (2000).
42. den Dekker E, Hoenderop JG, Nilius B, Bondels RJ. The epithelial calcium channels, TRPV5 & TRPV6: from identification towards. *Cell Calcium. 2003 May-Jun;33(5-6):497-507.*, (2003).
43. Caterina MJ, Schumacher MA, Tominaga M, Rosen TA, Levine JD, Julius D. The capsaicin receptor: a heat-activated ion channel in the pain pathway. *Nature 389, 816-824*., (1997).
44. Tominaga M, Caterina MJ, Malmberg AB, Rosen TA, Gilbert H, Skinner K, *et al.* The cloned capsaicin receptor integrates multiple pain-producing stimuli. *Neuron. 1998 Sep;21(3):531-43.*, (1998).
45. Xu H, Blair NT, Clapham DE. Camphor activates and strongly desensitizes the transient receptor potential. *J Neurosci. 2005 Sep 28;25(39):8924-37.*, (2005).
46. Macpherson L*,* Geierstanger BH, Viswanath V, Bandell M, Eid SR, Hwang S, *et al.* The pungency of garlic: activation of TRPA1 and TRPV1 in response to allicin. *Curr Biol 15(10):929-34.*, (2005).
47. Macpherson LJ, Xiao B, Kwan KY, Petrus MJ, Dubin AE, Hwang S*, et al.* An ion channel essential for sensing chemical damage. *J Neurosci 27(42):11412-11415.,* (2007).
48. Yoshida T*,* Morii T, Takahashi N, Yamamoto S, Hara Y, Tominaga M, *et al.* Nitric oxide activates TRP channels by cysteine S-nitrosylation. *Nat Chem Biol. 2006 Nov;2(11):596-607.,* (2006).
49. Siemens J, Zhou S, Piskorowski R, Nikai T, Lumpkin EA, Basbaum AI, *et al.* Spider toxins activate the capsaicin receptor to produce inflammatory pain. *Nature. 2006 Nov 9;444(7116):208-12.,* (2006).
50. Trevisani M, Smart D, Gunthorpe MJ, Tognetto M, Barbieri M, Campi B, *et al.* Ethanol elicits and potentiates nociceptor responses via the vanilloid receptor-1. *Nature* Neuroscience 5(6):546-551., (2002).
51. Ahern G, Brooks IM, Miyares RL, Wang XB, *et al.* Extracellular cations sensitize and gate capsaicin receptor TRPV1 modulating pain. *J Neurosci 25(21):5109-16.,* (2005).
52. Doly S, Fischer J, Salio C, Conrath M. The vanilloid receptor-1 is expressed in rat spinal dorsal horn astrocytes. *Neurosci Lett 357(2):123-6.,* (2004).
53. Tominaga M & Tominaga T. Structure and function of TRPV1. *Pflugers Arch. 2005 Oct;451(1):143-50.,* (2005).
54. Ji RR, Samad TA, Jin SX, Schmoll R, Woolf CJ. p38 MAPK activation by NGF in primary sensory neurons after inflammation. *Neuron. 2002 Sep 26;36(1):57-68.*, (2002).
55. Zhang X, Huang J, McNaughton PA. NGF rapidly increases membrane expression of TRPV1 heat-gated ion channels. *EMBO J. 2005 Dec 21;24(24):4211-23.,* (2005).
56. Mohapatra DP & Nau C. Desensitization of capsaicin-activated currents in the vanilloid receptor TRPV1. *J Biol Chem. 2003 Dec 12;278(50):50080-90.,* (2003).
57. Chuang HH, Prescott ED, Kong H, Shields S, Jordt SE, Basbaum AI, *et al.* Bradykinin and nerve growth factor release the capsaicin receptor from. *Nature. 2001 Jun 21;411(6840):957-62.*, (2001).

58. Hwang SW, Cho H, Kwak J, Lee SY, Kang CJ, Jung J, *et al.* Direct activation of capsaicin receptors by products of lipoxygenases: endogenous. *Proc Natl Acad Sci U S A. 2000 May 23;97(11):6155-60.,* (2000).
59. Amadesi S, Nie J, Vergnolle N, Cottrell GS, Grady EF, Trevisani M, *et al.* Protease-activated receptor 2 sensitizes the capsaicin receptor transient. *J Neurosci. 2004 May 5;24(18):4300-12.*, (2004).
60. Amadesi S, Cottrell GS, Divino L, Chapman K, Grady EF, Bautista F, *et al.* Protease-activated receptor 2 sensitizes TRPV1 by protein kinase Cepsilon- and A-dependent mechanisms in rats and mice. *J Physiol. 2006 Sep 1;575(Pt 2):555-71.,* (2006).
61. Liedtke W*,* Choe Y, Martí-Renom MA, Bell AM, Denis CS, Sali A, *et al.* Vanilloid receptor-related osmotically activated channel (VR-OAC), a candidate vertebrate osmoreceptor. *Cell. 2000 Oct 27;103(3):525-35.*, (2000).
62. Delany NS, Hurle M, Facer P, Alnadaf T, Plumpton C, Kinghorn I, *et al.* Identification and characterization of a novel human vanilloid receptor-like protein, VRL-2. *Physiol Genomics. Jan 19;4(3):165-74.,* (2001).
63. Wissenbach U, Bödding M, Freichel M, Flockerzi V. Trp12, a novel Trp related protein from kidney. *FEBS Lett. 2000 Nov 24;485(2-3):127-34.*, (2000).
64. Suzuki M, Mizuno A, Kodaira K, Imai M. Impaired pressure sensation in mice lacking TRPV4. *J Biol Chem. 2003 Jun 20;278(25):22664-8.,* (2003).
65. Guler AD, Lee H, Iida T, Shimizu I, Tominaga M, *et al.* Heat-evoked activation of the ion channel, TRPV4. *J Neurosci. 2002 Aug 1;22(15):6408-14.*, (2002).
66. Grant A, Amadesi S, Bunnett NW. Protease-Activated Receptors: Mechanisms by Which Proteases Sensitize TRPV Channels to Induce Neurogenic Inflammation and Pain. (eds. WB, L., S, H. & At) (2007).
67. Strotmann R, Harteneck C, Nunnenmacher K, Schultz G, Plant TD. OTRPC4, a nonselective cation channel that confers sensitivity to extracellular osmolarity. *Nat Cell Biol. 2000 Oct;2(10):695-702.,* (2000).
68. Gao X, Wu L, O'Neil RG. Temperature-modulated diversity of TRPV4 channel gating: activation by physical. *J Biol Chem. 2003 Jul 18;278(29):27129-37.,* (2003).
69. Watanabe H, Vriens J, Suh SH, Benham CD, Droogmans G, Nilius B. Heat-evoked activation of TRPV4 channels in a HEK293 cell expression system and in native mouse aorta endothelial cells. *J Biol Chem. 2002 Dec 6;277(49):47044-51*., (2002).
70. Watanabe H, Vriens J, Prenen J, Droogmans G, Voets T, Nilius B. Anandamide and arachidonic acid use epoxyeicosatrienoic acids to activate TRPV4 channelS. *Nature. 2003 Jul 24;424(6947):434-8.*, (2003).
71. O' Neil RG & Leng l. Osmo-mechanically sensitive phosphatidylinositol signaling regulates a Ca2+. *Am J Physiol. 1997 Jul;273(1 Pt 2):F120-8.*, (1997).
72. Pedersen S, Lambert IH, Thoroed SM, Hoffmann EK. Hypotonic cell swelling induces translocation of the alpha isoform of cytosolic phospholipase A2 but not the gamma isoform in Ehrlich ascites tumor cells. *Eur J Biochem. 2000 Sep;267(17):5531-9* (2000).
73. Xu H, Zhao H, Tian W, Yoshida K, Roullet JB, Cohen DM Regulation of a transient receptor potential (TRP) channel by tyrosine phosphorylation. SRC family kinase-dependent tyrosinephosphorylation of TRPV4 on TYR-253

mediates its response to hypotonic stress. *J Biol Chem. 2003 Mar 28;278(13):11520-7.,* (2003).
74. Alessandri-Haber N, Dina OA, Joseph EK, Reichling D, Levine JD. A transient receptor potential vanilloid 4-dependent mechanism of hyperalgesia is engaged by concerted action of inflammatory mediators. *J Neurosci. 2006 Apr 5;26(14):3864-74.*, (2006).
75. Chen Y, Yang C, Wang ZJ. Proteinase-activated receptor 2 sensitizes transient receptor potential vanilloid 1, transient receptor potential vanilloid 4, and transient receptor potential ankyrin 1 in paclitaxel-induced neuropathic pain. *Neuroscience. 2011 Oct 13;193:440-51.,* (2011).
76. Soyombo A, Tjon-Kon-Sang S, Rbaibi Y, Bashllari E, Bisceglia J, Muallem S, *et al.* TRP-ML1 regulates lysosomal pH and acidic lysosomal lipid hydrolytic activity. *J Biol Chem. 2006 Mar 17;281(11):7294-301.,* (2006).
77. Hanaoka K, Qian F, Boletta A, Bhunia AK, Piontek K, Tsiokas L, *et al.* Co-assembly of polycystin-1 and -2 produces unique cation-permeable currents. *Nature. 2000 Dec 21-28;408(6815):990-4.*, (2000).
78. Nagata K, Duggan A, Kumar G, García-Añoveros J. Nociceptor and hair cell transducer properties of TRPA1, a channel for pain and hearing. *J Neurosci. 2005 Apr 20;25(16):4052-61.,* (2005).
79. Story GM, Peier AM, Reeve AJ, Eid SR, Mosbacher J, Hricik TR, *et al.* ANKTM1, a TRP-like channel expressed in nociceptive neurons, is activated by cold temperatures. *Cell 112, 819-829.,* (2003).
80. Jaquemar D, Schenker T & Trueb B. An ankyrin-like protein with transmembrane domains is specifically lost after oncogenic transformation of human fibroblasts. *J Biol Chem 274, 7325-7333.,* (1999).
81. Jordt S, Bautista DM, Chuang HH, McKemy DD, Zygmunt PM, *et al.* Mustard oils and cannabinoids excite sensory nerve fibres through the TRP channel ANKTM1. *Nature. 2004 Jan 15;427(6971):260-5.,* (2004).
82. Nilius B, Owsianik G. The transient receptor potential family of ion channels. *Genome Biol. 2011;12(3):218.,* (2011).
83. Nilius B, Appendino G, Owsianik G.The transient receptor potential channel TRPA1: from gene to pathophysiology. - *Pflugers Arch. 2012 Nov;464(5):425-58.,* (2012).
84. Chen J, Kim D, Bianchi BR, Cavanaugh EJ, Faltynek CR, Kym PR, *et al.* Pore dilation occurs in TRPA1 but not in TRPM8 channels. *Mol Pain. 2009 Jan 21;5:3*., (2009).
85. Banke t, Chaplan SR, Wickenden AD. Dynamic changes in the TRPA1 selectivity filter lead to progressive but reversible pore dilation. *Am J Physiol Cell Physiol. 2010 Jun;298(6):C1457-68.,* (2010).
86. Voets T, Droogmans G, Wissenbach U, Janssens A, Flockerzi V, Nilius B. The principle of temperature-dependent gating in cold- and heat-sensitive TRP channels. *Nature. 2004 Aug 12;430(7001):748-54.*, (2004).
87. Karashima Y, Prenen J, Meseguer V, Owsianik G, Voets T, Nilius B. Modulation of the transient receptor potential channel TRPA1 by hosphatidylinositol 4,5-biphosphate manipulators. *Pflugers Arch. 2008 Oct;457(1):77-89.,* (2008).
88. Gaudet R. A primer on ankyrin repeat function in TRP channels and beyond. *Mol Biosyst. 2008 May;4(5):372-9.,* (2008).
89. Wang L, Cvetkov TL, Chance MR, Moiseenkova-Bell VY. Identification of in vivo disulfide conformation of TRPA1 ion channel. *J Biol Chem. 2012 Feb 24;287(9):6169-76.,* (2012).

90. Andersson, DA, Gentry C, Moss S, Bevan S. Clioquinol and pyrithione activate TRPA1 by increasing intracellular Zn2+. - *Proc Natl Acad Sci U S A. 2009 May 19;106(20):8374-9.,* (2009).
91. Hu H, Bandell M, Petrus MJ, Zhu MX, Patapoutian A. Zinc activates damage-sensing TRPA1 ion channels. *Nat Chem Biol. 2009 Mar;5(3):183-90*., (2009).
92. Wang Y, Chang RB, Waters HN, McKemy DD, Liman ER. The nociceptor ion channel TRPA1 is potentiated and inactivated by permeating calcium ions. *J Biol Chem. 2008 Nov 21;283(47):32691-703.,* (2008).
93. Sura L, Zíma V, Marsakova L, Hynkova A, Barvík I, Vlachova V.C-terminal acidic cluster is involved in Ca2+-induced regulation of human transient receptor potential ankyrin 1 channel. *J Biol Chem. 2012 May 25;287(22):18067-77.,* (2012).
94. Doerner JF, Gisselmann G, Hatt H, Wetzel CH. Transient receptor potential channel A1 is directly gated by calcium ions. *J Biol Chem. 2007 May 4;282(18):13180-9.,* (2007).
95. Zurborg S, Yurgionas B, Jira JA, Caspani O, Heppenstall PA. Direct activation of the ion channel TRPA1 by Ca2+. *Nat Neurosci. 2007 Mar;10(3):277-9.,* (2007).
96. Cvetkov TL, Huynh KW, Cohen MR, Moiseenkova-Bell VY. Molecular architecture and subunit organization of TRPA1 ion channel revealed by electron microscopy. *J Biol Chem. 2011 Nov 4;286(44):38168-76.,* (2011).
97. Hjerling-Leffler J, Alqatari M, Ernfors P, Koltzenburg M. Emergence of functional sensory subtypes as defined by transient receptor potential channel expression. *J Neurosci. 2007 Mar 7;27(10):2435-43.*, (2007).
98. Bhattacharya MR, Bautista DM, Wu K, Haeberle H, Lumpkin EA, Julius D. Radial stretch reveals distinct populations of mechanosensitive mammalian somatosensory neurons. Proc Natl Acad Sci U S A 105, 20015-20020., (2008).
99. Hayashi, s, Nakamura E, Endo T, Kubo Y, Takeuchi K. Impairment by activation of TRPA1 of gastric epithelial restitution in a wound model using RGM1 cell monolayer. *Inflammopharmacology. 2007 Oct;15(5):218-22.,* (2007).
100. Du S, Araki I, Kobayashi H, Zakoji H, Sawada N, Takeda M. Differential expression profile of cold (TRPA1) and cool (TRPM8) receptors in human urogenital organs. *Urology. 2008 Aug;72(2):450-5.,* (2008).
101. Nassini R, Pedretti P, Moretto N, Fusi C, Carnini C, *et al.* Transient receptor potential ankyrin 1 channel localized to non-neuronal airway cells promotes non-neurogenic inflammation. *PLoS One 7(8): e42454.,* (2012).
102. Caceres AI, Brackmann M, Elia MD, Bessac BF, del Camino D, D'Amours M, *et al.* A sensory neuronal ion channel essential for airway inflammation and hyperreactivity in asthma. *Proc Natl Acad Sci U S A. 2009 Jun 2;106(22):9099-104.,* (2009).
103. Gratzke C, Weinhold P, Reich O, Seitz M, Schlenker B, Stief CG*, et al.* - Transient receptor potential A1 and cannabinoid receptor activity in human normal and hyperplastic prostate: relation to nerves and interstitial cells. *Eur Urol. 2010 May;57(5):902-10.,* (2009).
104. Nozawa K, Kawabata-Shoda E, Doihara H, Kojima R, Okada H, Mochizuki S, *et al.* TRPA1 regulates gastrointestinal motility through serotonin release from enterochromaffin cells. *Proc Natl Acad Sci U S A. 2009 Mar 3;106(9):3408-13.,* (2009).

105. Earley S, Gonzales AL, Crnich R. Endothelium-dependent cerebral artery dilation mediated by TRPA1 and Ca2+-Activated K+ channels. *Circ Res. 2009 Apr 24;104(8):987-94.,* (2009).
106. Bellono N, Kammel LG, Zimmerman AL, Oancea E. UV light phototransduction activates transient receptor potential A1 ion channels in human melanocytes. *Proc Natl Acad Sci U S A. 2013 Feb 5;110(6):2383-8.,* (2013).
107. Yu s, Gao G, Peterson BZ, Ouyang A. TRPA1 in mast cell activation-induced long-lasting mechanical hypersensitivity of vagal afferent C-fibers in guinea pig esophagus. *Am J Physiol Gastrointest Liver Physiol. 297(1):G34-42.*, (2009).
108. Hox v, Vanoirbeek JA, Alpizar YA, Voedisch S, Callebaut I, Bobic S, *et al.* Crucial role of transient receptor potential ankyrin 1 and mast cells in. *Am J Respir Crit Care Med. 1;187(5):486-93.,* (2013).
109. Son AR, Yang YM, Hong JH, Lee SI, Shibukawa Y, Shin DM.Odontoblast TRP channels and thermo/mechanical transmission. *J Dent Res. 88(11):1014-9.,* (2009).
110. Caterina MJ. Transient receptor potential ion channels as participants in thermosensation and termoregulation. *Am J Physiol Regul Integr Comp Physiol. 2007 Jan;292(1):R64-76.,* (2007).
111. Bandell M, Story GM, Hwang SW, Viswanath V, Eid SR, Petrus MJ, *et al.* Noxious cold ion channel TRPA1 is activated by pungent compounds and bradykinin. *Neuron 41:849-857.,* (2004).
112. Sawada Y, Hosokawa H, Matsumura K, Kobayashi S. Activation of transient receptor potential ankyrin 1 by hydrogen peroxide. *Eur J Neurosci 27:1131-1142.,* (2008).
113. Bautista DM, Siemens J, Glazer JM, Tsuruda PR, Basbaum AI, Stucky CL*, et al.* The menthol receptor TRPM8 is the principal detector of environmental cold. *Nature. 448(7150):204-8.,* (2007).
114. Karashima Y, Talavera K, Everaerts W, Janssens A, Kwan KY, Vennekens R, *et al.* TRPA1 acts as a cold sensor in vitro and in vivo. *Proc Natl Acad Sci U S A 106:1273-1278.,* (2009).
115. Abrahamsen B*,* Zhao J, Asante CO, Cendan CM, Marsh S, Martinez-Barbera JP,*et al.* The cell and molecular basis of mechanical, cold, and inflammatory pain. *Science 321:702-705.,* (2008).
116. Kwan KY, Allchorne AJ, Vollrath MA, Christensen AP, Zhang DS, Woolf CJ, *et al.* TRPA1 contributes to cold, mechanical, and chemical nociception but is not essential for hair-cell transduction. *Neuron 50:277-289.,* (2006).
117. Bautista DM, Jordt SE, Nikai T, Tsuruda PR, Read AJ, Poblete J, *et al.* TRPA1 mediates the inflammatory actions of environmental irritants and proalgesic agents. *Cell 124:1269-1282.,* (2006).
118. Petrus M*,* Peier AM, Bandell M, Hwang SW, Huynh T, Olney N, *et al.* A role of TRPA1 in mechanical hyperalgesia is revealed by pharmacological inhibition. *Mol Pain 3:40.,* (2007).
119. Zhang XF, Chen J, Faltynek CR, Moreland RB, Neelands TR. Transient receptor potential A1 mediates an osmotically activated ion channel. *Eur J Neurosci 27: 605-61.,* (2008).
120. Bang S & Hwang SW. Polymodal ligand sensitivity of TRPA1 and its modes of interactions. *J Gen Physiol. 2009 Mar;133(3):257-62.,* (2009).
121. Hinman A, Chuang HH, Bautista DM, Julius D. TRP channel activation by reversible covalent modification. *Proc Natl Acad Sci U S A 103:19564-*

19568., (2006).
122. Macpherson LJ, Dubin AE, Evans MJ, Marr F, Schultz PG, Cravatt BF, *et al.* Noxious compounds activate TRPA1 ion channels through covalent modification of cysteines. *Nature 445:541-545.,* (2007).
123. Trevisani M, Siemens J, Materazzi S, Bautista DM, Nassini R, Campi B*, et al.* 4-Hydroxynonenal, an endogenous aldehyde, causes pain and neurogenic inflammation through activation of the irritant receptor TRPA1. *Proc Natl Acad Sci U S A 104:13519-13524.,* (2007).
124. Benedetti A, Comporti M, Esterbauer H. Identification of 4-hydroxynonenal as a cytotoxic product originating from the peroxidation of liver microsomal lipids. *Biochim Biophys Acta. 1980 Nov 7;620(2):281-96.,* (1980).
125. Esterbauer H, Schaur RJ, Zollner H. Chemistry and biochemistry of 4-hydroxynonenal, malonaldehyde and related aldehydes. *Free Radic Biol Med. 1991;11(1):81-128.,* (1991).
126. Taylor-Clark TE*,* McAlexander MA, Nassenstein C, Sheardown SA, Wilson S, Thornton J, *et al.* Relative contributions of TRPA1 and TRPV1 channels in the activation of vagal bronchopulmonary C-fibres by the endogenous autacoid 4-oxononenal. *J Physiol. 586(14):3447-59.,* (2008).
127. Andersson DA, Gentry C, Moss S, Bevan, S. Transient receptor potential A1 is a sensory receptor for multiple products of oxidative stress. *J Neurosci 28(10):2485-2494.,* (2008).
128. Bessac BF, Sivula M, von Hehn CA, Escalera J, Cohn L, Jordt SE. TRPA1 is a major oxidant sensor in murine airway sensory neurons. *J Clin Invest 118, 1899-1910.,* (2008).
129. Taylor-Clark TE, Ghatta S, Bettner W, Undem BJ. Nitrooleic acid, an endogenous product of nitrative stress, activates nociceptive sensory nerves via the direct activation of TRPA1. *Mol Pharmacol 75(4):820-829.,* (2009).
130. Materazzi S, Nassini R, Andrè E, Campi B, Amadesi S, Trevisani M, *et al.* Cox-dependent fatty acid metabolites cause pain through activation of the irritant receptor TRPA1. *Proc Natl Acad Sci U S A 105(339:12045-12050.,* (2008).
131. Taylor-Clark T, Undem BJ, Macglashan DW Jr, Ghatta S, Carr MJ, McAlexander MA. Prostaglandin-induced activation of nociceptive neurons via direct interaction with transient receptor potential A1 (TRPA1). *Mol Pharmacol. 2008 Feb;73(2):274-81.,* (2008).
132. Miyamoto R, Otsuguro K, Ito S. Time- and concentration-dependent activation of TRPA1 by hydrogen sulfide in rat DRG neurons. *Neurosci Lett. 2011 Jul 20;499(2):137-42.,* (2011).
133. Wang YY, Chang RB, Liman ER. TRPA1 is a component of the nociceptive response to CO2. *J Neurosci. 2010 Sep 29;30(39):12958-63*., (2010).
134. Fujita F, Uchida K, Moriyama T, Shima A, Shibasaki K, Inada H, *et al.* Intracellular alkalization causes pain sensation through activation of TRPA1 in mice. *J Clin Invest. 2008 Dec;118(12):4049-57.,* (2008).
135. Nassini R, Materazzi S, Andrè E, Sartiani L, Aldini G, Trevisani M, *et al.* Acetaminophen, via its reactive metabolite N-acetyl-p-benzo-quinoneimine and transient receptor potential ankyrin-1 stimulation, causes neurogenic inflammation in the airways and other tissues in rodents. *FASEB J. 2010 Dec;24(12):4904-16.,* (2010).
136. Sadofsky LR, Boa AN, Maher SA, Birrell MA, Belvisi MG, Morice AH. TRPA1 is activated by direct addition of cysteine residues to the N-

hydroxysuccinyl esters of acrylic and cinnamic acids. *Pharmacol Res. 2011 Jan;63(1):30-6.,* (2011).
137. Dalle-Donne I, Aldini G, Carini M, Colombo R, Rossi R, Milzani A. Protein carbonylation, cellular dysfunction, and disease progression. *J Cell Mol Med. 2006 Apr-Jun;10(2):389-406.,* (2006).
138. Fischer MJ, Leffler A, Niedermirtl F, Kistner K, Eberhardt M, Reeh PW, *et al.* The general anesthetic propofol excites nociceptors by activating TRPV1 and TRPA1 rather than GABAA receptors. *J Biol Chem. 2010 Nov 5;285(45):34781-92.,* (2010).
139. Leffler A, Lattrell A, Kronewald S, Niedermirtl F, Nau C. Activation of TRPA1 by membrane permeable local anesthetics. *Mol Pain. 2011 Aug 23;7:62.,* (2011).
140. Motter AL & Ahern GP. TRPA1 is a polyunsaturated fatty acid sensor in mammals. *PLoS One. 2012;7(6):e38439.,* (2012).
141. Karashima Y, Damann N, Prenen J, Talavera K, Segal A, Voets T, *et al.* Bimodal action of menthol on the transient receptor potential channel TRPA1. *J Neurosci 27(37):9874-9884.,* (2007).
142. McKemy DD, Neuhausser WM, Julius D. Identification of a cold receptor reveals a general role for TRP channels in thermosensation. *Nature. 2002 Mar 7;416(6876):52-8.,* (2002).
143. Peier AM, Moqrich A, Hergarden AC, Reeve AJ, Andersson DA, Story GM, *et al.* A TRP channel that senses cold stimuli and menthol. *Cell. 2002 Mar 8;108(5):705-15.*, (2002).
144. Hu H, Tian J, Zhu Y, Wang C, Xiao R, Herz JM, *et al.* Activation of TRPA1 channels by fenamate nonsteroidal anti-inflammatory drugs. *Pflugers Arch. 2010 Mar;459(4):579-92.,* (2009).
145. McMahon SB, Cafferty WB, Marchand F. Immune and glial cell factors as pain mediators and modulators. *Exp Neurol. 2005 Apr;192(2):444-62*., (2005).
146. Dray A & Perkins M. Bradykinin and inflammatory pain. *Trends Neurosci. 1993 Mar;16(3):99-104.*, (1993).
147. Dai Y, Wang S, Tominaga M, Yamamoto S, Fukuoka T, Higashi T, *et al.* Sensitization of TRPA1 by PAR2 contributes to the sensation of inflammatory pain. *J Clin Invest 117, 1979-1987.,* (2007).
148. Diogenes A, Akopian AN, Hargreaves KM. NGF up-regulates TRPA1: implications for orofacial pain. *J Dent Res. 2007 Jun;86(6):550-5.*, (2007).
149. McNamara CR, Mandel-Brehm J, Bautista DM, Siemens J, Deranian KL, Zhao M, *et al.* TRPA1 mediates formalin-induced pain. *Proc Natl Acad Sci U S A 104(33):13525-13530.,* (2007).
150. Kerstein PC, del Camino D, Moran MM, Stucky CL. Pharmacological blockade of TRPA1 inhibits mechanical firing in nociceptors. *Mol Pain. 2009 Apr 21;5:19.,* (2009).
151. Wei H, Hamalainen MM, Saarnilehto M, Koivisto A, Pertovaara A. Attenuation of mechanical hypersensitivity by an antagonist of the TRPA1 ion channel in diabetic animals. *Anesthesiology 111(1):147-154.,* (2009).
152. Cavaletti G & Marmioli P. Chemotherapy-induced peripheral neurotoxicity. *Nat Rev Neurol. 2010 Dec;6(12):657-66.,* (2010).
153. Windebank AJ & Grisold W. Chemotherapy-induced neuropathy. *J Peripher Nerv Syst. 2008 Mar;13(1):27-46.,* (2008).
154. Joseph, EK, Chen X, Bogen O, Levine JD. Oxaliplatin acts on IB4-positive nociceptors to induce an oxidative stress-dependent acute painful peripheral

neuropathy. *J Pain 9(5):463-472.,(*2008).
155. Pachman DR, Barton DL, Watson JC, Loprinzi CL. Chemotherapy-induced peripheral neuropathy: prevention and treatment. *Clin Pharmacol Ther. 2011 Sep;90(3):377-87.,* (2011).
156. Bolcskei K, Helyes Z, Szabó A, Sándor K, Elekes K, Németh J, *et al.* Investigation of the role of TRPV1 receptors in acute and chronic nociceptive. *Pain. 2005 Oct;117(3):368-76.,* (2005).
157. Materazzi S, Fusi C, Benemei S, Pedretti P, Patacchini R, Nilius B, *et al.* TRPA1 and TRPV4 mediate paclitaxel-induced peripheral neuropathy in mice via a glutathione-sensitive mechanism. *Pflugers Arch 463(4):561-569.,* (2012).
158. Nassini R, Gees M, Harrison S, De Siena G, Materazzi S, Moretto N, *et al.* Oxaliplatin elicits mechanical and cold allodynia in rodents via TRPA1 receptor stimulation. *Pain 152(7):1621-1631.,* (2011).
159. Trevisan G, Materazzi S, Fusi C, Altomare A, Aldini G, Lodovici M, *et al.* Novel therapeutic strategy to prevent chemotherapy-induced persistent sensory neuropathy by TRPA1 blockade. *Cancer Res 73(10):3120-3131.,* (2013).
160. Gibson L, Lawrence D, Dawson C, Bliss J. Aromatase inhibitors for treatment of advanced breast cancer in postmenopausal women. *Cochrane Database Syst Rev (4):CD003370.,* (2009).
161. Burstein HJ, Prestrud AA, Seidenfeld J, Anderson H, Buchholz TA, Davidson NE, *et al.* American Society of Clinical Oncology clinical practice guideline: update on adjuvant endocrine therapy for women with hormone receptor-positive breast cancer. *J Clin Oncol* 28(23):3784-3796., (2010).
162. Connor C. & Attai D. Adjuvant endocrine therapy for the surgeon: options, side effects, and their management. *Ann Surg Oncol 20:3188-3193., (*2013).
163. Mouridsen HT. Incidence and management of side effects associated with aromatase inhibitors in the adjuvant treatment of breast cancer in postmenopausal women. *Curr Med Res Opin 22, 1609-1621.,* (2006).
164. Crew KD, Greenlee H, Capodice J, Raptis G, Brafman L, Fuentes D, *et al.* Prevalence of joint symptoms in postmenopausal women taking aromatase inhibitors for early-stage breast cancer. *J Clin Oncol* 25:3877-3883., (2007).
165. Henry NL, Giles JT, Stearns V. Aromatase inhibitor-associated musculoskeletal symptoms: etiology and strategies for management. *Oncology (Williston Park) 22:1401-1408.,* (2008).
166. Laroche F, Coste J, Medkour T, Cottu PH, Pierga JY, Lotz JP, *et al.* Classification of and risk factors for estrogen deprivation pain syndromes related to aromatase inhibitor treatments in women with breast cancer: a prospective multicenter cohort study. *J Pain 15(3):293-303.,* (2014).
167. Henry NL, Giles JT, Ang D, Mohan M, Dadabhoy D, Robarge J, *et al.* Prospective characterization of musculoskeletal symptoms in early stage breast cancer patients treated with aromatase inhibitors. *Breast Cancer Res Treat 111(2)365-372.,* (2008).
168. Burstein HJ & Winer EP. Aromatase inhibitors and arthralgias: a new frontier in symptom management for breast cancer survivors. *J Clin Oncol 25:3797-3799.,* (2007).
169. Presant CA, Bosserman L, Young T, Vakil M, Horns R, Upadhyaya G, *et al.* Aromatase inhibitor-associated arthralgia and/ or bone pain: frequency and characterization in non-clinical trial patients. *Clin Breast Cancer 7: 775-778.,* (2007).

170. Morales L, Pans S, Paridaens R, Westhovens R, Timmerman D, Verhaeghe J, *et al.* Debilitating musculoskeletal pain and stiffness with letrozole and exemestane: associated tenosynovial changes on magnetic resonance imaging. *Breast Cancer Res Treat 104(1):87-9.,* (2007).
171. Sestak I, Cuzick J, Sapunar F, Eastell R, Forbes JF, Bianco AR, *et al.* Risk factors for joint symptoms in patients enrolled in the ATAC trial: a retrospective, exploratory analysis. *Lancet Oncol 9(9):866-872.,* (2008).
172. Liu H & Talalay P. Relevance of anti-inflammatory and antioxidant activities of exemestane and synergism with sulforaphane for disease prevention. *Proc Natl Acad Sci U S A 110, 19065-19070.,* (2013).
173. Brone B, Peeters PJ, Marrannes R, Mercken M, Nuydens R, Meert T, *et al.* Tear gasses CN, CR, and CS are potent activators of the human TRPA1 receptor. *Toxicol Appl Pharmacol 231(2):150-156.,* (2008).
174. Fusi C, Materazzi S, Benemei S, Coppi E, Trevisan G, Marone IM, *et al.* Steroidal and non-steroidal third-generation aromatase inhibitors induce pain-like symptoms via TRPA1. *Nat Commun 5:5736.,* (2014).
175. Gallicchio L, Macdonald R, Wood B, RushovicH E, Helzlsouer KJ. Androgens and musculoskeletal symptoms among breast cancer patients on aromatase inhibitor therapy. *Breast Cancer Res Treat 130:569-577.,* (2011).
176. Ghosh D, Griswold J, Erman M, Pangborn W. Structural basis for androgen specificity and oestrogen synthesis in human aromatase. *Nature 457:219-223.,* (2009).
177. Bayliss WM. On the origin from the spinal cord of the vaso-dilator fibres of the hind-limb. *J Physiol. 1901 Feb 28;26(3-4):173-209.*, (1901).
178. Salvatore CA, Hershey JC, Corcoran HA, Fay JF, Johnston VK, Moore EL, *et al.* Pharmacological characterization of MK-0974 [N-[(3R,6S)-6-(2,3-difluorophenyl)-2-oxo-1-(2,2,2-trifluoroethyl)azepan-3-yl]-4-(2-oxo-2,3-dihydro-1H-imidazo[4,5-b]pyridin-1-yl)piperidine-1-carboxamide], a potent and orally active calcitonin gene-related peptide receptor antagonist for the treatment of migraine. *J Pharmacol Exp Ther 324:416-421.,* (2008).
179. Sinclair SR, Kane SA, Van der Schueren BJ, Xiao A, Willson KJ, Boyle J, *et al.* Inhibition of capsaicin-induced increase in dermal blood flow by the oral CGRP receptor antagonist, telcagepant (MK-0974). *Br J Clin Pharmacol 69(1):15-22.,* (2010).
180. Goldstein DJ, Wang O, Saper JR, Stoltz R, Silberstein SD, Mathew NT*, et al.* Ineffectiveness of neurokinin-1 antagonist in acute migraine: a crossover study. *Cephalalgia 17:785-790.,* (1997).
181. Ho TW, Ferrari MD, Dodick DW, Galet V, Kost J, Fan X, *et al.* Efficacy and tolerability of MK-0974 (telcagepant), a new oral antagonist of calcitonin gene-related peptide receptor, compared with zolmitriptan for acute migraine: a randomised, placebo-controlled, parallel-treatment trial. *Lancet 372:2115-2123.,* (2008).
182. Diener HC. RPR100893, a substance-P antagonist, is not effective in the treatment of migraine attacks. *Cephalalgia 23:183-185.,* (2003).
183. Courteau JP, Cushman R, Bouchard F, Quévillon M, Chartrand A, Bhérer L. Survey of construction workers repeatedly exposed to chlorine over a three to six. *Occup Environ Med. 1994 Apr;51(4):219-24.*, (1994).
184. Kelman L. The triggers or precipitants of the acute migraine attack. *Cephalalgia. 2007 May;27(5):394-402.,* (2007).

185. Lima AM , Sapienza GB, Giraud Vde O, Fragoso YD. Odors as triggering and worsening factors for migraine in men. *Arq Neuropsiquiatr. 2011;69(2B):324-7.,* (2011).
186. Rozen TD. Cluster headache as the result of secondhand cigarette smoke exposure during. *Headache. 2010 Jan;50(1):130-2.,* (2010).
187. Andre E, Campi B, Materazzi S, Trevisani M, Amadesi S, Massi D, *et al.* Cigarette smoke-induced neurogenic inflammation is mediated by alpha,beta-unsaturated aldehydes and the TRPA1 receptor in rodents. *J Clin Invest 118(7):2574-2582.,* (2008).
188. Bang S, Kim KY, Yoo S, Kim YG, Hwang SW. Transient receptor potential A1 mediates acetaldehyde-evoked pain sensation. *Eur J Neurosci. 2007 Nov;26(9):2516-23.,* (2007).
189. Talavera K, Gees M, Karashima Y, Meseguer VM, Vanoirbeek JA, Damann N, *et al.* Nicotine activates the chemosensory cation channel TRPA1. *Nat Neurosci. 2009 Oct;12(10):1293-9.,* (2009).
190. Lundberg JM & Saria A. Capsaicin-induced desensitization of airway mucosa to cigarette smoke, mechanical and chemical irritants. *Nature 302: 251-253.,* (1983).
191. Kunkler PE, Ballard CJ, Oxford GS, Hurley JH. TRPA1 receptors mediate environmental irritant-induced meningeal vasodilatation. *Pain 152:38-44.,* (2011).
192. Geppetti P, Nassini R, Materazzi S, Benemei S. The concept of neurogenic inflammation. *BJU Int. 2008 Mar;101 Suppl 3:2-6.*, (2008).
193. Anderson PJ, Lau GS, Taylor WR, Critchley JA. Acute effects of the potent lacrimator o-chlorobenzylidene malononitrile (CS) tear gas. *Hum Exp Toxicol. 1996 Jun;15(6):461-5.*, (1996).
194. Irlbacher k & Meyer BU. Nasally triggered headache. *Neurology. 2002 Jan 22;58(2):294.*, (2002).
195. Wantke F, Focke M, Hemmer W, Bracun R, Wolf-Abdolvahab S, Götz M, *et al.* Exposure to formaldehyde and phenol during an anatomy dissecting course. *Allergy. 2000 Jan;55(1):84-7.*, (2000).
196. Bessac BF & Jordt SE. Sensory detection and responses to toxic gases: mechanisms, health effects, and countermeasures. *Proc Am Thorac Soc. 2010 Jul;7(4):269-77.,* (2010).
197. Shevel E. The extracranial vascular theory of migraine--a great story confirmed by the fact. *Headache. 2011 Mar;51(3):409-417.,* (2011).
198. Thomsen LL & Olesen J. Nitric oxide in primary headaches. *Curr Opin Neurol. 2001 Jun;14(3):315-21.*, (2001).
199. Iversen HK & Olesen J. Headache induced by a nitric oxide donor (nitroglycerin) responds to sumatriptan. A human model for development of migraine drugs. *Cephalalgia. 1996 Oct;16(6):412-8.*, (1996).
200. Amin FM, Asghar MS, Ravneberg JW, de Koning PJ, Larsson HB, Olesen J, *et al.* The effect of sumatriptan on cephalic arteries: A 3T MR-angiography study in healthy volunteers. *Cephalalgia. 2013 Sep;33(12):1009-16.*, (2013).
201. Asghar MS, Hansen AE, Amin FM, van der Geest RJ, Koning Pv, Larsson HB, *et al.* Evidence for a vascular factor in migraine. *Ann Neurol. 2011 Apr;69(4):635-45.*, (2011).
202. Tvedskov JF, Tfelt-Hansen P, Petersen KA, Jensen LT, Olesen J. CGRP receptor antagonist olcegepant (BIBN4096BS) does not prevent glyceryl rinitrate-induced migraine. *Cephalalgia. 2010 Nov;30(11):1346-53.*, (2010).

203. Eltorp CT, Jansen-Olesen I, Hansen AJ. Release of calcitonin gene-related peptide (CGRP) from guinea pig dura mater in inhibited by sumatriptan but unaffected by nitric oxide. *Cephalalgia. 2000 Nov;20(9):838-44.*, (2000).
204. Wei EP, Moskowitz MA, Boccalini P, Kontos HA. Calcitonin gene-related peptide mediates nitroglycerin and sodium nitroprusside-induced vasodilation in feline cerebral arterioles. Circ Res. 1992 Jun;70(6):1313-9., (1992).
205. Fanciullacci M, Alessandri M, Figini M, Geppetti P, Michelacci S. Increase in plasma calcitonin gene-related peptide from the extracerebral circulation during nitroglycerin-induced cluster headache attack. *Pain. 1995 Feb;60(2):119-23.*, (1995).
206. Miyamoto T, Dubin AE, Petrus MJ, Patapoutian A. TRPV1 and TRPA1 mediate peripheral nitric oxide-induced nociception in mice. *PLoS One 4(10):e7596.,* (2009).
207. Iversen HK. Experimental headache in humans. *Cephalalgia. 1995;15(4):281-7.*, (1995).
208. Immel D. California Laurel. *USDA Natural Resources Conservation Service* (2006).
209. Benemei S, Appendino G, Geppetti P. Pleasant natural scent with unpleasant effects: cluster headache-like attacks triggered by Umbellularia californica. *Cephalalgia 30:744-746.,* (2009).
210. Nassini R, Materazzi S, Vriens J, Prenen J, Benemei S, De Siena G, *et al.* The 'headache tree' via umbellulone and TRPA1 activates the trigeminovascular system. *Brain* 135(Pt2):376-390., (2012).
211. Avula B, Wang YH, Wang M, Smilli TJ, Khan IA. Simultaneous determination of sesquiterpenes and pyrrolizidine alkaloids from the rhizomes of Petasites hybridus (L.) G.M. et Sch. and dietary supplements using UPLC-UV and HPLC-TOF-MS methods. *J Pharm Biomed Anal 70: 53-63.,* (2012).
212. Danesch U & Rittinghausen R. Safety of a patented special butterbur root extract for migraine prevention. *Headache 43(1):76-78.,* (2003).
213. Grossmann M & Schmidramsl H. An extract of Petasites hybridus is effective in the prophylaxis of migraine. *Int J Clin Pharmacol Ther 38:430-435.,* (2000).
214. Lipton RB, Gobel H, Einhaupl KM, Wilks K, Mauskop A. Petasites hybridus root (butterbur) is an effective preventive treatment for migraine. *Neurology 63: 2240-2244.,* (2004).
215. Pothmann R. & Danesch U. Migraine prevention in children and adolescents: results of an open study with a special butterbur root extract. *Headache 45:196-203.,* (2005).
216. Thomet OA, Wiesmann UN, Blaser K, Simon HU. Differential inhibition of inflammatory effector functions by petasin, isopetasin and neopetasin in human eosinophils. *Clin Exp Allergy 31:1310-1320.,* (2001).
217. Wang GJ, Shum AY, Lin YL, Liao JF, Wu XC, Ren J, *et al.* Calcium channel blockade in vascular smooth muscle cells: major hypotensive mechanism of S-petasin, a hypotensive sesquiterpene from Petasites formosanus. *J Pharmacol Exp Ther* 297: 240-246., (2001).
218. Wang GJ, Wu XC, Lin YL, Ren J, Shum AY, Wu YY, *et al.* Ca2+ channel blocking effect of iso-S-petasin in rat aortic smooth muscle cells. *Eur J Pharmacol 445:239-245.,* (2002).

219. Ko WC, Lei CB, Lin YL, Chen CF. Mechanisms of relaxant action of S-petasin and S-isopetasin, sesquiterpenes of Petasites formosanus, in isolated guinea pig trachea. *Planta Med 67:224-229.,* (2001).
220. Holland S*,* Silberstein SD, Freitag F, Dodick DW, Argoff C, Ashman E, *et al.* Evidence-based guideline update: NSAIDs and other complementary treatments for episodic migraine prevention in adults: report of the Quality Standards Subcommittee of the American Academy of Neurology and the American Headache Society. *Neurology 78:1346-1353.,* (2012).
221. Avonto C, Taglialatela-Scafati O, Pollastro F, Minassi A, Di Marzo V, De Petrocellis L, *et al.* An NMR spectroscopic method to identify and classify thiol-trapping agents: revival of Michael acceptors for drug discovery? *Angew Chem Int Ed Engl 50:467-471.,* (2011).
222. Staruschenko A, Jeske NA, Akopian AN. Contribution of TRPV1-TRPA1 interaction to the single channel properties of the TRPA1 channel. *J Biol Chem 285:15167-15177.,* (2010).
223. Cuzick J, Sestak I, Baum M, Buzdar A, Howell A, Dowsett M*, et al.* Effect of anastrozole and tamoxifen as adjuvant treatment for early-stage breast cancer: 10-year analysis of the ATAC trial. *Lancet Oncol 11:1135-1141.,* (2013).
224. Desta Z, Kreutz Y, Nguyen AT, Li L, Skaar T, Kamdem LK, *et al.* Plasma letrozole concentrations in postmenopausal women with breast cancer are associated with CYP2A6 genetic variants, body mass index, and age. *Clin Pharmacol Ther 90:693-700.,* (2011).
225. Trainor DC & JonesRC. Headaches in explosive magazine workers. *Arch Environ Health 12:231-234.,* (1966).
226. Thadani U & Rodgers T. Side effects of using nitrates to treat angina. *Expert Opin Drug Saf 5:667-674.,* (2006).
227. Sicuteri F, Del Bene E, Poggioni M, Bonazzi A. Unmasking latent dysnociception in healthy subjects. *Headache 27:180-185.,* (1987).
228. Iversen HK, OlesenJ, Tfelt-Hansen P. Intravenous nitroglycerin as an experimental model of vascular headache. Basic characteristics. *Pain 38:17-24.,* (1989).
229. Thomsen LL, Kruuse C, IversenHK, Olesen J. A nitric oxide donor (nitroglycerin) triggers genuine migraine attacks. *Eur J Neurol* 1*:73-80.,* (1994).
230. Olesen J. The role of nitric oxide (NO) in migraine, tension-type headache and cluster headache. *Pharmacol Ther 120:157-171.,* (2008).
231. Reuter U, Bolay H, Jansen-Olesen I, Chiarugi A, Sanchez del Rio M, Letourneau R, *et al.* Delayed inflammation in rat meninges: implications for migraine pathophysiology. *Brain 124:2490-2502.,* (2001).
232. Ferrari LF, LevineJD, Green PG. Mechanisms mediating nitroglycerin-induced delayed-onset hyperalgesia in the rat. *Neuroscience 317:121-129.,* (2016).
233. Ramachandran R, Bhatt DK, Ploug KB, Hay-Schmidt A, Jansen-Olesen I, Gupta S, Olesen J. Nitric oxide synthase, calcitonin gene-related peptide and NK-1 receptor mechanisms are involved in GTN-induced neuronal activation. *Cephalalgia 34:136-147.,* (2014).
234. Strecker T, Dux M, Messlinger K. Nitric oxide releases calcitonin-gene-related peptide from rat dura mater encephali promoting increases in meningeal blood flow. *J Vasc Res 39:489-496.,* (2002).
235. Edvinsson L. The Journey to Establish CGRP as a Migraine Target: A

Retrospective View. *Headache 55:1249-1255.,* (2015).
236. Ho TW, Edvinsson L, Goadsby, PJ. CGRP and its receptors provide new insights into migraine pathophysiology. *Nat Rev Neurol 6:573-582.,* (2010).
237. Tassorelli C, Greco R, Wang D, Sandrini M, Sandrini G, Nappi G. Nitroglycerin induces hyperalgesia in rats--a time-course study. *Eur J Pharmacol 464: 159-162.,* (2003).
238. Bates EA, Nikai T, Brennan KC, Fu YH, Charles AC, Basbaum AI, *et al.* Sumatriptan alleviates nitroglycerin-induced mechanical and thermal allodynia in mice. *Cephalalgia 30:170-178.,* (2010).
239. Thomsen LL, Brennum J, Iversen HK, Olesen J. Effect of a nitric oxide donor (glyceryl trinitrate) on nociceptive thresholds in man. *Cephalalgia 16:169-174.,* (1996).
240. Trevisan G, Benemei S, Materazzi S, De Logu F, De Siena G, Fusi C, *et al.* TRPA1 mediates trigeminal neuropathic pain in mice downstream of monocytes/macrophages and oxidative stress. *Brain 139:1361-1377.,* (2016).
241. Trevisan G, Hoffmeister C, Rossato MF, Oliveira SM, Silva MA, Silva CR, *et al.* TRPA1 receptor stimulation by hydrogen peroxide is critical to trigger hyperalgesia and inflammation in a model of acute gout. *Free Radic Biol Med 72: 200-209.,* (2014).
242. Andersson DA, Gentry C, Alenmyr L, Killander D, Lewis SE, Andersson A, *et al.* TRPA1 mediates spinal antinociception induced by acetaminophen and the cannabinoid Delta(9)-tetrahydrocannabiorcol. *Nat Commun 2:551.,* (2011).
243. Nassini R, Fusi C, Materazzi S, Coppi E, Tuccinardi T, Marone IM*, et al.* The TRPA1 channel mediates the analgesic action of dipyrone and pyrazolone derivatives. *Br J Pharmacol 172:3397-3411.,* (2014).
244. Benemei S, De Logu F, Li Puma S, Marone IM, Coppi E, Ugolini F, *et al.* The anti-migraine component of butterbur extracts, isopetasin, desensitizes peptidergic nociceptors by acting on TRPA1 cation channel. *Br J Pharmacol 16:13917.,* (2017).
245. Materazzi S*,* Benemei S, Fusi C, Gualdani R, De Siena G, Vastani N, *et al.* Parthenolide inhibits nociception and neurogenic vasodilatation in the trigeminovascular system by targeting the TRPA1 channel. *Pain 3959:00438-00437.,* (2013).
246. Sutherland A. & Sweet BV. Butterbur: an alternative therapy for migraine prevention. *Am J Health Syst Pharm 67:705-711.,* (2010).
247. Aydin AA, Zerbes V, Parlar H, Letzel T. The medical plant butterbur (Petasites): analytical and physiological (re)view. *J Pharm Biomed Anal 75: 220-229.,* (2013).
248. Nilius B & Szallasi A. Transient receptor potential channels as drug targets: from the science of basic research to the art of medicine. *Pharmacol Rev* 66*: 676-814.,* (2014).
249. Chaplan SR, Bach FW, Pogrel JW, Chung JM, Yaksh TL. Quantitative assessment of tactile allodynia in the rat paw. *J Neurosci Methods 53:55-63.,* (1994).
250. Dixon WJ. Efficient analysis of experimental observations. *Annu Rev Pharmacol Toxicol 20:441-462.,* (1980).
251. Doig J, Griffiths LA, Peberdy D, Dharmasaroja P, Vera M, Davies FJ, *et al.* In vivo characterization of the role of tissue-specific translation elongation factor 1A2 in protein synthesis reveals insights into muscle atrophy. *Febs J 280: 6528-6540.,* (2013).

252. la Marca G, Malvagia S, Filippi L, Fiorini P, Innocenti M, Luceri F, *et al.* Rapid assay of topiramate in dried blood spots by a new liquid chromatography-tandem mass spectrometric method. *J Pharm Biomed Anal 48: 1392-1396.,* (2008).
253. Mao JJ, Chung A, Benton A, Hill S, Ungar L, Leonard CE, *et al.* Online discussion of drug side effects and discontinuation among breast cancer survivors. *Pharmacoepidemiol Drug Saf 22:256-262.,* (2013).
254. Steinhoff MS, von Mentzer B, Geppetti P, Pothoulakis, C, Bunnett NW. Tachykinins and their receptors: contributions to physiological control and the mechanisms of disease. *Physiol Rev 94:265-301.,* (2014).
255. Reagan-Shaw S, Nihal M, Ahmad N. Dose translation from animal to human studies revisited. *Faseb J 22:659-661.,* (2008).
256. Lintermans A, Van Calster B, Van Hoydonck M, Pans S, Verhaeghe J, Westhovens R, *et al.* Aromatase inhibitor-induced loss of grip strength is body mass index dependent: hypothesis-generating findings for its pathogenesis. *Ann Oncol 22:1763-1769.,* (2011).
257. Jin SJ, Jung JA, Cho SH, Kim UJ, Choe S, Ghim JL, *et al.* The pharmacokinetics of letrozole: association with key body mass metrics. *Int J Clin Pharmacol Ther 50:557-565.,* (2012).
258. Jukanti R, Sheela S, Bandari S, Veerareddy PR. Enhanced bioavailability of exemestane via proliposomes based transdermal delivery. *J Pharm Sci* 1*00: 3208-3222.,* (2011).
259. Valle M, Di Salle E, Jannuzzo MG, Poggesi I, Rocchetti M, Spinelli R, *et al.* A predictive model for exemestane pharmacokinetics/pharmacodynamics incorporating the effect of food and formulation. *Br J Clin Pharmacol 59:355-364.,* (2005).
260. Wang S, Dai Y, Fukuoka T, Yamanaka H, Kobayashi K, Obata K, *et al.* Phospholipase C and protein kinase A mediate bradykinin sensitization of TRPA1: a molecular mechanism of inflammatory pain. *Brain 131:1241-1251.,* (2008).
261. Vergnolle N, Bunnett NW, Sharkey KA, Brussee V, Compton SJ, Grady EF, *et al.* Proteinase-activated receptor-2 and hyperalgesia: A novel pain pathway. *Nat Med 7: 821-826.,* (2001).
262. Dalle-Donne I, Carini M, Vistoli G, Gamberoni L, Giustarini D, Colombo R, *et al.* Actin Cys374 as a nucleophilic target of alpha,beta-unsaturated aldehydes. *Free Radic Biol Med 42:583-598.,* (2007).
263. Oballa RM, Truchon JF, Bayly CI, Chauret N, Day S, Crane S, *et al.* A generally applicable method for assessing the electrophilicity and reactivity of diverse nitrile-containing compounds. *Bioorg Med Chem Lett 17:998-1002.,* (2007).
264. Moran MM, McAlexander MA, Biro T, Szallasi A. Transient receptor potential channels as therapeutic targets. *Nat Rev Drug Discov 10:601-620.,* (2011).
265. Henry NL, Pchejetski D, A'Hern R, Nguyen AT, Charles P, Waxman J, *et al.* Inflammatory cytokines and aromatase inhibitor-associated musculoskeletal syndrome: a case-control study. *Br J Cancer 103:291-296.,* (2010).
266. Kennecke HF, Olivotto IA, Speers C, Norris B, Chia SK, *et al.* Late risk of relapse and mortality among postmenopausal women with estrogen responsive early breast cancer after 5 years of tamoxifen. *Ann Oncol 18:45-51.,* (2007).
267. Sies H. Role of metabolic H_2O_2 generation: redox signaling and oxidative

stress. *J Biol Chem 289:8735-8741.,* (2014).
268. Spinelli O*, et al.* Pharmacokinetics (PK) of Aromasin ® (exemestane, EXE) after single and repeated doses in healthy postmenopausal volunteers (HPV). *Eur J Cancer 35:S295.,* (1999).
269. Dowsett M, Cuzick J, Howell A, Jackson I. Pharmacokinetics of anastrozole and tamoxifen alone, and in combination, during adjuvant endocrine therapy for early breast cancer in postmenopausal women: a sub-protocol of the 'Arimidex and tamoxifen alone or in combination' (ATAC) trial. *Br J Cancer 85:317-324.,* (2001).
270. Bradford MM. A rapid and sensitive method for the quantitation of microgram quantities of protein utilizing the principle of protein-dye binding. *Anal Biochem 72:248-254.,* (1976).
271. Kelly E, Lu CY, Albertini S, Vitry A. Longitudinal trends in utilization of endocrine therapies for breast cancer: an international comparison. *J Clin Pharm Ther 40:76-82.,* (2015).
272. Rezvanfar MA*,* Rezvanfar MA, Ahmadi A, Saadi HA, Baeeri M, Abdollahi M. Mechanistic links between oxidative/nitrosative stress and tumor necrosis factor alpha in letrozole-induced murine polycystic ovary: biochemical and pathological evidences for beneficial effect of pioglitazone. *Hum Exp Toxicol 31:887-97.,* (2012).
273. Nassini R, Materazzi S, Benemei, S,Geppetti P. The TRPA1 channel in inflammatory and neuropathic pain and migraine. *Rev Physiol Biochem Pharmacol 167:1-43.,* (2014).
274. Sadofsky LR*,* Sreekrishna KT, Lin Y, Schinaman R, Gorka K, Mantri Y*, et al.* Unique Responses are Observed in Transient Receptor Potential Ankyrin 1 and Vanilloid 1 (TRPA1 and TRPV1) Co-Expressing Cells. *Cells 3:616-626.,* (2014).
275. Schaefer M. Homo- and heteromeric assembly of TRP channel subunits. *Pflugers Arch 451:35-42.,* (2005).
276. Salas MM, Hargreaves KM, Akopian AN. TRPA1-mediated responses in trigeminal sensory neurons: interaction between TRPA1 and TRPV1. *Eur J Neurosci 29:1568-1578.,* (2009).
277. Akopian AN, Ruparel NB, Jeske NA, Hargreaves KM. Transient receptor potential TRPA1 channel desensitization in sensory neurons is agonist dependent and regulated by TRPV1-directed internalization. *J Physiol 583: 175-193.,* (2007).
278. Ruparel NB, Patwardha AM, Akopian AN, Hargreaves KM. Homologous and heterologous desensitization of capsaicin and mustard oil responses utilize different cellular pathways in nociceptors. *Pain* 135:271-279., (2008).
279. FDA, C.f.d.e.a.r. Letrozole - Clinical pharmacology and biopharmaceutic review, NDA 20-726. Vol. 2016 NDA (1997).
280. Bautista DM, Pellegrino M, Tsunozaki M. TRPA1: A gatekeeper for inflammation. *Annu Rev Physiol 75:181-200.,* (2013).
281. Kilic N, Yavuz Taslipinar M, Guney Y, Tekin E, Onuk E. An investigation into the serum thioredoxin, superoxide dismutase, malondialdehyde, and advanced oxidation protein products in patients with breast cancer. *Ann Surg Oncol 21:4139-4143.,* (2014).
282. Mittal M, Siddiqui MR, Tran K, Reddy SP, Malik AB. Reactive oxygen species in inflammation and tissue injury. *Antioxid Redox Signal 20:1126-1167.,* (2014).

283. Guan Z, Kuhn JA, Wang X, Colquitt B, Solorzano C, Vaman S, *et al.* Injured sensory neuron-derived CSF1 induces microglial proliferation and DAP12-dependent pain. *Nat Neurosci 19:94-101.,* (2016).
284. Zurborg S, Piszczek A, Martínez C, Hublitz P, Al Banchaabouchi M, Moreira P, *et al.* Generation and characterization of an Advillin-Cre driver mouse line. *Mol Pain 7:66.,* (2011).
285. Zappia KJ, O'Hara CL, Moehring F, Kwan, KY, Stucky CL. Sensory Neuron-Specific Deletion of TRPA1 Results in Mechanical Cutaneous Sensory Deficits. *eNeuro 4:0069-0016.,* (2017).
286. Elliott MB, Oshinsky ML, Amenta PS, Awe OO, Jallo J.I. Nociceptive neuropeptide increases and periorbital allodynia in a model of traumatic brain injury. *Headache 52:966-984.,* (2012).
287. Altenhofer S, Radermacher KA, Kleikers PW, Wingler K, Schmidt HH. Evolution of NADPH Oxidase Inhibitors: Selectivity and Mechanisms for Target Engagement. *Antioxid Redox Signal 23:406-427.,* (2015).
288. Glowka TR, Steinebach A, Stein K, Schwandt T, Lysson M, Holzmann B, *et al.* The novel CGRP receptor antagonist BIBN4096BS alleviates a postoperative intestinal inflammation and prevents postoperative ileus. *Neurogastroenterol Motil 27:1038-1049.,* (2015).
289. Nozaki-Taguchi N & Yamamoto T. Involvement of nitric oxide in peripheral antinociception mediated by kappa- and delta-opioid receptors. *Anesth Analg 87:388-393.,* (1998).
290. Rossato MF, Velloso NA, de Oliveira Ferreira AP, de Mello CF, Ferreira J. Spinal levels of nonprotein thiols are related to nociception in mice. *J Pain 11:545-554.,* (2010).
291. Marquez de Prado B, Hammond DL, Russo AF. Genetic enhancement of calcitonin gene-related Peptide-induced central sensitization to mechanical stimuli in mice. *J Pain 10:992-1000.,* (2009).
292. Mogil JS, Miermeister F, Seifert F, Strasburg K, Zimmermann K, Reinold H, *et al.* Variable sensitivity to noxious heat is mediated by differential expression of the CGRP gene. *Proc Natl Acad Sci U S A 102:12938-12943.,* (2005).
293. Pecze L, Pelsoczi P, Kecskés M, Winter Z, Papp A, Kaszás K, *et al.* Resiniferatoxin mediated ablation of TRPV1+ neurons removes TRPA1 as well. *Can J Neurol Sci 36: 234-241.,* (2009).
294. Chung MK, Asgar J, Lee J, Shim MS, Dumler C, Ro JY. The role of TRPM2 in hydrogen peroxide-induced expression of inflammatory cytokine and chemokine in rat trigeminal ganglia. *Neuroscience 297:160-169.,* (2015).
295. Holzer P. Capsaicin: cellular targets, mechanisms of action, and selectivity for thin sensory neurons. *Pharmacol Rev 43:143-201.,* (1991).
296. Sullivan MN, Gonzales AL, Pires PW, Bruhl A, Leo MD, Li W, *et al.* Localized TRPA1 channel Ca2+ signals stimulated by reactive oxygen species promote cerebral artery dilation. *Sci Signal 8:ra2.,* (2015).
297. Eid SR, Crown ED, Moore EL, Liang HA, Choong KC, Dima S, *et al.* HC-030031, a TRPA1 selective antagonist, attenuates inflammatory- and neuropathy-induced mechanical hypersensitivity. *Mol Pain 4:48.,* (2008).
298. Beretta M, Gruber K, Kollau A, Russwurm M, Koesling D, Goessler W, *et al.* Bioactivation of nitroglycerin by purified mitochondrial and cytosolic aldehyde dehydrogenases. *J Biol Chem 283:17873-17880.,* (2008).
299. WenzL MV, Beretta M, Gorren AC, Zeller A, Baral PK, Gruber K, *et al.* Role of the general base Glu-268 in nitroglycerin bioactivation and

superoxide formation by aldehyde dehydrogenase-2. *J Biol Chem 284:19878-19886.,* (2009).
300. Dalle-Donne I, Rossi R, Colombo R, Giustarini D, Milzani A. Biomarkers of oxidative damage in human disease. *Clin Chem 52:601-623.,* (2006).
301. Brame CJ, Salomon RG, Morrow JD, Roberts LJ 2nd. Identification of extremely reactive gamma-ketoaldehydes (isolevuglandins) as products of the isoprostane pathway and characterization of their lysyl protein adducts. *J Biol Chem 274:13139-13146.,* (1999).
302. Bedard K & Krause KH. The NOX family of ROS-generating NADPH oxidases: physiology and pathophysiology. *Physiol Rev 87:245-313.,* (2007).
303. Demartini C, Tassorelli C, Zanaboni AM, Tonsi G, Francesconi O, Nativi C, *et al.* The role of the transient receptor potential ankyrin type-1 (TRPA1) channel in migraine pain: evaluation in an animal model. *J Headache Pain 18:94.,* (2017).
304. Farkas S, Bölcskei K, Markovics A, Varga A, Kis-Varga Á, Kormos V, *et al.* Utility of different outcome measures for the nitroglycerin model of migraine in mice. *J Pharmacol Toxicol Methods 77:33-44.,* (2016).
305. Koza D, Kabasawa Y, Ebert M, Kiyonaka S; Firman, Otani Y *et al.* Transnitrosylation directs TRPA1 selectivity in N-nitrosamine activators. *Mol Pharmacol 85:175-185.,* (2014).
306. Zhang Y & Hogg N. Formation and stability of S-nitrosothiols in RAW 264.7 cells. *Am J Physiol Lung Cell Mol Physiol 287:L467-474.,* (2004).
307. Shimizu S, Takahashi N, Mori Y. TRPs as chemosensors (ROS, RNS, RCS, gasotransmitters). *Handb Exp Pharmacol. 223:767-794.,* (2014).
308. Edvinsson L. Blockade of CGRP receptors in the intracranial vasculature: a new target in the treatment of headache. *Cephalalgia 24:611-622.,* (2004).
309. Kopruszinski CM, Xie JY, Eyde NM, Remeniuk B, Walter S, Stratton J, *et al.* Prevention of stress- or nitric oxide donor-induced medication overuse headache by a calcitonin gene-related peptide antibody in rodents. *Cephalalgia 37:560-570.,* (2017).
310. Bigal ME, Bordini CA, Tepper SJ, Speciali JG. Intravenous dipyrone in the acute treatment of migraine without aura and migraine with aura: a randomized, double blind, placebo controlled study. *Headache. 42:862-871.,* (2002).
311. Kilkenny C, Browne W, Cuthill IC, Emerson M, Altman DG. Animal research: reporting in vivo experiments: the ARRIVE guidelines. *Br J Pharmacol 160:1577-1579.,* (2010).
312. McGrath JC & Lilley E. Implementing guidelines on reporting research using animals (ARRIVE etc.): new requirements for publication in BJP. *Br J Pharmacol 172:3189-3193.,* (2015).
313. Liedtke W & Friedman JM. Abnormal osmotic regulation in trpv4$^{-/-}$ mice. *Proc Natl Acad Sci U S A 100:13698-13703.,* (2003).
314. Luccarini P, Childeric A, Gaydier AM, Voisin D, Dallel R. The orofacial formalin test in the mouse: a behavioral model for studying physiology and modulation of trigeminal nociception. *J Pain 7:908-914.,* (2006).
315. Curtis MJ, Bond RA, Spina D, Ahluwalia A, Alexander SP, Giembycz MA, *et al.* Experimental design and analysis and their reporting: new guidance for publication in BJP. *Br J Pharmacol 172:3461-3471.,* (2015).
316. Nicoletti P, Trevisani M, Manconi M, Gatti R, De Siena G, Zagli G, *et al.* Ethanol causes neurogenic vasodilation by TRPV1 activation and CGRP

release in the trigeminovascular system of the guinea pig. *Cephalalgia 28:9-17.,* (2008).
317. Benemei S, Fusi C, Trevisan G, Geppetti P. The TRPA1 channel in migraine mechanism and treatment. *Br J Pharmacol 171:2552-2567.,* (2014).
318. Andrade EL, Ferreira J, Andre E, Calixto JB. Contractile mechanisms coupled to TRPA1 receptor activation in rat urinary bladder. *Biochem Pharmacol 72:104-114.,* (2006).
319. Arnold E, Benz T, Zapp C, Wink M. Inhibition of Cytosolic Phospholipase A2alpha (cPLA2alpha) by Medicinal Plants in Relation to Their Phenolic Content. *Molecules. 2015 Aug 20:15033-15048.,* (2015).
320. Lee DK, Carstairs IJ, Haggart K, Jackson CM, Currie GP, Lipworth BJ. Butterbur, a herbal remedy, attenuates adenosine monophosphate induced nasal responsiveness in seasonal allergic rhinitis. *Clin Exp Allergy. 33:882-886.,* (2003).
321. Schapowal A. Randomised controlled trial of butterbur and cetirizine for treating seasonal allergic rhinitis. *Bmj. 324:144-146.,* (2002).
322. Edvinsson L. CGRP receptor antagonists and antibodies against CGRP and its receptor in migraine treatment. *Br J Clin Pharmacol 80:193-199.,* (2015).
323. Bigal ME*,* Edvinsson L, Rapoport AM, Lipton RB, Spierings EL, Diener HC*, et al.* Safety, tolerability, and efficacy of TEV-48125 for preventive treatment of chronic migraine: a multicentre, randomised, double-blind, placebo-controlled, phase 2b study. *Lancet Neurol 14:1091-1100.,* (2015).
324. Ramacciotti AS, Soares BG, Atallah AN. Dipyrone for acute primary headaches. *Cochrane Database Syst Rev 18:CD004842.,* (2007).
325. Pietrobon D & Moskowitz MA. Pathophysiology of migraine. *Annu Rev Physiol. 75:365-91*., (2013).
326. Murray CJ & Lopez AD. Measuring the global burden of disease. *N Engl J Med. 369(5):448-57.,* (2013).